Springer Tracts in Electrical and Electronics Engineering

Praveen K. Malik
Prasad N. Shastry *Editors*

Internet of Things Enabled Antennas for Biomedical Devices and Systems

Impact, Challenges and Applications

Springer

Springer Tracts in Electrical and Electronics Engineering

Springer Tracts in Electrical and Electronics Engineering (STEEE) publishes the latest developments in Electrical and Electronics Engineering - quickly, informally and with high quality. The intent is to cover all the main branches of electrical and electronics engineering, both theoretical and applied, including:

- Signal, Speech and Image Processing
- Speech and Audio Processing
- Image Processing
- Human-Machine Interfaces
- Digital and Analog Signal Processing
- Microwaves, RF Engineering and Optical Communications
- Electronics and Microelectronics, Instrumentation
- Electronic Circuits and Systems
- Embedded Systems
- Electronics Design and Verification
- Cyber-Physical Systems
- Electrical Power Engineering
- Power Electronics
- Photovoltaics
- Energy Grids and Networks
- Electrical Machines
- Control, Robotics, Automation
- Robotic Engineering
- Mechatronics
- Control and Systems Theory
- Automation
- Communications Engineering, Networks
- Wireless and Mobile Communication
- Internet of Things
- Computer Networks

Within the scope of the series are monographs, professional books or graduate textbooks, edited volumes as well as outstanding PhD theses and books purposely devoted to support education in electrical and electronics engineering at graduate and post-graduate levels.

Review Process

The proposal for each volume is reviewed by the main editor and/or the advisory board. The books of this series are reviewed in a single blind peer review process.

Ethics Statement for this series can be found in the Springer standard guidelines here https://www.springer.com/us/authors-editors/journal-author/journal-author-helpdesk/before-you-start/before-you-start/1330#c14214

Praveen K. Malik · Prasad N. Shastry
Editors

Internet of Things Enabled Antennas for Biomedical Devices and Systems

Impact, Challenges and Applications

Springer

Editors
Praveen K. Malik
School of Electronics and Electrical Engineering
Lovely Professional University
Phagwara, Punjab, India

Prasad N. Shastry
Department of Electrical and Computer Engineering
Bradley University
Peoria, IL, USA

ISSN 2731-4200 ISSN 2731-4219 (electronic)
Springer Tracts in Electrical and Electronics Engineering
ISBN 978-981-99-0211-8 ISBN 978-981-99-0212-5 (eBook)
https://doi.org/10.1007/978-981-99-0212-5

This Springer imprint is published by the registered company Springer Nature Singapore Pte Ltd.
The registered company address is: 152 Beach Road, #21-01/04 Gateway East, Singapore 189721, Singapore

I dedicate this book to my beloved father in heaven who taught me to be an independent and determined person, without whom I would never be able to achieve my objectives and success in life

Praveen Malik

I dedicate this book to my teachers and mentors because of whom I am who I am today
Prasad Shastry

Contents

Editors and Contributors

About the Editors

Praveen K. Malik is a Professor at the School of Electronics and Electrical Engineering, Lovely Professional University, Phagwara, Punjab, India. He received his Ph.D. with a specialization in wireless communication and antenna design. He has over 40 research papers and three edited/authored books published to his credit. He has guided many students leading to M.E./M.Tech. and guiding students leading to Ph.D. His current interest areas are microstrip antenna design, MIMO, vehicular communication, and IoT. He has been a Guest Editor/Editorial Board Member of many international journals and a Keynote Speaker at many international conferences and invited as a Program Chair, Publications Chair, Publicity Chair, and Session Chair at many international conferences. He has been granted two design patents, and a few are in the pipeline.

Prasad N. Shastry is a Professor of RF, microwave, and wireless engineering in the Department of Electrical and Computer Engineering at Bradley University, Peoria, Illinois, USA. He is also the Founder of Shastry Associates Global Enterprise (SAGE). He worked at the University of Wisconsin-Madison for 9 years as a Post-doctoral Researcher and Adjunct Faculty Member before joining Bradley University. He has 40 years of experience teaching courses from Sophomore to Ph.D. levels in addition to 45 years of research experience. Since joining Bradley in 1991, he has spearheaded the development of the curriculum, laboratories, and an active research program in the area of microwave and wireless engineering at Bradley. He has established a National Science Foundation-funded advanced microwave engineering laboratory for designing and testing monolithic microwave integrated circuits (MMICs), an anechoic chamber for antenna measurements, a CAD laboratory for the designs of RF circuits and antennas, a laboratory for tests and measurements of RF circuits, and microwave integrated circuit fabrication facility. His areas of research are wideband distributed amplifiers, wideband distributed architecture circuits, wideband antennas, reconfigurable active and passive circuits, reconfigurable antennas,

wireless power transfer, and ambient RF energy harvesting. During the past forty-five years, he has made significant contributions in his area of expertise in industry-university collaborative projects sponsored by several leading microwave companies in the USA. He was the Director of RF development at Validus Technologies, LLC, from 2006 to 2014. He has advised Endotronix, Inc., since its start-up stage. He is Advisor to the Center for Antennas and RF Systems, MSRIT, and the company ELDAAS in Bangalore. Dr. Shastry was awarded a Ph.D. degree in microwave engineering by IIT Bombay in 1980. During his doctoral research, he invented the widely used Linearly Tapered Slotline Antenna (LTSA). He earned an M.Tech. degree in microwave and radar engineering from IIT Kharagpur in 1974, where he worked on phased array antennas, and a Bachelor of Engineering (Electronics) degree from University Visveshwaraih College of Engineering, Bangalore University, in 1972. He was awarded Post-doctoral Fellowship in the Department of Electrical and Computer Engineering at the University of Wisconsin, Madison, in 1982. Dr. Shastry is the Author or Co-author of over one hundred manuscripts and publications which include archival journal articles, refereed conference papers, book chapters, edited books, and project reports. He also holds two U.S. patents on Electronically Tunable Active Duplexers. He is an Invited Speaker at international conferences, universities/colleges, R&D organizations, companies, and professional societies. He has advised and supervised numerous post-graduate and undergraduate student projects and theses for over forty years. He has served as an Expert Reviewer for IEEE Transactions and other international journals, international conferences, and books. He has also served on expert proposal review panels of the National Science Foundation and technical program committees of the IEEE MTT-S International Microwave Symposium. Dr. Shastry has been recognized for his outstanding performance in teaching and exemplary innovations in the field of microwave engineering by IETE, India, and Bradley University.

Contributors

Sumit Agarwal Pennsylvania State University, State College, Pennsylvania, Philadelphia, US

Basim Alhadidi Computer Information Systems, Prince Abullah Bin Ghazi Faculty of Information and Communication Technology, Al-Balqa Applied University, As-Salt, Jordan

Waleed Saleh Alnumay Computer Science Department, King Saud University, Riyadh, Saudi Arabia

Gokul Basavaraj Department of Electronics and Communication Engineering, KPR Institute of Engineering and Technology, Coimbatore, Tamil Nadu, India; Central Queensland University, Victoria, Melbourne, Australia

Nitinkumar J. Bathani Department of Electronics and Communication Engg, Government Engineering College, Modasa, Gujarat, India

S Durga Padmaja Bikkuri GITAM University, Bengaluru, India

Mukesh Chand Poornima College of Engineering, Jaipur, India

Dharmendra V. Chauhan V T Patel Department of E&C Engineering, Chandubhai S Patel Institute of Technology, Charotar University of Science and Technology (CHARUSAT), Changa, India

Sanjay Chouhan Jawaharlal Institute of Technology, Borawan-Khargone, India

E. L. Dhivya Priya Department of ECE, Sri Krishna College of Technology, Coimbatore, Tamilnadu, India

Mohamed El Bakkali Faculty of Sciences of Rabat, Mohammed Five University of Rabat, Rabat, Morocco

Jeet Ghosh Chaitanya Bharati Institute of Technology (A), Hyderabad, India

K. R. Gokul Anand Department of ECE, Dr Mahalingam College of Engineering and Technology, Pollachi, Tamilnadu, India

L. Govinda Cancer Science Institute of Singapore, National University of Singapore, Singapore, Singapore

Md. Shakhawat Hossen Rajshahi University of Engineering & Technology, Rajshahi, Bangladesh

Sweety Jain Samrat Ashok Technological Institute, Vidisha, Madhya Pradesh, India

S. Kannadhasan Department of Electronics and Communication Engineering, Study World College of Engineering, Coimbatore, India

Ramani kannan Department of Electrical and Electronic Engineering, University of Teknologi Petronas, Bandar Seri Iskandar, Tronoh Perak, Malaysia

Parminder Kaur Chitkara University Institute of Engineering and Technology, Chitkara University, Rajpura, Punjab, India

Habibullah Khan ALRC R&D, ECE Department, Koneru Lakshmaiah Education Foundation, Guntur, Andhra Pradesh, India

Maleeha Khan McGill University, Montreal, QC, Canada

Dheeraj Kumar Department of Physics and Electronics, Rajdhani College (University of Delhi), Delhi, India

R. Sanjeev Kumar Department of Physics, Coimbatore Institute of Technology, Coimbatore, India

Vivek Singh Kushwah Amity University, Gwalior, Madhya Pradesh, India

Joan Lu Department of Computer Science, University of Huddersfield, Huddersfield, UK

B. T. P. Madhav ALRC R&D, ECE Department, Koneru Lakshmaiah Education Foundation, Guntur, Andhra Pradesh, India

Keyur Mahant V T Patel Department of E&C Engineering, Chandubhai S Patel Institute of Technology, Charotar University of Science and Technology (CHARUSAT), Changa, India

Shivani Malhotra Chitkara University Institute of Engineering and Technology, Chitkara University, Rajpura, Punjab, India

Praveen Kumar Malik School of Electronics and Electrical Engineering, Lovely Professional University, Jalandhar, Punjab, India

Garima Mathur Poornima College of Engineering, Jaipur, India

Utkal Mehta Electrical and Electronics Engineering, The University of the South Pacific, Laucala Campus, Suva, Fiji Islands

Hiren Mewada Prince Mohmmad Bin Fahad University, Al Khobar, Saudi Arabia

Sovan Mohanty SRMS College of Engineering and Technology, Bareilly, India

Baibaswata Mohapatra Chandigarh University, Chandigarh, India

Mehaboob Mujawar Research Scholar, Glocal University, Saharanpur, Uttar Pradesh, India

R. Nagarajan Department of Electrical and Electronics Engineering, Gnanamani College of Technology, Namakkal, India

Arshi Naim Department of Information Systems, AlSamer, University Campus, King Khalid University, Aseer, Abha, Kingdom of Saudi Arabia

K. S. Nisaar Salman Bin Abdul Aziz University, Al-Kharj, Kingdom of Saudi Arabia

S. Nithya Department of Electronics and Communication Engineering, KPR Institute of Engineering and Technology, Coimbatore, Tamil Nadu, India

Ahmed J. Obaid Department of Computer Science, Faculty of Computer Science and Mathematics, University of Kufa, Najaf, Iraq

Shuchismita Pani Amity University, Uttar Pradesh, Noida, India

Amit Patel V T Patel Department of E&C Engineering, Chandubhai S Patel Institute of Technology, Charotar University of Science and Technology (CHARUSAT), Changa, India

Sagar patel V T Patel Department of E&C Engineering, Chandubhai S Patel Institute of Technology, Charotar University of Science and Technology (CHARUSAT), Changa, India

T. Poornima Space Machines Company, Bangaluru, India

R. Prabhu Robert Bosch, Coimbatore, India

A. Praveena PSG College of Technology, Coimbatore, India

E. L. Dhivya Priya Department of ECE, Erode Sengunthar Engineering College, Erode, India

K. C. Rajarajeshwari Department of ECE, Dr Mahalingam College of Engineering and Technology, Pollachi, Tamilnadu, India

R. Ramesh Department of ECE, PSG College of Technology, Coimbatore, India

Jagdishkumar M. Rathod Electronics Department, B.V.M. Engineering College, Vallabh Vidhyanagar, Anand, Gujarat, India

S. Salma Department of ECE, Sri Venkateshwara College of Engineering, Karakambadi Road, Tirupati, India

D. Ram Sandeep Department of ECE, Raghu Engineering College, Dakamarri, Bheemunipatnam, Visakhapatnam, India

G. Saranya Department of Electronics and Communication Engineering, Rajalakshmi Engineering College, Chennai, Tamil Nadu, India

T. Sathiyapriya ECE Department, Dr. Mahalingam College of Engineering and Technology, Coimbatore, India

V. Seethalakshmi Department of Electronics and Communication Engineering, KPR Institute of Engineering and Technology, Coimbatore, Tamil Nadu, India

Manish Sharma Chitkara University Institute of Engineering and Technology, Chitkara University, Rajpura, Punjab, India

A. Sharmila Department of ECE, Bannari Amman Institute of Technology, Sathyamangalam, India

M. Singaram KPR Institute of Engineering and Technology, Arasur, Coimbatore, India

S. Suganyadevi Department of Electronics and Communication Engineering, KPR Institute of Engineering and Technology, Coimbatore, Tamil Nadu, India

Malay Ranjan Tripathy Amity University, Uttar Pradesh, Noida, India

E. Udayakumar Department of ECE, KIT-Kalaignarkarunanadhi Institute of Technology, Coimbatore, India

G. Umamaheswari PSG College of Technology, Coimbatore, India

Alpesh Vala V T Patel Department of E&C Engineering, Chandubhai S Patel Institute of Technology, Charotar University of Science and Technology (CHARUSAT), Changa, India

G. Vetrichelvi Jansons Institute of Technology, Coimbatore, India

Shanmugam Bhaskar Vignesh NTU, Singapore, Singapore

Chapter 1
Biomedical Application Single-Element/MIMO Patch Antenna for WBAN/Implantable in Ultra-wideband and ISM Band

Manish Sharma, Praveen Kumar Malik, and Waleed Saleh Alnumay

Abstract This chapter focuses on the application of microstrip patch antennae in ultra-wideband as well as ISM band for bio-medical and telemetry applications. The antenna discussed finds applications in Wireless Body Area Networks (WBAN), for wearable and implantable purposes. The utilization of a very thin substrate such as jeans for wearable purposes provides super-wideband bandwidth. The cotton and jeans material corresponds to the permittivity of 1.50 (thickness 0.242 mm) and 1.67 (thickness 0.75 mm) for wearable medical applications. The capsule antenna is used for deep tissue implantation use to study the human intestine and head at 2.45 and 0.91 GHz, respectively.

Keywords UWB · ISM · WBAN · Implantable · Wearable antenna · Human intestine and head

Introduction

The antenna development technology, especially microstrip patch antenna, plays a vital role in modern communication. This has led to the application of the proposed antenna in medical field applications which is useful in diagnosing breast cancer, brain tumor, various skin-related diseases and endoscopy. They also find applications in energy harvesting which can trigger different sensors useful in medical technology. The enormous amount of electromagnetic energy available in nature

M. Sharma (✉)
Chitkara University Institute of Engineering and Technology, Chitkara University, Rajpura, Punjab, India
e-mail: manishengineer1978@gmail.com; manish.sharma@chitkara.edu.in

P. K. Malik
School of Electronics and Electrical Engineering, Lovely Professional University, Jalandhar, Punjab, India

W. S. Alnumay
Computer Science Department, King Saud University, Riyadh, Saudi Arabia

P. K. Malik and P. N. Shastry (eds.), *Internet of Things Enabled Antennas for Biomedical Devices and Systems*, Springer Tracts in Electrical and Electronics Engineering,
https://doi.org/10.1007/978-981-99-0212-5_1

which is ubiquitous can be transformed into energy harvesting with the help of a rectifier section and can be stored for different embedded applications (Koohestani et al. 2020). Body Area Networks (BANs) are another recent research area in the field of medical science. Several wireless communication devices are linked with the body and ultra-wideband (UWB) is one among them. Also, exploration for super-wideband antennae can provide short as well as long-range communication in ubiquitous applications. Several antennae for WBAN find fabric as a substrate which can be wearable and can be designed as a planar antenna. A super-wideband antenna includes Global Positioning System bandwidth (GPS: 1.57042–1.58042 GHz), Personal Communication System 900 (1.850–1.990 GHz), International Telecommunication/Universal Mobile Telecommunication System (UMTS) with a bandwidth of 1.885–2.200 GHz, Wireless-Fidelity (WiFi: 2.400 GHz/5.800 GHz), Bluetooth with a center frequency of 2.40 GHz and Ultra-wideband (3.10–10.60 GHz) which are all useful for WBAN applications. This wider bandwidth is achieved with a triangular-shaped fractal patch and semi-circular ground with an etched rectangular slot (Karimyian-Mohammadabadi et al. 2015). A high-impedance surface is used to improve the impedance bandwidth at 2.45 GHz which provides a maximum gain of 6.19 dBi. The antenna also features a wearable-loop antenna in line with High Impedance Surface (HIS) which is useful for the human arm and can monitor vital parameters (Bait-Suwailam et al. 2020). The loop antenna with High Impedance Surface (HIS) structure is fabricated on cotton jeans for wearable applications. A monocone antenna produces wider bandwidth of 2.50–2.40 GHz for S11 <-10.0 dB which is lower in profile with height 0.05 λ_0 which finds applications for WBAN (Yang et al. 2018). A dual band antenna with a frequency centered at 2.40 and 5.80 GHz is fabricated on regular dielectric material and an electromagnetic Band Gap structure. The designed antenna is investigated for human-arm and legs (right or left). The two ISM bands are realized for Specific-Absorption Rate (SAR) values less than 2 watts/Kg (Afridi et al. 2013). WBAN antenna at 2.45 GHz with dual port pattern diversity is directed toward the omni-azimuth plane which is directed to form a radiation pattern (Masood et al. 2017). Also, the spurious mode is suppressed in an Electronic-Textile antenna (Shah and Patel 2021) targeted for bandwidth of 2.30–2.49 GHz with a center frequency of 2.45 GHz that is designed for investigation on the body with an evaluation of SAR checked for a minimum distance of 1 mm corresponding to SAR = 0.208 watts/Kg. An improved WBAN MIMO antenna produces UWB bandwidth with a rejection of LTE-A 43 band (3.90–4.20 GHz) and WLAN band (5.10–5.85 GHz). The orthogonal polarization with defected ground structure achieves higher isolation between the inter-spaced radiating elements (Suriya and Anbazhagan 2019). A textile antenna with a printed circular patch on one plane and corrugated ground on the opposite plane ensures the guiding of waves along the surface of the ground (Tak et al. 2015). A MIMO-UWB antenna designed on a Liquid Crystal Polymer substrate offers bending and is used for WBAN applications (Du and Jin 2021). Endoscopy antenna designed at 2450 MHz with individual MIMO element size corresponding to 6×6 mm^2 is fabricated on LCP and is tested on homogenous phantom liquid resembling human characteristics (Biswas et al. 2021). A compact WBAN antenna with size 0.318 $\lambda_0 \times 0.318$ λ_0 produces gain of 2.06 dBi which is

tested on HUGO voxel model for bio-medical application (Arif et al. 2019). A linearly polarized antenna with center frequencies 2.45 and 5.80 GHz is useful for WBAN applications for which the wavelength corresponds to λ/4 and 3λ/4 (Bhattacharjee et al. 2019). A WBAN antenna at 2.45 GHz and a 5G antenna at 3.50 GHz occupies space of 47.2×31 mm^2 (Mashagba et al. 2021; Singh et al. 2016; Bhattacharjee et al. 2018). An EBG textile antenna at 2.45 GHz designed for center frequency occupies space of $46 \times 46 \times 2.4$ mm^3 and is useful for wearable device applications (Ashyap et al. 2017). An Electromagnetic Band Gap and Frequency Selective Surface (FSS) is utilized in wearable fabric antennae which is useful for medical-BAN. The size of the antenna corresponds to $60 \times 60 \times 2.4$ mm^3 (Ashyap et al. 2018), and an implantable antenna plays a vital role in monitoring several healthcare parameters in telemetry (Malik et al. 2021). An ISM band antenna designed at a 2.45 GHz band is capable of reconfiguration where two groups of PIN diodes are used in implantable applications. The two orthogonal polarizations are available in the x- and y-directions (Yang et al. 2019). An ultra-wideband 5G-New Radio (n257/n258 and n261) is designed for MIMO configuration providing an impedance bandwidth of 24.80–44.45 GHz. This configuration of a four-port MIMO antenna offers a gain of 8.60 dBi with an efficiency of more than 85% (Patel et al. 2022). A dual band antenna resonating at 0.91 and 2.45 GHz ISM band utilizes meandered line resonators for telemetry applications and is easily implantable as a biomedical device due to its compact size of $5.60 \times 5.80 \times 0.25$ mm^3 (Al-Hasan et al. 2021). An ISM band antenna comprising a slotted cross-elliptical patch (dragonfly shape) and the stepped ground is useful for the medical monitoring system of the vital parameters of the patient. The MIMO antenna elements are placed orthogonally for better isolation, and upgradation of the same is achieved by using fan-type parasitic element (Kaboutari and Hosseini 2021).

Role of Electromagnetics in Medical Applications (Choudhury and El-Nasr 2015)

The interaction of controlled electromagnetic energy with the human body has brought an evolution in the field of medical science. The radiations do interact with biological systems of the body and find applications in X-Rays, MRIs, Laser therapy involving the healing of cataract, identification of bone fractures and reading the inner-body structure by using endoscopy antenna capsule. The common components in the human body such as blood and urine constitute the vital component which is used to diagnose several chronicle diseases. The above said components offer the characteristics of dielectric material which may include disease components such as diabetes mellitus. The diabetic disease is experimentally verified by using the Debye model where different glycosuria groups can be harnessed and hence the chronic diabetic disease can be cured. The metallic-complex mediums used in monitoring the urine samples are treated for Turbadar-Kretschmann-Raether (TKR) configuration. This is done by using sculptured-thin-films (STFs) and columnar-thin-films

(CTFs). These two concepts are used for sensing purposes. The meta-material is used in sensing the temperature of marrow bone by application of microwave frequencies. They are also used in sensing hemoglobin in blood samples, problems in diabetics and infection in the urine. The biosensor is designed on Chiral-meta-material used to sense the temperature of the biological tissues of pigs. This is experimentally verified and compared with simulated results. The titrated high strength radiation by electromagnetic is commonly used to treat thyroids and cancer. The impulse-radiated antenna is used for this application as long duration signal can permanently damage the tissues. On the other hand, the biological tissues do interact with electromagnetic energy and can be considered as a dispersive electric medium irrespective of frequency. Also, the human body is also the source of propagation of electromagnetic waves in the frequency range of 5.0–50.0 MHz (Choudhury and El-Nasr 2015).

Wireless Body Area Network Antenna

It is well known that the ultra-wideband bandwidth 3.10–10.60 GHz has managed to attract researchers due to the features including broadband, lower cost with higher data transmission and provide an omni-directional radiation pattern for wide coverage. They have been handy in applications such as shorter wireless communication applications, mobile communication, imaging related to medical applications and radar systems (Du and Jin 2021). Figure 1.1 represents the development of a Wireless Body Area Network (WBAN) MIMO antenna with a 2 × 2 configuration and placed orthogonally providing the S-parameter corresponding to S_{11}, S_{12}, S_{21} and S_{22}. The S_{11}/S_{22} indicates the reflection coefficient, whereas S_{12}/S_{21} corresponds to the transmission coefficient. Figure 1.1a shows the two-port MIMO antenna fabricated on the substrate Rogers Ultralam 3850 with permittivity 2.90 and loss tangent 0.002. For flexible configuration of the antenna configuration, it is required to use a very thin substrate, and the MIMO configuration uses 0.10 mm thickness dielectric material. They generally fall under the category of Liquid Crystal Polymer. The compact size of 30 mm × 56.50 mm provides easy integration on the motherboard of different hand-held devices used in medical applications. As per the observation, Fig. 1.1a provides the ultra-wideband frequencies as mentioned by the above UWB bandwidth. However, there are a few wireless communication applications that are also working simultaneously in the UWB bandwidth such as WiMAX or WLAN. This causes interference and has to be mitigated by the introduction of the filter. Figure 1.1b shows the etching of a semi-circular slot on the surface of the radiating patch which stops the bandwidth 3.20–3.90 GHz from radiation. Figure 1.1c shows the introduction of a parasitic element placed between the two orthogonally placed radiating elements so that higher isolation can be achieved. The distribution of surface current over the surface of patch and ground concludes that there is a lot of interaction between the radiating element with the de-coupling structure which largely affects the diversity performance. However, in the presence of the de-coupling structure, the interfering signals from Antenna1 to Antenna2 are absorbed by the parasitic structure

for larger bandwidth of the radiating signals. In comparison to the far-field result, the omni-directional pattern is achieved. The diversity performance is also calculated due to the MIMO configuration concluding the difference of Mean Effective Gain <-3.0 dB, Envelope Correlation Coefficient <0.005 with approximately Diversity Gain at 10.0 dB and Total Active Reflection Coefficient at $\theta = 0°$, 60°, 120° and 180° less than 10.0 dB. The MIMO antenna also offers a maximum measured gain of 5.32 dBi at 5.53 GHz. Due to the application of the MIMO antenna for wearable applications, the bending of the antenna analysis is also studied to know the deviation of the S_{11} parameter. This is achieved by bending the antenna on the cylinder of radius say 30 and 45 mm. The change in S_{11} parameter in all three (non-bending, bending at cylinder radius of 30 and 45 mm) has not much change in the S_{11} result, and it can be concluded that the antenna is well suited for flexible applications. The direct effects of the antenna are evaluated in the form of Specific-Absorption-Rate (SAR) with different human parameters corresponding to skin, fat, muscle and bone. Table 1.1 shows the RF parameter of the human.

Figure 1.2 (Yang et al. 2019) shows the working model of polarization reconfigurable PIFA antenna in the real world of a wireless communication channel. This antenna is designed at a 2.45 GHz frequency of the ISM band. Interestingly, the antenna is reconfigured to achieve polarization in either x- or y-direction by means of switches to ensure connectivity all the time irrespective of any direction. Figure 1.2

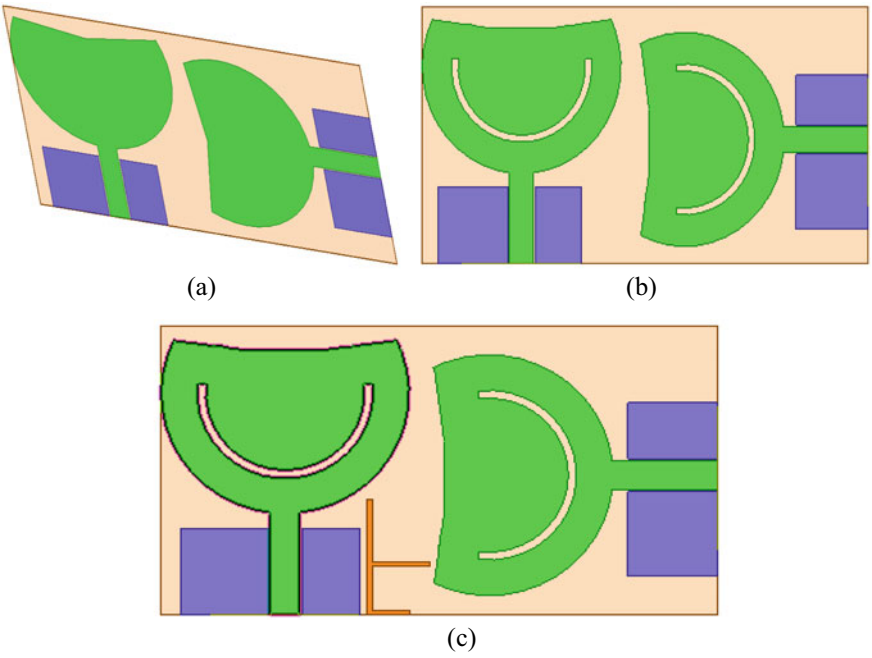

Fig. 1.1 WBAN antenna. **a** Perspective orientation, **b** MIMO configuration (without isolation element) and **c** MIMO configuration (with isolation element)

Table 1.1 The human body tissue model parameters

Tissue model	Size (mm^3)	Permittivity	Resistivity (S/m)
Skin	40 × 66.5 × 2.0	37.95	1.49
Fat	40 × 66.5 × 5.0	5.27	0.11
Muscle	40 × 66.5 × 20.0	52.67	1.77
Bone	40 × 66.5 × 13.0	18.49	0.82

shows a patient suffering from a chronic disease such as diabetes can be monitored continuously from a remote location wirelessly by a doctor who can monitor the patient's glucose level continuously. This application is known as medical telemetry. However, the wireless link may suffer the connectivity issue due to the fact that the multi-path indoor reflections can create a mismatch between the implantable antenna and the receiver.

The Specification Absorption Rate (SAR) can be defined as

$$SAR = \int \frac{\sigma(r)\left|\overrightarrow{E}(r)\right|^2}{\rho(r)} dr \tag{1.1}$$

where $\sigma(r)$ corresponds to conductivity (tissue), $\overrightarrow{E}(r)$ is electric field and $\rho(r)$ is tissue density (Yang et al. 2019). The IEEE standard (C95.1 (1999)) specifies that

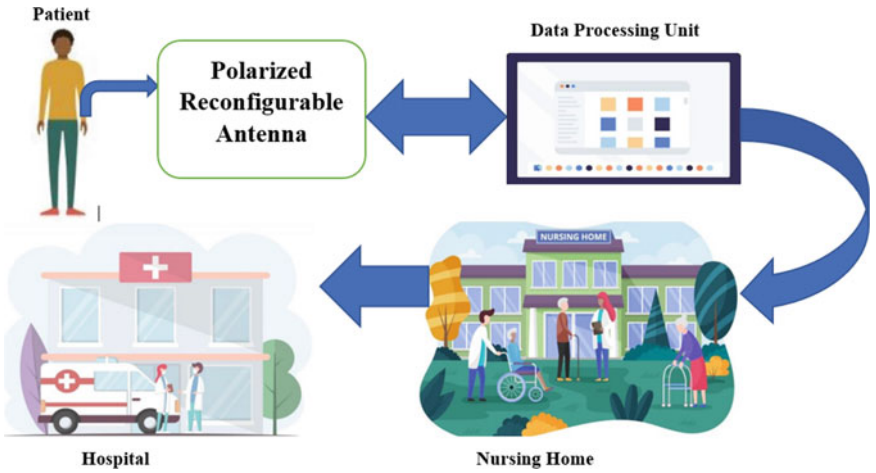

Fig. 1.2 Application of WBAN antenna (Yang et al. 2019)

the SAR values should be $\leq$1.6 watts/Kg for 1 g of the tissue with maximum input power not exceeding more than 22 mW.

Figure 1.3 shows the configuration of single-element and four-port version of the 5G-mmWave antenna. The antenna is fabricated on Rogers RT/Duroid 5880 microwave substrate of dimension 12 $\times$ 12 mm^2 and thickness of 0.80 mm. The combination of a circular patch of radius 3.75 mm and partial ground of dimension 9 $\times$ 9.6 mm^2 forms the antenna configuration providing the bandwidth for 5GmmWave New Radio application covering n257/n258/n261 bands. For better matching of the impedance, an elliptical slot is etched on the circular patch with an additional two circular parasitic patches placed on the plane containing the radiating patch. This transformation not only improves the operating bandwidth but also provides three resonating frequencies centered at 25.20, 28.0 and 36.10 GHz, respectively. Further in the WBAN application, it is expected to get connected seamlessly between the transmitter and the receiver and thus multiple path fading has to be reduced. This is achieved by transforming a single-element antenna to a four-port MIMO configuration as shown in Fig. 1.3b. The four-port MIMO configuration consists of four radiating patches and respective ground placed in an orthogonal fashion. This MIMO antenna configuration suffers large interaction of radiating elements with neighboring elements thereby increasing the interference and reducing the diversity performance. The diversity performance is improved by placing the slotted ring parasitic structure in the plane containing ground as shown in Fig. 1.3c. This improves the isolation between the inter-spaced elements while preserving the operating bandwidth. The designed MIMO antenna offers an efficiency of more than 85% with a gain ranging 6.0–9.0 dBi and is well suited for WBAN applications.

Present State-of-the-Art Medical Application Antenna

Table 1.2 shows the comparison of the medical application antenna. The size of the antenna is very compact when it comes to the application for endoscopy. However, wearable antennae do show variable sizes from 8 $\times$ 60 to 60 $\times$ 70 mm^2. The medical application antenna utilizes the substrate such as FR4, LCP, jeans, denim and Rogers RT/Duroid 5880 substrate.

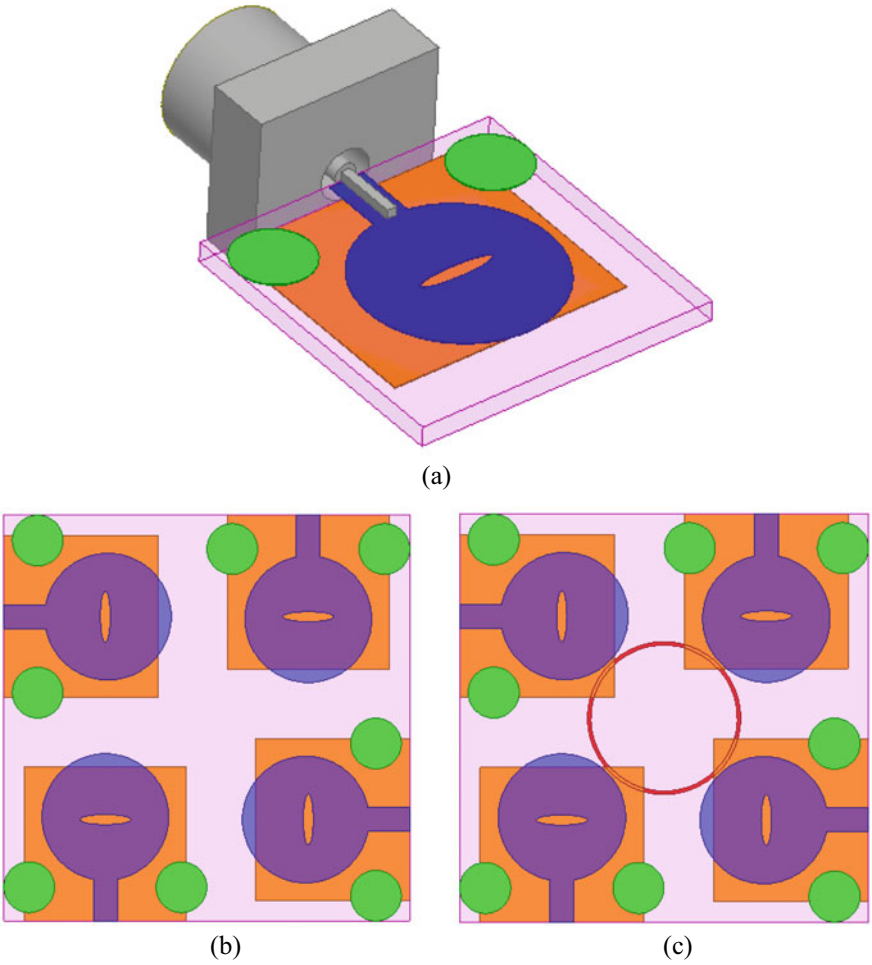

Fig. 1.3 **a** Single element antenna, **b** MIMO configuration without isolation and **c** addition of ring shape isolation element in ground plane of 4-port MIMO (Patel et al. 2022)

Table 1.2 Comparison of medical application antenna

Refs.	Size of the antenna (mm^2)	Operating bandwidth/center resonating frequency (GHz)	Substrate used	MIMO configuration	Potential applications
Koohestani et al. (2020)	24.9 × 8.60	2.45	FR4	No	WBAN
Karimyian-Mohammadabadi et al. (2015)	60 × 80	1.40–20.0	Polyester fabric	No	WBAN
Bait-Suwailam et al. (2020)	50 × 35	2.45	Textile cotton	No	Wearable
Afridi et al. (2013)	8 × 60	2.40, 5.80	Felt	No	Wearable
Shah and Patel (2021)	60 × 70	2.54, 3.72	Denim	No	Wearable
Du and Jin (2021)	30 × 56.50	2.40–11.30	Liquid crystal polymer	Yes	Flexible
Biswas et al. (2021)	6 × 6	2.45	Liquid crystal polymer	No	Endoscopy
Arif et al. (2019)	39 × 39	2.36–2.55	Rogers RT/Duroid 5880	No	Wearable-WBAN
Ashyap et al. (2017)	46 × 46	2.17–2.83	Denim	No	Wearable medical applications
Ashyap et al. (2018)	60 × 60	2.40	Jeans	No	Medical-BAN
Al-Hasan et al. (2021)	5.60 × 5.80	0.91, 2.45	RO3010	No	Implantable medical devices
Kaboutari and Hosseini (2021)	30 × 35	2.16–3.20	FR4	Yes	ISM

Conclusions

The role of electromagnetics in the field of medical science with recent technology breakthroughs in solving or monitoring chronic diseases such as diabetes was discussed. Also, a flexible 2 × 2 MIMO antenna for WBAN applications characterized for SAR calculation of human skin, fat, muscle and bone was studied. A 4 × 4 MIMO antenna provided the 5G-mmWave application designed for n257/n258/n261 bands. The present state-of-the-art antenna for medical applications was also discussed.

References

Afridi A, Ullah S, Khan S, Ahmed A, Khalil AH, Tarar MA (2013) Design of dual band wearable antenna using metamaterials. J Microw Power Electromagn Energy 47(2):126–137

Al-Hasan M, Sura PR, Iqbal A, Tiang JJ, Mabrouk IB (2021) Low-profile dual-band implantable antenna for compact implantable biomedical devices. Int J Electron Commun 138(153896):1–10

Arif A, Zubair M, Ali M, Khan MU, Mehmood MQ (2019) A compact, low-profile fractal antenna for wearable on-body WBAN applications. IEEE Antennas Wirel Propag Lett 18(5):981–985

Ashyap AYI et al (2017) Compact and low-profile textile EBG-based antenna for wearable medical applications. IEEE Antennas Wirel Propag Lett 16:2550–2553

Ashyap AYI et al (2018) Highly efficient wearable CPW antenna enabled by EBG-FSS structure for medical body area network applications. IEEE Access 6:77529–77541

Bait-Suwailam MM, Labiona II, Alomainy A (2020) Impedance enhancement of textile grounded loop antenna using high-impedance surface (HIS) for healthcare applications. Sensors (Basel) 20(14)

Bhattacharjee S, Maity S, Chaudhuri SRB, Mitra M (2019) A compact dual-band dual-polarized omnidirectional antenna for on-body applications. IEEE Trans Antennas Propag 67(8):5044–5053

Bhattacharjee S, Midya M, Bhadra Chaudhuri SR, Mitra M (2018) Design of a miniaturized dual-band textile antenna using characteristic modal analysis for on-body applications. J Electromagn Waves Appl 32(18):2415–2430

Biswas B, Karmakar A, Chandra V (2021) Hilbert curve inspired miniaturized MIMO antenna for wireless capsule endoscopy. AEU Int J Electron Commun 137

Choudhury PK, El-Nasr MA (2015) Electromagnetics for biomedical and medicinal applications. J Electromagn Waves Appl 29(17):2275–2277

Du C, Jin G (2021) A compact CPW-fed band-notched UWB-MIMO flexible antenna for WBAN application. J Electromagn Waves Appl 35(8):1046–1058

Kaboutari K, Hosseini V (2021) A compact 4-element printed planar MIMO antenna system with isolation enhancement for ISM band operation. Int J Electron Commun 134(153687):1–12

Karimyian-Mohammadabadi M, Dorostkar MA, Shokuohi F, Shanbeh M, Torkan A (2015) Super-wideband textile fractal antenna for wireless body area networks. J Electromagn Waves Appl 29(13):1728–1740

Koohestani M, Tissier J, Latrach M (2020) A miniaturized printed rectenna for wireless RF energy harvesting around 2.45 GHz. AEU Int J Electron Commun 127

Malik NA, Sant P, Ajmal T, Ur-Rehman M (2021) Implantable antennas for bio-medical applications. IEEE J Electromagn RF Microw Med Biol 5(1):84–96

Mashagba HA et al (2021) A hybrid mutual coupling reduction technique in a dual-band MIMO textile antenna for WBAN and 5G applications. IEEE Access 9:150768–150780

Masood R, Person C, Sauleau R (2017) A dual-mode, dual-port pattern diversity antenna for 2.45-GHz WBAN. IEEE Antennas Wirel Propag Lett 16:1064–1067

Patel A, Desai A, Elfergani I, Vala A, Mewada H, Mahant K, Patel S, Zebiri C, Rodriguez J, Ali E (2022) UWB CPW fed 4-port connected ground MIMO antenna for sub-millimeter-wave 5G applications. Alex Eng J 61:6645–6658

Shah A, Patel P (2021) E-textile slot antenna with spurious mode suppression and low SAR for medical wearable applications. J Electromagn Waves Appl 35(16):2224–2238

Singh VK, Dhupkariya S, Bangari N (2016) Wearable ultra wide dual band flexible textile antenna for WiMax/WLAN application. Wirel Pers Commun 95(2):1075–1086

Suriya I, Anbazhagan R (2019) Inverted-A based UWB MIMO antenna with triple-band notch and improved isolation for WBAN applications. AEU Int J Electron C 99:25–33

Tak J, Lee S, Choi J (2015) Design of an all-textile circular patch antenna with corrugated ground for guided wave along the body surface for WBAN applications. J Electromagn Waves Appl 29(7):905–924

Yang D, Hu J, Liu S (2018) A low profile UWB antenna for WBAN applications. IEEE Access 6:25214–25219

Yang X-T, Wong H, Xiang J (2019) Polarization reconfigurable planar inverted-F antenna for implantable telemetry applications. IEEE Access 7:141900–141909. https://doi.org/10.1109/ACCESS.2019.2941388

Chapter 2
Performance Improvement of an H-Shaped Antenna for Biomedical Devices

S. Kannadhasan, R. Nagarajan, and Basim Alhadidi

Abstract An antenna with a new structure of H-Shaped antenna for biomedical applications in the ISM band has been suggested (2.4–3.4 GHz). The suggested antenna design uses CPW as a feeding technique to achieve maximum frequency responsiveness. Today, biomedical applications play an important role in medical diagnosis and treatment, as well as a field of study. Remote monitoring enables illness diagnosis and may be used as a hospital application from home; the installation of equipment lowers the length of stay in the hospital. Key antenna properties such as VSWR, gain, return loss, and radiation pattern are investigated. The modest size and improved correctness of the recommended task are its key advantages. The proposed mirror H-shape patch may thus be used for a variety of medical implants. In recent years, the wireless communication system has advanced significantly with the aid of microstrip patch antennas. Microstrip patch antennas are better suited for wireless devices because of their tiny size, simplicity in manufacture, and installation. This article talks about wireless devices' ultra-wideband slotted modified H-shaped microstrip patch antenna. With a 50-Ω microstrip line feeding and a low-cost FR4 substrate with a dielectric constant of 4.2, the recommended antenna is constructed and computer-simulated using High-Frequency Structural Simulator (HFSS) v15 software. The words "slotted patch" and "partial ground" refer to the ground plane and patch, respectively, which are used to miniaturise the antenna. Overall, the antenna measures 35 * 35 * 11 mm. The results of the experiments and simulations are contrasted with those of the suggested antenna.

S. Kannadhasan (✉)
Department of Electronics and Communication Engineering, Study World College of Engineering, Coimbatore, India
e-mail: s.kannadasan@swehg.com

R. Nagarajan
Department of Electrical and Electronics Engineering, Gnanamani College of Technology, Namakkal, India

B. Alhadidi
Computer Information Systems, Prince Abullah Bin Ghazi Faculty of Information and Communication Technology, Al-Balqa Applied University, As-Salt, Jordan

P. K. Malik and P. N. Shastry (eds.), *Internet of Things Enabled Antennas for Biomedical Devices and Systems*, Springer Tracts in Electrical and Electronics Engineering,
https://doi.org/10.1007/978-981-99-0212-5_2

Keywords Biomedical · Gain · H-shaped · ISM · Radiation pattern and VSWR

Introduction

More than ever, flexible implanted antennas are needed for biological applications. These physical barriers between the human body and external monitoring equipment provided by these subcutaneous antennas are essential to communication systems. Due to biocompatibility, miniaturisation, and patient safety, the design of implanted antennas is highly challenging. A multipolarisation-reconfigurable circular antenna with a four-dipole radiator is used in body-centric wireless communication (BWCS) to enhance the wireless connection quality. The antenna resonates between 2.2 and 3.1 GHz and has an impedance bandwidth of 34%. The 5.2 dB stated peak gain is the greatest. A double-layered bow-tie antenna is presented as a way to increase the electrical length of the antenna utilising a coaxial feeding mechanism.

To minimise size and enhance impedance matching, a patch antenna with CP implants is inserted into the centre square slot. A conformal rectangular patch antenna with a rectangular slot and split ring resonators (SRR) has been created for use in ISM band biomedical applications. The antenna has a gain of 19.6 dB, a 400 MHz impedance bandwidth, and a 2.41–2.81 GHz frequency range. A compact folded meander line structure antenna is made in order to reduce the size of the antenna with a gain of 23.7 dB. An ultra-low profile dual band antenna and a square shape CSRR have been developed to operate the antenna for biomedical telemetry applications. These modifications are intended to improve antenna impedance matching and reduce detected body power (Srinivasan and Shanmuganantham 2015; Kim and Rahmat-Samii 2004; Sukhija and Sarin 2017; Lee et al. 2008; Fernandez et al. 2010).

The irregular shapes of the patches, in contrast to traditional rectangular patch antennas, cause irregularity in the current distribution throughout the radiating patch, which results in limited polarisation and asymmetry in radiation patterns. A ring patch antenna in a circle was made to obtain circular polarisation. To boost the antenna's bandwidth, a dual-element ring slot antenna has been created. This antenna's frequency coverage spans 4.25–12.5 GHz. Antenna testing has been done on or close to the human body to look at the characteristics of directional, omni-directional, and pattern radiation. For usage in ISM bands, a patch antenna with a hexagonal shape and a CPW feed has also been created. Wireless communication needs a small, lightweight antenna that is easy to connect in order to operate effectively. Consequently, an effective antenna design is required for integration into wireless equipment. Microstrip patch antennas are the only alternatives that meet all the criteria. However, the same patch antennas also have a small bandwidth and weak signal. A few techniques for increasing a patch antenna's bandwidth have been discussed in earlier research articles, including the use of thick substrates, low permittivity substrates, and etching resonant gaps inside the patch. Etching slots in the patch and ground plane boosts bandwidth by introducing multiband characteristics and condensing the antenna size. Numerous resonant slots are taken up in the

patch in this article in order to create resonance overlapping and, eventually, give ultra-wideband characteristics. The proposed antenna spans the frequency ranges from 2.68 to 3.14 GHz in the graph's early part and from 3.37 to 10 GHz in the graph's later half. The planned antenna is modelled using high-frequency structural simulator (HFSS) software, which also plots its return loss, gain, VSWR, radiation pattern, and bandwidth for measurement.

Studying the communication methods used to establish a wireless link between the implanted device and the external station becomes essential when considering biomedical applications. The implanted system has to be compact and radiation-resistant. An antenna may be built using either the atmosphere or the human body's dielectric. To function as well as be feasible when implanted inside the human body, the implanted antenna must be built with consideration for the impacts on the body and the environment in which it is meant to operate. The dielectric properties of biological tissues, such as skin, fat, and bone, must thus be taken into consideration for optimum performance. Animals, and tissue-equivalent liquids and mimicking gels, or both may be used to study them (Chow et al. 2013; Merli et al. 2011; Chen et al. 2009; Gosalia et al. 2005; Palanivel Rajan 2015).

An implantable, miniature E-shaped antenna for the 2.4 GHz ISM (Industrial Scientific Medical) band is described in this study. Between the patch and the ground plane, there is a shorting pin. We also demonstrate how the shorting pin method may be used to reduce the size of the E-shaped PIFA antenna. The recommended antenna is compact and has a measured return loss of −10 dB over the chosen ISM band. IMDs serve a crucial purpose and are widely used to safeguard patient security and safety in the quickly changing international environment. IMDs provide a number of benefits, including temperature monitoring, diagnostics, and more. It may be surgically implanted into the human body. Biomedical sensors are also very advantageous to the biotelemetry sector. When an interstitial is sufficiently present, these sensors may detect functional restrictions. They may thus make things successfully and efficiently as a result.

Numerous frequency bands are open to implantable medical devices. The vast majority of medical applications are found in the MICS (401–406 MHz) range. The Industrial Scientific and Medical (ISM) band makes use of planer Inverted-F antenna (PIFA), as well as circular, square, and many other types of antennas (2.4–2.4835 GHz). For wireless communication, a low-profile antenna that enables wideband and multiband operations is required. The planar inverted-F antenna satisfies these requirements. This antenna is compact, has a patch that spans a quarter wavelength, and produces little inverted radiation. Millions of people now rely on surgically implanted medical gadgets to live normal lives. Additionally, it is challenging to account for any experimental versus numerical inaccuracies while making tiny antenna prototypes. In this field, biomedical sensors are also crucial. Despite having certain limitations, the interstitial fluid that surrounds this sensor helps with functioning.

According to the most recent biomedical research studies, an implanted antenna considerably enhances a patient's quality of life and medical care. Theoretical studies and research towards implantable antennas are now highly intriguing and piquing

some scientific curiosity. The implanted antenna, which operates in the ISM band (2.4–2.48 GHz) and MICS band (401–406 MHz), is only one example of the electromagnetic field and radio frequency application range (Kim and Rahmat-Samii 2004). Patch antennas are often used in implanted medical devices because of their tiny size, particularly for telemetry purposes. It enhances the relationship between doctors and patients, resulting in better treatments, faster diagnosis, and better health care. By changing the operating frequency, the permittivity and conductivity of human body tissue may be changed. The three most important considerations for an implanted patch antenna are its size, operational frequency, and tissue permittivity. The patch structure is produced without wires and makes effective use of wireless networking (Tiwari and Malik 2021; Wadhwa et al. 2021; Kaur and Malik 2021). The antenna's feeding mechanism is a Coplanar Waveguide (CPW), which is designed for greater frequency responsiveness. This reduces back radiation while potentially considerably improving the correctness of the suggested structure. The antenna was used to investigate the relative dielectric constants, electrical conductivity, mass density, and permittivity of muscle, fat, and skin. The antenna's parameters, such as VSWR, return loss, gain, and radiation pattern, are also measured (Rajan et al. 2016; Ribana and Pradeep 2018; Paranthaman and Berlin 2017; Vijayprasath and Palanivel Rajan 2015; Palanivel Rajan et al. 2012; Kannadhasan et al. 2022).

Proposed Work

An innovative split ground plane ultra-wideband slotted modified H-shaped microstrip patch antenna is presented in this work. A bandwidth is seen in the ultra-wideband between 8.75 and 13.75 GHz. Both of these bands provide advantages for wireless devices including WLAN, Wi-Fi, WiMAX, IMT, LTE, and many more. Over the last 10 years, the utilisation of wireless communication systems in biomedical engineering has increased dramatically. The creation of implanted biomedical devices that might improve people's health, well-being, and quality of life has attracted a lot of attention. As a result, several antennas and techniques for implanting into the human body have been proposed. With the advent of central X-beam inquiry, electromagnetic application in the medical sector has risen. The standard for illness detection and treatment has been increased by the development of electromagnetic waves. Microwave and EM waves are widely used in the treatment of malignant development, imaging of damaged cells, and the identification of wound evidence. In relation to this, the development of remote communication contributes to improving the level of comfort offered to the sick, for example by lowering the intrusiveness of electromagnetic (EM) medical equipment. The field of medicine has broadened with the creation of pacemakers and drugs that patients may ingest and detect. Therefore, just as remote communication improved, so did the use of in-body implants for monitoring and diagnosing diseases. The implanted gadgets make use of remote technology to allow for remote patient monitoring. Heart rate and glucose content measurements are two examples. There are two distinct biological

goals for the use of implanted receiving devices in humans. They are biotelemetry and biomedical treatment. The human body and the environment may interact across long distances, thanks to biotelemetry. Biomedical therapy integrates the treatment of numerous illnesses and enables the physical health of the people being treated to be monitored. These programmes reduce the length of the patient's hospital stay.

The Remote Body Area Network (WBAN) technology for monitoring the human body controls implants that are placed within the body. This facility provides human-assisted in-home patient care. The design of implanted radio wires, which must be optimal for human body conditions and the closeness to certain tissues that sometimes may affect the operation of the transmitting component, is the key factor to be taken into account. Radio wires are required in the inserts since they must be able to communicate with the outside equipment. The design of a specialised radiator is the key element of an implanted device that operates in a WBAN that is two or three metres wide. Implanted receiving wires with lower zone occupancy and greater diagnostic capacity are ultimately required. This research includes in-depth details on the development and assessment of implanted receiving apparatus.

The radio wires that are implanted must be biocompatible in order to safeguard the patients who have been equipped with inserts. Implanted receiving wires may short-circuit if they come in touch with the material of the receiving apparatus since human tissues may conduct electricity. Biocompatibility and the capacity to reduce severe short circuits are key considerations in the design of implanted receiving wires for prolonging the life of inserts. The most thorough method for safeguarding the device's biocompatibility while acquiring equipment. The other method is to construct receiving wire utilising biocompatible materials. An antenna design is influenced by a number of variables, including the frequency, substrate material preference, and relative permittivity of the antenna material. It is designed for an 8.75 GHz resonance frequency. For the antenna, there are engravings on the 35 * 35 * 11 mm FR4 volume. Relative permittivity of 8.2 is what the antenna is designed to have. The mirror H-form patch is triggered by coplanar ground plane feeding and designed for biomedical applications in the ISM (8.75–13.75 GHz).

The recommended antenna's length, breadth, feed length, and feed width are initialised at random. The initial antenna structure is set up in a layered phantom to ensure that it is biocompatible. A −20 dB ideal value is used to compute and verify return loss S11. The design process is repeated using different initial values until the structure achieves a return loss of −20 dB or less. If the structure achieves a return loss of −20 dB or less, it is considered to be the final antenna design. This chapter presents the design and modelling of an H-shaped microstrip patch antenna. These antennas were created using the HFSS software. The three essential elements that must be comprehended in order to build a microstrip patch antenna have already been mentioned. Selecting settings for these basic parameters is the first step. After selecting these three key requirements, the patch's shape and size must be chosen. To radiate, an antenna must have a return loss of at least −10 dB. Even though the planned antenna was functioning effectively at the needed frequency, there was still potential for improvement. We thus cut the patch. Additional return loss reduction is provided by slitting. The antenna is modelled on a FR4 substrate and has a dielectric

constant of 4.2 and a loss tangent of 0.01. Its thickness is 1.6 mm. The antenna is 30.78 mm wide and 40.02 mm long. The literature review makes it clearly clear that adding slots to the patch would enhance an antenna's output characteristics. We cut two slots into our design.

For medical wireless applications like implanted devices and on-body sensors to transmit and receive electromagnetic signals from the human body, an antenna is required. As a result, developing a trustworthy implanted antenna is essential for communication. We chose to employ an H-shaped printed PIFA antenna in this case since it may provide much broader bandwidths than conventional patch antennas. The implementation of the design is split into two steps. First, the implanted E-shaped antenna with a shorting post was designed to operate in the 2.4 GHz ISM band in free space. In order for the antenna to resonate at 2.4 GHz, it is then given a single-layer superstrate and placed within several layers of human tissue made to resemble phantoms (Fig. 2.1).

The H-shaped antenna's feeding structure consists of coaxial feeding and a shorting pin with a 50 Ω impedance. The E-shaped antenna's impedance may be adjusted to a 50 Ω load by altering the distance between the post and the feed. To guarantee the performance of a wideband antenna, the feed and pin positions must be altered. The thickness and dielectric properties of the skin affect the antenna's characteristics since implanted antennas are often placed under the skin of the body. However, in other circumstances, such as in applications for inter-body communication, an antenna will be placed beneath body fat and/or muscle. As a result, both muscle and fat properties must be taken into account.

We use a length of 100 mm for the phantom in numerical calculations. Additionally, we assume that the antenna is buried at a depth of 2.0 mm under the phantoms' fat

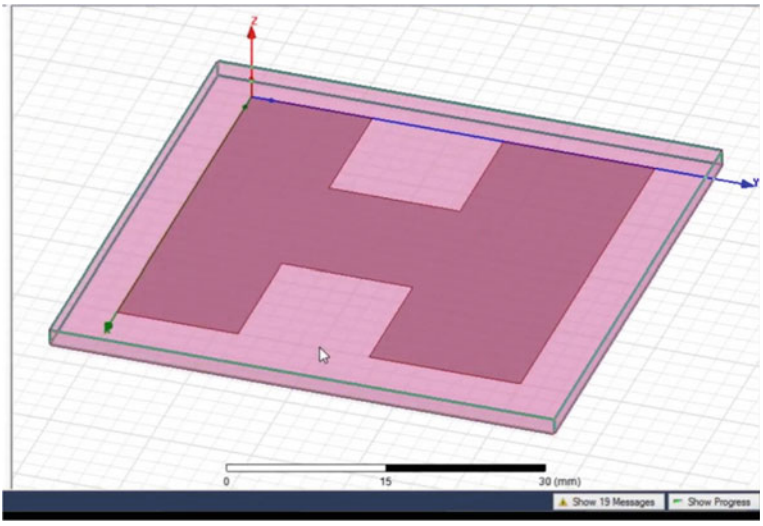

Fig. 2.1 H-shaped antenna

layer. In order to simulate implantation into a human arm, a multi-layered phantom with a cylindrical shape was used. In addition, we replicated the implantation of antennas under human chests using a stack of rectangular block phantoms. Simulations are used to determine the antenna's dimensions. There is growing interest in the development of implanted devices for a range of applications in both humans and animals. Locating dependent individuals or lost animals, keeping an eye on blood pressure and temperature, and wirelessly transmitting diagnostic information from a pacemaker or other implanted electronic device to an external RF receiver are a few examples of usage. Small, implanted biomedical devices may enhance the lives of many people. Patients who have had an antenna implanted in their body have regular checkups at the hospital to ensure the health of the patient and the integrity of the implant.

Data captured by the implanted antenna may be wirelessly sent to the receiving station using RF technology while the patient sits in the waiting area. Some patients could need daily examinations. The patient's home might be used as a home care facility in this case. The gadget may be able to communicate with the medical implant, exchange data on a regular basis with the hospital's responsible party, and be connected to the phone network or the Internet. In actuality, the antenna is still too big to be implanted despite a seven-fold decrease in size and consideration for the effects on the body during design. The reflection coefficient value reported in the research is only a simulation and not a measurement, even if the simulated MICS bandwidth is partially covered. There is growing interest in the development of implanted devices for a range of applications in both humans and animals. Locating dependent individuals or lost animals, keeping an eye on blood pressure and temperature, and wirelessly transmitting diagnostic information from a pacemaker or other implanted electronic device to an external RF receiver are a few examples of usage. Small, implanted biomedical devices may enhance the lives of many people. Patients who have had an antenna implanted in their body have regular checkups at the hospital to ensure the health of the patient and the integrity of the implant. Data captured by the implanted antenna may be wirelessly sent to the receiving station using RF technology while the patient sits in the waiting area. Some patients could need daily examinations. The patient's home might be used as a home care facility in this case.

The gadget may be able to communicate with the medical implant, exchange data on a regular basis with the hospital's responsible party, and be connected to the phone network or the Internet. In actuality, the antenna is still too big to be implanted despite a seven-fold decrease in size and consideration for the effects on the body during design. The reflection coefficient value reported in the research is only a simulation and not a measurement, even if the simulated MICS bandwidth is partially covered. The radiation patterns, gain pattern, and radiation efficiency value are coupled to the rescaled antenna and a rescaled resonance frequency of 980 MHz. Additionally, neither the wire nor the antenna was ever covered in a biocompatible material throughout the experimentation. There are two dual-band implantable antennas on display that perform well in both the MICS band and the ISM band. The dielectric nominal values have since been modified by a factor of 50%. To ensure that the antenna functions well in all potential body settings, several

simulations were run. The radiation characteristics of the antenna were modelled in terms of E-field and gain using FDTD computations.

Given the rapid expansion of wireless communication applications in contemporary biomedical industries, implantable devices are crucial for maintaining a strong connection with external equipment. Due to the unique way they collect and store real-time data, implantable antennas are growing in popularity. However, because of its particular implanted circumstance, the fundamental requirement of compact size must be completely met. It is also conceivable to implement this feature since circular polarisation provides the advantages of reducing multipath loss and eliminating polarisation mismatching problems. In this case, receiving antennas could react differently to sender antennas with various orientations. Numerous organisations have concentrated their efforts on studying implantable antennas. To accomplish the core goals of miniaturisation, a range of methods may be used to successfully shrink an item. By creating openings in the radiator patch or ground plane, it may be possible to extend the current path and achieve a considerable reduction in size. An implantable hollow slot antenna was developed in the form of an H. By loading shorting strips or pins, which may decrease the size by 50%, a standing wave structure from open to short circuit may be achieved. To forecast the radiation field of the microstrip antenna, one may use either a magnetic current model or an electric current model. The electric current model employing the current directly determines the far-field radiation pattern. The electrical flow is included in patch mode (1, 0). If the substrate is ignored, the radiation pattern may be derived directly from image theory (and in its substitute, air is used). When the substrate has been studied and is assumed to be infinite, the far-field pattern may be discovered using the reciprocity technique. According to the equivalence principle, the patch in the magnetic current model is replaced by the magnetic surface current that circulates around the patch's edge. Figure 2.2 displays the antenna's return loss. Figure 2.3 displays the antenna's VSWR.

In the electric current concept, the current directly controls the pattern of far-field radiation. Current is in the (1, 0) patch mode. Without considering the substrate (instead of using air), the radiation pattern may be estimated, and the pattern can then be produced directly from image theory. If the substrate is taken into account and treated as infinite, the far-field pattern may be calculated using the reciprocity technique. The magnetic current model uses the equivalence principle to replace the patch with a magnetic surface current that circulates around the patch's edge.

Figure 2.4 depicts the gain, yet another useful parameter for evaluating an antenna's effectiveness. This evaluation takes into account the antenna's efficiency and directional capabilities even if the gain of the antenna and its directivity are closely related. Remember that the pattern is the only thing that may have an impact on directivity as it is just a measurement of the antenna's directional qualities. Gain is described as "the ratio of the intensity in a given direction to the radiation intensity that would be reached if the antenna's power were radiated isotropically" (in a given direction). Figure 2.5 illustrates the radiation intensity that corresponds to the isotropically radiated power by dividing the power that the antenna absorbs (inputs) by four.

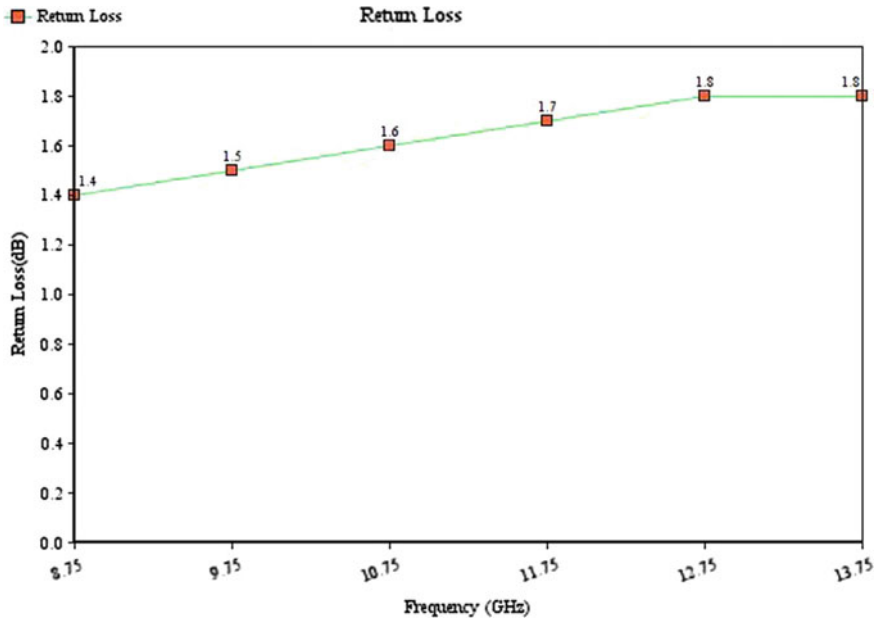

Fig. 2.2 Return loss of the proposed antenna

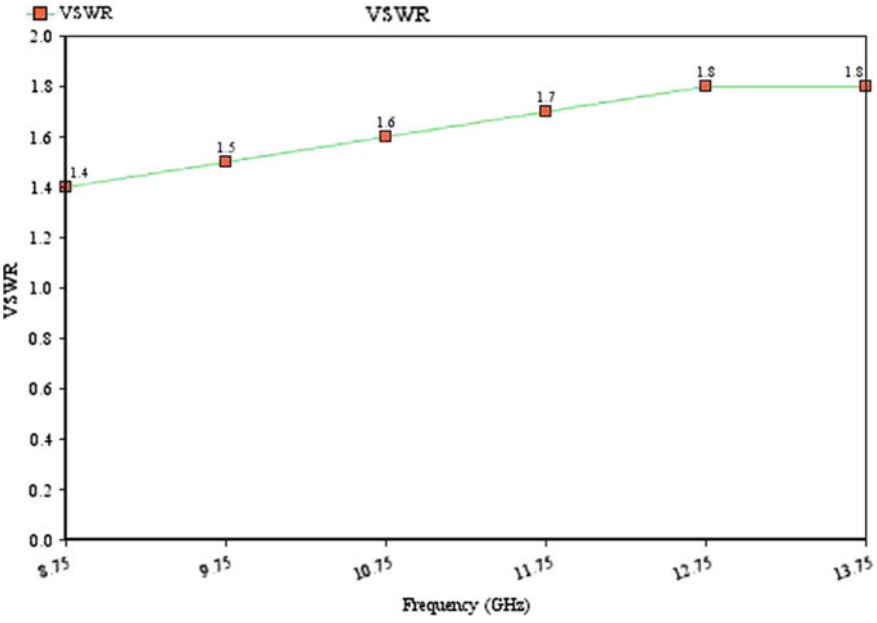

Fig. 2.3 VSWR of the proposed antenna

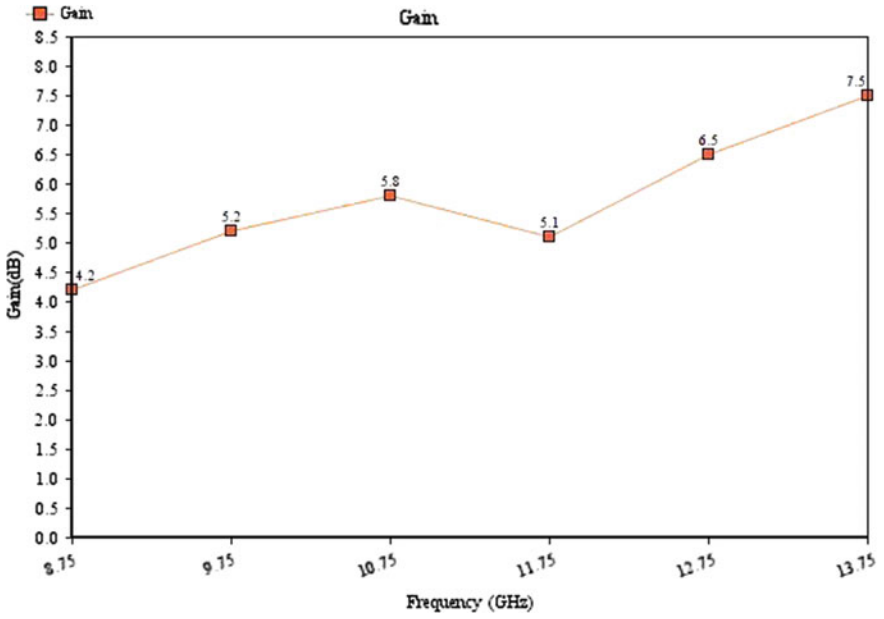

Fig. 2.4 Gain of the proposed antenna

Conclusion

This work develops an H-shaped patch antenna for biomedical applications. This antenna design may be inserted into a powerful Phantom human model in order to assess its performance in a biological setting. Human tissue has a return loss of -30.06 dB at the resonance frequency of 404 MHz. The in-body biocompatible antenna requirement was validated by the voltage standing wave ratio (VSWR), which was found to be 1.646 and was also very good. The far-field radiation pattern and Specific Absorption Rate (SAR) of 0.0124 W/kg, which is more than sufficient for biomedical applications, demonstrated the antenna's directivity and safety. The H-shaped wideband microstrip patch antenna used in this study is constructed, simulated, optimised, and tested using High-Frequency Structure Simulator (HFSS) software version 13.0. The intended antenna's bandwidth, gain, return loss, VSWR, and radiation pattern were all analysed. The design was optimised to get the best result. The substrate used has a dielectric constant of 1.06 and is air. The wideband antenna can operate in the frequency range of 8.75–13.75 GHz, with 8.73 GHz acting as its ideal frequency, according to the results. The potential to include the proposed antenna in the many portable devices using GPS applications is apparent.

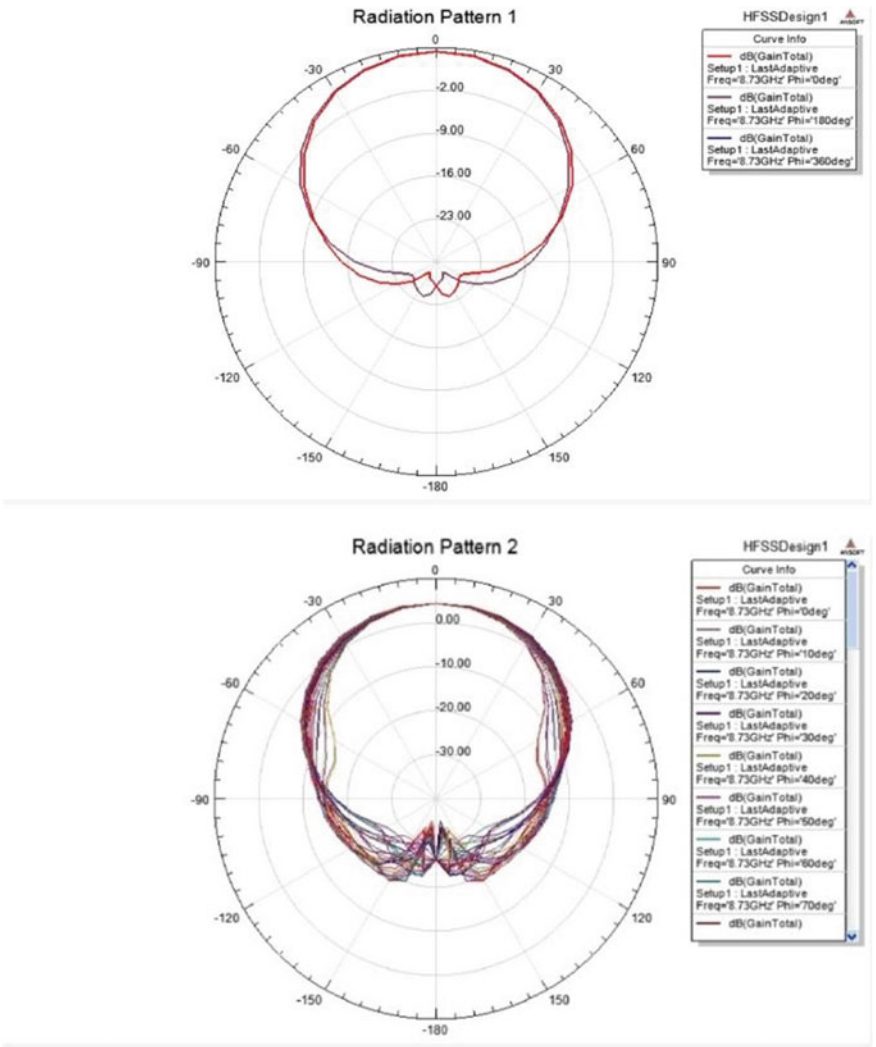

Fig. 2.5 Radiation pattern

References

Chen ZN, Liu GC, See TSP (2009) Transmission of RF signals between MICS loop antennas in free space and implanted in the human head. IEEE Trans Antennas Propag 57(6):1850–1854

Chow EY, Morris MM, Irazoqui PP (2013) Implantable RF medical devices: the benefits of high-speed communication and much greater communication distances in biomedical applications. IEEE Microw Mag 14(4):64–73

Fernandez CJS, Teruel OQ, Carrion JR, Sanchez LI, Iglesias ER (2010) Dual-band microstrip patch antenna based on short-circuited ring and spiral resonators for implantable medical devices. IET Microw Antennas Propag 4(8):1048–1055

Gosalia K, Humayun MS, Lazzi G (2005) Impedance matching and implementation of planar space-filling dipoles as intraocular implanted antennas in a retinal prosthesis. IEEE Trans Antennas Propag 53(8):2365–2373

Kannadhasan S, Nagarajan R, Banupriya R (2022) Performance improvement of an ultra wide band antenna using textile material with a PIN diode. Textile Res J.https://doi.org/10.1177/00405175221089690journals.sagepub.com/home/trj

Kaur A, Malik PK (2021) Multiband elliptical patch fractal and defected ground structures microstrip patch antenna for wireless applications. Prog Electromagn Res B 91:157–173. https://doi.org/10.2528/PIERB20102704. ISSN 1937-6472

Kim J, Rahmat-Samii Y (2004) Implantable antennas inside a human body: simulations, designs and characterizations. IEEE Trans Microw Theory Tech 52(8):1934–1943

Lee CM, Yo TC, Huang FJ, Luo CH (2008) Dual-resonant π-shape with double L-strips PIFA for implantable biotelemetry. Electron Lett 44(14):837–839

Merli F, Fuchs B, Mosig JR, Skrivervik AK (2011) The effect of insulating layers on the performance of implanted antennas. IEEE Trans Antennas Propagat 59(1):21–31

Palanivel Rajan S (2015) Review and investigations on future research directions of mobile based tele care system for cardiac surveillance. J Appl Res Technol 13(4):454–460

Palanivel Rajan S, Sukanesh R, Vijayprasath S (2012) Analysis and effective implementation of mobile based tele-alert system for enhancing remote health-care scenario. HealthMED J 6(7):2370–2377. ISSN No. 1840–2291

Paranthaman M, Berlin A (2017) Design of adaptive changing structures with bandwidth control for wideband applications. Int J Innov Res Electr Electron Instrum Control Eng 5(2):26–28

Rajan S P, Vivek C, Paranthaman M (2016) Feasibility analysis of portable electroencephalography based abnormal fatigue detection and tele-surveillance system. Int J Comput Sci Inf Secur 14(8):711–722

Ribana K, Pradeep S (2018) Contrast enhancement techniques for medical images. Int J Pure Appl Math 118:695–700

Srinivasan AK, Shanmuganantham T (2015) Analysis and design of implantable Z-monopole antennas at 2.45 GHz ISM band for biomedical applications. Microw Opt Technol Lett 57(2):468–473

Sukhija S, Sarin RK (2017) A U-shaped meandered slot antenna for biomedical applications. Prog Electromagn Res 62:65–77

Tiwari P, Malik PK (2021) Wide band micro-strip antenna design for higher "X" band. Int J e-Collab (IJeC) 17(4):60–74. https://doi.org/10.4018/IJeC.2021100105. ISSN 1548-3673. Oct 2021

Vijayprasath S, Palanivel Rajan S (2015) Performance investigation of an implicit instrumentation tool for deadened patients using common eye developments as a paradigm. Int J Appl Eng Res 10(1):925–929. ISSN No. 0973-4562

Wadhwa DS, Malik PK, Khinda JS (2021) High gain antenna for n260- & n261-bands and augmentation in bandwidth for mm-wave range by patch current diversions. World J Eng. https://doi.org/10.1108/WJE-03-2021-0133. ISSN 1708-5284

Chapter 3
Advanced Tapered-Fed Compact Two-Port Circularly Polarized MIMO Antenna for IoT Wireless Communication Applications

S. Salma, Habibullah Khan, B. T. P. Madhav, D. Ram Sandeep, and Ramani kannan

Abstract This article details the development of a compact circularly polarized MIMO antenna on an FR-4 substrate. The antenna is methodically designed from a single element to a dual input MIMO antenna. The designed antennas have fed with the tapered model feed lines, and this mechanism will aid the surface currents in passing through its narrow structural design. The aerodrome control tower shape inspires the antenna design. The core structure has been the same in every step, from the single element to the dual radiating element antenna. However, a few modifications like opening the slots and varying the defective ground structure has been made to operate the developed antenna in the circular polarization. The defective ground structures play a crucial role in this examination. They are carefully modified in all the iterations to achieve the circular polarization characteristic and IoT operating ranges under the 6 GHz frequency. The designed antenna is developed on an FR-4 substrate, and this prototype is authenticated in an anechoic chamber. The measured reflection coefficient, coupling isolation, radiation patterns, and axial ratios of the antenna are

S. Salma (✉)
Department of ECE, Sri Venkateshwara College of Engineering, Karakambadi Road, Tirupati, India
e-mail: salmaa.syed24@gmail.com; salma.sy@svce.edu.in

H. Khan · B. T. P. Madhav
ALRC R&D, ECE Department, Koneru Lakshmaiah Education Foundation, Guntur, Andhra Pradesh, India
e-mail: habibulla@kluniversity.in

B. T. P. Madhav
e-mail: btpmadhav@kluniversity.in

D. R. Sandeep
Department of ECE, Raghu Engineering College, Dakamarri, Bheemunipatnam, Visakhapatnam, India

R. kannan
Department of Electrical and Electronic Engineering, University of Teknologi Petronas, Bandar Seri Iskandar, Tronoh Perak, Malaysia
e-mail: ramani.kannan@petronas.com.my

P. K. Malik and P. N. Shastry (eds.), *Internet of Things Enabled Antennas for Biomedical Devices and Systems*, Springer Tracts in Electrical and Electronics Engineering,
https://doi.org/10.1007/978-981-99-0212-5_3

in good match with the simulation values. These parameters legitimize the compact MIMO antenna applicability in IoT wireless communication applications.

Keywords Circular polarization · MIMO antenna · Sub-6 GHz frequencies · IoT wireless communication applications

Introduction

For the last few decades, researchers have been trying to develop compact and efficient gadgets in mobile communications which can simultaneously incorporate multiple communication functionalities. In such devices, antennas play an essential role by enabling two-way communication. Among such antennas, MIMO antennas (Multiple Input and Multiple Output) have far advantages of having high channel capacity, efficient power handling features, and multiple transmission and reception capabilities through their various channels. MIMO antennas were vastly used to enhance spectrum efficiency and channel capacity with high data rates (Zhu et al. 2020; Hasan et al. 2019). In the MIMO antenna system, the antennas are tightly packed, making an unwanted coupling. Therefore, to reduce these coupling effects, many decoupling techniques are proposed. Some utilize the metamaterial structures in the radiating elements, opening slits/slots in the patch and the ground elements, and finally making the ground as defected ground structures (DGS (Thomas and Sreenivasan 2010; Salma et al. 1982)). Apart from these methods, some other decoupling techniques are widely used, mainly in altering surface currents. They are inserting decoupling networks, parasitic elements, and establishing a neutralization line (Salma et al. 1995; Syed et al. 2021; Iqbal et al. 2017).

Signals are received and transmitted by multiple antenna elements in the MIMO Technique, which increases the efficiency, data rate, and reliability of wireless systems. MIMO channel capacity can be improved by reducing coupling between antenna components. Gain enhancement can also be accomplished by increasing the number of antenna components. However, these antennas suffer due to their size and mutual coupling, but they are highly capable of handling multiple streams of data (Iqbal et al. 2017). Compact dimensions are difficult to obtain, but they provide a low correlation and high data transmission benefit over single-element antennas. The antenna characteristics were influenced by changing the ground plane. So, at low frequencies, the ground plane provides a path for the return current and sometimes forms part of the radiating structure, and changes in the ground structure can cause a difference in the surface currents (Zhang and Pedersen 2016; Qu et al. 2018; Deng et al. 2016). Considering all these aspects in this work, we have developed a multi-band resonating circularly polarized MIMO antenna for sub-6 GHz IoT applications. A detailed stepwise analysis and design methodologies are explained from the single-element model to the dual-element model. The unique feature of this work is the circular polarization feature attained by the tapered feed method; also,

the antenna size was made as compact as possible (Tiwari and Malik 2021; Wadhwa et al. 2021; Kaur and Malik 2021).

Antenna Design

Single-Element Antennas Evolution

The proposed single-element antenna was devised on a 1.6 mm thick FR-4 substrate with a 0.02 loss tangent, 1.4 relative permittivity, and a compact size of 20 × 20 mm. Figure 3.1 shows the proposed antenna's iteration-wise evolution. An air traffic tower structure inspires the patch element, and later L-shaped slots are open for operating it in the lower frequencies. The ground plane evolved from full ground to a staircase-like design with stub on it.

As illustrated in Fig. 3.1a, the patch in iteration 1 considers a polygon-like element and takes over a full ground structure. Iteration 1 resonates at 9 GHz with −10 dB of return loss, as shown in Fig. 3.2. Figure 3.1b illustrates the antenna with a half-ground structure, and triangular-like L-shaped steps were added to the patch to alter the surface currents. This iteration operates at 6.5 GHz with a −15 dB return loss. The next iteration, illustrated in Fig. 3.1c, consists of opened L-shaped inverted slots on the radiator. It also has a pillar stub on the antenna's ground plane for operating it in lower frequencies. This iteration resonates with a −13 and −25 dB return loss at 4.5 and 7 GHz.

In Fig. 3.1d, staircase-like Defected Ground Structure has been developed, and more L-shaped slots are placed in the patch to observe the changes in the frequencies. The final iteration has the operating ranges in the sub-6 GHz frequency with a −25.7 dB return loss value. The single-element antenna's overall dimensions are given as: $L_{\_Sub1} = 20$, $W_{\_Sub1} = 20$, $h = 1.6$, $L_{\_f} = 10$, $W_{\_f} = 4$, $L_{\_p} = 9$, $W_{\_P} = 18$, $L_{\_p} = 9$, $W_{\_g} = 20$, $L_{\_g} = 10$, $W_{\_sg1} = 5$, $L_{\_sg1} = 19$, $W_{\_S1} = 4$, $L_{\_S1} = 3$, $W_{\_sg2} = 2$, $L_{\_sg2} = 11$, $W_{\_sg3} = 6$, $L_{\_sg3} = 3$, $W_{\_S2} = 5$, $L_{\_S2} = 4$, $W_{\_S3} = 7$, $L_{\_S3} = 6$, $G_{\_1} = 0.5$, $G_{\_2} = 0.3$, $G_{\_3} = 0.3$.

Conversion of Single Element into MIMO Antenna

The developed single-element antenna successfully achieved a sub-6 GHz operating frequency. The dimensions of the dual-element MIMO antenna radiator structures were the same as in the single-element model. The final dual-element model is created by adding another similar radiation element to the existing one against the complete ground structure. The dimensions of the MIMO antenna are 20 × 40 mm in length and width with a thickness of 1.6 mm, fabricated on an FR-4 substrate. The maximum and minimum distance between the two radiators in the dual-element model are 1.8

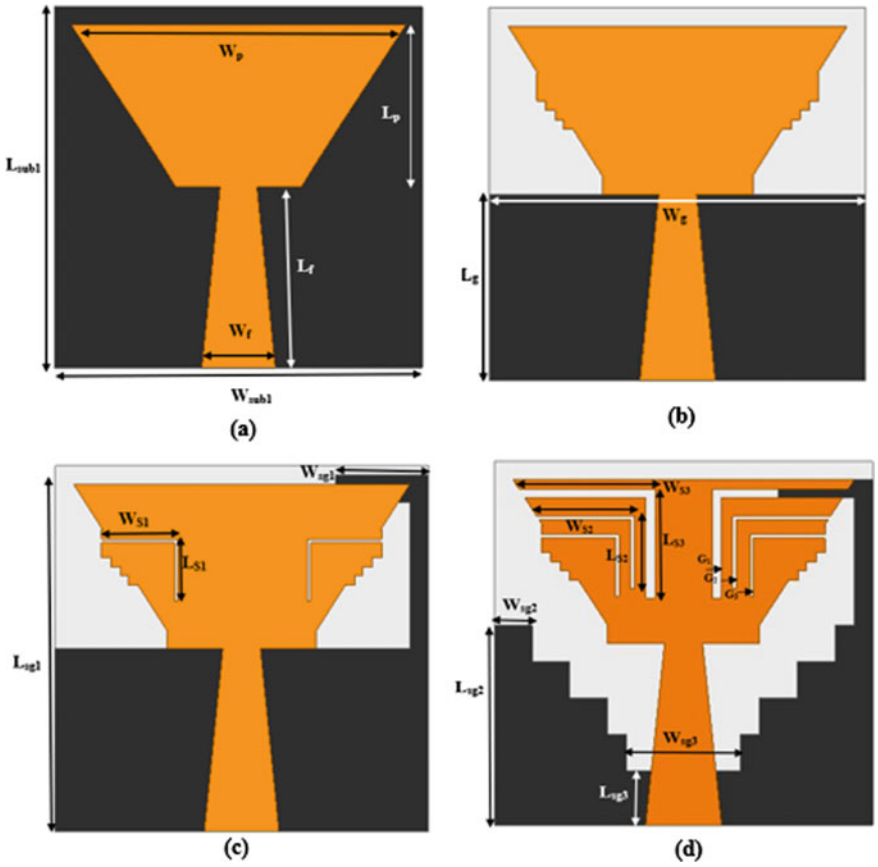

Fig. 3.1 Evolution of single element antenna

and 0.8 mm, respectively. Table 3.1, provides the overall dimension of the MIMO antenna. Figure 3.3 depicts the dual-element MIMO antenna iterations.

The defective ground structure evolves in four iterations, creating a staircase-like ground. Multiple iterations were performed on the ground structure to reduce mutual coupling and to resonate at the desired frequencies. The proposed antenna's output is highly dependent on its ground element, critical for improved impedance matching and the antenna's components isolation. Figure 3.4 depicts the entire design of the proposed MIMO antenna.

In each iteration step, the effects on the antenna's resonating frequencies concerning the changes in the ground structure are presented in Fig. 3.5. From iteration 1, it's observed that with a complete ground plane, the antenna resonates at four bands of 3.5, 3.8, 4.6, and 5.6 GHz with a −26 dB return loss at 4.6 GHz frequency.

From iteration 2, it's noted that the half-ground plane resonates at five frequencies of 3.3, 3.6, 4.5G, 4.7, and 5.4 GHz, with a maximum return loss of −42 dB at 5.4 GHz

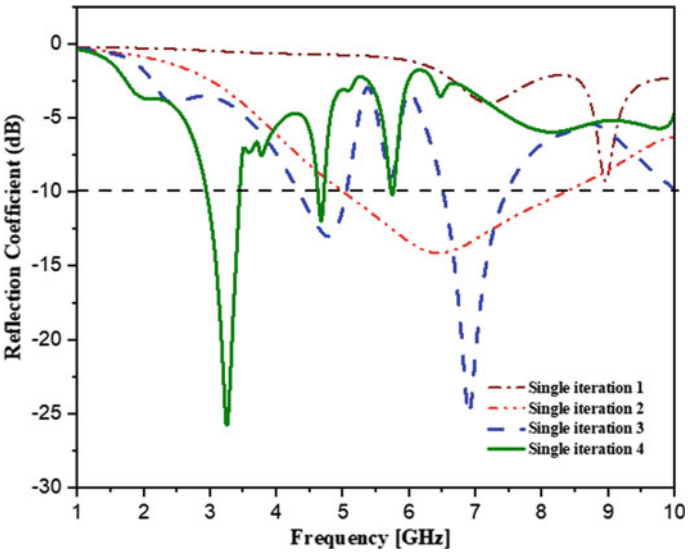

Fig. 3.2 Single element antennas reflection coefficients-iteration wise

Table 3.1 Proposed MIMO antenna design parameters

Antenna parameters	Dimensions in mm	Antenna parameters	Dimensions in mm
L_s	20	L_s2	4
W_s	40	W_s2	4.8
L_p	9	L_s3	3.4
W_p	18	W_s3	4
L_f	10	G_sl	2
W_f	4	G_s1w	16
L_s1	6	G_s2w	12
W_s1	7.1	G_s3w	8
G_s4w	4	W_g	40

frequency. In iteration 3, the two rectangular slots with different widths and the same lengths are removed from the half-ground plane resulting in bands' shifting. In this iteration, the bands are obtained at 4.1, 4.5, 5.2, and 5.6. The IoT applications are usually used in 5.2 and 5.8 GHz bands of ISM; However, in the third iteration, only 5.2 GHz bands were attained, and further modifications are attended to make use of the other 5.8 GHz ISM band. In the final iteration, another two rectangular slots are etched to get a 5.8 GHz band with maximum return loss. This iteration makes the antenna operate at frequencies of 3.9, 4.4, 5.1, 5.5, and 5.9 GHz with −12, −18, −27, and −24 dB return losses. Also, functions with a wide band from 5.99 to 9 GHz with −22 dB return loss, which has potential applications for 5G communications.

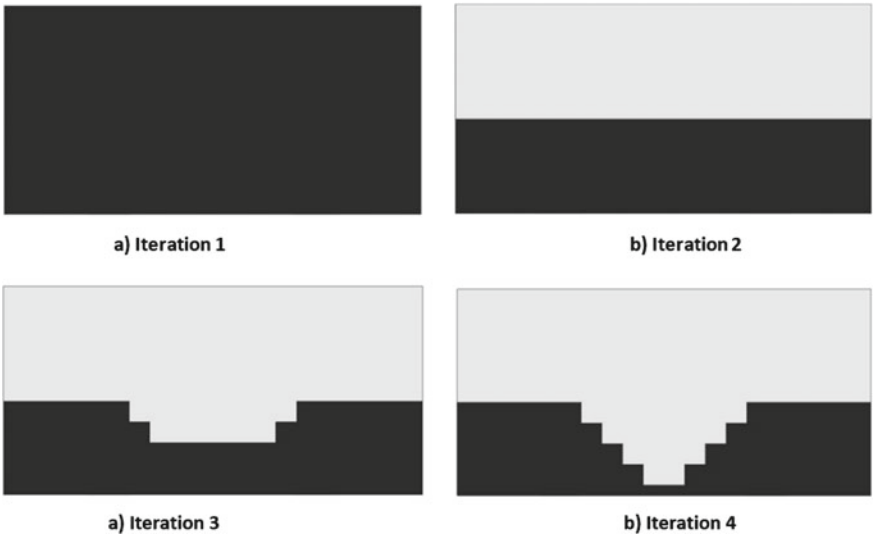

Fig. 3.3 The final MIMO antenna's ground plane iterations

The final model also attained a circular polarization function in the ISM band's 5–5.35 GHz frequency. Thus, the proposed antenna works at frequencies of 4 GHz (satellite communication), 4.5 GHz (Fixed mobile), 5.2 and 5.8 GHz (ISM), and 5.6 GHz (Radio navigation). Figure 3.6. shows the proposed MIMO antenna simulated and measurement |S11| results. The fabricated prototype is authenticated inside an anechoic chamber using a combinational network analyzer. The 2D radiation patterns of the operating bands at 4.0, 4.5, 5.2, and 5.6 GHz is shown in Fig. 3.7, where the blue line indicates the measurement, and the red line indicates the simulation results at operating frequencies.

The proposed antenna achieves circular polarization at 5.2 GHz (ISM band) frequency. Figure 3.8 shows the current movements for a varying phase shift from 0 to 360 degrees. The currents are moving circularly, which is the required movement in the circular polarization effect. Figure 3.9 shows the axial ratio of the band of 5.2 GHz, which has a good match between measured and simulated results, and both values are under the value 3. Hence, its circular polarized antenna is used for IoT applications.

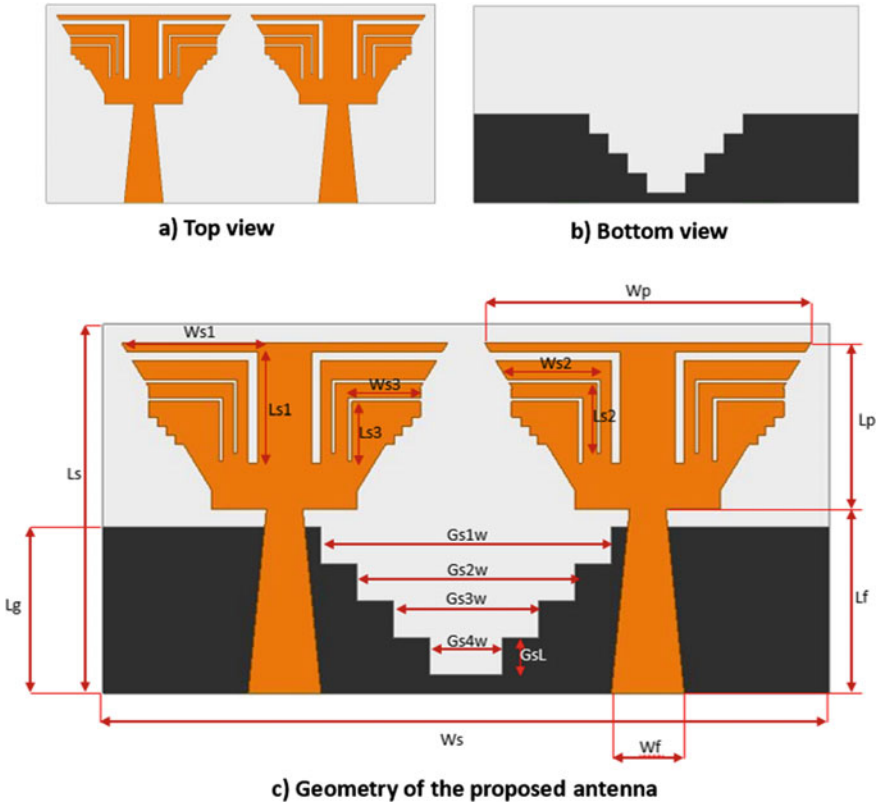

Fig. 3.4 Proposed MIMO antenna topology

Conclusion

A 40 × 20 mm^2 dual-element MIMO antenna is designed on a 1.6 mm thick FR-4 substrate. The designed antenna operates at multiple sub-6 GHz frequencies targeting the IoT applications of the ISM band. The antenna is progressed from the single-element antenna to the dual element. In all the design iterations, the tapered fed line is used to feed the radiating parts. The L-shaped slots are crucial in resonating the antenna in lower frequencies. Initially, the first model with an L-shaped slot operated in the single sun-6 GHz frequency. This antenna was turned into a MIMO antenna with identical patch elements and a stub-like ground element. This model works in 3, 3.5, and 6.2 GHz frequencies. Finally, an analytical study has been made by altering the ground plane of the developed antenna. The patch has been constant as in the previous design, and the ground plane is tuned as a staircase structure. This model works in the frequencies of ISM and fixed-mobile application bands. The circular polarization feature also holds good in the 5.2 GHz ISM band. Prototypes are built and validated experimentally in the anechoic chamber in all the iterations. The radiations

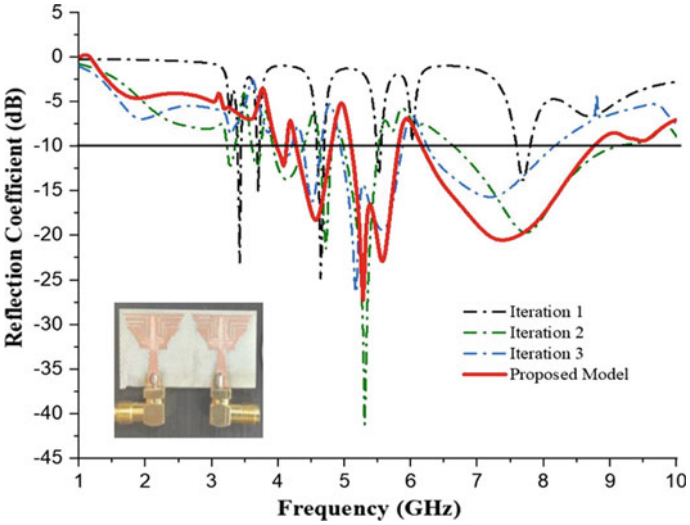

Fig. 3.5 Reflection coefficient of the proposed antenna iteration wise

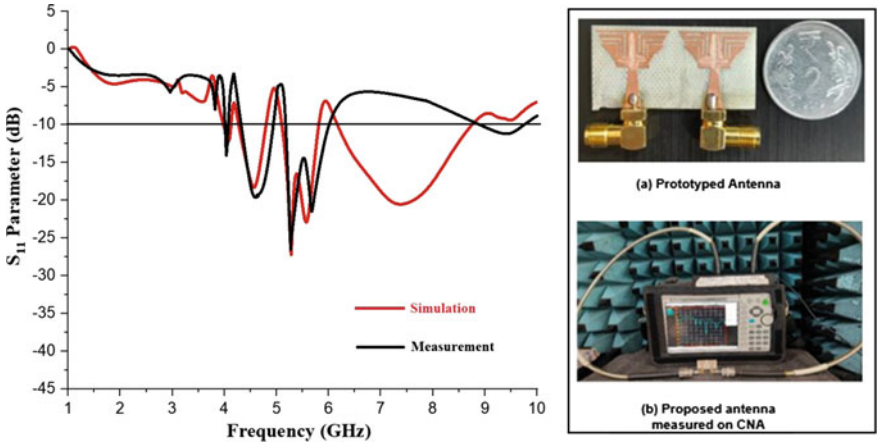

Fig. 3.6 Proposed antenna S-parameter simulated and measured curves

characteristics of the antenna obtained from the simulations are practically measured, and a decent match has been marked between them. These practical, measured values show the robust functional behaviour of the developed MIMO antenna for portable IOT wireless communication applications.

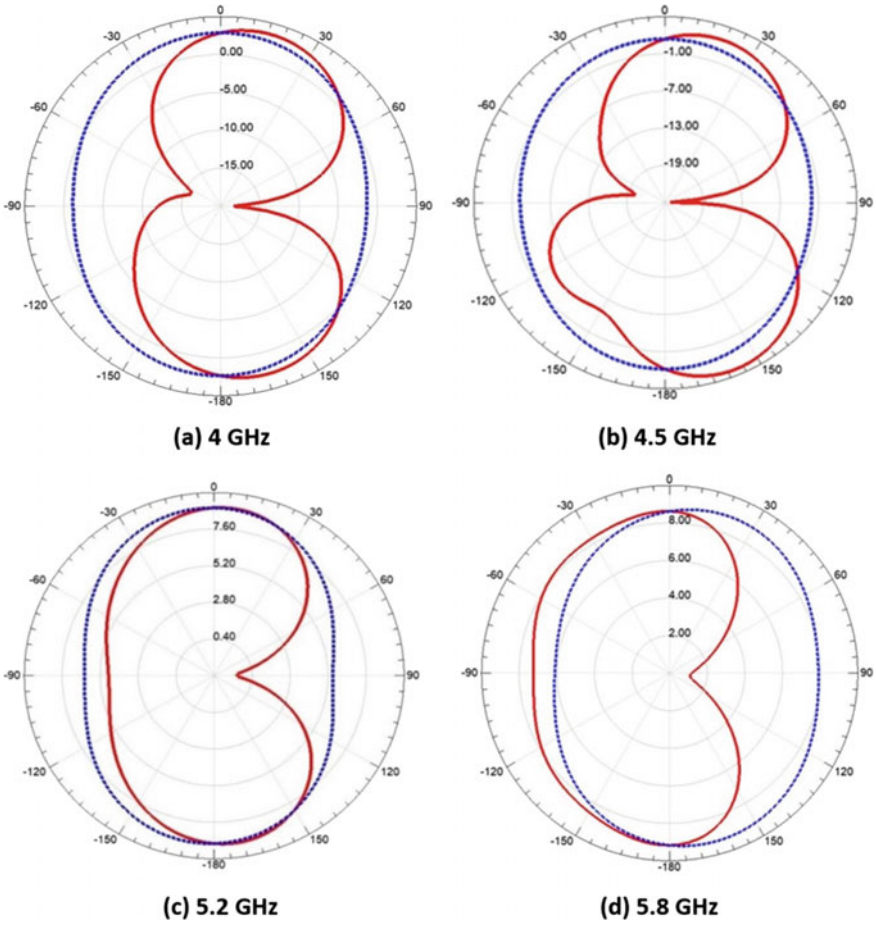

Fig. 3.7 2D radiation patterns of the antenna at 4.0, 4.5, 5.2, and 5.8 GHz

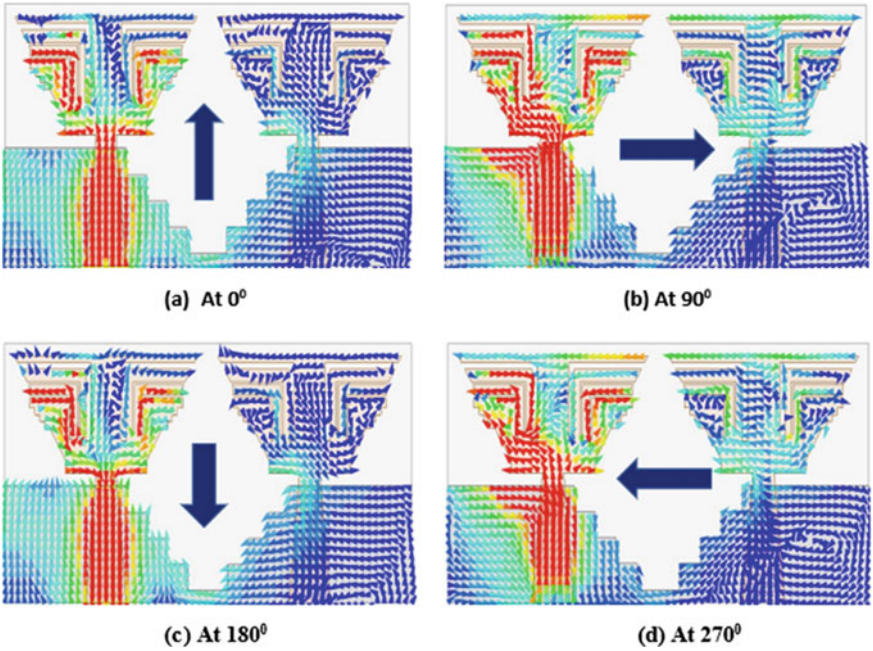

Fig. 3.8 Surface current movements concerning phase shift at 5.2 GHz

Fig. 3.9 The axial ratio curves at 5.2 GHz

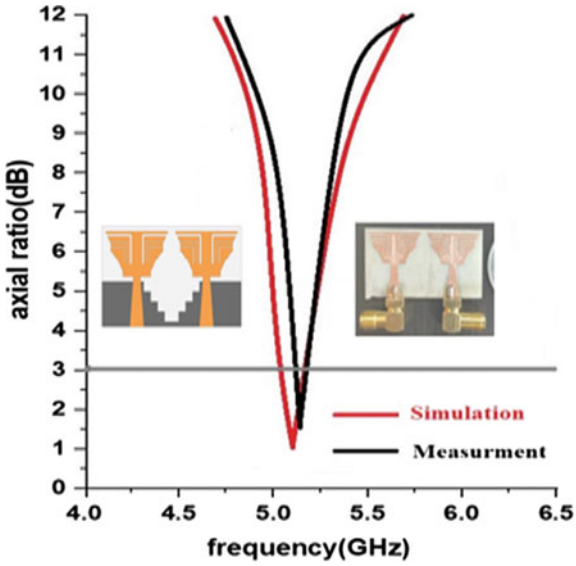

References

Deng J-Y, Guo L-X, Liu X-L (2016) An ultrawideband MIMO antenna with high isolation. IEEE Antenna Wirel Propag Lett 15:182–185

Hasan MdN, Chu S, Bashir S (2019) A DGS monopole antenna loaded with U-shape stub for UWB MIMO applications. Microwave Opt Technol Lett 61(9):2141–2149

Iqbal A, Saraereh OA, Ahmad AW, Bashir S (2017) Mutual coupling reduction using F-shaped stubs in UWB-MIMO antenna. IEEE Access 6:2755–2759

Kaur A, Malik PK (2021) Multiband elliptical patch fractal and defected ground structures microstrip patch antenna for wireless applications. Progr Electromagnet Res B 91:157–173. https://doi.org/10.2528/PIERB20102704 (ISSN: 1937-6472)

Qu L, Piao H, Qu Y, Kim H-H, Kim H (2018) Circularly polarized MIMO ground radiation antennas for wearable devices. Electron Lett 54(4)

Salma S, Khan H, Reddy KRVN, Mahidhar D, Sandeep DR, Rao MC (1982) Design and analysis of circularly polarized dual-element MIMO antenna with DGS for satellite communication, fixed mobile, ISM, and radio navigation applications. Int J Adv Sci 29:19942020

Salma S, Khan H, Reddy BN, Maheswari GU, Prathyusha KR, Sandeep DR, Rao MC (1995) Design and analysis of circularly polarized MIMO antenna with defective ground structure for maritime radio navigation, Wi-MAX and fixed satellite communication applications. Int J Adv Sci 29:20102020

Syed S, Khan H, Madhav B, Sandeep D, Suman M (2021) Design and analysis of a hybrid circularly polarized multi-band MIMO antenna for sub 6 GHz applications. Int J Electron Telecommun 67:570–577. https://doi.org/10.24425/ijett.2021.137848

Thomas KG, Sreenivasan M (2010) A simple ultrawideband planar rectangular printed antenna with band dispensation. IEEE Trans Antennas Propag 58(1):27–34

Tiwari P, Malik PK (2021) Wide band micro-strip antenna design for higher "X" band. Int J of e-Collab (IJeC) 17(4):60–74. https://doi.org/10.4018/IJeC.2021100105 (ISSN:1548-3673)

Wadhwa DS, Malik PK, Khinda JS (2021) High gain antenna for n260- & n261-bands and augmentation in bandwidth for mm-wave range by patch current diversions. World J Eng 19(5):689–696.https://doi.org/10.1108/WJE-03-2021-0133 (ISSN: 1708–5284)

Zhang S, Pedersen GF (2016) Mutual coupling reduction for UWB MIMO antennas with a wideband neutralization line. IEEE Antenna Wirel Propag Lett 15:166–169

Zhu Y, Chen Y, Yang S (2020) Integration of 5G rectangular MIMO antenna array and GSM antenna for dual-band base station applications. IEEE Access 8:63175–63187

Chapter 4
Performance Analysis of Flexible Textile Antenna for Health Monitoring of Elderly Alone at Home

V. Seethalakshmi, S. Nithya, S. Suganyadevi, Gokul Basavaraj, and G. Saranya

Abstract Rapid technological advancements have been followed by a spike in the use of technology in healthcare. A major role for antenna is currently being played in biomedical engineering to enhance health and quality of life. Among the medical devices that make use of antenna and wireless body area networks are pacemakers, deep brain implants, endoscopy, magnetic resonance imaging, microwave imaging, and therapeutic thermal ablation equipment. To transmit diagnosis information from the human body to the external device and then to the doctor or concerned person over the internet, antennas can be implanted, applied to the body, and swallowed. Additionally, variations in an antenna's electrical parameters, such as impedance and reflection coefficient, can be examined to non-invasively diagnose illnesses. Some of the crucial uses for antennas include the detection of breast and brain tumours, malignancy, and motion. Additionally, the electromagnetic field's heating action is useful for treating tissues with cancerous cell growth. In contrast to conventional antennas, which are composed of rigid materials, textile antennas are a specific class of antennas that are made entirely or mostly of textile materials. Electrotextiles,

V. Seethalakshmi (✉) · S. Nithya · S. Suganyadevi · G. Basavaraj
Department of Electronics and Communication Engineering, KPR Institute of Engineering and Technology, Coimbatore, Tamil Nadu, India
e-mail: seethav@kpriet.ac.in

S. Nithya
e-mail: s.nithya@kpriet.ac.in

S. Suganyadevi
e-mail: suganyadevi.s@kpriet.ac.in

G. Basavaraj
e-mail: gokul.basavaraj@cqumail.com

G. Basavaraj
Central Queensland University, Victoria Melbourne, Australia

G. Saranya
Department of Electronics and Communication Engineering, Rajalakshmi Engineering College, Chennai, Tamil Nadu, India
e-mail: saranya.g@rajalakshmi.edu.in

P. K. Malik and P. N. Shastry (eds.), *Internet of Things Enabled Antennas for Biomedical Devices and Systems*, Springer Tracts in Electrical and Electronics Engineering,
https://doi.org/10.1007/978-981-99-0212-5_4

also known as electrically conductive textiles, are used for the antenna's radiating and grounding components, whereas dielectric materials are used for the antenna's insulating components.

Keywords Electro textiles · ISM band · Return loss · Textile antenna · VSWR

Introduction

With wearable technology integrated into the "smart" garment, smart textile systems represent a new idea in clothing that offers additional capabilities like detecting, actuating, and communicating in addition to more traditional uses like protecting the body from the environment. In order to monitor the wearer's status (such as body temperature, heart rate, and position) and/or the state of the environment around them, sensing functions are implemented via sensors built into the fabric of textile garments (i.e., external temperature and humidity). In order to inform, command, or warn the wearer about specific events relating to his or her state or the state of the surrounding environment, garment-integrated actuators enable actuating functions. Finally, wireless communication is accomplished using a wearable transceiver and an integrated wearable textile antenna.

When antennas are incorporated into clothes for Internet of Things applications, the clothing acts as a smart interface between the user and network communication. The wearable antennas must also be inexpensive to produce and market. They should be small, light, durable, easy to maintain, and resistant to use and washing cycles. In view of the aforementioned, textile planar antennas of the microstrip patch type have been suggested for use in clothing applications since they exhibit all of the foregoing qualities as well as being adaptable to any surface. The microstrip patch antenna also radiates perpendicular to a ground plane, which acts as a shield to the antenna radiation, ensuring that only a very small amount of the radiation is absorbed by the human body.

ISM (Industrial, Scientific, and Medical) band resonance is targeted by a wearable microstrip patch antenna. The suggested multiband antenna is a textile garment made from denim, which has a substrate with a relative permittivity of 1.6. The antenna's physical measurements are 28 mm × 32 mm × 1.56 mm. The slots are etched into the patch in order to produce the necessary antenna for use in the ISM band. The suggested antenna has a return loss of about −33 dB and resonates at 2.48 GHz. At 2.48 GHz, the antenna gain is 2.9 dB, the directivity is 5.2 dB, and the VSWR is 1.21 dB. Experimental testing has proven that the suggested wearable textile antenna is appropriate in the ISM band (2.48–2.484 GHz), which is typically utilised for medical applications. The designed antenna is compatible and flexible as it is designed in cloth substrate. The structure has outstanding performance at various angles, and is safe to use with less power consumption. The antenna is mounted on the kneecap and this antenna can be utilised in health monitoring and fall detection of senior persons.

Fig. 4.1 Proposed antenna mounted on the kneecap

Textile Antenna

A planar structure and flexible materials are the two fundamental prerequisites for a textile wearable antenna. The performance of the antenna is influenced by a variety of flexible material characteristics. For instance, the bandwidth and efficiency of a microstrip antenna are influenced by the thickness of the dielectric material. The impedance of the antenna is typically reduced and increased by surface wave losses due to the low dielectric constant of textile materials. In some medical applications, the body's biometric information is continually tracked. To do this, an antenna that transmits biometric information to the outside world must be kept as adjacent to the skin as possible. The nature of conventional antennas, which are rigid, makes them poor choices for such monitoring systems because they cannot be held connected to the human body for a long time. In the modern world, textile antennas are found to be more significant in a variety of communication domains. This proposed antenna is used for the health monitoring of elderly people alone at home. As most old people wear kneecaps, the antenna along with sensors for health monitoring and fall detection is mounted on the kneecap as shown in Fig. 4.1.

A Review of Wearable Antennas for Medical Application

Textile antennas' primary goal is to be simply incorporated into clothing. They are made with conductive yarn and thread made from textile materials. The technology and materials used to make textile antennas, the interface between the antenna and the top of the skin, and the environment present the most problems (Sreelakshmy

et al. 2017). The most common kind of antennas utilised in wearable demands are textile antennas. Cotton, denim, fleece, and other common textiles can be utilised as dielectric substrates. Because they are strong, elastic, and waterproof, polymer-based materials are also taken into consideration as potential substrates. The conductive portion of the wearable antenna should have similar qualities to regular clothing, like being cosy, inconspicuous, washable, elastic in all directions, etc. The antenna can be incorporated completely into clothing by weaving or embroidering conductive threads or yarn into textiles (Izquierdo et al. 2010; Kellomäki 2012; Rais et al. 2009).

Metal-plated polymer fibres or thin solid metal wires are both examples of conductive threads. The human body, a lossy dielectric, is in close contact with the textile antenna where it operates. The human body absorbs some of the radiated power which lowers the efficiency and gain. If exposure restrictions are not followed, the person could be showing EM waves that may have harmful possessions on their health (Kumar and Thangavelu 2014). Wearable antennas might tune in both on-body and also off-body operations (where EM wave might sent into empty space where the propagation along the body surface is desired) (Kumar and Thangavelu 2015a). The antenna must be designed to account for mechanical contortion such as bending, stretching, and crumpling that can occur when it is worn on the body (Talukder et al. 2012).

When armed forces are taken into account, wearable antennas are frequently necessary to function under challenging conditions (rain, heat, snow, etc.). Moisture in the textile substrate has a significant impact on the antenna radiation parameters. The application of suitably waterproof textile substrates or antenna coverings is a common method to reduce the impact of severe environments (Kumar and Thangavelu 2015b; Chen and Tao 2011). A wideband reconfigurable antenna with extended band coverage is proposed to be compatible with mobile terminals (Seethalakshmi et al. 2019). A novel model of planar monopole antenna with high gain and directivity is proposed where the square loop unit cell is positioned inside the substrate, increasing the antenna's directivity to work at frequencies of 3.0, 8.3, 11, and 12 GHz (Seethalakshmi et al. 2021; Nithya and Seethalakshmi 2022) (Tiwari and Malik 2020; Gupta et al. 2020; Roges et al. 2022).

Antenna Design Parameters

As a wearable antenna, presentation at various bending positions will be taken into account. Different antenna performances may result from antenna bending. This effort's antenna for wearable applications has a small size, a low return loss, and electrical characteristics of fabric. We must prevent wave deterioration in the complicated human environment when designing wearable antenna. Miniaturisation requires more consideration than any other parameter. Due to the attenuated effects of the human body, this structure is mostly used in wearable demands in the 2.48 GHz ISM band.

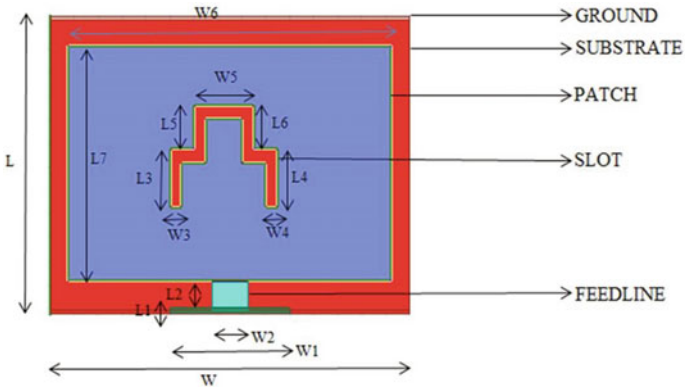

Fig. 4.2 Architecture of antenna design

The textile antenna is printed on denim fabric with a permittivity of 1.6, copper will be the radiating element here. To reduce the radiation influence on the body, the suggested antenna configuration includes a ground path and a route fueled by a tiny strip. The projected assembly's ground flat covers the complete end surface, which lessens the effects of radiation on people's bodies. The width (W) and length of a microstrip antenna affect how well it performs (L).

The geometrical view of a textile antenna for wearable demands in ISM band is shown in Fig. 4.2. The substrate is 1.6 permittivity denim fabric. This antenna structure has dimensions of 28 mm × 32 mm × 1.56 mm thickness. Copper is used for the radiator and ground, and it has a 60 μm thickness. The antenna feed is a 50 microstrip feed with dimensions of 3 mm in width and 4 mm in length. Figure 4.2 depicts a textile antenna from a geometric perspective for wearable applications in the ISM band.

Denim fabric with a permittivity of 1.6 is the substrate. The dimensions and thickness of this antenna structure are 28 mm × 32 mm × 1.56 mm, respectively. Copper with a 60 μm thickness makes up the ground and radiator. Table 4.1 gives the dimension of the proposed antenna.

Results and Discussion

Using the CST Studio suite, textile antenna design and analysis are carried out. The dimensions and performance of the optimised antenna design were verified. In Fig. 4.3, the return loss S11 characteristic of a textile antenna is displayed. An antenna's return error could be least than −10 dB. The planned antenna has S-parameter of −33 dB and spans the frequency is 2.488 GHz. The performance will be better since interference between the signals will be reduced as return loss is

Table 4.1 Dimension of the designed antenna

Parameters	Values (mm)
L1	1.5
L2	2.5
L3	5
L4	5
L5	5
L6	5
L7	20
W1	10
W2	3
W3	1
W4	1
W5	3
W6	27

higher or when reflection is low. The largest return loss occurs at a frequency of 2.488 GHz, around −33 dB.

Figure 4.4 displays the 2.48 GHz radiation pattern and gain. The major lobes' benefit, however, is constant across all bending scenarios. A radiation pattern measurement is used to determine the gain of the suggested antenna. The graph shows that the antenna's gain is essentially ideal during the resonant band frequency. Additionally, it should be renowned that the gain vigour worth does not change. The suggested system's elevation and azimuth patterns demonstrate its high gain of 2.9 dB. The bandwidth obtained at 2.48 GHz is 165 MHz. In light of this, the suggested textile antenna is the ideal choice for wearable applications. Figure 4.5 shows the directivity of the designed antenna is 5.2 dB. Figure 4.6 shows the VSWR of 1.21 of the proposed antenna. Table 4.2 depicts the results of the proposed antenna. Figures 4.7 and 4.8 shows the simulated far-field directivity and gain of the planned aerial.

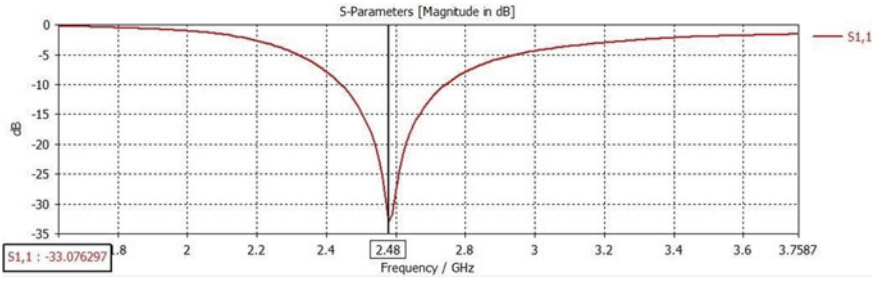

Fig. 4.3 Return loss characteristic

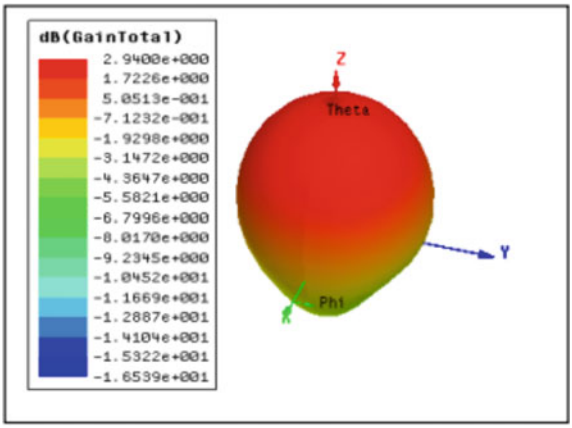

Fig. 4.4 Radiation pattern at 2.48 GHz

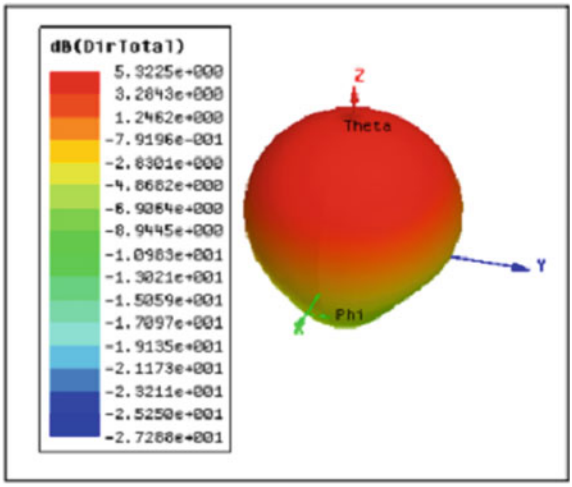

Fig. 4.5 Directivity at 2.48 GHz

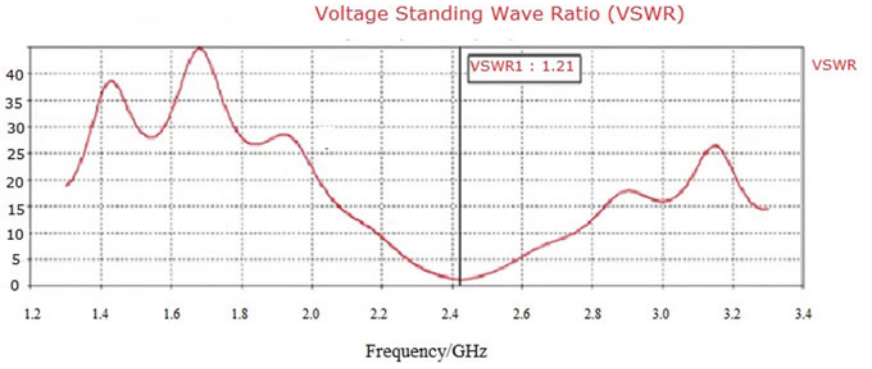

Fig. 4.6 Voltage standing ratio of proposed antenna

Table 4.2 Simulated results for proposed antenna

Frequency	Return loss	Gain	Directivity	VSWR
2.48 GHz	−20 dB	3.9 dB	5.2 dB	1.21

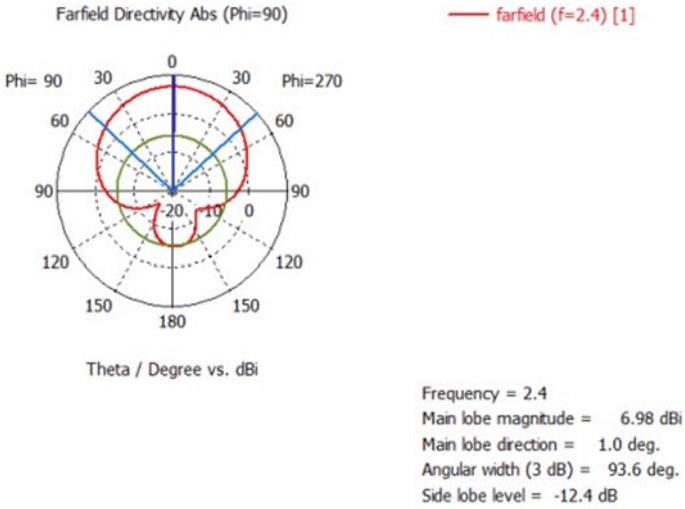

Fig. 4.7 Simulated far field directivity

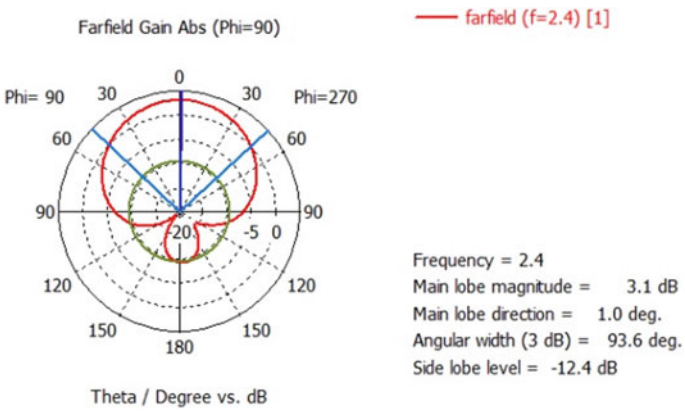

Fig. 4.8 Simulated far field gain

Summary

For wearable applications at the 2.48 GHz ISM Band frequency, a textile antenna is created. The dielectric constant of the substrate used to replicate the textile antenna

was 1.6. Based on the findings, it can be concluded that the construction performance improved through an s11 of −20 dB at 2.48 GHz. Applications like health monitoring, fall detection, and remote monitoring of older persons can all be done with this. Denim was chosen as the material because it is strong, weather-resistant, and stain-resistant. The proposed antenna's design and construction are extremely challenging. Within the frequency band, the measured radiation patterns are consistent.

References

Chen HY, Tao Y (2011) Performance improvement of a U-slot patch antenna using a dual-band frequency selective surface with modified cross elements. IEEE Trans Antennas Propag 59:3482–3486

Gupta NP, Malik PK, Ram BS (2020) A review on methods and systems for early breast cancer detection. In: 2020 International conference on computation, automation and knowledge management (ICCAKM), pp 42–46. https://doi.org/10.1109/ICCAKM46823.2020.9051554. ISBN: 978-1-7281-0666-3. https://ieeexplore.ieee.org/document/9051554. Accessed 09 Jan 2020

Izquierdo S, Batchelor JC, Sobhy MI (2010) Button antenna on textiles for WLAN on body application. IET Micro Ant Prop 4:1980–1987

Kellomäki T (2012) Analysis of circular polarization of cylindrically bent micro strip antennas. Int J Antennas Propag 2012:1–8

Kumar SA, Thangavelu S (2014) Design and analysis of implantable CPW fed X-monopole antenna for ISM band applications. Telemed e-Health 20(3):246

Kumar SA, Thangavelu S (2015a) CPW fed monopole implantable antenna for 2.485 GHz ISM band applications. Int J Electron Lett 3(3):152–159

Kumar SA, Thangavelu S (2015b) CPW fed implantable Z-monopole antennas for ISM band biomedical applications. Int J Microw Wirel Tech 7(5):529–533

Nithya S, Seethalakshmi V (2022) MIMO antenna with isolation enrichment for 5G mobile information. Mobile information systems, vol 2022. Hindawi Publisher

Rais N, Soh P, Hall P (2009) A review of wearable antenna. In: Lough Borough, International conference, pp 120–126

Roges R, Malik PK, Sharma S (2022) A compact wideband antenna with DGS for IoT applications using LoRa technology. In: 2022 10th International conference on emerging trends in engineering and technology—signal and information processing (ICETET-SIP-22), pp 1–4. https://doi.org/10.1109/ICETET-SIP-2254415.2022.9791725

Seethalakshmi V, Sowndharya N, Swatiga B, Uma K (2019) Design and analysis of wideband antenna for 5G wireless communication. Int J Innov Res Sci Eng Technol 8(3)

Seethalakshmi V, Kalirajan K, Nithya S, Sumathi K (2021) Performance analysis of multiple frequency selective antenna. In: Planar antenna: design, fabrication, testing, and application. Nova Publications, pp 295–317

Sreelakshmy R, Kumar SA, Shanmuganantham T (2017) A wearable type embroidered logo antenna at ISM band for military applications. Micro Opt Tech Lett 59:2159–2163

Talukder A, Karmokar D, Morshed K, Mollah N (2012) Low profile inverted-F-L antenna for 5.5 GHz Wi MAX applications. ACEEE Int J Commun 3:12–19

Tiwari P, Malik PK (2020) Design of UWB antenna for the 5G mobile communication applications: a review. In: 2020 International conference on computation, automation and knowledge management (ICCAKM), pp 24–30. https://doi.org/10.1109/ICCAKM46823.2020.9051556. ISBN: 978-1-7281-0666-3. https://ieeexplore.ieee.org/document/9051556. Accessed 09 Jan 2020

Chapter 5
Investigation on Performance Characteristics of Wearable Textile Patch Antenna

S. Nithya, V. Seethalakshmi, G. Vetrichelvi, M. Singaram, R. Prabhu, and Sumit Agarwal

Abstract The production of elements and equipment that individuals can carry in their pockets or even attach to their bodies as an integral part of their clothes is being encouraged by the enormously increased shrinking of electronic devices and the massive development in wearable computing technology. Wearable antennas built onto garments are now necessary for uninterrupted communication to occur. A wearable antenna's design and development must take four criteria into mind. When the antenna is worn as part of clothing and is in close contact with the human body, it must first perform as the intended radiator. To maintain successful and efficient communication, there should be very little variation, or rather deviation, in the operation of these wearable antennas when operating close to body tissues. There are further restrictions, though, when making an antenna genuinely wearable. The ability to be emblazoned more easily than traditional antennas is one requirement for textile antennas. If anything can simultaneously bend in all directions, it is said to be drapable. The wearable antenna can be made truly drapable by using cutting-edge materials or methods. Last but not least, full integration of these components into the fabrics at the point of production is required if wearable antennas are to

S. Nithya (✉) · V. Seethalakshmi · M. Singaram
KPR Institute of Engineering and Technology, Arasur, Coimbatore, India
e-mail: s.nithya@kpriet.ac.in

V. Seethalakshmi
e-mail: seethav@kpriet.ac.in

M. Singaram
e-mail: m.singaram@kpriet.ac.in

G. Vetrichelvi
Jansons Institute of Technology, Coimbatore, India
e-mail: kavena290302@gmail.com

R. Prabhu
Robert Bosch, Coimbatore, India

S. Agarwal
Pennsylvania State University, State College, PA 16802, USA
e-mail: sua347@psu.edu

P. K. Malik and P. N. Shastry (eds.), *Internet of Things Enabled Antennas for Biomedical Devices and Systems*, Springer Tracts in Electrical and Electronics Engineering,
https://doi.org/10.1007/978-981-99-0212-5_5

revolutionise the commercial market. Patch antennas are useful for measuring some physical events because of their tiny size, which allows them to be integrated into small devices. The constant measurement and transmission of various bio signals from the human body medical devices is one of the main uses of patch antennas. The wearer's comfort and safety can be increased by integrating this kind of bio-sensor with a patch antenna into clothing for continuous monitoring. Due to their small size, excellent flexibility, and ease of incorporation into clothes, textile antennas are useful for wireless communications. The goal of the current effort is to create a body-worn textile antenna operating at 2.4 GHz that is appropriate for the ISM band. Since wearable antenna must always be worn on the body, all antennas are also examined in bending and flat skin conditions. A body phantom model with various dielectric layers, such as muscle, fat, and skin, each with its own dielectric constant and thickness, was employed for this. The power that is returned to it is absorbed by the human body, a lossy medium. These back radiations raise body temperature and speed up particular absorption, which is bad for the user and hazardous. EBG is employed to reduce the back radiation and an enhanced SAR is seen, which allays this worry in the case of a bent antenna.

Keywords Body phantom model · EBG · Human body · ISM band · SAR · Textile antenna

Introduction

The wearable microstrip antenna has undergone innovative modernisation over the past few years by creating fresh concepts to detect numerous abnormal limitations in and around the human body and has been utilised to diagnose various types of disorders. Numerous methods, including magnetic resonance imaging (MRI), computer tomography (CT) scans, ultrasound imaging scanning, and positron emission tomography (PET), are employed to find diseases and damage within the human body. Microwave signals outperform X-ray, MRI, and mammogram radiation as a non-ionising radiation (Abbasi et al. 2013). Wearable textile antenna applications are essential since wireless communication has recently been incorporated into fabric materials. The most current advancement in textile technology allows for continuous monitoring of a person's bio signals and transmission of that information through the atmosphere to offer information about their whereabouts and physical condition. However, antennas are required for a wireless contact bond between the cloth and a pedestal station. The best way to incorporate an antenna is by the assembly of the antenna from fabric made of a certain type of textile. The industries have access to conductive textile resources, also known as electro textiles, which equips them with textile antennas and gets them ready for a rebellious component of the wearable textile programme. In their early stages of development, wireless technologies for human body-worn systems remain immobile. By integrating cloth into the communication organism, the wearable textile antenna reduces the visibility of electronic gadgets.

Wearable antennas claim to be small, quick, fun, strong, inexpensive, and easily integrated into RF (radio frequency) circuits in order to get better concert. In their infancy, wireless technologies for devices that people wear on their bodies are still immobile. Small size antennas may be needed in high performance applications such satellites, aeroplanes, missiles, and spacecraft where weight, size, cost, aerodynamic profile, and simplicity of installation profiles are constraints. To satisfy these needs, microstrip antennas can be employed. Electronic gadgets become less obvious thanks to the wearable textile antenna, which incorporates cloth into the communication organism. Wearable antennas brag to be thin, brief in duration, frivolous, energetic, inexpensive, as well as easily integrated into RF (radio frequency) circuits, in order to achieve improved concert. Planar antennas, which pass a high-quality amalgamation of the antenna among the feeding lines, are, therefore, the preferred category of an antenna to achieve the highest data rate. For electrically small antennas, throughput is noticeably lower than the highly speculative perimeter. Additionally, radio frequency circuits are the same circuits found in a typical multi-deposit board material. This allows for its minimally obtrusive incorporation into the cloth. Microstrip patch antennas are the best antennas for wearable applications because they perpendicularly project close to a planar arrangement, maintain the wearer's valuable body tissues, and have an earth plane. An excellent printed resonant antenna in microwave wireless mode of communication is the microstrip patch antenna (Ahmad et al. 2012). Solely on a single side of a dielectric substrate is a ground plane, while on the other is a radiating patch.

In Fig. 5.1, the microstrip antenna system is illustrated; generally, a patch is constructed of a conducting substance, such as copper or gold, and can take on any geometric design (Ahmed et al. 2018). It allows for both circular and linear polarisation. In order for the microstrip antenna to work in a flexible manner, the substrate is essential. Other hard substrates can be used in place of textile ones. The microstrip antenna's dimensions are determined by fringing fields, and the borders of the antenna also experience straying. The patch's width affects the fringing effect. The dielectric constant of the uniform dielectric material is known as the effective dielectric constant. In contrast to tougher substrates, soft substrates are soft and flexible, as opposed to textile substrates like FR4, glass, cotton, polyester, and wool. Based on their unique dielectric constants, which vary for different substrates, different substrates will have distinct properties. Microstrip antennas are ideally suited for bio applications, while textile antennas can be easily integrated, are less expensive, weigh less, and operate at microwave frequencies. When designing a flexible antenna, it is predictable to use various patch shapes, soft substrates, and conducting materials. For on-body and off-body analysis, the interaction between the tissue and antenna interface when this antenna is put on the body is crucial. Since the 1970s, commercial and governmental applications for microstrip patch antenna have grown in popularity. A radiating patch and conductive ground plane are placed around a non-conductive substrate to create a microstrip patch antenna. There are many different antenna shapes, but due to their simplicity in analysis and design, circular and rectangular shapes are most frequently utilised. The matching networks, power dividers, radiators, and phasing circuits can all be designed as planar configurations

on a printing circuit board. Additionally, the solid metallic surfaces of spacecraft and missiles can be simply attached with microstrip antennas that have a conductor as the ground plane. In addition, a microstrip antenna is more suitable for high-frequency applications than other low-frequency conventional antennas. Despite these benefits, microstrip antennas have some significant drawbacks, including low efficiency, poor polarisation purity, high Q (quality factor), spurious feed radiation, low power, subpar scan performance, and a very small bandwidth. Low bandwidth is preferred for some security system applications, though. But if surface waves are excluded, raising the height of the substrate can increase bandwidth (up to 35%) and efficiency (up to 90%). However, a rise in substrate height causes an increase in surface wave, which is extremely undesirable because it reduces the total amount of power available for direct radiation (space wave). Patch antennas are widely used in medical equipment for the continuous transmission and monitoring of various bio signals from the human body. This kind of bio-sensor with a patch antenna can be incorporated into clothing for continuous monitoring with a higher level of wearer safety and comfort. Textile antennas are advantageous for wireless communications because of their low bulk, great flexibility, and simplicity of integration into clothing. However, it is not always viable to provide a flat surface to attach the antenna when it is being used for on-body communication. Therefore, a textile antenna ought to function better even under bending and crumpling circumstances. The researchers have noticed increased power absorption because of the capacitive interaction of the antenna with the body. Due to variations in body temperature and humidity, an antenna's dielectric characteristics are liable to alter when it is put on a human body. This causes the antenna's radiation pattern to be distorted, its resonance frequency to shift, and its impedance matching to become out of tune. Additionally, because of the mismatch between the antenna and the human body, back lobe radiations are produced and absorbed by the body, which lowers the radiations' available power and lowers the antenna's gain in the desired direction. A specific absorption rate is used to assess the absorbed power from back radiations (SAR). The body absorbs back radiations at a specific rate due to reflected waves. By separating the antenna from the body component, these reflected waves can be reduced to a minimum. To prevent reflection at a design frequency, one solution is to employ a synthetic substance called metamaterial. Although metamaterials do not exist in nature as such, they can be created by spacing out the tiny resonant units in a predictable way. EBG is the kind of metamaterial utilised in antenna applications (electromagnetic band gap). In the microwave frequency range, an EBG prevents electricity flowing from a patch antenna to body tissue. The goal of the current effort is to create a body-worn textile antenna that operates in the ISM band at a frequency of 2.4 GHz. The performance of the developed antenna is next examined independently on several textile substrates with varied dielectric constants and thicknesses, such as wash cotton, curtain cotton, polyester, and polycot. Performance metrics including return loss, gain, and directivity are monitored, analysed, and compared across all cases. All antennas are further tested on a flat body surface as well as bending conditions since wearable antenna must be worn on the body. A body phantom model with various dielectric layers, including skin, muscle, and fat, each with its own dielectric constant and thickness, was employed for this.

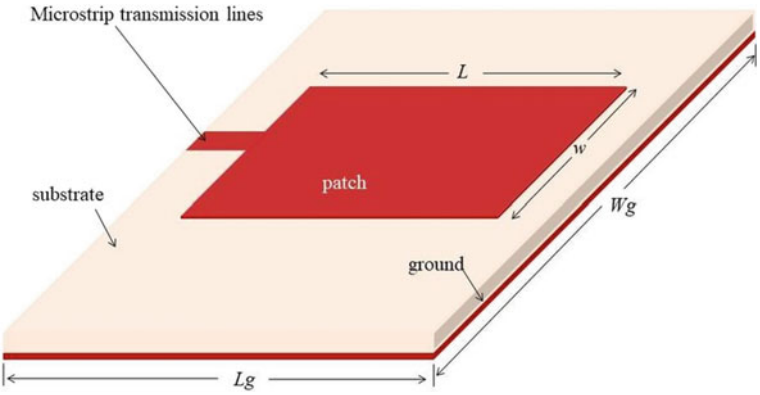

Fig. 5.1 Flexible microstrip antenna

Literature Survey

A dual-band antenna that operates in the 2.45 and 5 GHz frequency bands was presented in Zhu and Langley (2008). High conductivity zelt fabric is used as the patch and ground plane for the antenna's design. As a substrate, thin felt is used. Being a body-wearing antenna, SAR increases when worn on the body due to back radiation. To successfully remove back radiation and reduce the SAR value to within an allowed limit, an EBG approach is applied.

In this research (Zhu and Langley 2009), they offer a dual-band antenna that operates at the wireless network bands of 2.45 and 4.5 GHz. A CPW (coplanar waveguide) is employed to feed this antenna, and parameter results are contrasted with those of a microstrip feed patch antenna. The impact of antenna back radiations on the human body is also studied because these antennas are intended to be placed on the body. The patch and substrate of the antenna are designed with textile materials to provide comfort and flexibility. Zelt fabric is used for conducting antenna components such as the patch, feed line, and ground plane. The substrate of this antenna is 1.1 mm thick. The designed antenna is put to the test in both flat and bent conditions. A SAR analysis is additionally performed on 1 g and 10 g of tissue. A substance called EBG (electromagnetic) is utilised to reduce back lobe radiation. Because of its high impedance surface and conductive ground plane, the EBG lowers the antenna's SAR value.

A flexible and lightweight textile antenna based on E technology has been proposed in Bayram (2010). Due to their excellent mechanical compatibility, single wall carbon nanotubes (SWNT) and textiles with an Ag coating were used to create this antenna. Superior RF performance is provided by polymer composites with permittivity ranges of 3–13. This research simulates and fabricates an E-textile antenna in both flat and bending conditions. Different performance metrics are analyzed. From their investigation, they deduced that the sample patch had a gain

of 6 dB, which is 2 dB less than the antenna under ideal circumstances and with the same dimensions.

In addition to being completely integrable into shielding clothing, a Twin Polarised Patch Antenna (TPPA) at the 2.4–2.45 GHz ISM (Industrial Scientific and Medical) radio band is strong to channel fading. Carla Hertleer, Luigi Vallozzi, and Hendrik Rogier in Hertleer et al. (2009) created this wearable fabric system for rescue personnel in 2008 and 2009.

Bai and Langley (2010) demonstrated a two-dimensional dual-band antenna under stressing conditions in 2010. Felt fabric with a 1.38 dielectric constant serves as the foundation for this antenna, and "Zelt" fabric serves as the conductor. Twin band frequencies like 2.45 and 5.8 GHz were used to characterise the input impedance and radiation patterns. Even when the radiation pattern doesn't change, crumbling causes the antenna return loss to change.

In 2015, Choi et al. in (2015) proposed an entire textile antenna fabricated using leather as substrate and conductive fabric as patch and operated in the industrial, scientific, and medical (ISM) 2.45 GHz band and 4.5 GHz band in the shape of a crossed LV fashioned logo (Louis Vuitton logo). For the lower and higher frequency band, there are two long thin arms and two shorter thick arms. Small-size antennas may be necessary for high-performance applications such as spacecraft, satellites, aeroplanes, and missiles when weight, size, cost, aerodynamics, and ease of installation characteristics are restrictions (Nithya et al. 2021; Seethalakshmi et al. 2021; Nithya and Seethalakshmi 2022). These requirements can be satisfied using microstrip wearable antennas (Bisht and Malik 2022; Pandey et al. 2022; Vishnoi et al. 2023).

Significance of ISM Band

The term "SM band" refers to portions of the radio spectrum that are legally reserved for the use of radio frequency (RF) energy for industrial, medical, and scientific applications as opposed to communication needs. The ISM band at 2.54 GHz is a widely used band for activities around the world. Among the devices that use this ISM band are cordless phones, microwave ovens, medical diathermy devices, WiFi, Bluetooth, and military radars. These ISM devices produce electromagnetic interference, which interferes with radio transmissions using the same frequency. As a result, this equipment was restricted to a certain range of frequencies. The ISM bands are made available for use in wireless LANs and mobile communications by the Federal Communications Commission (FCC) of the United States. Food is cooked using microwaves in ISM device applications like 2.45 GHz microwave ovens. Induction heating, plastic softening, microwave heat treating, and plastic welding methods are all used in the industry. Radio waves in the ISM bands are used by diathermy machines in medical settings to administer deep warmth and kill cancer cells.

Because of this, the flexible microstrip antenna uses textile substrates. In body area network observation, various textile substrate wearable antennas that operate

in the ISM band have been created. This affects the tissues of the human body. The specific absorption rate regulates the influence of antenna radiation. When the antenna absorbs moisture from the air, the performance of the antenna changes because the antenna's high dielectric constant dominates it and lowers its resonance frequency. The performance parameters of a textile antenna alter when it is worn close to human flesh due to the fabric's characteristic of dampness. Therefore, the flexible antenna must be built and function properly in the region of the human body known as the Body Area Network (BAN). The SAR analysis must be taken into consideration. Certain crucial factors, including flexibility, working in a bending environment, ISM band operation, and SAR analysis close to the human body, must be taken into account when an antenna is worn on the body.

Design of Textile Antenna

The design of a flexible microstrip antenna is shown in Fig. 5.2. The antenna is built using a denim textile substrate with a W × L dimension, a thickness of 1 mm, and a loss tangent of 0.025. Copper tape with adhesive properties was used to make a rectangle patch measuring $W_1 \times L_1$ on the denim substrate. In addition, a redesigned ground plane has been employed to expand the bandwidth with improved impedance matching; while a microstrip feed line of $W_f \times L_f$ dimension has been used to activate the antenna. The updated ground was made using two newly introduced slots. The basic patch has a rectangle-shaped notch eliminated, and a metallic stub has been added by folding the patch over on the right side to increase impedance compatibility and bandwidth augmentation.

It is essential to start by comprehending a number of terms associated with flexible patch antennas, formally known as antenna parameters, such as resonant frequency, bandwidth, directivity, gain, and return loss. It is also necessary to understand how these terms relate to human body interactions, such as specific absorption rates, skin effects, dielectric effects, near-field communications, and electromagnetic properties of human tissues.

Simulation Results

Figure 5.3 displays the 3D human body-specific model for assessing the SAR effect of the triple-band textile antenna. The following model includes the layers of skin, fat, and muscle along with their electrical characteristics. Table 5.1 provides the biological electrical characteristics results of the various human bodily organs.

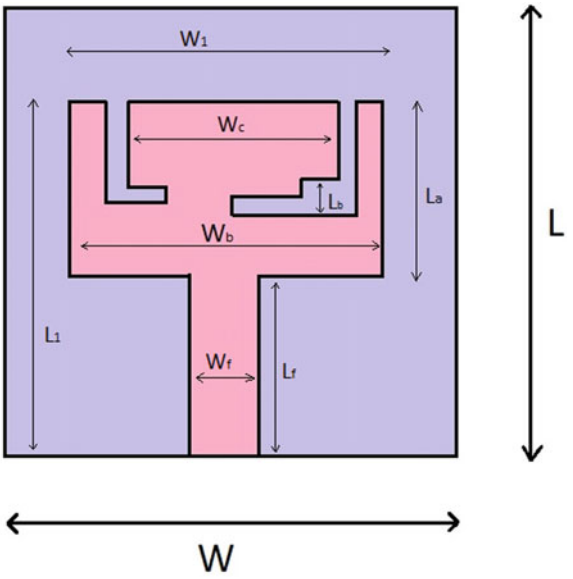

Fig. 5.2 Design of proposed textile antenna

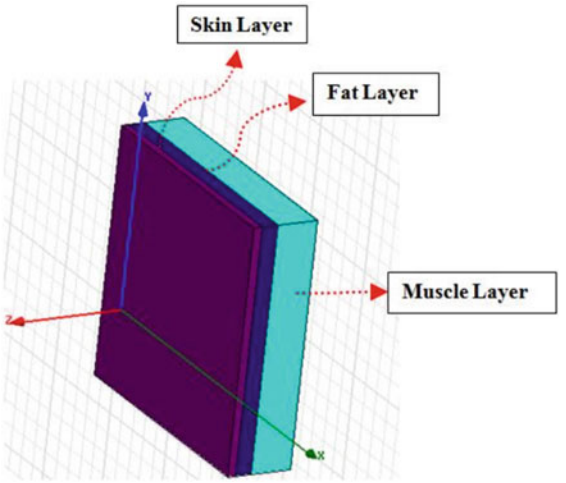

Fig. 5.3 3D human body customised model

Table 5.1 Biological electrical characteristics

Layer	Permittivity (ε_r)	Conductivity (S/m)	Loss tangent	Density
Skin	43	1.55618	0.2672	1120
Fat	5.3853	0.09235	0.1345	912
Muscle	53.191	1.695	0.2341	1010

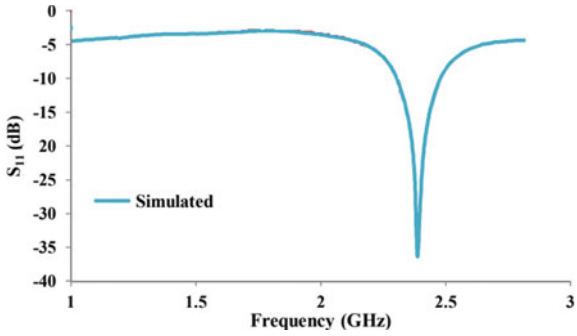

Fig. 5.4 Return loss characteristics of wearable antenna

S Parameter

A Return loss, which does not reflect back, shows how much power was lost to the load. The return loss curve of an antenna is a graph of S_{11} of an antenna versus frequency. A graph must exhibit a drop in the operating frequency for it to function optimally. The S_{11}, which contains the return loss and its resonant frequency, is shown in Fig. 5.4. As it is necessary to modify the antenna size for a fixed operational ISM band frequency, for WBAN, this parameter is found to play a key role in antenna research. Decibel is the unit of return loss (dB).

The S_{11} return loss metric of a textile antenna is shown. The return error of an antenna could be as low as −10 dB. The proposed antenna spans the frequency of 2.45 GHz and has an S-parameter of −37 dB. Performance will improve as return loss increases or when reflection is minimal because interference between the signals will be decreased.

Radiation Pattern

Figure 5.5 shows the radiation pattern which clearly states that antenna gain is experimentally achieved. Always a negative gain is achieved with a normal ground structure; due to the introduction of the defect in the ground plane, the gain was very well improved. However, the advantage of the major lobes remains the same under all bending conditions. The gain of the proposed antenna is determined using a radiation pattern measurement. The graph demonstrates that during the resonant band frequency, the antenna's gain is nearly perfect. It should also be noted that the increase in vigour value remains constant. The elevation and azimuth patterns of the proposed system show its high gain of 3.996 dB.

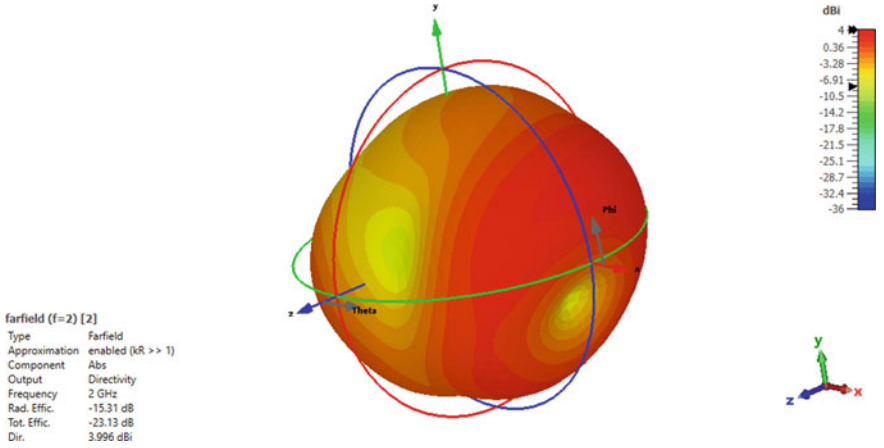

Fig. 5.5 Radiation pattern of the proposed antenna

Far-Field Gain and Directivity

These additional crucial performance indicators shed light on the usability of the chosen antenna. The planned antenna's far-field gain and directivity under bending conditions with various textile substrates are listed below. The far-field gain and directivity of the antenna are shown in Fig. 5.6.

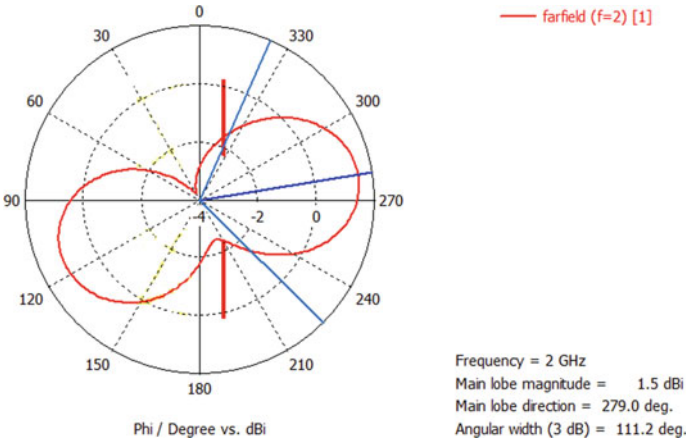

Fig. 5.6 Far-field gain and directivity characteristics

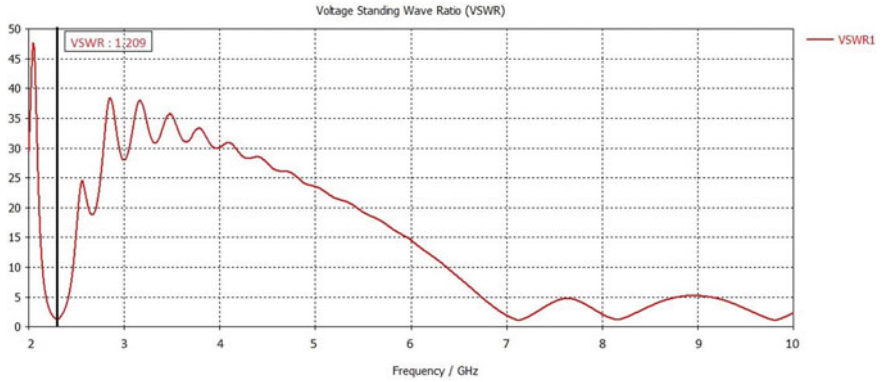

Fig. 5.7 VSWR characteristics of proposed antenna

VSWR (Voltage Standing Wave Ratio)

The design and analysis of textile antennas are completed using the CST Studio suite. The optimised antenna design's size and functionality were confirmed. Figure 5.7 shows the result of VSWR. The voltage standing wave ratio of the proposed antenna is found to be 1.209. For perfect radiation and functioning of the antenna, the VSWR should lie between 1 to 2.

Summary

This article presented a design for a textile patch antenna using materials in the ISM band with a central frequency of 2.45 GHz is reported and various performance analyses were done on the basis of S Parameter, Far-field directivity, gain, and radiation pattern. Exacerbated by the fact that textile substrate materials can be used in its construction, the rectangular microstrip patch antenna performs superbly for wearable applications. The dielectric constant of the textile material is low, falling between one and two. As a result, it can lower surface wave losses and increase an antenna's bandwidth.

References

Abbasi QH, Rehman MU, Yang X, Alomainy A, Quaraqe K, Serpedin E (2013) Ultra wideband band-notched flexible antenna for wearable applications. IEEE Antennas Wirel Propag Lett 12:1606–1609

Ahmad S, Saidin NS, Chelsa CM (2012) Development of embroidered Sierpinski carpet antenna. In: Proceedings of the IEEE Asia-Pacific conference on applied electromagnetics, vol 8, pp 123–127

Ahmed MI, Ahmed MF, Shaalan AEH (2018) Novel electro-textile patch antenna on jeans substrate for wearable applications. Prog Electromagnet Res 83:255–265

Bai Q, Langley R (2010) Textile antenna bending and crumpling. In: Proceedings of the fourth European conference on antennas and propagation

Bayram Y et al (2010) E-textile conductors and polymer composites for conformal lightweight antennas. IEEE Trans Antennas Propag 2:45–60. https://doi.org/10.1109/TAP.2010.2050439

Bisht N, Malik PK (2022) Adoption of microstrip antenna to multiple input multiple output microstrip antenna for wireless applications: a review. In: Singh PK, Singh Y, Chhabra JK, Illés Z, Verma C (eds) Recent innovations in computing. Lecture notes in electrical engineering, vol 855. Springer, Singapore. https://doi.org/10.1007/978-981-16-8892-8_15

Choi J, Tak J et al (2015) Design of an all-textile circular patch antenna with corrugated ground for guided wave along the body surface for WBAN applications. J Electromagn Waves Appl 1–20

Hertleer C, Vallozzi L, Rogier H (2009) A textile patch antenna with dual polarization for rescue workers' garments. In: IEEE transactions, 3rd European conference on antennas and propagation. EuCAP 2009, pp 967–970

Nithya S, Seethalakshmi V (2022) MIMO antenna with isolation enrichment for 5G mobile information. Mobile Inf. Syst. 1802352 2022:1–15

Nithya S et al (2021) Design of MIMO microstrip patch antenna for 5G applications. Planar Antenna Des Fab Test Appl 2021:261–271

Pandey U, Gupta NP, Malik P (2022) Review on miniaturized flexible wearable antenna for body area network. In: Singh PK, Singh Y, Chhabra JK, Illés Z, Verma C (eds) Recent innovations in computing. Lecture notes in electrical engineering, vol 855. Springer, Singapore. https://doi.org/10.1007/978-981-16-8892-8_4

Seethalakshmi V, Kalirajan K, Nithya S, Sumathi K (2021) Performance analysis of multiple frequency selective antenna. Planar Antenna Des Fab Test Appl 2021:295–317

Vishnoi V, Singh P, Budhiraja I, Malik PK (2023) Multiband dual-layer microstrip patch antenna for 5G wireless applications. In: Singh PK, Wierzchoń ST, Tanwar S, Rodrigues JJPC, Ganzha M (eds) Proceedings of third international conference on computing, communications, and cybersecurity. Lecture notes in networks and systems, vol 421. Springer, Singapore. https://doi.org/10.1007/978-981-19-1142-2_7

Zhu SZ, Langley R (2008) Dual-band wearable antenna. IEEE Trans Antennas Propag 3:25–30. https://doi.org/10.1109/LAPC.2008.4516853

Zhu SZ, Langley R (2009) Dual-band wearable textile antenna on an EBG substrate. IEEE Trans Antennas Propag 57:926–935. https://doi.org/10.1109/TAP.2009.2014527

Chapter 6
Implantable Antennas for Bio-telemetry Application

Jeet Ghosh and S Durga Padmaja Bikkuri

Abstract In recent times, the healthcare industry is bridging with information and communication technology to provide efficient and personalized services to patients. This paradigm shift enthused to the development of advanced implantable medical devices with the telemetry feature. The major demand for the bio-telemetry application is that the communication should be reliable, secure, and safe for human being. In this regard, the implantable antenna unit is the key player in the system. In this chapter, a detailed explanation of the design and development steps of the implantable antenna is discussed. In addition to this, a comprehensive review is presented with a focus on implantable antenna and telemetry link. Furthermore, several issues related to the safety of human health and biocompatibility have also been addressed.

Keywords Antenna placement analysis · Bio-telemetry · Ex vivo testing · Implantable antenna · Ingestible antenna · In vitro testing · In vivo testing

Introduction

Over the last decade, the medical and healthcare industry is facing several difficulties based on data management, personalization treatment, patient handling in the hospital, etc. Due to the recent COVID-19 pandemic, the problem increases in multiple folds and forced the researcher, medical practitioner, and policy maker to think and incorporate new technologies, such as the Internet of Things (IoT), Big data analysis, and Cloud computing, into the healthcare system (Tian et al. 2019). By adopting modern technology, conventional healthcare units are moving toward the smart industry. This transformation is mainly fueled by the rapid advancement in information and communication technology (ICT). The smart healthcare industry is

J. Ghosh (✉)
Chaitanya Bharati Institute of Technology (A), Hyderabad, India
e-mail: jeetghosh_ece@cbit.ac.in

S. D. P. Bikkuri
GITAM University, Bengaluru Campus, Bengaluru, India
e-mail: pbikkuri@gitam.edu

P. K. Malik and P. N. Shastry (eds.), *Internet of Things Enabled Antennas for Biomedical Devices and Systems*, Springer Tracts in Electrical and Electronics Engineering,
https://doi.org/10.1007/978-981-99-0212-5_6

more versatile, more personalized, and more efficient as well as convenient compared to the traditional one. Apart from versatile and personalized treatment, smart healthcare systems are capable of remote health monitoring facilities. Due to this feature, this advanced system would be more convenient for senior citizens. As per the recent population survey within the year 2045, the population of the senior citizen became more than the adults (Zikali 2018). Thus, it can be stated that, shortly, the smart healthcare industry turns out to be an inevitable part of the healthcare system. As a result of this, the smart hospital market was valued at USD 22.2 Billion worldwide in 2018 and it will be increased by a compound annual growth rate of 18% and reached USD 83.1 Billion in 2026 (Market and growing at a CAGR of 2021).

In the smart healthcare system, wireless medical devices play a pivotal role in continuously monitoring physiological data and simulating specific functionalities. These new generations of medical devices are incorporated with a telemetry unit to monitor the patient's physiological data and control the devices remotely. Generally, medical devices are categorized into three types according to their location inside or outside the patient's body (Kiourti and Nikita 2017). A schematic of different types of biomedical devices is shown in Fig. 6.1.

A. Wearable medical devices: These devices can be worn by the patient. The wearable devices are in form of accessories or embedded into the clothing and monitor several physiological data such as glucose or cardiac events and transmit it to the user's mobile or any control unit.
B. Implantable and Indigestive devices:

    a. Implantable Devices: These devices are implanted inside the patient's body through a surgical operation. These devices are mainly used for several applications such as artificial retinas, cardiac pacemakers, and intracranial pressure monitoring system.

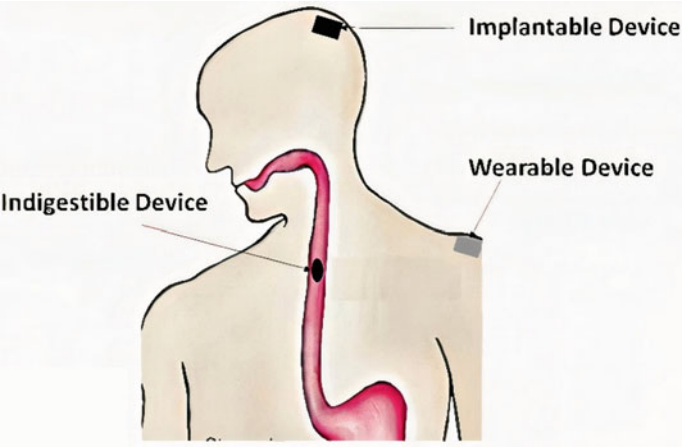

Fig. 6.1 Different types of medical telemetry devices

b. Ingestible Devices: This type of device is mainly used to monitor the physiological event in the food pipe and gastrointestinal tract. The ingestible devices are integrated over the capsule or pill in a way that the patient can swallow it easily.

Nowadays, implantable and ingestible devices are becoming the most popular and versatile for monitoring physiological data and simulating different functionalities. As the devices are implanted inside the human body, in the trial, these devices should pass the certain criterion proposed by the governing body such as the Federal Communications Commission (FCC) in Europe and the Department of Health and Human Services (HHS) of the Food and Drug Administration (FDA) in the USA.

These implantable biomedical devices have several advanced applications (Nikita 2014). These applications can be classified as follows:

a. Remote monitoring: A single device used to monitor the physiological data of a patient suffering from chronic diseases like diabetes, hypertension, etc.
b. Smart sensor network: Multiple interconnected sensor devices are engaged to collect different physiological data from the inside or over the human body.
c. Drug delivery feedback loop: Implantable devices deliver the drug at a particular location in the human body and continuously monitor the physiological data.
d. Rehabilitation: Implantable devices are used for the rehabilitation of the aged person.

Already, millions of patients affected by several diseases got benefited from the help of implantable telemetry devices (Topol 2013). Traditionally, wired biomedical devices are used for telemetry applications. However, wired connectivity has several drawbacks like restricted communication range, patient discomfort, and limited activity level. Due to these drawbacks, researchers are oriented to the development of wireless connectivity between the implantable unit and the remote/control section. In wirelessly connected biomedical devices, one of the most important sections is the antenna unit for providing connectivity.

Radio Frequency Allocation for Implantable Antenna

In the entire electromagnetic spectrum, certain spectra are retained for wireless medical applications in the radio frequency region. The allocated spectrum for medical applications will vary based on the regulations of the accredited organizations. The radio frequency spectrum is classified in terms of the license acquired for a particular application and the shared radio spectrum for other applications. Wireless medical device systems are regulated by three authorized agencies. The Federal Communication Commission (FCC) takes control of allocating the radio frequency spectrum, the Food and Drug Administration (FDA) looks at patient safety, and the Center for Medicare and Medicaid Services (CMS) is responsible for regulating the

cost. According to FCC (Federal Communication Commission), frequency spectrum allocations are classified as short range and long range.

Short-Range Telemetry Application

Frequency spectrum allocation for short-range medical devices regulated by FCC is as follows:

a. Inductive Implant—Small amount of data can be transmitted using Inductive Implant devices in their allocated frequency spectrum of 100 kHz (Soliman et al. 2021).
b. Medical Device Radio Communication Service (MDRC)—Wearable medical applications are band-limited to 100 kHz in 401–402 kHz and 405–406 kHz bands, respectively. From 402 to 405 kHz bandwidth of 300 kHz is permitted on the other hand (Fish & Richardson 2017).
c. Ultra-wide Band (UWB)—Especially for medical applications UWB is an emerging wireless frequency band with operability in 3.1–10.6 GHz frequency region. For short-range communication less than 1 m wireless medical devices operating under the UWB band support high data rate transfer of 1 Gbps.
d. Medical Micropower Networks (MMNs)—The MMNs frequency band is assigned from 413 to 457 MHz. This frequency band is subdivided into four frequency segments with a 6 MHz frequency region (Zhao et al. 2010).
e. Medical Body Area Networks (MBANs)—Medical body area networks aim to monitor human body conditions in the allocated spectrum of 2360–2400 MHz (Chirwa et al. 2003).
f. Wi-Fi, Bluetooth, and Zigbee—FCC has declared frequency spectrum which can be used for short-range digital communication suitable for medical implants in 902–928, 2400–2483.5, and 5725–5850 MHz bands. These bands are named Wi-Fi, Bluetooth, and Zigbee.

Long-Range Telemetry Application

When the communication is happening between 30 m and 10 km for medical applications, then the type of medical devices used for establishing communication is termed Long-Range Medical Devices and the communication is Long-range communication. For diverse medical applications, the frequency spectrum allocation is as follows:

a. Wireless Medical Telemetry Services (WMTS)—The objective of WMTS is to monitor patients' health conditions through wireless links bi-directionally. FCC has allotted 13 MHz spectrum for WMTS in the 608–614, 1395–1400, and 1427–1429 MHz.

b. World Interoperability for Microwave Access (WiMAX)—WiMAX is very efficient in data transfer which is required for establishing communication between hospitals and ambulances. As per IEEE 802.16, the frequency band allocated for WiMAX is 2.5 GHz with data transmitting capabilities of nearly 70 Mbps.

Challenges for the Designing of the Implantable Antenna

As explained in the above section, a limited number of the frequency band is allocated for the implantable telemetry application. Thus, the antenna and the transmitting unit should be tuned properly to transmit and receive the electromagnetic signal in a specific frequency region. Apart from this, there are several factors that are need to be considered for designing the implantable antenna unit.

Effect of Human Tissue on the Antenna Performance

The propagation, reflection, and attenuation of the electromagnetic waves are strongly affected by the human tissue. Thus, in the implantable antenna, we need to consider the effect of lossy tissue on the radiation property of the antenna. It should be stated that the temperature and the perfusion of liquid shall also affect the property of the radiated wave. However, these secondary effects are not normally considered.

In order to understand the effect of human tissue, one needs to model the different type of tissue with the help of electromagnetic parameters such as permittivity (ε), permeability (μ), and conductivity (σ) in a software simulation platform. As the human body is non-magnetic, the permeability of the tissues is assigned to unity. In the case of magnetic resonance imaging, one needs to consider the permeability separately (Nikita 2014). The main challenge of modeling the dielectric parameter of the human body is that for a different type of tissue $\varepsilon and \sigma$ are different. Apart from this, the tissue parameters are also frequency-dependent.

In this regard, Gabriel et. al. reported a comprehensive study of measuring the permittivity and conductivity of 25 types of tissue in the human body. They measure these parameters by open-ended coax technique at 20–37 °C temperature for the 1 MHz to 20 GHz frequency range (Gabriel et al. 1996). A model based on 4 Cole–Cole expressions is reported to find out the dielectric constant of the human tissue (Gabriel et al. 1996; Fujii et al. 2003). The expression is expressed as

$$\varepsilon_r(\omega) = \varepsilon_\infty + \sum_{m=1}^{4}\left[\frac{\Delta\epsilon_m}{1+(j\omega\tau_m)^{1-\alpha_m}}\right] + \frac{\sigma_i}{j\omega\varepsilon_o} \tag{6.1}$$

In this expression, ε_∞ is the material's relative permittivity at the THz frequency region. The ε_o indicate the free space impedance. The variables ϵ_m, τ_m, and α_m indicate the material parameters at the specific dispersion regions. As the dielectric

constant is a complex term, it can be expressed as

$$\varepsilon_r(\omega) = \varepsilon_r^{'}(\omega) - j\varepsilon_r^{''}(\omega) \tag{6.2}$$

The conductivity and skin depth (δ) are defined as

$$\sigma(\omega) = \varepsilon_r^{''}(\omega)\varepsilon_o\omega \tag{6.3}$$

And

$$\delta(\omega) = \frac{1}{\omega}\left\{\frac{\mu^{'}\varepsilon_o\varepsilon_r^{'}(\omega)}{2}\left[\left(1+\left(\frac{\sigma(\omega)}{\omega\varepsilon_o\varepsilon^{'}(\omega)}\right)^2\right)^{\frac{1}{2}}-1\right]\right\} \tag{6.4}$$

With the help of Eqs. (6.1) to (6.4), one can model the different tissues in the human body. Generally, human tissue can be divided into two types based on water content. The low water content tissues have low permittivity and conductivity such as fat and bone. On the other hand, if the tissue contains more water, the permittivity and conductivity are increased, like muscle, skin, heart, etc. Almost all internal organ tissues with high water content have similar electromagnetic (EM) properties. With the increase in frequency, the permittivity of the human tissue decreases whereas the conductivity increases. This phenomenon indicates that at the higher frequency region, the human tissue became lossy. To model a human torso, a multilayer model is required. As the internal organs have a similar dielectric property to muscle, they can be grouped. The dielectric property of the human tissue in the MICS band (402 MHz) is enlisted in Table 1 (Kiourti et al. 2012).

Biocompatibility Issues in Implantable Antenna

In the implantable environment, the biocompatibility of the material is one of the important issues to be a concern. Biocompatibility can be defined as the capability of a material to exist in harmony with a biological tissue environment. Thus, the implantable devices should be developed or encapsulated by a biocompatible material. Moreover, as the human tissues are conductive, the implantable unit would be short-circuited if it is not covered by an insulator. Considering this fact, the most popular approach is to cover the antenna with the superstrate dielectric layer. Commonly, the biocompatible material such as Teflon ($\varepsilon r = 2.1$, $\tan\delta = 0.001$), MACOR ($\varepsilon r = 6.1$, $\tan\delta = 0.005$), and ceramic alumina ($\varepsilon r = 9.4$, $\tan\delta = 0.006$) (Soontornpipit et al. 2004) are used. In some reported work, for achieving biocompatibility, a low-cost thin coating (e.g., zirconia ($\varepsilon r = 29$, $\tan\delta \approx 0$) (Skrivervik and Merli 2011), polyether ether ketone (PEEK) ($\varepsilon r = 3.2$, $\tan\delta = 0.01$) (Skrivervik and Merli 2011), and Silastic MDX–4210 Biomedical-Grade Base Elastomer ($\varepsilon r = 3.3$, $\tan\delta \approx 0$)) are used. It is also reported in the literature (Abadia et al. 2009) that

a properly designed biocompatible encapsulation can help to lower the amount of loading effect over the implantable antenna and also offer a smooth transition of the electromagnetic energy to the dispersive human tissue medium.

Safety Consideration of the Implantable Antenna

After the design, the medical devices should pass all the safety standards. Generally, the safety performance of the devices is tested by the in-vivo and animal explanations. The actual field density, dissipated electromagnetic power, and absorbed energy are monitored and further extrapolated to the human being. One of the important parameters regarding safety is the specific absorption rate (SAR) and defined as (Nikita 2014)

$$SAR = \sigma \frac{|E|^2}{\rho} \tag{6.5}$$

where E is the RMS value of the electric field (V/m), σ is the conductivity (S/m) of the human tissue, and ρ is the tissue density (kg/m^3). Particularly, it is specified by the FCC that the maximum SAR limit is 1.6 W/kg as averaged over 1 g of tissue.

Size Consideration of Implantable Antenna

One of the most important aspects of designing the implantable antenna is the size of the unit. It is well known that the implantable antenna size should be as small as possible. However, the antenna should operate in the allocated frequency region and have a sufficient gain for the communication. If the designer considers designing a $\lambda/4$ or $\lambda/2$ antenna at a lower MICS frequency band, the dimension of the antenna makes them useless and impractical in implantable conditions. There are several techniques used by the researcher to reduce the size of the antenna.

a. *Use of High-Permittivity Dielectric Material*: By using the high-permittivity material as a substrate, the resonance frequency of the antenna is shifted to the lower frequency region (Kiourti et al. 2011).
b. *Lengthening the current flow path*: It is well known that the resonance frequency of the antenna depends on the effective inductance and capacitance of the structure. If the designer can enhance the effective inductance of the structure, the antenna resonates at the lower frequency region. This phenomenon can be achieved by increasing the length of the metallic strip as well as the current flow path. As a result of it, the reactance component of the structure enhances and the resonance frequency-shifted towards the left side (Kiourti et al. 2011; Kiourti and Nikita 2011).

c. *Inclusion of the shorting pin*: By including the shorting pin between the ground plane and the radiator plane, one can be able to increase the inductance of the structure. As a result, the structure resonates at the lower frequency region (Kiourti et al. 2011).
d. Stacking multiple patches: By stacking multiple patches and sorting pins, one can reduce the antenna size.

Far-Field Gain Consideration

As the implantable antennas in biomedical devices are used for telemetry operation, the gain in the far field is an important factor. Generally, the exterior unit is placed around a 2 m distance from the patient's body (Nikita 2014). Thus, the signal should be transmitted with enough power that the exterior unit can catch and process the same. It should be mentioned that due to patient safety and interference issues, the input power in the implantable antenna is limited. Thus, to enhance the range of the communication, the gain of the implantable antenna should be sufficient. However, the miniaturized antenna has a very small effective aperture which degrades the gain of the antenna. The designer should tackle these tradeoffs between the size and gain of the antenna. Furthermore, the dielectric property of the human tissues is highly complex and asymmetric. The lossy nature of the tissues reduces the effective gain of the antenna and the asymmetric dielectric property provides a distorted and inhomogeneous radiation pattern (Kiourti et al. 2011; Kiourti and Nikita 2012). Thus, for designing an implantable antenna, engineers should consider all of these criterias. In the next section of this chapter, state-of-the-art scenario of the implantable antenna technology is discussed in brief.

Recent Development in Implantable Antenna Technology

By considering the abovementioned facts, several strategies are used to design implantable antenna units. For a better understanding of the reported works, we subdivided the section into the following parts.

Miniaturized Linearly Polarized Implantable Antenna

As discussed in the previous section, one of the main features of the implantable antenna is its miniaturized size of the antenna. For the telemetry application, in Xia et al. (2009), an H-shaped cavity slot antenna has been reported. In this work, a 2/3 human muscle phantom model is used for analyzing the antenna performance.

Despite the very miniaturized dimension of 1.6mm × 2.8mm × 4mm, the three-dimensional configuration may not be suitable for several applications. To provide more miniaturization and compactness, researchers are mainly focusing on the planar geometry-based configuration. The most conventional technique for miniaturization is to enhance the current flow path of the antenna. By embedding the meander slot and open slot in the ground plane along with the inclusion of shorting pin, a significant size reduction is achieved (Liu et al. 2012). Due to the modification of the ground plane, with the dimension of 10mm × 16mm × 1.27mm, the antenna is operating at a low MICS band of 402–405 MHz frequency region. In (Liu et al. 2012), a significant reduction in the height of the antenna is observed. A similar type of approach has been presented in Li and Xiao (2014) for the reduction of the size of the antenna. For more miniaturization and compactness, several researchers loaded periodic structures over the antenna. In (Das and Mitra 2018), Das et. al. reported a miniaturized grounded metamaterial-loaded implantable antenna for the telemetry application. In this work, a 2 × 2 metamaterial unit cell is incorporated over the slot antenna for achieving miniaturization and better radiation property. By including the metamaterial unit cell, the lateral dimension is reduced to 10mm × 10mm and provides a bandwidth of 57%.

Apart from the single band of operation, for several advanced applications, the dual and multiband operation is more desirable. Generally, dual frequency is required for providing a bio-telemetry link and wake-up signal. As power management is an important consideration of the implantable device, the device need not be active all the time for some specific application. Thus, a wake-up signal is required to transmit from the external units toward the implant. In this aspect, the MICS band is used for the bio-telemetry application whereas the ISM band is utilized for the wake-up signal reception (Samanta and Mitra 2019). Thus, in practical applications, such as an implantable continuous glucose monitoring system (CGM), a dual-band antenna is required to transmit and receive the physiological data and control signal simultaneously. For the CGM, system, a meander-shaped dual-band antenna operated at 402 MHz and 2.4 GHz has been presented in Karacolak et al. (2008). A multilayer solution has been reported by Sanchez-Fernandez et. al. for providing dual frequency of operation of the implant (Sánchez-Fernández et al. 2010). In this work, the feed line and the antenna are situated in different layers. As a result, a significant lateral size reduction has been achieved. A differential feed dual-band antenna has been reported in Duan et al. (2012) which can easily connect two different circuitries. An on-body repeater-based dual-band configuration has been proposed by Kiourti et al. (2014). In this work, a repeater is placed on the body to receive a signal from the implantable unit and retransmit it to the external unit. This type of configuration enhanced the telemetry range of the system. A scalp implantable miniaturized dual-band antenna system has been reported in Shah et al. (2019). The main feature of this simple antenna is its size. Within the volume of 24 mm^3, the structure provides a satisfactory gain in two frequency bands, i.e., 915 and 2450 MHz. A triple-band spiral-shaped implantable antenna operated at 402 MHz, 1.6 GHz, and 2.45 GH has been proposed (Xiao et al. 2016). With a very small size, 7 × 6.5 × 0.377 mm^3, the antenna provides a significant gain of more than -30 dB in all frequency regions.

It is noticeable that the gain of the antenna unit is always a concern for the designer. To overcome this problem, a multiple antenna approach is taken by several researchers. Apart from the miniaturization, one of the critical challenges for the designer is to control the coupling between the radiating elements. Due to coupling, the gain and pattern of the multiple antenna would be distorted (Ghosh et al. 2016). A helix line dual antenna structure has been reported in Xiao et al. (2016) for the MedRadio frequency band. A four-element MIMO antenna loaded with a decoupling unit consisting of an electromagnetic band gap (EBG) structure has been proposed by Fan. et. al. The incorporation of the EBG structure enhanced the complexity and loss of the structure (Fan et al. 2018). An alternative solution of loading vertical metallic strips in a multiple antenna approach is reported in Matekovits et al. (2017). The vertical strip is used to control the coupling between elements in the cost of increment in the vertical height of the antenna. In (Singh et al. 2021), the authors proposed an innovative hybrid method to control the coupling based on neutralized lines and defective ground structures. This planar solution provides significant gain and improvement in link margin without disturbing the radiation properties of the elements. However, all the aforementioned antennas are linearly polarized antennas. As the linear polarized antennas are affected due to the orientation, circular polarized (CP) antennas are the solutions.

Circular Polarized Implantable Antenna

In this section of the chapter, several reported implantable circular polarized antennas are discussed. In the case of a linear polarized antenna, the implantable antenna should maintain a fixed orientation. Due to the posture and mobility of the human body, it is difficult for the implantable device to maintain its orientation. To overcome this drawback, the circular polarized (CP) antenna would be the best solution. In (Liu et al. 2014a), a capacitively loaded microstrip patch antenna was reported. This multilayer configuration provides RHCP wave with a realized gain of −32 dB. A meander line loaded implantable CP antenna is reported in Liu et al. 2014b. Due to the loading of the meander line, the reported structure became miniaturized and operated at the 2.45 GHz frequency region (Liu et al. 2014b). For biocompatibility purposes, the antenna is encapsulated by silicon. A shorting pin and slot-loaded structure have been presented in Yang et al. (2017) and the antenna radiated RHCP wave at ISM band frequency. A wideband circular shape CP antenna with a bandwidth of 12.2% has been reported in Zhang et al. (2018). The diagonal slot in the reported antenna is mainly responsible for providing CP radiated waves at the 915 MHz frequency band. An ultra-miniaturized CP antenna with a dimension of 10.02mm × 10.02mm × 0.675mm has been reported in Xu et al. (2014). The reported structure radiates circularly polarized waves at 400 and 2400 MHz frequency regions. Another wideband solution for a continuous glucose monitoring system has been proposed in Li et al. (2016). The unequal length of the arm in this design is mainly responsible for the CP radiation. A dual-band reactive impedance surface-loaded implantable

antenna has been reported by Samanta et al. In this journal paper, the author has proposed a meander shape loop antenna loaded with a rectangular ring reactive impedance surface (Samanta and Mitra 2019). This reported antenna provides a 123% impedance bandwidth with 15% and 8.7% axial ratio bandwidth at 920 MHz and 2.45 GHz frequency bands. A sufficient gain is obtained at both bands which maintains a link margin of more than 0 dB for a transmission distance of up to 10 m. A circular reactive impedance surface-loaded antenna has been also reported by Samanta et al. in Samanta and Mitra (2020). In this work, the authors encapsulated the antenna with Al_2O_3 for biocompatibility issues. Recently, a circular polarized cubic multi-antenna system is reported in Kaim et al. (2020). However, the CP wave is affected by the depolarization due to human tissues and essentially results in linear polarization (Bao 2018). Thus, it is noticeable that like a linear polarized antenna, circular polarized antennas also have some drawbacks which became acute for some specific applications such as deep implant systems. In (Bhattacharjee et al. 2019), Bhattacharjee et al. has proposed a dual-polarized antenna for implantable application. In this proposed design, the reported antenna provides LP radiation at 2.4 GHz frequency and CP radiation at 5.8 GHz frequency region.

Capsule and Ingestible Antenna

Ingestible and capsule medical devices are mainly used for endoscopy purposes. These devices look like a capsule and can be swallowed by the patient. The capsule antennas are installed over this pill-like medical device. Thus, the antenna size should be very small and miniaturized. While this type of capsule medical device traveling through the gastrointestinal track, it collects and transmits real-time video and other physiological data to the external unit. This capsule Endoscopy has become a promising wireless technique for detecting GI (Gastrointestinal)-related diseases. For the telemetry application, capsule medical devices should contain very miniaturized microstrip-based antennas. A schematic of a capsule-based implantable device is shown in Fig. 6.2. The meandering configuration of the antenna is a very popular technique for miniaturization (Wang et al. 2022; Neebha and Nesasudha 2018). Besides this, conformal antennas are also very useful for endoscopy applications.

Antenna Placement Analysis

The placement of the antenna and its analysis is one of the important aspects for the antenna designer. The radiation property of the antenna is affected by the closely placed other electronic equipment such as sensor, battery, and RF circuitry. In (Shah and Yoo 2018), the antenna is placed in the two types of system architecture and the radiation property of the antenna has been analyzed. The schematic of the system architecture is shown in Fig. 6.3. As the electronic equipment such as circuitry and

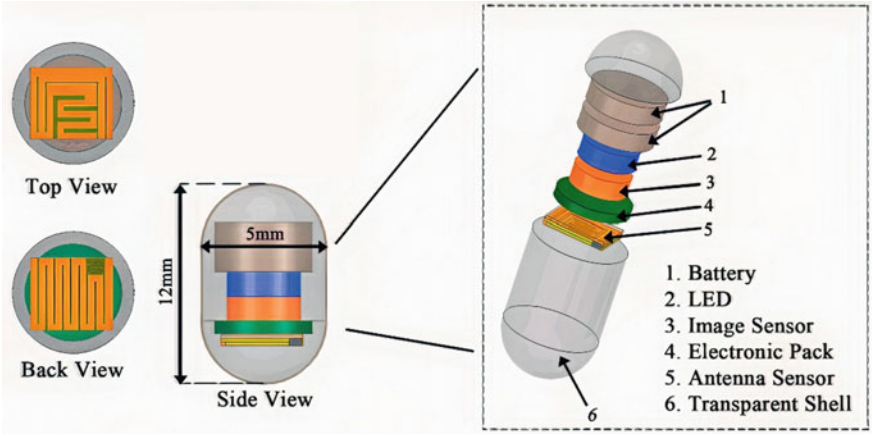

Fig. 6.2 Detailed architecture of the capsule endoscopy system (Wang et al. 2022)

battery are shielded by the metallic box, a PEC layer can be used to mimic the electronic equipment. In the reported system architecture, the radiation property of the antenna have been analyzed. The schematic of the system architecture is shown in Fig. 6.3. As the electronic equipment such as circuitry and battery are shielded by the metallic box, a PEC layer can be used to mimic the electronic equipment. In the reported work (Shah and Yoo 2018; Singh et al. 2021), it is observed that the antenna should be placed in such a way that the radiation property is not affected significantly. A novel approach based on the mantle cloaking method is presented in Ghosh and Mitra (2020). Here, the author proposed that the radiation property of the antenna was restored by covering the electronic equipment with an efficiently designed mantle.

Measurement and Testing of the Antenna

After the design and fabrication of the device as well as the antenna, one needs to test and measure the devices in the actual environment. However, for primary testing, we cannot use the human body. The alternative approach is to use the animal sample for testing. However, animal testing is very expensive and highly regulated. Thus, live testing should be performed as the last stage of the development of an implantable antenna. At the design stage, benchtop testing is the best suitable option. There are two types of benchtop testing (a) Ex Vivo and (b) In vitro. After the successful Bench top testing, one should go for In vivo testing for final validation (Green et al. 2021; Smart Antennas: Latest Trends in Design and Application, "Springer" 2022; Malik et al. 2021; Rahim and Malik 2020).

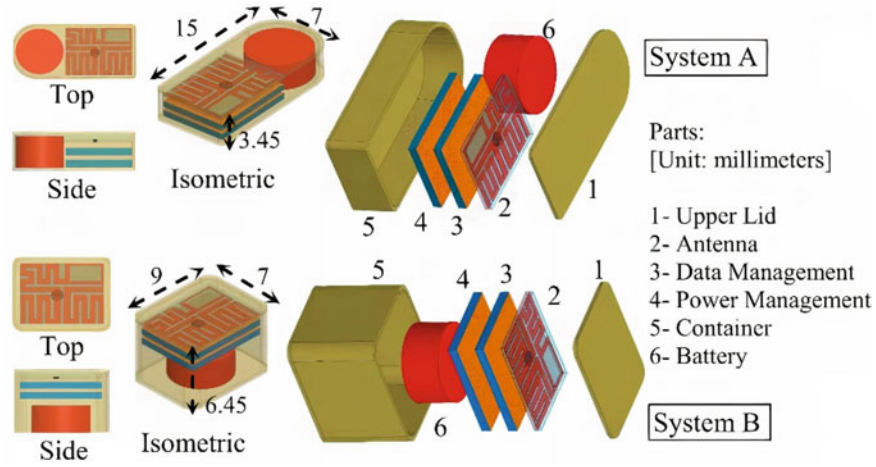

Fig. 6.3 Implantable antenna with the system (Shah and Yoo 2018)

Ex Vivo Testing

"Ex vivo" is a Latin word that means "out of the living". In the ex vivo testing, we measure the implantable devices inside the extracted tissue from the animal. The tissue can be extracted from the laboratory animal or from the slaughterhouse. It should be mentioned that the tissue should be used very soon after the extraction. The Ex Vivo method is very useful for the measurement of the radiation property of the antenna. However, it has some limitations. After separating the tissue from the animal model, the tissues started to decay very quickly and change their dielectric property.

In Vitro Testing

To overcome the problem of ex vivo testing, in vitro testing is an alternative method. "In Vitro" means "inside the glass". In this technique, tissues are artificially developed outside the glass. For the antenna measurement purpose, dielectrically similar tissue-mimicking phantom. Though this phantom mimics the dielectric property of the tissue, it is unable to replicate the thermal, biological, and mechanical property of the tissue. Thus, the "in vitro" testing can only be used and reused for measurement and making them researcher and student-friendly.

In Vivo Testing

The "Ex vivo" and "In Vitro" testing methods have some advantages and disadvantages. But, these methods are not able to provide complete results. In this regard, in the final stage of product development, scientists need to test their implantable device in the "In vivo" or "In the living" technique. However, for the "In vivo" test model, one needs to take permission from the regulatory body.

Conclusion

In this chapter, we mainly focus on the design and development procedure of implantable antenna for bio-telemetry applications. In specific, frequency selection, challenges, biocompatibility, and safety features of implantable antennas have been addressed thoroughly along with the state-of-the-art scenario implantable antenna. Furthermore, the measurement and testing of the implantable system are also discussed in brief. Thus, it can be concluded that the designing of the implantable antenna is a very sophisticated field. The designing team should consist of several interdisciplinary researchers with expertise in different fields such as material science, electronics, chemistry, and biology. Thus, it is necessary to re-consider and perform a rigorous research for analysis of the safety feature of implantable devices for the healthcare system. In the very near future, these implantable medical devices with telemetry features became an inevitable part of the healthcare system.

References

Abadia J, Merli F, Zürcher JF, Mosig JR, Skrivervik AK (2009) 3D-spiral small antenna design and realization for biomedical telemetry in the MICS band. Radioengineering 18:359–367

Bahl I, Bhartia P, Stuchly S (1982) Design of microstrip antennas covered with a dielectric layer. IEEE Trans Antennas Propag 30(2):314–318

Bao Z (2018) Comparative study of dual-polarized and circularly-polarized antennas at 2.45 GHz for ingestible capsules. IEEE Trans Antennas Propag 67(3):1488–1500

Bhattacharjee S, Maity S, Chaudhuri SRB, Mitra M (2019) A compact dual-band dual-polarized omnidirectional antenna for on-body applications. IEEE Trans Antennas Propag 67(8):5044–5053

Chirwa LC, Hammond PA, Roy S, Cumming DR (2003) Electromagnetic radiation from ingested sources in the human intestine between 150 MHz and 1.2 GHz. IEEE Trans Biomed Eng 50(4):484–492

Das S, Mitra D (2018) A compact wideband flexible implantable slot antenna design with enhanced gain. IEEE Trans Antennas Propag 66(8):4309–4314

Duan Z, Guo YX, Xue RF, Je M, Kwong DL (2012) Differentially fed dual-band implantable antenna for biomedical applications. IEEE Trans Antennas Propag 60(12):5587–5595

Fan Y, Huang J, Chang T, Liu X (2018) A miniaturized four-element MIMO antenna with EBG for implantable medical devices. IEEE J Electromagnet RF Microwaves Med Biol 2(4):226–233

Fish and Richardson (2017) Wireless medical technologies: navigating government regulation in the new medical age. Fish & Richardson, Boston, MA, USA, pp 1–36
Fujii K, Ito K, Tajima S (2003) A study on the receiving signal level in relation with the location of electrodes for wearable devices using human body as a transmission channel. In: IEEE antennas and propagation society international symposium. Digest. Held in conjunction with: USNC/CNC/URSI North American Radio Sci. Meeting (Cat. No. 03CH37450), vol 3). IEEE, pp 1071–1074
Gabriel S, Lau RW, Gabriel C (1996) The dielectric properties of biological tissues: III. Parametric models for the dielectric spectrum of tissues. Phys Med Biol 41(11):2271
Ghosh J, Mitra D (2020) Restoration of antenna performance in the vicinity of metallic cylinder in implantable scenario. IET Microw Antennas Propag 14(12):1440–1445
Ghosh J, Ghosal S, Mitra D, Chaudhuri SRB (2016) Mutual coupling reduction between closely placed microstrip patch antenna using meander line resonator. Progress Electromagnet Res Lett 59:115–122
(2021) Global Smart Hospital Market growing at a CAGR of 18.0%. In: GMI Research. https://www.gmiresearch.com/global-smart-hospital-market-share-trends-growth-opportunity/
Green RB, Smith MV, Topsakal E (2021) In vitro and in vivo testing of implantable antennas. Antenna Sensor Technol Modern Med Appl 145–189
Kaim V, Kanaujia BK, Rambabu K (2020) Quadrilateral spatial diversity circularly polarized MIMO cubic implantable antenna system for biotelemetry. IEEE Trans Antennas Propag 69(3):1260–1272
Karacolak T, Hood AZ, Topsakal E (2008) Design of a dual-band implantable antenna and development of skin mimicking gels for continuous glucose monitoring. IEEE Trans Microw Theory Tech 56(4):1001–1008
Kiourti A, Nikita KS (2012) Miniature scalp-implantable antennas for telemetry in the MICS and ISM bands: design, safety considerations and link budget analysis. IEEE Trans Antennas Propag 60(8):3568–3575
Kiourti A, Nikita KS (2017) A review of in-body biotelemetry devices: implantables, ingestibles, and injectables. IEEE Trans Biomed Eng 64(7):1422–1430
Kiourti A, Costa JR, Fernandes CA, Santiago AG, Nikita KS (2012) Miniature implantable antennas for biomedical telemetry: from simulation to realization. IEEE Trans Biomed Eng 59(11):3140–3147
Kiourti A, Costa JR, Fernandes CA, Nikita KS (2014) A broadband implantable and a dual-band on-body repeater antenna: design and transmission performance. IEEE Trans Antennas Propag 62(6):2899–2908
Kiourti A, Nikita KS (2011) Meandered versus spiral novel miniature PIFAs implanted in the human head: tuning and performance. In: International conference on wireless mobile communication and healthcare. Springer, Berlin, Heidelberg, pp 80–87
Kiourti A, Christopoulou M, Nikita KS (2011) Performance of a novel miniature antenna implanted in the human head for wireless biotelemetry. In: 2011 IEEE international symposium on antennas and propagation (APSURSI). IEEE, pp 392–395
Li R, Xiao S (2014) Compact slotted semi-circular antenna for implantable medical devices. Electron Lett 50(23):1675–1677
Li H, Guo YX, Xiao SQ (2016) Broadband circularly polarised implantable antenna for biomedical applications. Electron Lett 52(7):504–506
Liu C, Guo YX, Xiao S (2012) A hybrid patch/slot implantable antenna for biotelemetry devices. IEEE Antennas Wirel Propag Lett 11:1646–1649
Liu C, Guo YX, Xiao S (2014a) Circularly polarized helical antenna for ISM-band ingestible capsule endoscope systems. IEEE Trans Antennas Propag 62(12):6027–6039
Liu C, Guo YX, Xiao S (2014b) Capacitively loaded circularly polarized implantable patch antenna for ISM band biomedical applications. IEEE Trans Antennas Propag 62(5):2407–2417
Malik PK, Kumar P, Kumar S, Singh DK (2021) Smart antennas: recent trends in design and applications. Bentham Science, Sharjah, United Arab Emirates. ISSN: 2717–5421 (Print), ISSN:

2717–543X (Online), ISBN: 978–1–68108–860–0 (Print). https://doi.org/10.2174/9781681088594121020 1

Malik P, Lu J, Madhav BTP, Kalkhambkar G, Amit S (eds) (2022) Smart antennas: latest trends in design and application. Springer. ISBN 978–3–030–76636–8. https://doi.org/10.1007/978-3-030-76636-8

Matekovits L, Huang J, Peter I, Esselle KP (2017) Mutual coupling reduction between implanted microstrip antennas on a cylindrical bio-metallic ground plane. IEEE Access 5:8804–8811

Neebha TM, Nesasudha M (2018) Analysis of an ultra miniature capsule antenna for gastrointestinal endoscopy. Eng Sci Technol Int J 21(5):938–944

Nikita KS (ed) (2014) Handbook of biomedical telemetry. John Wiley & Sons

Rahim A, Malik PK (2020) Design methodologies and tools for 5G network development and application, Ch 10: analysis and design of planner wide band antenna for wireless communication applications: fractal antennas, vol 13. IGI Global USA, pp 196–208. https://doi.org/10.4018/978-1-7998-4610-9.ch010

Samanta G, Mitra D (2019) Dual-band circular polarized flexible implantable antenna using reactive impedance substrate. IEEE Trans Antennas Propag 67(6):4218–4223

Samanta G, Mitra D (2020) Miniaturised and radiation efficient implantable antenna using reactive impedance surface for biotelemetry. IET Microw Antennas Propag 14(2):177–184

Sánchez-Fernández CJ, Quevedo-Teruel O, Requena-Carrión J, Inclán-Sánchez L, Rajo-Iglesias E (2010) Dual-band microstrip patch antenna based on short-circuited ring and spiral resonators for implantable medical devices. IET Microw Antennas Propag 4(8):1048–1055

Shah SAA, Yoo H (2018) Scalp-implantable antenna systems for intracranial pressure monitoring. IEEE Trans Antennas Propag 66(4):2170–2173

Shah IA, Zada M, Yoo H (2019) Design and analysis of a compact-sized multiband spiral-shaped implantable antenna for scalp implantable and leadless pacemaker systems. IEEE Trans Antennas Propag 67(6):4230–4234

Singh MS, Ghosh J, Ghosh S, Sarkhel A (2021) Miniaturized dual-antenna system for implantable biotelemetry application. IEEE Antennas Wirel Propag Lett 20(8):1394–1398

Skrivervik AK, Merli F (2011) Design strategies for implantable antennas. In: 2011 loughborough antennas & propagation conference. IEEE, pp 1–5

Soliman MM, Chowdhury ME, Khandakar A, Islam MT, Qiblawey Y, Musharavati F, Zal Nezhad E (2021) Review on medical implantable antenna technology and imminent research challenges. Sensors 21(9):3163

Soontornpipit P, Furse CM, Chung YC (2004) Design of implantable microstrip antenna for communication with medical implants. IEEE Trans Microw Theory Tech 52(8):1944–1951

Tian S, Yang W, Le Grange JM, Wang P, Huang W, Ye Z (2019) Smart healthcare: making medical care more intelligent. Global Health J 3(3):62–65

Topol EJ (2013) The creative destruction of medicine: how the digital revolution will create better health care. Basic Books

Wang GB, Xuan XW, Jiang DL, Li K, Wang W (2022) A miniaturized implantable antenna sensor for wireless capsule endoscopy system. AEU-Int J Electron Commun 143:154022

Xia W, Saito K, Takahashi M, Ito K (2009) Performances of an implanted cavity slot antenna embedded in the human arm. IEEE Trans Antennas Propag 57(4):894–899

Xiao S, Liu C, Li Y, Yang XM, Liu X (2016) Small-size dual-antenna implantable system for biotelemetry devices. IEEE Antennas Wirel Propag Lett 15:1723–1726

Xu LJ, Guo YX, Wu W (2014) Miniaturized dual-band antenna for implantable wireless communications. IEEE Antennas Wirel Propag Lett 13:1160–1163

Yang ZJ, Xiao SQ, Zhu L, Wang BZ, Tu HL (2017) A circularly polarized implantable antenna for 2.4-GHz ISM band biomedical applications. IEEE Antennas Wirel Propag Lett 16:2554–2557

Zhang Y, Liu C, Liu X, Zhang K, Yang X (2018) A wideband circularly polarized implantable antenna for 915 MHz ISM-band biotelemetry devices. IEEE Antennas Wirel Propag Lett 17(8):1473–1477

Zhao D, Hou X, Wang X, Peng C (2010) Miniaturization design of the antenna for wireless capsule endoscope. In: 2010 4th international conference on bioinformatics and biomedical engineering. IEEE, pp 1–4

Zikali Z (2018) No suitable care for SA's elderly population | Health-e. In: Health-e. https://health-e.org.za/2018/08/22/no-suitable-care-for-sas-elderly-population/

Chapter 7
Design of Compact Low-Profile Antenna for Wearable Medical Applications

T. Sathiyapriya, K. C. Rajarajeshwari, T. Poornima, and Sumit Agarwal

Abstract The development of Multifunctional Fabric Antennas for Biomedical Applications at 2.36–2.45 GHz ISM Band is proposed here. Using Wireless Body Area Network (WBAN) technology, a low-profile Wearable microstrip patch antenna is built and proposed in this study for continuous detection of patient monitoring, including cardiac output, heartbeat, and respiration. During the course of our work, we developed prototype antennas using a variety of substrate materials, including Teflon, Polyimide, Polytetrafluoroethylene (PTFE), Nylon, and Polystyrene. For metrics like Reflection coefficient, Gain, Directivity, VSWR, Efficiency, and Bandwidth, the built-in antenna was simulated and compared. To achieve better return loss, VSWR, and gain, geometry is modified like S-shaped antenna that operates at 2.5 GHz. At 2.5 GHz, the optimum reflection coefficient values of −45, −38, −25, and −28 dB were obtained against different substrates like polyimide, Teflon, PTFE, and polystyrene, respectively.

Keywords Biomedical antenna · WBAN · Wearable · IoT healthcare

T. Sathiyapriya (✉) · K. C. Rajarajeshwari
ECE Department, Dr. Mahalingam College of Engineering and Technology, Coimbatore, India
e-mail: sathyatsp@gmail.com

K. C. Rajarajeshwari
e-mail: rajarajeshwari@drmcet.ac.in

T. Poornima
Space Machines Company, Bangaluru, India
e-mail: poorvipoornima.t@gmail.com

S. Agarwal
Pennsylvania State University, State College, PA 16802, USA
e-mail: sua347@psu.edu

P. K. Malik and P. N. Shastry (eds.), *Internet of Things Enabled Antennas for Biomedical Devices and Systems*, Springer Tracts in Electrical and Electronics Engineering,
https://doi.org/10.1007/978-981-99-0212-5_7

Introduction

As a result of longer lifespans, which is mostly due to the significant advancements in public health, nutrition, and medicine, the world's aging population has been quickly expanding. By 2035, it is expected that there will be an increasing number of older people; the number of people aged 85 years and over was estimated to be 1.7 million in 2020 (2.5% of the UK population) and this is projected to almost double to 3.1 million by 2045 (4.3% of the UK population) (Office of National Statistics 2022), nearly two times as many people over the age of 65 in the United States (National Institute and on Aging (NIA) 2016), twice as many people over the age of 60 in the People's Republic of China (https://worldpopulationreview.com/countries/china-population, 2022), and by 2050, Japan will have the oldest population in recorded history, with an average age of 52 (https://worldpopulationreview.com/countries/china-population, 2022). In many affluent nations, public healthcare systems are simultaneously dealing with a rise in the number of individuals being diagnosed with chronic conditions like obesity and diabetes. These chronic diseases are caused by improper food, a sedentary lifestyle, and insufficient physical exercise rather than just the aging of the population (U.S. Department of Health and Human Services 2020; World Health Organization, Food and Agriculture Organization of the United Nations 2018). By 2030, diabetes is predicted to overtake heart disease as the seventh greatest cause of death, according to the World Health Organization (WHO) (https://www.who.int/news-room/fact-sheets/detail/noncommunicable-diseases#:~:text=Key%20facts,%2D%20and%20middle%2Dincome%20countries). Diabetes is a significant condition due to its chronic nature, both for members and for healthcare organizations. These estimates and figures show that the expense of healthcare systems is rising dramatically as a result of the ongoing provision of medical treatment to patients with chronic illnesses and the growing population of older individuals with varied health issues (Switzerland. xxxx; Bodenheimer et al. 2009; Hayes and Gillian 2020). As a result, healthcare systems cannot continue as they are now (Bodenheimer et al. 2009; Bhargava 2021). Early disease identification and diagnosis, in the opinion of scientists (Jazieh and Kozlakidis 2020; Botha et al. 2014; Tossaint-Schoenmakers et al. 2021; Lehnert et al. 2011), is crucial because it both helps to successfully halt the progression of sickness (Lehnert et al. 2011; Yach et al. 2004; Leifer 2003) and greatly lowers the expense of healthcare systems.

The use of wireless technology in medical devices has increased recently. Implantable and wearable wireless sensors may now include radio transceivers and biological sensor devices due to significant advancements in microelectronics. These gadgets record and keep track of a patient's essential physiological data before sending it to a remote node within, on, or near the body (Levin and Stevens 2011) (Fig. 7.1).

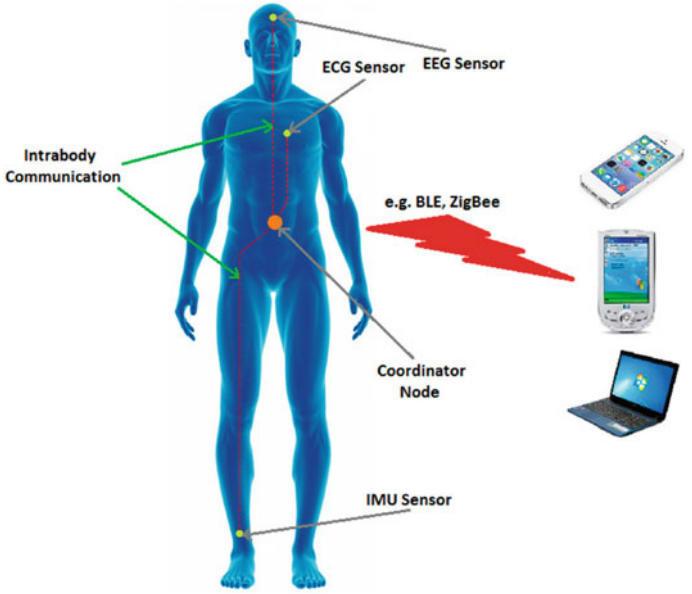

Fig. 7.1 Remote health monitoring systems

The classification of body-centric wireless communication

Off-body, on-body, or in-body wireless body-centric communication is categorized as part of personal area networks and body-area networks (Alzheimer's Association Report 2011). The first kind of communication occurs between an off-body system or device and an on-body one. Within on-body networks and wearable devices, the second class serves as the wireless communication interface. The third class is wireless communication to sensor networks and medical implants (Fig. 7.2). In reality, all three types of body-centric communication are used in an integrated system, and clear distinctions between them may not always be made. Even yet, the categorization may be used to show the many difficulties that wearable and implantable antennas must overcome.

IOT-based Wireless Healthcare monitoring system

The IoT-enabled health monitoring system is very different than the conventional health care system. Because of this, IoT makes it harder to get the results and performance that are needed. As all sensors are connected to voltage signals, working with IoT systems is analogous to working in the embedded domain (Pahwa and Lyons 2010). Initially, equipment such as sensors, detectors, monitors, and the microcontroller are connected so that they can operate in accord. The microcontroller performs the analog-to-digital conversion so that data may be read in the proper digital format. The converted data is sent as an input signal to a Microcontroller in an IoT Board, with Raspberry Pi being the most often used microcontroller these days (Fig. 7.3).

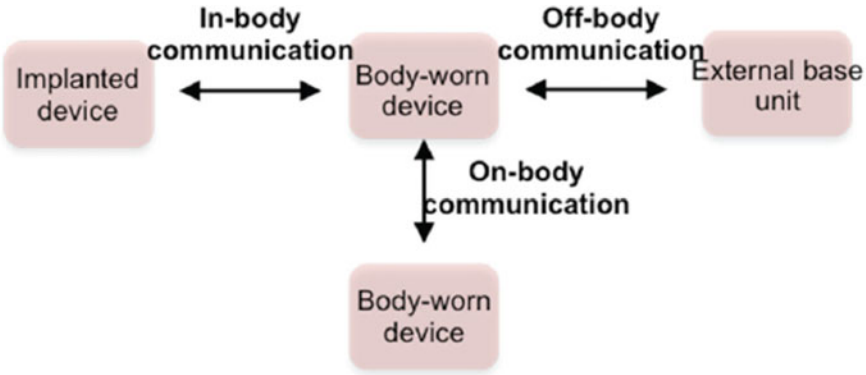

Fig. 7.2 Body-centric wireless communication

Fig. 7.3 Autonomous health monitoring system

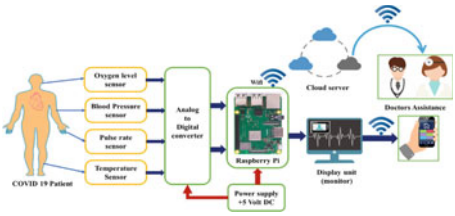

System Support during Covid Pandemic

The global spread of the COVID-19 pandemic has significantly altered people's daily lives dramatically. The delayed manufacturing and distribution of vaccinations has put a strain on both developing and wealthy nations' health systems (Garcia-Pardo et al. 2018). Thus, various governments are quite concerned about the surveillance of COVID-19 infected and recovered patients in the wards (Hall and Hao 2006; Bhardwaj et al. 2022; Momtazmanesh et al. 2020; Iftekhar et al. 2021). As COVID-19 spread can be mitigated by implementing an Internet of things (IoT)-based remote health monitoring system. Biomedical signals can provide information about a person's health; a large amount of data can be collected, and suitable conclusions can be drawn from observation. The Internet of Things has revolutionized the lives of individuals, particularly senior patients, by providing continuous monitoring of health issues. Wearables such as fitness bands and other remotely connected gadgets such as blood pressure and pulse monitors provide patients with access to individualized care. These devices may be customized to send reminders for step count, water consumption, doctor's visits, blood pressure variations, and more. Pulse count, SPO2, temperature, blood pressure, and some other biological data might be detected to identify the COVID-19. Artificial Intelligence techniques might be used to detect COVID-19 patients from a vast quantity of data by monitoring health markers and storing them on the cloud via IoT (Thapliyal et al. 2021). The

combination of machine learning with IoT will be beneficial in a variety of ways. IoT technology would assist public health officials in segregating patients who require immediate care from those who might be isolated at home removing the big patient bubble from hospitals and neighborhood health centers (Priesemann et al. 2021).

The smart health monitoring system based on IoT might minimize the need for O2 in hospitals. This device might possibly be equipped with a GPS chip to track the position of the rescued patient. During a lockdown situation, the individuals' data is shared with the health authorities, and the potentially contaminated individuals are isolated as soon as feasible. An autonomous health monitoring system that reacts or generates an alarm in the event of a patient's severe condition is to be devised (Islam et al. 2020; Kumar and Mukesh 2013). The data is evaluated using the Node MCU microcontroller to deliver notifications to physicians and concerned individuals through emails. It also stores and keeps track of previous diagnostic information about the patient's health. The patient's real status is relayed to medical specialists via an Internet portal, and the right medication may be administered to cure the patient.

System Requirements and challenges of WBAN

1. **Challenges Presented by E-Textiles**

The characterization of the physical layer of the network is an essential phase in the process of developing a WBAN. This step involves making an estimate of the delay spread as well as the path loss between any two nodes located on the body. In order to accomplish this goal, a comprehensive assessment of the electromagnetic wave propagation and antenna behavior close to the human body is required. For both the conductive portions and the substrate, textile materials may be used effectively. Electronic chips and, in general, surface-mounted components (SMCs) must be able to be soldered to the conductive sections using tin solder (Levin and Stevens 2011) (Fig. 7.4).

2. **Data Rates**

Data rates vary significantly in the healthcare context due to the variety of Wireless Body Area Network applications. Low-data-rate sensors are required for On-Body sensors, while high-data-rate systems are encouraged for multimedia data transmission to the cloud (Khan et al. 2021). Burst transmission uses a lot of energy since it transmits data at a very high speed for a very short period of time. The reliability of wireless monitoring systems in medical applications depends on the data rates used. High data rate devices are best employed in low BER settings, while low data rate devices can survive high Bit Error Rate (BER) situations.

3. **Security and Privacy**

WBAN systems need security measures to ensure the safety, privacy, reliability, and confidentiality of patient health information. A supporting WBAN infrastructure must apply particular security processes (Khan et al. 2021). WBAN systems provide the security and privacy of patient information. Data is secure while sent, gathered,

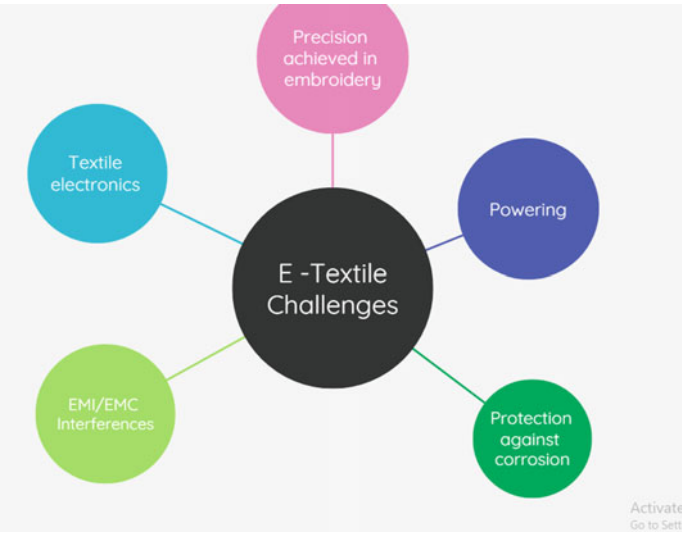

Fig. 7.4 E-textile challenges

processed, and stored. A patient may not want his/her information shared with insurance companies, which might deny coverage. Intruders may also modify information by physically grabbing a node, which can lead to a patient's death. Medical records may be used to find a patient's rivals. This sensitive and vital information should be protected from unwanted access, usage, and alterations (Islam et al. 2020; Srividya and Satyanarayana 2018; Roges and Malik 2021; Rahim and Malik 2021; Malik et al. 2020) (Fig. 7.5).

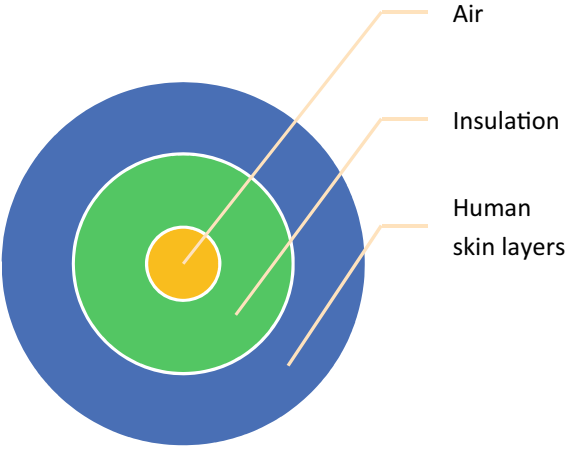

Fig. 7.5 Body sample for designing biomedical antenna

Antenna Layout

Implantable antennas must be bioavailable in order to guarantee human community safety implant rejection. Moreover, cell lines are sensitive, and if enabled to come into direct touch with the implanted antenna's passivation, they would short-circuit it. The prevention of unwanted short circuits is especially important in the case of antennas intended for long-term implantation. The hypothesized inverse E-shaped microstrip monopole antenna is mathematically constructed using ADS software to operate in the 2.5 GHz ISM band. The antenna is positioned on a different substrate material with a different dielectric constant. The overall dimensions of the antenna are $27 \times 15 \times 0.16$ mm^3, highlighting the design's compactness when compared to current antennas. Initially, the proposed antenna was designed without any ground structure and the reflection coefficient was very low. Then defected ground structure was made to improve the reflection coefficient. Even another dielectric layer was added to improve the desired gain. Different substrates were used to obtain the required results.

As shown in Fig. 7.6, the computed and measured reflection coefficients of the antenna in free space, with and without the DGS and dielectric ground structure, are compared. Meanwhile, the suggested EBG-enhanced antenna significantly increased. When the DGS and dielectric substrate is incorporated, both results show good impedance matching with a slight shift in the resonant frequency. The need for excellent dielectric (substrate/superstrate) materials: High-permittivity dielectrics are picked for surgically implanted radiating patch since they truncate the efficacious wavelength as well as lead to reduced resonance frequencies, aiding and abetting in antenna size reduction. Even with such high-permittivity dielectrics, the substrate layer insulates the antenna from the higher-permittivity tissue. Thicker substrates raise the working frequency of the antenna, necessitating larger physical dimensions to refine resonance. Dielectric materials with high permittivity values and thin substrate layers are therefore sought.

Result and Comparison

The return loss at 2.5 GHz seems to be good polyimide, Teflon, PTFE, and polystyrene substrate. The respective return losses are −45, −38, −25, and −28 dB. The comparison graph is given in Figure (Figs. 7.7 and 7.8) (Table 7.1).

Medical implant communication systems (MICS) are made up of an implanted screening tool and an additional surveillance device that is positioned a certain distance (usually 2 m) outward. Preferable connections are being used to alter device parameters, transmit stored information, and transmit effective performance measurement tracking data. Thus, irrespective of resource restrictions, the implanted antenna must pass the message powerful enough for it to be picked up by the external

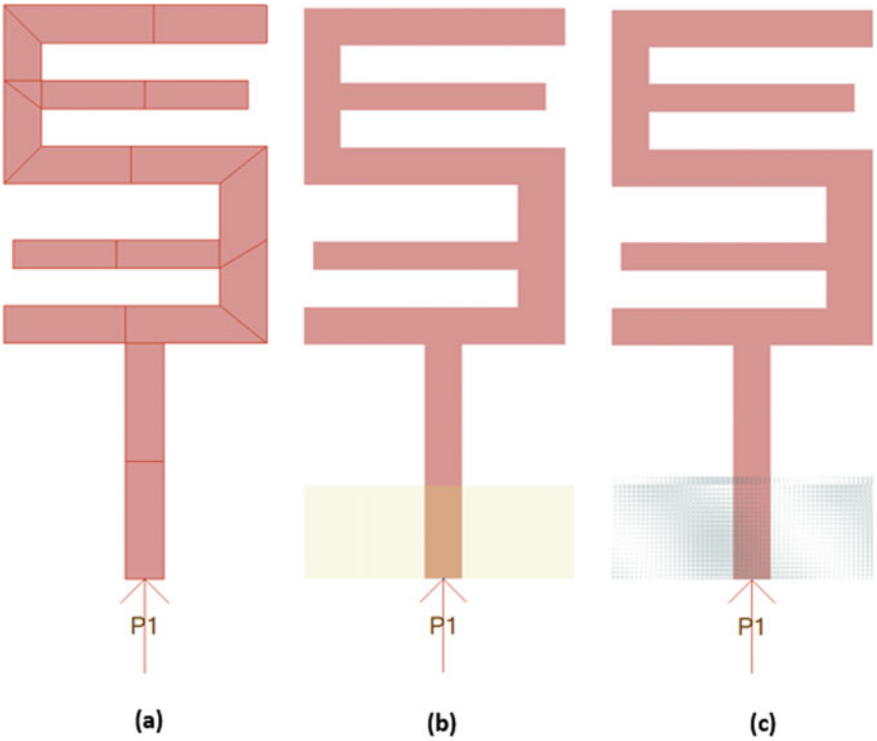

Fig. 7.6 Proposed antenna design **a** without ground structure, **b** with monopole ground structure, and **c** with dielectric structure

device. It is critical to emphasize that, in addition to patient safety, intervention difficulties restrict the permissible limits intensity incident on the implanted antenna. The field strength of the proposed antenna is shown in Fig. 7.9.

The gain is high for Polyimide which is 7 dB and next to it Polystyrene which is 6 dB and next is Polytetrafluoroethylene (PTFE) which is 5 dB. The comparison of the same is given in Fig. 7.10 and Table 7.2.

Conclusion

In this work, we attempted to provide a quick summary of the issues encountered and remedies proposed for the development, modeling, and constraints of implanted antennas for biomedical applications. The development of implanted antennas is primarily concerned with miniaturization and nontoxicity, despite the fact that electrically tiny antennas have poor transmission efficacy and generally limited bandwidths. Gain improvement is important since it affects the quality of the results. Patch antennas are fundamentally based on two numerical models: Finite-Element

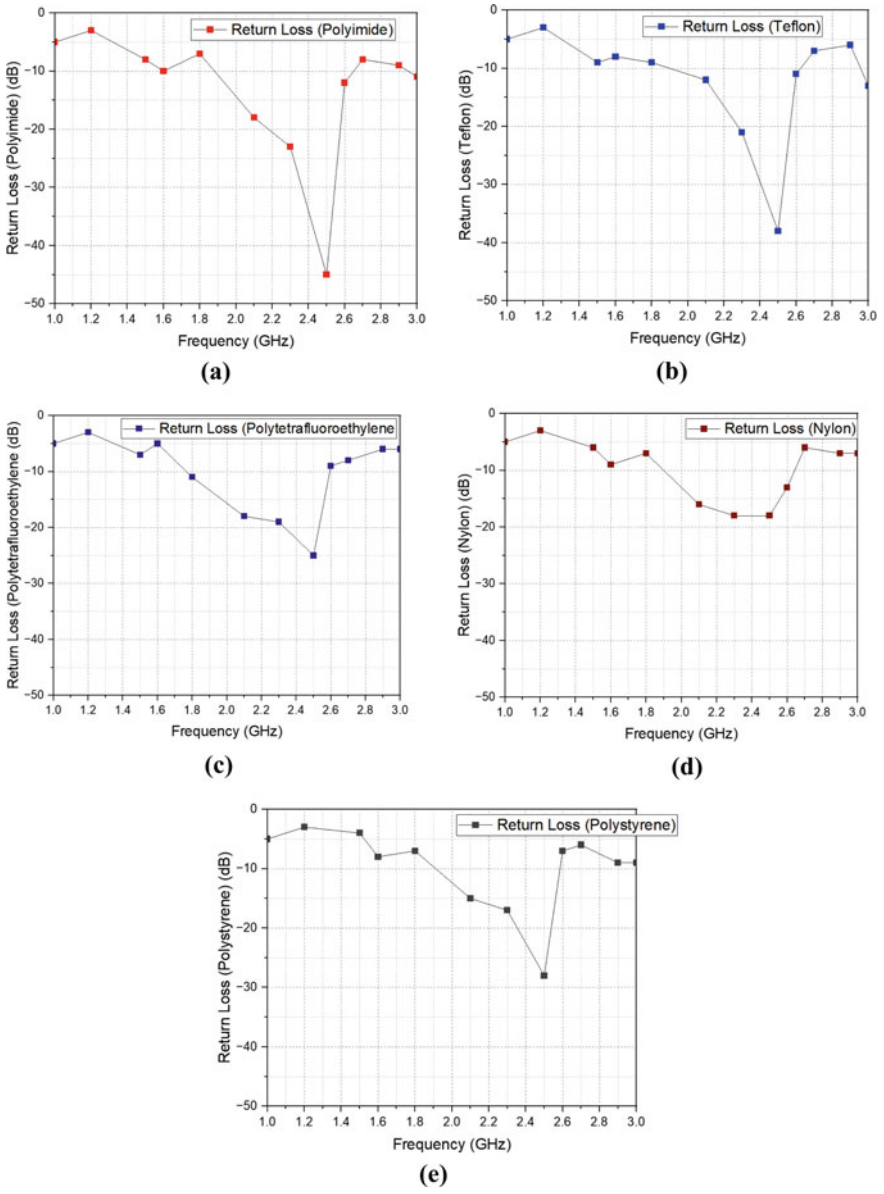

Fig. 7.7 **a** Return loss for the proposed antenna with polyimide substrate, **b** return loss for the proposed antenna with Teflon substrate, **c** return loss for the proposed antenna with polytetrafluoroethylene (PTFE) substrate, **d** return loss for the proposed antenna with nylon substrate, and **e** return loss for the proposed antenna with polystyrene substrate

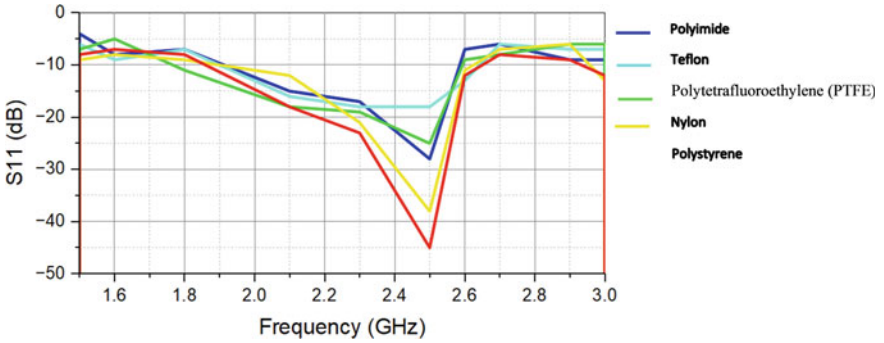

Fig. 7.8 Comparison of return loss for various substrates at 2.5 GHZ

Table 7.1 Return loss for various substrates at 2.5 GHz

S. No	Frequency (GHz)	Return loss (dB)				
		Polyimide	Teflon	Polytetrafluoroethylene (PTFE)	Nylon	Polystyrene
1.	1.5	−8	−9	−7	−6	−4
2.	1.6	−7	−8	−5	−9	−8
3.	1.8	−8	−9	−11	−7	−7
4.	2.1	−18	−12	−18	−16	−15
5.	2.3	−23	−21	−19	−18	−17
6.	2.5	−45	−38	−25	−18	−28
7.	2.6	−12	−11	−9	−13	−7
8.	2.7	−8	−7	−8	−6	−6
9.	2.9	−9	−6	−6	−7	−9
10.	3	−12	−13	−6	−7	−9

and Finite-Difference Time-Domain Methods. Simplified tissue models have been demonstrated to be capable of replacing sophisticated anatomical tissue models, therefore speeding up simulations. A bio-friendly antenna with dimensions of 27 × 15 × 0.16 mm^3 was developed and successfully simulated at various substrates with high gain, return loss, and field pattern at 2.5 GHz.

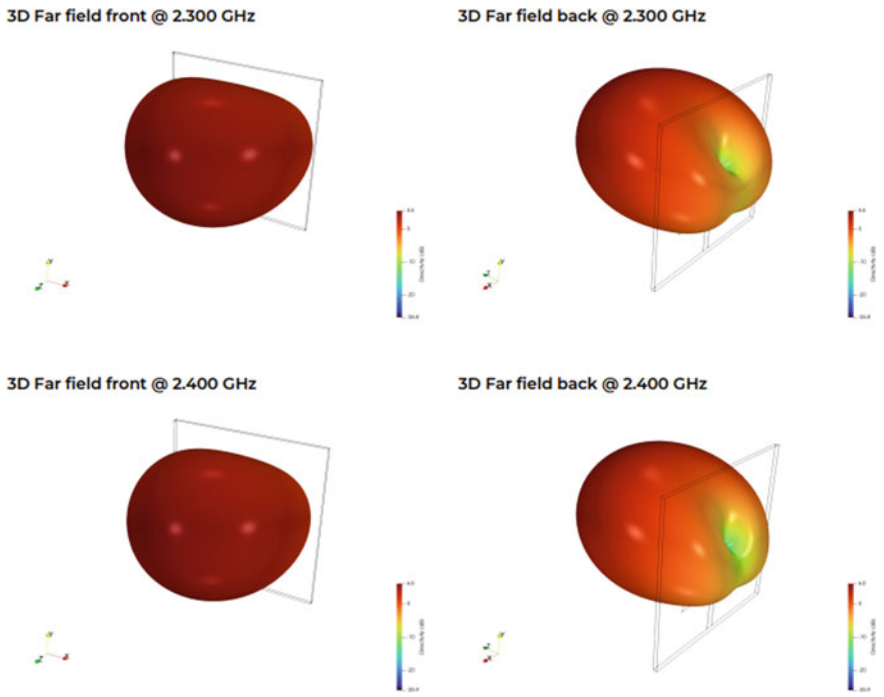

Fig. 7.9 Field strength of the proposed antenna at ISM band

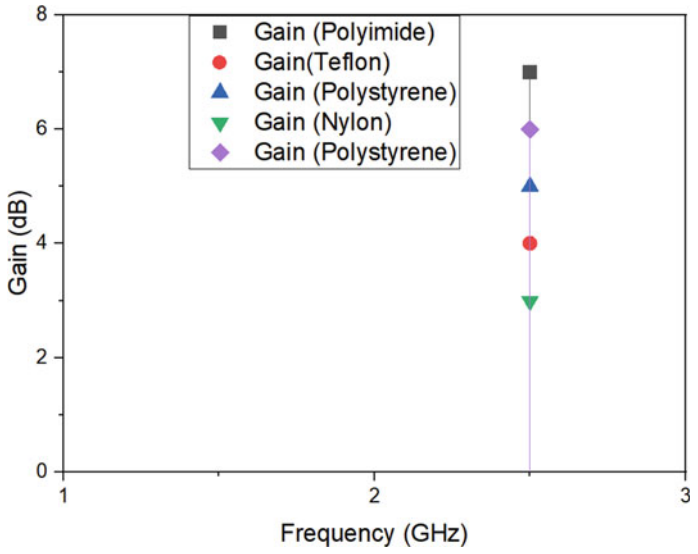

Fig. 7.10 Gain comparison for various substrates for the proposed antenna

Table 7.2 Gain obtained for various substrates

S. No	Name of the substrate	Dielectric constant	Gain obtained at 2.5 GHz (dB)
1.	Polyimide	3.5	7
2.	Teflon	2	4
3.	Polytetrafluoroethylene (PTFE)	2.1	5
4.	Nylon	3.1	3
5.	Polystyrene	2.5	6

References

Alzheimer's Association Report (2011) 2011 Alzheimer's disease facts and figures. Alzheimer's Demen J Alzheimer's Assoc 7:208–244

Bhardwaj V, Joshi R, Gaur AM (2022) IoT-based smart health monitoring system for COVID-19. SN Comput Sci 3:137. https://doi.org/10.1007/s42979-022-01015-1

Bhargava B (2021) Wanted a revolution in healthcare system. The Hindu Businessline

Bodenheimer T, Chen E, Bennett HD (2009) Confronting the growing burden of chronic disease: Can the US health care workforce do the job. Health Aff 28:64–74

Botha M et al (2014) The benefits and challenges of e-health applications: a content analysis of the South African context. In: Conference: the international conference on computer science, computer engineering, and social media (CSCESM2014)

Ferdous MdS, Chowdhury F, Moniruzzaman Md (2007) A taxonomy of attack methods on peer-to-peer network. In: Proceedings of the 1st Indian conference on computational intelligence and information security (ICCIIS, 07)

Garcia-Pardo C, Andreu C, Fornes A, Castello-Palacios S, Perez Simbor S, Barbi M, Vallés-Lluch A, Cardona N (2018) Ultra wideband technology for medical in-body sensor networks: an overview of the human body as a propagation medium, phantoms, and approaches for propagation analysis. IEEE Antennas Propag Mag 1–1. https://doi.org/10.1109/MAP.2018.2818458

Hall PS, Hao Y (2006) Antennas and propagation for body centric communications. In: 2006 first European conference on antennas and propagation

Hayes TO, Gillian S (2020) Chronic disease in the United States: a worsening health and economic crisis. 1–19

https://worldpopulationreview.com/countries/china-population (2022)

https://worldpopulationreview.com/countries/japan-population

https://www.who.int/news-room/fact-sheets/detail/noncommunicable-diseases#:~:text=Key%20facts,%2D%20and%20middle%2Dincome%20countries

Iftekhar EN et al (2021) A look into the future of the COVID-19 pandemic in Europe: an expert consultation. Lancet Reg Health Eur 8:100185

Islam MM, Rahaman A, Islam MR (2020) Development of smart healthcare monitoring system in IoT environment. SN Comput Sci 1(3):185

Islam MM, Rahmanand A, Islam MR (2020) Development of smart healthcare monitoring system in IoT environment. SN ComputSci 1(3)

Jazieh AR, Kozlakidis Z (2020) Healthcare transformation in the post-coronavirus pandemic era. Sec. Infectious diseases—surveillance, prevention and treatment

Kargar MJ, Ghasemi S, Rahimi O (2013) Wireless body area network: from electronic health security perspective. Int J Reliab Qual E-Healthc (IJRQEH) 2(4):38–47

Kavitha S, Gokul Anand KR, Poornima T, Sathiya Girija H (2022) IoT centered household security and person's health care system predominantly aimed at epidemic circumstances. Internet of things and data mining for modern engineering and healthcare applications. ISBN 9781032108544

Khan MM, Mehnaz S, Shaha A, Nayem M, Bourouis S (2021) IoT-based smart health monitoring system for COVID-19 patients. Comput Math Methods Med
Kumar R, Mukesh R (2013) State of the art: security in wireless body area networks. Int J Comput Sci Eng Technol (IJCSET) 4(05):622–630
Lehnert T, Heider D, Leicht H, Heinrich S, Corrieri S, Luppa M, Heller SR, Konig HH (2011) Review: health care utilization and costs of elderly persons with multiple chronic conditions. Med Care Res Rev 68:387–420
Leifer BP (2003) Early diagnosis of Alzheimer's disease: clinical and economic benefits. J Am Geriatr Soc 51:S281–S288
Levin A, Stevens PE (2011) Early detection of CKD: the benefits, limitations and effects on prognosis. Nat Rev Nephrol 7:446–457
Malik PK, Wadhwa DS, Khinda JS (2020) A survey of device to device and cooperative communication for the future cellular networks. Int J Wirel Inf Netw Springer 27:411–432. https://doi.org/10.1007/s10776-020-00482-8
Momtazmanesh S et al (2020) All together to fight COVID-19. Am J Trop Med Hyg 102(6):1181–1183
National Institute on Aging (NIA) (2016) NIH-funded Census Bureau U.S. nih.gov/news-events/news-releases/worlds-older-population-grows-dramatically
Office of National Statistics (2022) Statistical bulletin national population projections: 2020-based interim. https://www.ons.gov.uk/peoplepopulationandcommunity/populationandmigration/populationprojections
Pahwa R, Lyons KE (2010) Early diagnosis of Parkinson's disease: recommendations from diagnostic clinical guidelines. Am J Manag Care 16:94–99
Priesemann V et al (2021) Towards a European strategy to address the COVID-19 pandemic. Lancet 398(10303):838–839
Rahim A, Malik PK (2021) Analysis and design of fractal antenna for efficient communication network in vehicular model. Sustain Comput Inform Syst 31:100586. Elsevier. https://doi.org/10.1016/j.suscom.2021.100586. ISSN 2210-5379
Roges R, Malik PK (2021) Planar and printed antennas for internet of things-enabled environment: opportunities and challenges. Int J Commun Syst 34(15):e4940. https://doi.org/10.1002/dac.4940ISSN:1099-1131
Srividya, Satyanarayana V (2018) Personal lung function monitoring system for asthma patients using internet of things (IOT). Int J Res Electron Comput Eng 6
Switzerland. http://www.who.int/nmh/publications/ncd_report_full_en.pdf. Accessed 1 May 2016
Thapliyal H et al (2021) Consumer technology-based solutions for COVID-19. IEEE Consum Electron Mag 10(2):64–65
Tossaint-Schoenmakers R et al (2021) The challenge of integrating eHealth into health care: systematic literature review of the Donabedian model of structure, process, and outcome. J Med Internet Res
U.S. Department of Health and Human Services (2020) Physical activity guidelines for Americans, 2nd edn
World Health Organization, Food and Agriculture Organization of the United Nations (2018) The nutrition challenge: food system solutions. WHO/NMH/NHD/18.10
Yach D, Hawkes C, Gould L, Hofman KJ (2004) The global burden of chronic diseases: overcoming impediments to prevention and control. J Am Med Assoc 291:2616–2622

Chapter 8
Design and Analysis of an All-Textile Antenna Integrated Within Human Clothing for Safe Bio-medical Wireless Communication

D. Ram Sandeep, B. T. P. Madhav, S. Salma, and L. Govinda

Abstract This study presents the design and development of a portable textile antenna for bio-medical wireless communication at a 5.8 GHz ISM band application. The proposed antenna is built on a highly sustainable, low-cost, and flexible jute substrate. The famous Tai-Chi symbol inspires the present textile antenna design and operates in three frequencies 3.5, 4.9, and 5.8 GHz. The circular polarization characteristic is also achieved in the operating frequencies. This feature enables the antenna to receive the signal without proper orientation between the receiver and transmitter, thus enabling a stable wireless link for wireless bio-medical communication applications. The developed antenna was methodologically investigated on the three-layer body model and the real human tissue to access SAR ranges. All the ranges were under the safe limits of US and EU standards. The obtained results have remarkably proven that the antenna is safe to use on the human body in all the functioning frequencies.

Keywords Textile antenna · Bio-medical communication · Circular polarization · SAR analysis · Three-layer body model

D. Ram Sandeep (✉)
Department of ECE, Raghu Engineering College, Dakamarri, Bheemunipatnam, Visakhapatnam, India
e-mail: askram91@gmail.com

B. T. P. Madhav
ALRC, R&D, Department of ECE, KLEF, Guntur, AP, India

S. Salma
Department of ECE, Sri Venkateshwara College of Engineering, Karakambadi Road, Tirupati, India

L. Govinda
Cancer Science Institute of Singapore, National University of Singapore, Singapore, Singapore

P. K. Malik and P. N. Shastry (eds.), *Internet of Things Enabled Antennas for Biomedical Devices and Systems*, Springer Tracts in Electrical and Electronics Engineering,
https://doi.org/10.1007/978-981-99-0212-5_8

Introduction

Wearable electronics are devices worn on or implanted in the human body. At the same time can also be concealed in the wearer's outfit (Düking et al. 2016). Wearable gadgets have the potential to connect to other devices through cellular connection or directly with each other. These devices consist of various components such as processing units, memory modules, sensors, transmitting and receiving modules, batteries, and antennas. The antennas are significant among these multiple components because they are vital in establishing the wearable wireless link.

In all the wearable devices, traditional rigid microstrip antennas are not found because they are difficult to mount on the user's body, and their sharp edges severely damage the skin. Wearable antennas are a particular kind where the antenna is made up of wearable materials specially designed to function while worn. The most common applications of these antennas are in the bio-medical radio frequency systems and on-body wearable wireless communication systems. Usually, the Wireless Body Area Networks (WBAN) connect these wearable antennas, and all these antennas are under the context of WBAN. The WBAN links IoT nodes, actuators, and sensors on the human skin or clothes of the wearer or other human body tissues and establishes a wearable wireless connection through a proper communication channel, as illustrated in Fig. 8.1 (Wang et al. 2017; Paracha et al. 2019).

All modern wearable devices are devised with compact wearable antennas. The antenna topology has relied on several requirements like radiating performance, electrical performance, size, efficiency, gain, bandwidth, polarization, and the wearable device's particular application. The daily used antenna topologies are planar inverted-F antennas (PIFAs), slot antennas, printed loops, monopole, printed dipole,

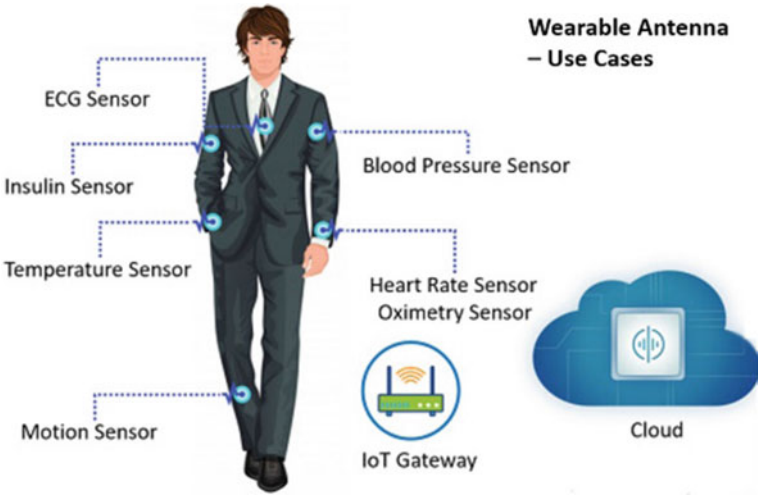

Fig. 8.1 Applications of wearable antennas

and microstrip antennas. The microstrip topology is the right choice for wearable antennas because of their compact size, ease to fabricate, flexibility and conformability, and ease of integration with wearers' clothing or wearable wireless devices (Balanis 2015; Kanitthika et al. 2016). For realizing a textile antenna, the insulating parts are made with various dielectric materials. At the same time, the radiating and ground structure is made up of electro-textiles or other fabrication techniques (Dong et al. 2022; Mahmood et al. 2020). This work considers the evolving methods in practice to develop a sustainable, safe, and circularly polarized multi-band textile antenna for Bio-Medical Wireless Communication applications.

Evolution Steps of the Proposed Textenna

The very famous Tai-Chi symbol inspires the present textile antenna design. Here in the sign, two equal forces acted upon each other, ultimately leading to the system's harmony. The design characteristics of the proposed antenna were done in Ansys High-Frequency Structure Simulator (HFSS) 19.0 software. Three iterations are carefully designed to achieve the Tai-Chi topology in the present antenna model, as seen in Fig. 8.2. For that purpose, together with simulation and practical development, the dimensions of the jute substrate are considered as $20 \times 16 \times 1.5$ mm^3 (20 mm of length, 16 mm of width, and a height of 1.5 mm) (Ram Sandeep et al. 2020). The antenna consists of a circular patch and ground elements in the first iteration. This design has an operating frequency of 4.8 GHz, as seen in Fig. 8.3. Later in design step-2, the circular elements were converted into half circles, and this model resonated at 2.2, 5.2, and 6.9 GHz. In the final step, the half circles were converted into crescent-shaped elements, and this design operates at 3.5, 4.9, and 5.8 GHz. The overall antenna design with geometry is shown in Fig. 8.4.

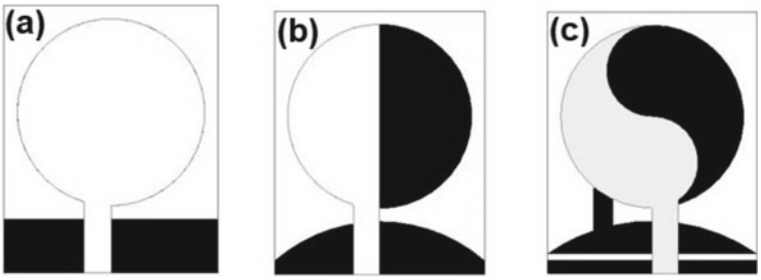

Fig. 8.2 The design procedure of the textenna: **a** step-1, **b** step-2, and **c** step-3

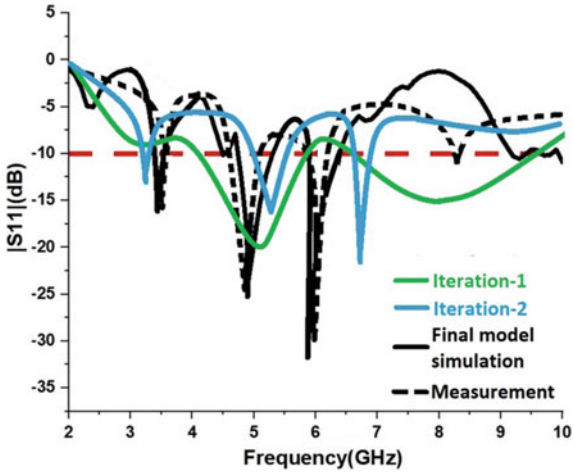

Fig. 8.3 The reflection coefficient concerning iterations

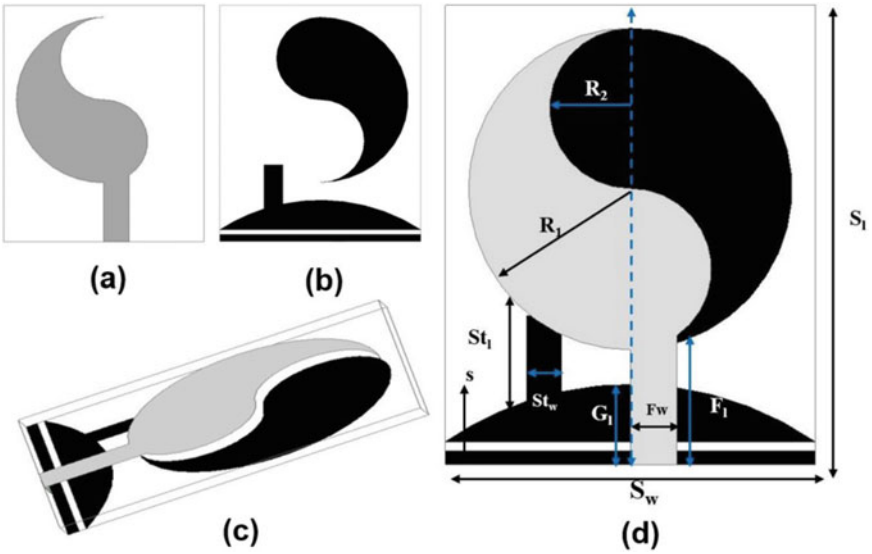

Fig. 8.4 The topology of the textile antenna: **a** patch perspective, **b** ground perspective, **c** lateral perspective, and **d** overall geometry

Validation of the Proposed Textenna

The fabricated prototype on a jute substrate is illustrated in Fig. 8.5; the patch and ground layers were realized through conductive paint. It is validated in an anechoic chamber to test its radiating behavior and circular polarization feature in the operating frequencies. To accomplish this task, initially, the resonating frequencies at the

Fig. 8.5 The photographic images of the prototype: **a** patch and **b** ground

operating bands were tested. This is followed by testing antennas' circular polarized features through the Axial ratios.

Reflection Coefficient |S11|

As seen in Fig. 8.6, the developed prototype is operating successfully at 3.5, 4.9, and 5.8 GHz. Also, there is a decent match that was observed between the practical measurement and the simulation.

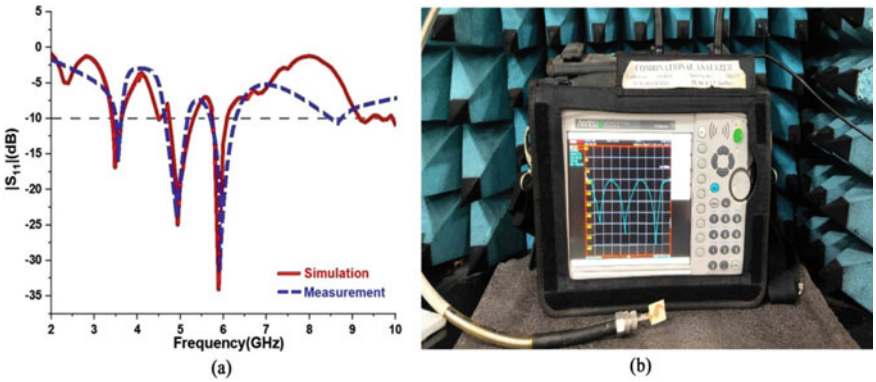

Fig. 8.6 |S11| measurement of the proposed textenna: **a** plot and **b** measurement setup

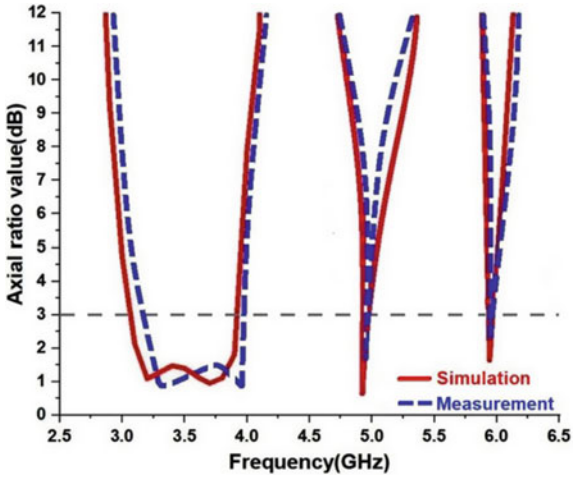

Fig. 8.7 Simulated and measured axial ratio (ARs) values of the proposed antenna

Axial Ratios

The circular polarization is primarily investigated by observing the Axial ratios. Axial ratios are described as the ratio of the major and minor axes of the polarization ellipse. Ideally, ARs value has to be one. In practice, the axial ratio values can't be unity (1) because the energy is emitted in a slightly elliptical form. So a value of less than three is widely considered as a standard limit for practical measurement of axial ratios. As seen in Fig. 8.7, the axial ratio values of the proposed model, both in the simulation and measurement, were under the 3 dB line; hence the antenna is operating with CP.

Specific Absorption Rate (SAR) Analysis

The human body is highly dispersed, lossy, and complex tissue. The performance of the antenna will be varied when it's operated in proximity to human tissue. The textenna's radiation behavior also changes, and long-time exposure to electromagnetic radiation will cause an adverse effect on human health. A proper investigation should be carried out on the textile antenna when it is designed for wearable applications. This study on the proposed textile antenna evaluates the SAR value and antenna's resonating behavior on the three-layered phantom model and also assesses directly the human body. As illustrated in Fig. 8.8, the body model comprises muscle, fat, and skin.

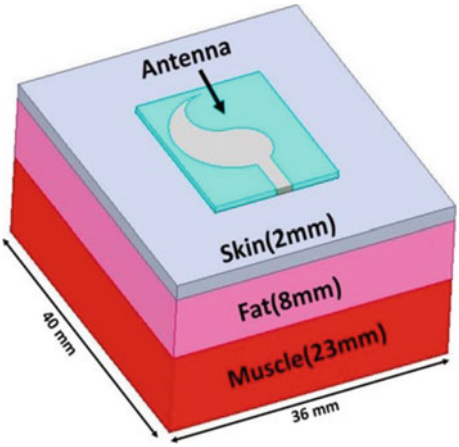

Fig. 8.8 Illustration of the textile antenna on top of the three-layer body phantom model

Proposed Textenna: Functional Behavior while Operating on the Human Body

As seen in Fig. 8.9, the textenna was placed directly on the human body and assessed in an anechoic space. Both in the simulation and measurement, a decent match has been noted. While placing the prototype jute antenna on the human body, a slight variation in the resonating frequencies is reported, and they are resonating at 3.45, 4.93, and 5.78 GHz. These reported variations are due to human tissue lossy and conductive behavior.

The IEEE standards (IEEE/IEC std 62,704) and European standards-International Commission on Non-Ionizing Radiation Protection (ICNIRP) have issued the guidelines for the safe SAR limits (IEEE Standards 1992). The threshold limit for

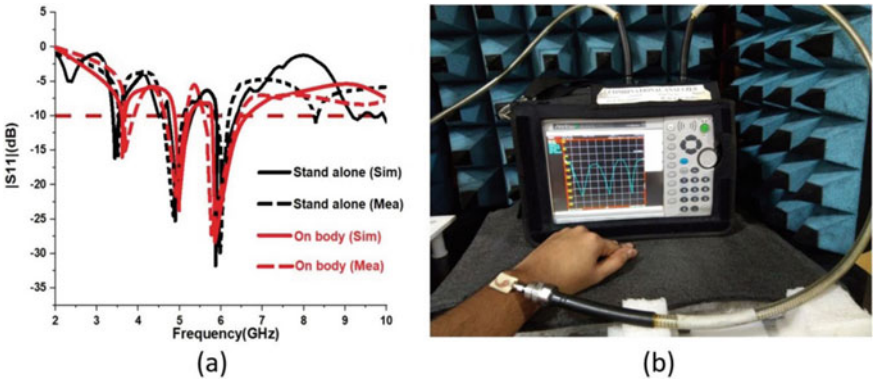

Fig. 8.9 The proposed textennas: **a** simulation and measurement of |S11| on the human body and **b** measurement setup

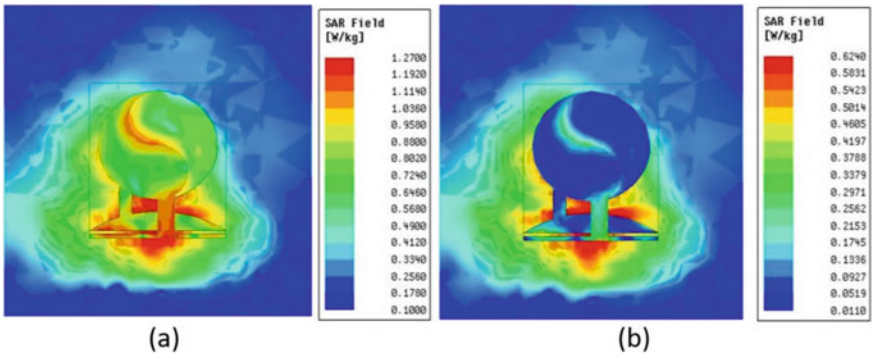

Fig. 8.10 The proposed textennas SAR analysis on body model at 3.5 GHz for **a** 1 and **b** 10 g of tissue

maximum SAR in 1 g of tissue is 1.6 W/Kg; the threshold limit for 10 g of tissue is 2W/Kg.

SAR Analysis at 3.5 GHz (Wi-MAX)

As illustrated in Fig. 8.10a, at 3.5 GHz frequency for 1 g of tissue, the SAR value is 1.270 W/Kg. Its corresponding value for 10 g of tissue is 0.6240 W/Kg, as shown in Fig. 8.10b. These values are under the IEEE and European standards' safe limits. So the proposed antenna has safe operating SAR limits at 3.5 GHz frequency of Wi-MAX band applications (Sandeep et al. 2021). Tiwari and Malik (2021), Failed (2021), Kaur and Malik 2021.

SAR Analysis at 4.9 GHz (WLAN)

As illustrated in Fig. 8.11a, at 4.9 GHz frequency for 1 g of tissue, the SAR value is 1.010 W/Kg. Its proportionate value for the 10 g of tissue is 0.5160 W/Kg, as shown in Fig. 8.11b. It concluded that the proposed antenna has safe operating SAR limits at 4.9 GHz frequency of WLAN band applications.

SAR Analysis at 5.8 GHz (ISM Band)

As illustrated in Fig. 8.12a, at 5.8 GHz frequency, for 1 g of tissue, the SAR value is 0.7300 W/Kg. Its equivalent value for the 10 g of tissue is 0.386 W/Kg, as shown

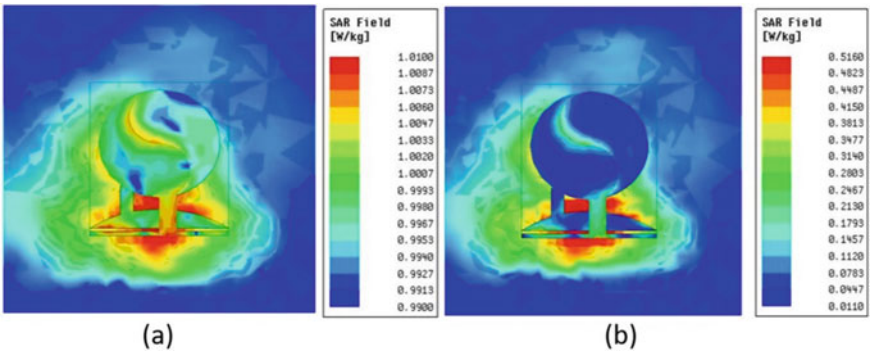

Fig. 8.11 The proposed textennas SAR analysis on body model at 4.9 GHz for **a** 1 and **b** 10 g of tissue

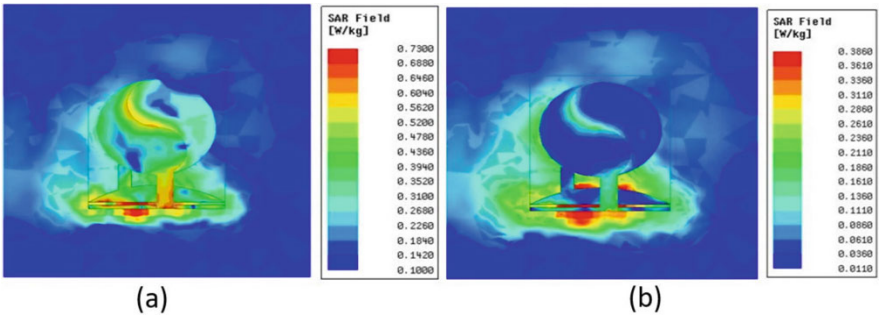

Fig. 8.12 The proposed textennas SAR analysis on body model at 5.8 GHz for **a** 1 and **b** 10 g of tissue

in Fig. 8.12b. Hence, it concluded that the proposed antenna has safe operating SAR limits at 5.8 GHz frequency of ISM band applications.

Conclusion

In this communication, a highly portable circularly polarized textile antenna was proposed and developed on a flexible jute substrate. The antenna is intended for bio-medical on-body wireless communication at 5.8 GHz. A safe SAR value is a must for such on-body communication since high SAR values possibly damage the human tissue on long exposures. So the antenna's SAR value is methodologically analyzed for 1 and 10 g of tissue. This analysis of the developed textenna concluded that for all the three operating frequencies, both at 1 and 10 g of tissue, the textenna performs well with safe SAR limits as prescribed by IEEE standards (IEEE/IEC std

62,704) and European standards (ICNIRP). So it is determined that this antenna is found safe to apply for on-body wireless communication applications as a whole.

References

Balanis CA (2015) Antenna theory: analysis and design. John wiley & sons

Dong Y, Li S, Hong W (2022) A review of wearable antenna research. Wearable Technol 2(2):92–100

Düking P, Hotho A, Holmberg H-C, Fuss FK, Sperlich B (2016) Comparison of non-invasive individual monitoring of the training and health of athletes with commercially available wearable technologies. Front Physiol 7:71

IEEE Standards Coordinating Committee, 28 (1992) IEEE standard for safety levels with respect to human exposure to radio frequency electromagnetic fields, 3 kHz to 300 GHz. IEEE C95, pp 1–1991

Kaur A, Malik PK (2021) Multiband elliptical patch fractal and defected ground structures microstrip patch antenna for wireless applications. Progress in Electromag Res B 91:157–173. https://doi.org/10.2528/PIERB20102704(ISSN:1937-6472)

Kanitthika K, Soochan K, Kaewkannate K, Kim S (2016) A comparison of wearable fitness devices. BMC Pub Health 16:433

Mahmood SN, Ishak AJ, Saeidi T, Alsariera H, Alani S, Ismail A, Soh AC (2020) Recent advances in wearable antenna technologies: a review. Electromag Res B 89 1–27

Paracha KN, Rahim SKA, Soh PJ, Khalily M (2019) Wearable antennas: a review of materials, structures, and innovative features for autonomous communication and sensing. IEEE Access 7:56694–56712

Ram Sandeep D, Prabakaran N, Madhav BTP, Narayana KL, Rakesh Kumar P (2020) Systematic investigation from material characterization to modeling of jute-substrate-based conformal circularly polarized wearable antenna. J Electron Mater 49(12):7292–7307

Sandeep DR, Prabakaran N, Madhav BTP, Lokesh Reddy D, Divya Sree K, Pavan Sai Kumar J, Salma S (2021) SAR analysis of jute substrate based Tri-band antenna for wearable applications. J Phys Conf Ser 1804(1):012203. IOP Publishing

Tiwari P, Malik PK (2021) Wide band micro-strip antenna design for higher "X" band Int J e-Collab (IJeC) 17(4):60–74. https://doi.org/10.4018/IJeC.2021100105 (ISSN:1548-3673)

Wadhwa DS, Malik PK, Khinda JS (2021) High gain antenna for n260- & n261-bands and augmentation in bandwidth for mm-wave range by patch current diversions. World J Eng. https://doi.org/10.1108/WJE-03-2021-0133 (ISSN: 1708-5284)

Wang Z, Yang Z, Dong T (2017) A review of wearable technologies for elderly care that can accurately track indoor position, recognize physical activities and monitor vital signs in real time. Sensors 17(2):341

Chapter 9
Microstrip Biomedical Patch Antenna with MIMO Capability and Challenges in Achieving Diversity Performance

Manish Sharma

Abstract The chapter discusses the microstrip patch antenna capability of transformation to $MIMO_{p\times q}$ antenna formation. A well-known fact for modern communication system needs to accommodate the higher data rate of transmission in the existing channel. The two aspects of the MIMO configuration are addressed in this chapter. The patch antenna needs to be useful for wireless communication applications and the other maintains isolation with good diversity performance evaluating ECC, DG, TARC, MEG, CCL. These are the challenges faced in designing the MIMO antenna, and the challenges are overcome in case of isolation by using different methods such as using neutralization line, using different fractals in-ground, using parasitic U-type between feed lines, placing radiating elements orthogonally, using meta-material structure, placing T-type stub in the commonly shared ground along with pair of etched comb-type slots, inverse L-type stub in the ground and interconnecting all the ground by using thin strips. These techniques provide either an additional current path between the radiating elements or by directing the current vectors in opposite direction thereby, canceling the unnecessary interference. Also, in medical applications, bandwidth of 402–405 MHz is used with power limitation of 25 W and are used in Implantation, Telemedicine applications. The ISM band of 2.45 GHz is used for detection of Skin Cancer.

Keywords MIMO · Diversity performance · Neutralization line · $ECC_{p\times q}$ · $DG_{p\times q}$ · $TARC_{p\times q}$ · $CCL_{p\times q}$ · Implantation · Telemedicine · Skin cancer

Introduction

Recent faster communication demanding the new concept of smart cities, artificial intelligence-based communication, etc. has emerged which has focused on the higher data rate transfer of information from source to destination with multiple users. However, SISO (Single–Input–Single–Output) system fulfills the requirement

M. Sharma (✉)
Chitkara University Institute of Engineering and Technology, Chitkara University, Punjab, India
e-mail: manishengineer1978@gmail.com

P. K. Malik and P. N. Shastry (eds.), *Internet of Things Enabled Antennas for Biomedical Devices and Systems*, Springer Tracts in Electrical and Electronics Engineering,
https://doi.org/10.1007/978-981-99-0212-5_9

to some extent but the operating bandwidth is compromised due to shortcomings such as multiple fading in real-time environment applications. However, the design of a microstrip MIMO antenna with smart reconfigurable technology will resolve the issues. Designing these MIMO antennas has to face lots of challenges and to name a few of them are maintaining reasonable isolation and achieving high diversity performance. The literature discussed here is an attempt to understand and overcome of above problems faced in a MIMO system. The two-port MIMO system (Tiwari et al. 2019a, b, 2020; Islam and Das 2020; Tang et al. 2020a, b; Pasumarthi et al. 2019; Wang et al. 2020; Vasu Babu and Anuradha 2019; Addepalli and Anitha 2020; Ameen et al. 2020; Hasan et al. 2019; Dkiouak et al. 2019, 2020; Hassan et al. 2020; Thakur et al. 2020; Azarm et al. 2019; Agarwal et al. 2020; Ahmed et al. 2018; Banerjee et al. 2017, 2020; Desai et al. 2022; Gupta and Kumar 2020; Gurjar et al. 2020; Mohanty and Behera 2020; Mark et al. 2019; Hadda et al. 2021; Sun et al. 2017; Sohi and Kaur 2020; Sharma et al. 2021a; Sharma 2020; Kumar et al. 2020; Oliveira et al. 2021; Kumar Biswas and Chakraborty 2019) is discussed where different methodologies have been employed for diversity performance and higher isolation between the inter-spaced elements. A neutralization line that is attached between the two adjacent radiators helps in achieving better isolation of ≤ -22 dB in the bandwidth range of 3.52–9.89 GHz (Tiwari et al. 2019a, b). Interestingly, a two-band antenna for WiMAX applications achieves isolation by etched U-shaped strip between the two feed lines (Islam and Das 2020). The two radiating elements placed face-to-face with parasitic U-type stub on opposite plane with printed stepped ground helps in achieving isolation of -15.0 dB (Tang et al. 2020a). The important technique in the form of meta-material structure is also used to obtain better isolation which is placed between the two antenna elements (Wang et al. 2020; Mark et al. 2019). Mutual coupling of more than 20 dB is achieved by using inverted L- and Ω-symbol in a 2×2 MIMO antenna (Vasu Babu and Anuradha 2019). The distance between the dual frequency bands maintains isolation of more than 15.0 dB for split-ring-resonator antennas (Ameen et al. 2020) and integrated T-type stub in ground achieves isolation of more than 21.0 dB (Tiwari et al. 2020; Tang et al. 2020b). A rectangular parasitic structure placed in ground for the orthogonally placed radiating elements is another technique to reduce isolation (Azarm et al. 2019). Addition of two rectangular strip in a CPW-fed Minkowski-fractal ground MIMO antenna improves isolation from 14.71 to 21.81 dB (Banerjee et al. 2017) and using Hilbert-fractal in ground also increases level of isolation (Banerjee et al. 2020; Gurjar et al. 2020). Also, in dual notched band UWB-MIMO antenna, isolation is achieved without using any decoupling element and placement of dual radiators at 90° to each other offers nil interaction between them (Hadda et al. 2021; Sharma et al. 2021a). 2-port $\text{MIMO}_{\text{p}\times\text{q}}$ with embedded T-type stub sharing commonly ground provides sufficient isolation to achieve permissible diversity performance (Sharma 2020; Kumar et al. 2020). The shape of integer "8" is used in the middle of ground providing better isolation and the designed antenna is useful for wearable applications (Kumar Biswas and Chakraborty 2019).

The reported literature also discusses four-port MIMO antenna configuration (Dhasarathan et al. 2020; Yussuf and Paker 2019; Srivastava et al. 2019a, b; Roy

et al. 2021; Bactavatchalame and Rajakani 2020; Sharma et al. 2020a, b, 2021b; Raheja et al. 2019, 2020; Khan et al. 2020; Mohammad Saadh et al. 2020; McHbal et al. 2020; Andrade-González et al. 2021; Sehrai et al. 2021; Agarwal et al. 2021; Hussain et al. 2022; Ali et al. 2021; Hassan et al. 2019; Arumugam et al. 2021; Khandelwal 2020; Mathur and Dwari 2018; Pahadsingh and Sahu 2018; Mohanty and Sahu 2021; Prabhu and Malarvizhi 2019; Singh et al. 2021; Fritz-Andrade et al. 2019) where different techniques are used to achieve higher isolation. In 4 × 4 hexagonal shape MIMO antenna with isolated ground, observes no decoupling structure for better isolation but the arrangement of all the four antennas is such that the radiated signal will not interfere (Dhasarathan et al. 2020). The mutual coupling in the 4 × 4 MIMO antenna is achieved by using a cross-shaped stub between the four radiators for improvement of the isolation (Yussuf and Paker 2019). An integrated Bluetooth UWB antenna arranged in orthogonal sequence needs no decoupling element to achieve better isolation (Srivastava et al. 2019a; Sharma et al. 2020a, b, 2021b; Mohammad Saadh et al. 2020; Sehrai et al. 2021; Ali et al. 2021; Arumugam et al. 2021; Raheja et al. 2020; Addepalli et al. 2022) and by using isolated meander line above the common-shared ground enhances the port-to-port isolation (Roy et al. 2021). Also, Electro-magnetic Band Gap Structure is used to achieve isolation which is also one of the prominent techniques in achieving isolation (Prabhu and Malarvizhi 2019). The literature work presented over here also discusses 6- and 8-port MIMO antenna configuration (Chung and Hsiao 2022; Mathur and Dwari 2019; Biswal and Das 2019) and utilizes various mechanisms to achieve higher isolation between the inter-element radiators. The 8 × 8 $\text{MIMO}_{p\times q}$ targeted for Ultra-WB usage utilizes 8-etched slits in-ground providing higher isolation (Mathur and Dwari 2019) and common-shared ground with eight radiators providing resonance at 5.50 GHz uses no additional isolation structure (Biswal and Das 2019). A significant review is conducted on chronic diseases involving instruments like MRI, X-Ray, mammography, ultrasound and different diagnosed diseases. The antennas are useful in telemedicine applications at frequency centered at 2.45 GHz (Arora et al. 2021). The skin model represented in Shreshtha et al. (2021) utilizes antenna with resonance of 2.45 GHz (Tiwari and Malik 2020; Gupta et al. 2020; Roges et al. 2022).

Two and Four-Port MIMO Antennas

The configuration of the 2- and 4-port MIMO antenna is depicted in Fig. 9.1. Figure 9.1a represents a 2-port MIMO antenna with a compact size of 21 × 34 × 1.6 mm^3. In this reported work (Tiwari et al. 2019a), FR4 substrate is used with a constant-dielectric value of 4.40 and a tangent (β) = 0.02 with a height of 1.60 mm. The width of the feed is 2.24 mm which corresponds to a matching of 50 Ω impedance. Introduction of a neutralization line between the two radiating elements offers a bandwidth of 3.53–9.91 GHz and maintains isolation of ≤ -22.0 dB. The surface current distribution over the surface is carried out at 3.53 and 9.91 GHz, respectively, as shown in Fig. 9.1c, d. It can be derived that the direction of the current flow in

the neutralization line and mid-ground are opposite to each other, thus canceling the interfering field which reduces the interference. This neutralization technique employed in the 2 × 2 MIMO antenna improves the matching of the impedance in the operating band and thus, improved S-parameters (S_{11}, S_{12}, S_{21}, S_{22}) are obtained. This MIMO antenna is useful in different wireless applications including HiperLAN operating between 5.00 and 6.00 GHz, maritime applications for different bands, and WLAN, WiMAX, and ISM bands. On the other hand, the diversity performance parameters include ECC to be 0.05 correspondingly Directive Gain is approximately 10.0 dB with CCL $\leq$ 0.26 bits/s/Hz (Tiwari et al. 2019a).

A four-port (Ali et al. 2021) MIMO antenna produces a single resonant frequency for a 5G n78/79 communication system. The designed four-port MIMO antenna is instrumental in hand-held 5G devices application with the compact size of 40 × 40 mm^2 and hence, shows the Specific-Absorption-Rate (SAR) value of 0.90 W/Kg and offers channel capacity of data transmission to be 18.7 bps/Hz. The single-element version is fabricated on an FR4 substrate with an overall size of 20 × 20 mm^2. The antenna or radiator is printed on one plane of the substrate which looks like an inverted L-type patch, and the opposite plane is printed with ground dimensions of 20 × 20 mm^2 with an etched rectangular slot below the radiating patch. This configuration of the antenna provides a narrow bandwidth with a center resonating frequency of 4.79 GHz. The S_{11}/S_{22} shows the resonant frequency centered at 4.85 and 4.82 GHz. This configuration of the $MIMO_{p\times q}$ antenna is intended to providing pattern diversity with maximum lobe directed at 280° for Ant. 1 and 208° for Ant. 3. Ant. 2 corresponds to the maximum gain lobe between 90° and 120° and opposite values of −90° to −120° for Ant. 4 (Ali et al. 2021).

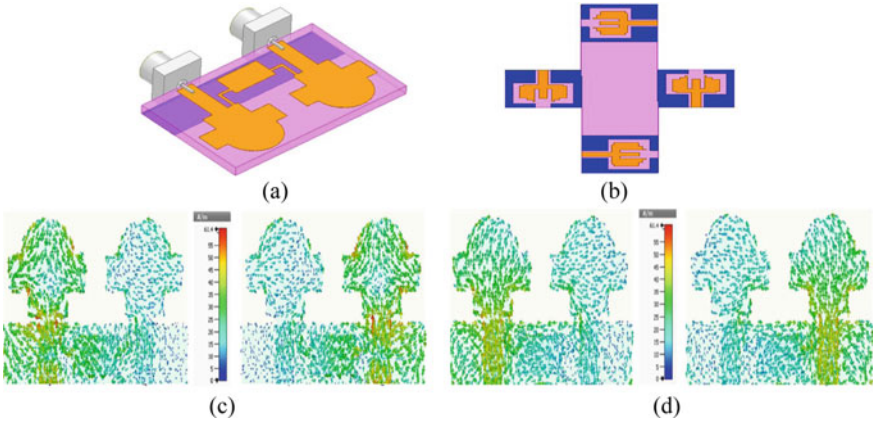

Fig. 9.1 MIMO configuration **a** 2-port with neutralization line (Tiwari et al. 2019a) **b** 4-port MIMO antenna (Mohammad Saadh et al. 2020) (**a**), (**b**) 3.53 GHz and 9.91 GHz (Tiwari et al. 2019a)

Understanding Eight-Port MIMO Antenna

A case study (Addepalli et al. 2022) is used to explain the working principle of an 8-port MIMO antenna. Figure 9.2 shows the single-element antenna configuration with a printed patch on one plane and ground on opposite plane of FR4 substrate. Figure 9.2 also illustrates the flower-shaped radiating patch with five leaves shaped stubs embedded in the semi-circular patch. The partial ground with a height of 13.50 mm is etched with a semi-elliptical slot placed below the microstrip for better matching of the impedance. Also, as per the observations from Fig. 9.2, two rectangular stubs and a pair of rotated L-strips are placed which act as reflectors and direct the signal in the direction of radiation.

Figure 9.3a, b shows the four-port configuration with a perspective view and transparent front view. Firstly, the substrate with an area of $D_1 \times D_2$ mm^2 is removed from all the four corners within the substrate of the dimension of $D_L \times D_W$ mm^2. The four-radiating patch is placed in an orthogonal fashion with their respective ground. Lastly, a square patch of dimension $D_5 \times D_6$ mm^2 is placed exactly at the center containing ground, and all the four ground are connected to the centrally placed patch by a rectangular strip of dimension $(D_2 + D_3 + D_4)$ mm. This ground modification is carried out to achieve higher isolation between the inter-spaced elements. The S_{11} parameter of the four-port transformed MIMO antenna is compared with the single-element antenna shown in Fig. 9.3c and can be concluded that the required impedance bandwidth for 5G-n77/78 band is achieved in both the cases with very good resonance at the center frequency. Figure 9.3c shows the isolation of Port 1 concerning Port 2, Port 3, and Port 4 providing isolation of more than 15.0 dB.

Finally, Fig. 9.4 shows an 8-port MIMO antenna with a fabricated prototype shown in Fig. 9.4a (Front + Ground), and Fig. 9.4b shows the simulation environment. As per the observations from Fig. 9.4a, b, eight radiating elements are used on the FR4 substrate with a total area of 2.147λg × 2.147 λg mm^2. It can be seen that the A_1/A_5,

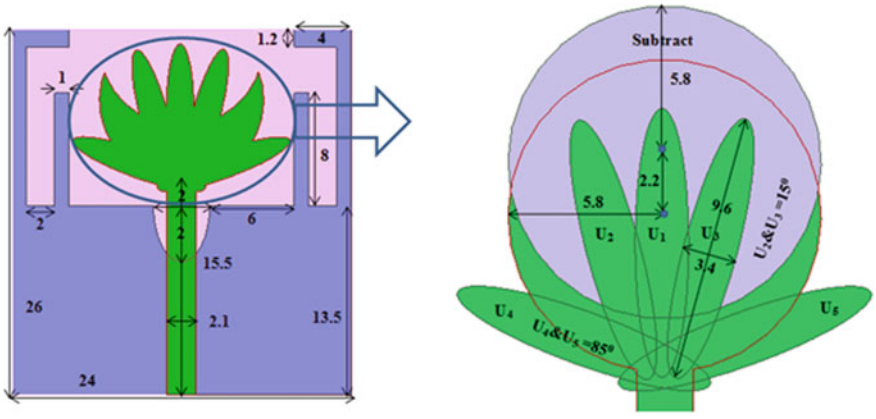

Fig. 9.2 Configuration of the single-element antenna (Addepalli et al. 2022)

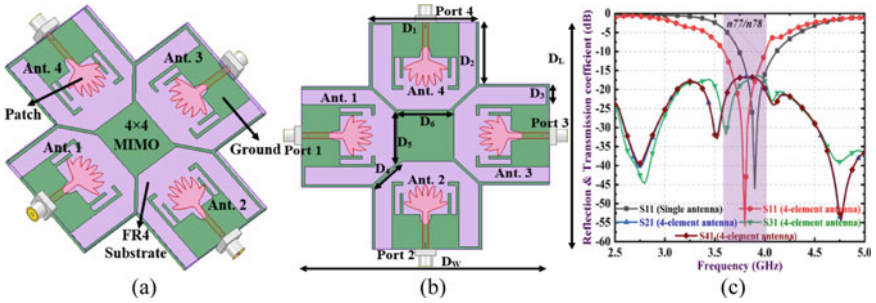

Fig. 9.3 Four port MIMO antenna **a** perspective view **b** transparent front view **c** reflection and transmission coefficients (Addepalli et al. 2022)

A_2/A_6, A_3/A_7, and A_4/A_8 are placed adjacent to each other with a spacing of 13.50 mm while all the four pairs are placed orthogonally. The ground of all the eight antennas is connected by rectangular strips with a dimension of 81.0 mm to the rectangle patch of dimension 30 × 30 mm^2 in the ground plane for better isolation. Figure 9.4c shows the comparison of the S_{11} parameter of all the three antennas discussed (Single-, Four-, and Eight-port) with all the three versions covering 5G-n77/n78 bands.

Figure 9.4d shows the measured reflection and transmission coefficients. It can be observed that the reflection coefficients $S_{11}/S_{22}/S_{33}/S_{44}$ are overlapped with each other in the 5G-n77/78 band with good impedance matching and the transmission coefficients of Port 1 concerning Port 2. Port 3, Port 4, Port 5, Port 6, Port 7, and Port 8 offers isolation of more than 20.0 dB.

Conclusions

The challenge in designing MIMO antenna configuration with two-, four-, and Eight-port was discussed. It was concluded that the few MIMO antennae with orthogonal placed required no additional isolation element to avoid the interference making the design simple. However, techniques such as neutralization line, which commonly connected ground by using thin rectangular stubs in-ground resulted in higher isolation between the closely placed radiating elements. It was also concluded that by maintaining isolation of more than 10 dB, the impedance bandwidth of all the individual radiating elements of the MIMO antenna was preserved without any deterioration.

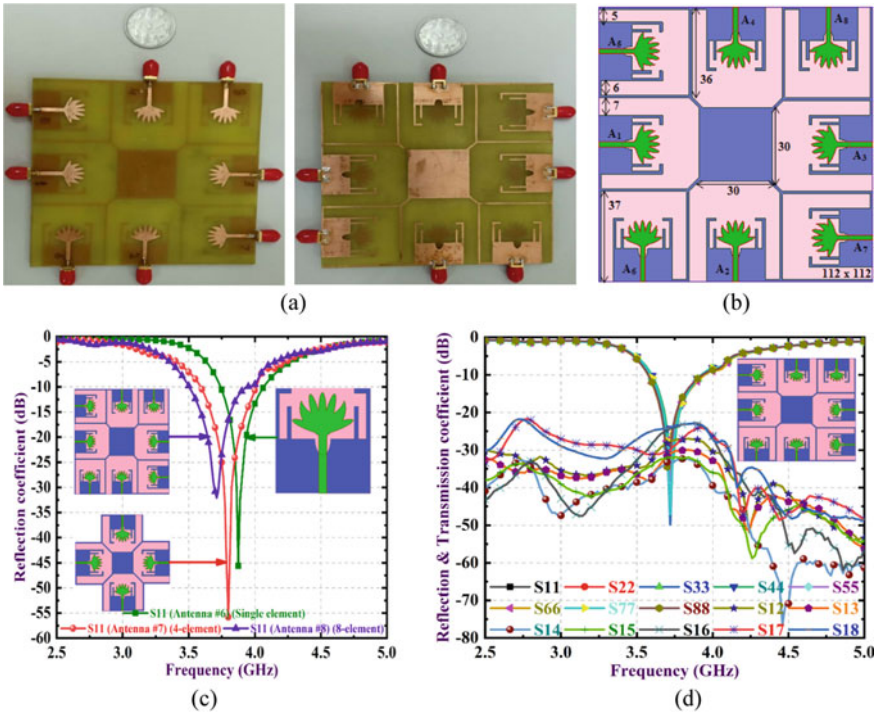

Fig. 9.4 Eight-port MIMO antenna **a** photograph of eight-port MIMO antenna (front + ground) **b** simulation environment **c** comparison of S-parameter (single-, four-, and eight-port MIMO antenna) **d** reflection and Transmission coefficients (Addepalli et al. 2022)

References

Addepalli T, Anitha VR (2020) A very compact and closely spaced circular shaped UWB MIMO antenna with improved isolation. AEU Int J Electron Commun 114

Addepalli T, Kamili JB, Bandi KK, Nella A, Sharma M (2022) Lotus flower-shaped 4/8-element MIMO antenna for 5G n77 and n78 band applications. J Electromagn Waves Appl. https://doi.org/10.1080/09205071.2022.2028683

Agarwal M, Dhanoa JK, Khandelwal MK (2020) Ultrawide band two-port MIMO diversity antenna with triple notch bands, stable gain and suppressed mutual coupling. AEU Int J Electron Commun 120

Agarwal S, Rafique U, Ullah R, Ullah S, Khan S, Donelli M (2021) Double overt-leaf shaped CPW-fed four port UWB MIMO antenna. Electronics 10(24)

Ahmed BT, Olivares PS, Campos JLM, Vázquez FM (2018) (3.1–20) GHz MIMO antennas. AEU-Int J Electron C 94:348–358

Ali H et al (2021) Four-port MIMO antenna system for 5G n79 band RF devices. Electronics 11(1)

Ameen M, Ahmad O, Chaudhary RK (2020) Single split-ring resonator loaded self-decoupled dual-polarized MIMO antenna for mid-band 5G and C-band applications. AEU Int J Electron Commun 124

Andrade-González EA, Tirado-Méndez JA, Jardón-Aguilar H, Reyes-Ayala M, Rangel-Merino A, Pascoe-Chalke M (2021) UWB four ports MIMO antenna based on inscribed Fibonacci circles. J Electromagn Waves Appl 35(9):1202–1220

Arora G, Maman P, Sharma A, Verma N, Puri V (2021) Systematic overview of microstrip patch antenna's for different biomedical applications. Adv Pharm Bull 11(3):439–449

Arumugam S, Manoharan S, Palaniswamy SK, Kumar S (2021) Design and performance analysis of a compact quad-element UWB MIMO antenna for automotive communications. Electronics 10(18)

Azarm B, Nourinia J, Ghobadi C, Majidzadeh M, Hatami N (2019) On development of a MIMO antenna for coupling reduction and WiMAX suppression purposes. AEU-Int J Electron C 99:226–235

Bactavatchalame P, Rajakani K (2020) Compact broadband slot-based MIMO antenna array for vehicular environment. Microw Opt Technol Lett 62(5):2024–2032

Banerjee J, Karmakar A, Ghatak R, Poddar DR (2017) Compact CPW-fed UWB MIMO antenna with a novel modified Minkowski fractal defected ground structure (DGS) for high isolation and triple band-notch characteristic. J Electromagn Waves Appl 31(15):1550–1565

Banerjee J, Gorai A, Ghatak R (2020) Design and analysis of a compact UWB MIMO antenna incorporating fractal inspired isolation improvement and band rejection structures. AEU Int J Electron Commun 122

Biswal SP, Das S (2019) Eight-element-based MIMO antenna with CP behaviour for modern wireless communication. IET Microw Antennas Propag 14(1):45–52

Chung M-A, Hsiao C-W (2022) Dual-band 6 × 6 MIMO antenna system for glasses applications compatible with Wi-Fi 6E and 7 wireless communication standards. Electronics 11(5)

Desai A et al (2022) Transparent 2-element 5G MIMO antenna for sub-6 GHz applications. Electronics 11(2)

Dhasarathan V, Nguyen TK, Sharma M, Patel SK, Mittal SK, Pandian MT (2020) Design, analysis and characterization of four port multiple-input-multiple-output UWB-X band antenna with band rejection ability for wireless network applications. Wirel Netw 26(6):4287–4302

Dkiouak A, Zakriti A, El Ouahabi M (2019) Design of a compact dual-band MIMO antenna with high isolation for WLAN and X-band satellite by using orthogonal polarization. J Electromagn Waves Appl 34(9):1254–1267

Dkiouak A, Zakriti A, El Ouahabi M, McHbal A (2020) Design of two element Wi-MAX/WLAN MIMO antenna with improved isolation using a short stub-loaded resonator (SSLR). J Electromagn Waves Appl 34(9):1268–1282

Fritz-Andrade E, Perez-Miguel A, Gomez-Villanueva R, Jardon-Aguilar H (2019) Characteristic mode analysis applied to reduce the mutual coupling of a four-element patch MIMO antenna using a defected ground structure. IET Microw Antennas Propag 14(2):215–226

Gupta A, Kumar V (2020) DGS-based wideband MIMO antenna for on–off body communication with port isolation enhancement operating at 2.45 GHz industrial scientific and medical band. J Electromagn Waves Appl 35(7):888–901

Gupta NP, Malik PK, Ram BS (2020) A review on methods and systems for early breast cancer detection. In: 2020 International conference on computation, automation and knowledge management (ICCAKM), pp 42–46. https://doi.org/10.1109/ICCAKM46823.2020.9051554. ISBN: 978-1-7281-0666-3. https://ieeexplore.ieee.org/document/9051554

Gurjar R, Upadhyay DK, Kanaujia BK, Kumar A (2020) A compact modified sierpinski carpet fractal UWB MIMO antenna with square-shaped funnel-like ground stub. AEU Int J Electron Commun 117

Hadda L, Sharma M, Gupta N, Kumar S, Singh AK (2021) On-demand reconfigurable WiMAX/WLAN UWB-X band high isolation 2×2 MIMO antenna for imaging applications. IETE J Res 1–13

Hasan MN, Bashir S, Chu S (2019) Dual band omnidirectional millimeter wave antenna for 5G communications. J Electromagn Waves Appl 33(12):1581–1590

Hassan MM et al (2019) A novel UWB MIMO antenna array with band notch characteristics using parasitic decoupler. J Electromagn Waves Appl 34(9):1225–1238
Hassan MM et al (2020) Two element MIMO antenna with frequency reconfigurable characteristics utilizing RF MEMS for 5G applications. J Electromagn Waves Appl 34(9):1210–1224
Hussain M et al (2022) Design and characterization of compact broadband antenna and its MIMO configuration for 28 GHz 5G applications. Electronics 11(4)
Islam SN, Das S (2020) Dual-band CPW fed MIMO antenna with polarization diversity and improved gain. Int J RF Microw Comput-Aided Eng 30(4)
Khan MS, Naqvi SA, Iftikhar A, Asif SM, Fida A, Shubair RM (2020) A WLAN band-notched compact four element UWB MIMO antenna. Int J RF Microw Comput-Aided Eng 30(9)
Khandelwal MK (2020) Metamaterial based circularly polarized four-port MIMO diversity antenna embedded with slow-wave structure for miniaturization and suppression of mutual coupling. AEU Int J Electron Commun 121
Kumar Biswas A, Chakraborty U (2019) Compact wearable MIMO antenna with improved port isolation for ultra-wideband applications. IET Microw Antennas Propag 13(4):498–504
Kumar A, Ansari AQ, Kanaujia BK, Kishor J, Kumar S (2020) An ultra-compact two-port UWB-MIMO antenna with dual band-notched characteristics. AEU Int J Electron Commun 114
Mark R, Rajak N, Mandal K, Das S (2019) Metamaterial based superstrate towards the isolation and gain enhancement of MIMO antenna for WLAN application. AEU-Int J Electron C 100:144–152
Mathur R, Dwari S (2018) Compact CPW-fed ultrawideband MIMO antenna using hexagonal ring monopole antenna elements. AEU-Int J Electron C 93:1–6
Mathur R, Dwari S (2019) 8-port multibeam planar UWB-MIMO antenna with pattern and polarisation diversity. IET Microw Antennas Propag 13(13):2297–2302
McHbal A, Amar Touhami N, Elftouh H, Dkiouak A (2020) Coupling reduction using a novel circular ripple-shaped decoupling mechanism in a four-element UWB MIMO antenna design. J Electromagn Waves Appl 34(12):1647–1666
Mohammad Saadh AW, Ashwath K, Ramaswamy P, Ali T, Anguera J (2020) A uniquely shaped MIMO antenna on FR4 material to enhance isolation and bandwidth for wireless applications. AEU Int J Electron Commun 123
Mohanty A, Behera BR (2020) Investigation of 2-port UWB MIMO diversity antenna design using characteristics mode analysis. AEU Int J Electron Commun 124
Mohanty A, Sahu S (2021) Integration of coupling resonator as port-isolator and MMLC-Minkowiski fractal loop for Wi-Max rejection in 4-port compact UWB MIMO antenna. J Electromagn Waves Appl 35(10):1359–1377
Oliveira JGD, D'Assunção Junior AG, Silva Neto VP, D'Assunção AG (2021) New compact MIMO antenna for 5G, WiMAX and WLAN technologies with dual polarisation and element diversity. IET Microw Antennas Propag 15(4):415–426
Pahadsingh S, Sahu S (2018) Four port MIMO integrated antenna system with DRA for cognitive radio platforms. AEU-Int J Electron C 92:98–110
Pasumarthi SR, Kamili JB, Avala MP (2019) Design of dual band MIMO antenna with improved isolation. Microw Opt Technol Lett 61(6):1579–1583
Prabhu P, Malarvizhi S (2019) Novel double-side EBG based mutual coupling reduction for compact quad port UWB MIMO antenna. AEU-Int J Electron C 109:146–156
Raheja DK, Kanaujia BK, Kumar S (2019) Compact four-port MIMO antenna on slotted-edge substrate with dual-band rejection characteristics. Int J RF Microw Comput-Aided Eng 29(7)
Raheja DK, Kumar S, Kanaujia BK (2020) Compact quasi-elliptical-self-complementary four-port super-wideband MIMO antenna with dual band elimination characteristics. AEU Int J Electron Commun 114
Roges R, Malik PK, Sharma S (2022) A compact wideband antenna with DGS for IoT applications using LoRa technology. In: 2022 10th International conference on emerging trends in engineering and technology—signal and information processing (ICETET-SIP-22), pp 1–4. https://doi.org/10.1109/ICETET-SIP-2254415.2022.9791725

Roy S, Biswas AK, Ghosh S, Chakraborty U, Sarkhel A (2021) Isolation improvement of dual-/quad-element textile MIMO antenna for 5G application. J Electromagn Waves Appl 35(10):1337–1353
Sehrai DA et al (2021) Compact quad-element high-isolation wideband MIMO antenna for mm-wave applications. Electronics 10(11)
Sharma M (2020) Design and analysis of MIMO antenna with high isolation and dual notched band characteristics for wireless applications. Wirel Pers Commun 112(3):1587–1599
Sharma M, Dhasarathan V, Patel SK, Nguyen TK (2020a) An ultra-compact four-port 4 × 4 super-wideband MIMO antenna including mitigation of dual notched bands characteristics designed for wireless network applications. AEU Int J Electron Commun 123
Sharma M, Vashist PC, Ashtankar PS, Mittal SK (2020b) Compact 2 × 2/4 × 4 tapered microstrip feed MIMO antenna configuration for high-speed wireless applications with band stop filters. Int J RF Microw Comput-Aided Eng 31(1)
Sharma M, Kumar R, Kaur P, Dhasarathan V, Nguyen TK (2021a) Design and analysis of on-demand reconfigurable WiMAX/WLAN high isolation 2 × 2 MIMO antenna oriented adjacent/orthogonally for imaging applications in UWB-X band. Int J RF Microw Comput-Aided Eng 32(1)
Sharma M, Vashist PC, Alsukayti I, Goyal N, Anand D, Mosavi AH (2021b) A wider impedance bandwidth dual filter symmetrical MIMO antenna for high-speed wideband wireless applications. Symmetry 14(1)
Shreshtha S, Aggarwal M, Ghane P, Varahramyan K (2021) Flexible microstrip antenna for skin contact application. Int J Antennas Propag Article ID 745426:1–6. https://doi.org/10.1155/2012/745426
Singh D et al (2021) Inverted-c ground MIMO antenna for compact UWB applications. J Electromagn Waves Appl 35(15):2078–2091
Sohi AK, Kaur A (2020) Hexa-band suppression characteristics from a fork-shaped UWB-MIMO antenna loaded with complementary split-ring resonator and slots. J Electromagn Waves Appl 34(16):2194–2219
Srivastava K, Kumar A, Kanaujia BK, Dwari S, Kumar S (2019a) A CPW-fed UWB MIMO antenna with integrated GSM band and dual band notches. Int J RF Microw Comput-Aided Eng 29(1)
Srivastava K, Kanaujia BK, Dwari S, Kumar S, Khan T (2019b) 3D cuboidal design MIMO/diversity antenna with band notched characteristics. AEU-Int J Electron C 108:141–147
Sun D, Wang P, Gao P, Zhang Y (2017) A novel dual-band MIMO antenna with two rings for WIMAX applications. J Electromagn Waves Appl 32(3):274–280
Tang X, Yao Z, Li Y, Zong W, Liu G, Shan F (2020a) A high performance UWB MIMO antenna with defected ground structure and U-shape branches. Int J RF Microw Comput-Aided Eng 31(2)
Tang Z, Zhan J, Wu X, Xi Z, Chen L, Hu S (2020b) Design of a compact UWB-MIMO antenna with high isolation and dual band-notched characteristics. J Electromagn Waves Appl 34(4):500–513
Thakur E, Jaglan N, Gupta SD (2020) Design of compact triple band-notched UWB MIMO antenna with TVC-EBG structure. J Electromagn Waves Appl 34(11):1601–1615
Tiwari P, Malik PK (2020) Design of UWB antenna for the 5G mobile communication applications: a review. In: 2020 International conference on computation, automation and knowledge management (ICCAKM), pp 24–30. https://doi.org/10.1109/ICCAKM46823.2020.9051556. ISBN: 978-1-7281-0666-3. https://ieeexplore.ieee.org/document/9051556
Tiwari RN, Singh P, Kanaujia BK (2019a) A compact UWB MIMO antenna with neutralization line for WLAN/ISM/mobile applications. Int J RF Microw Comput-Aided Eng 29(11)
Tiwari RN, Singh P, Kanaujia BK, Srivastava K (2019b) Neutralization technique based two and four port high isolation MIMO antennas for UWB communication. AEU Int J Electron Commun 110
Tiwari RN, Singh P, Kanaujia BK, Kumar S, Gupta SK (2020) A low profile dual band MIMO antenna for LTE/Bluetooth/Wi-Fi/WLAN applications. J Electromagn Waves Appl 34(9):1239–1253
Vasu Babu K, Anuradha B (2019) Design of inverted L-shape & ohm symbol inserted MIMO antenna to reduce the mutual coupling. AEU Int J Electron Commun 105:42–53

Wang C, Yang XS, Wang BZ (2020) A metamaterial-based compact broadband planar monopole MIMO antenna with high isolation. Microw Opt Technol Lett 62(9):2965–2970
Yussuf AA, Paker S (2019) Design of a compact quad-radiating element MIMO antenna for LTE/Wi-Fi application. AEU Int J Electron Commun 111

Chapter 10
Reconfigurable Antennas for Internet of Things (IoT) Devices

G. Umamaheswari, A. Praveena, and Shanmugam Bhaskar Vignesh

Abstract The Internet of Things (IoT) is a network that provides interoperability between wireless and a variety of low-power wireless devices linked via the Internet. It is a platform that requires the transmission of a large volume of data and a higher number of communication links, which leads to packet collision, reduced network efficiency, and increased power consumption for retransmission of lost packets. Today, advancements in technology are moving ahead towards higher and higher frequency bands to facilitate higher data rates. To better establish communication links between wireless devices, the selection and reconfigurability of the antennas for the IoT devices play a key role. Some characteristics of antennas such as operating frequency, radiation pattern, and polarization are electronically reconfigured by changing the surface currents on the antenna by using techniques such as biasing of diodes, digitally tuned capacitors, shorting pins, and so on. Frequency reconfigurable antennas meet the requirement of operating in more than one operating frequency which is vital in technologies such as the IoT, where multiple communication links among devices are needed. This article presents a review of various reconfigurable antennas for IoT, and a reconfigurable microstrip slot antenna is proposed for emerging 5G and IoT applications. An optimal-sized antenna at 28/60 GHz with multiple slots on the rectangular patch and defected ground structure is designed and simulated. The simulated antenna exhibits good antenna performance characteristics, such as a realized gain of 6.54 dB at 28 GHz and 2.27 dB at 60 GHz. A bandwidth of 8.8% and 11.25% at 28 GHz, 60 GHz, respectively, is achieved. The radiation efficiency of 81% at 28 GHz and 83% at 60 GHz are obtained. An antenna is constructed using an FR4 epoxy as dielectric material, with a size of 7×7 mm^2 and with thickness of 0.8 mm. An inset feed with a quarter-wave transformer is used for good impedance matching.

G. Umamaheswari · A. Praveena (✉)
PSG College of Technology, Coimbatore, India
e-mail: career.praveena@gmail.com

S. B. Vignesh
NTU, Singapore, Singapore

P. K. Malik and P. N. Shastry (eds.), *Internet of Things Enabled Antennas for Biomedical Devices and Systems*, Springer Tracts in Electrical and Electronics Engineering,
https://doi.org/10.1007/978-981-99-0212-5_10

Keywords Defected ground structure · Hybrid reconfigurable antenna · IoT devices · Polarization · Quarter-wave transformer · Reconfigurable antenna

Introduction

The massive rise of the Internet of Things (IoT) and smart industrial use cases has created many technical and scientific obstacles, requiring creative research from academia and industry to produce cost-effective, scalable, efficient, and reliable antenna systems for IoT. An IoT device collects or detects data from an object or environment and sends it through a wireless channel to another device or the cloud. The devices can be controlled remotely over the wireless channel. Thus, it is evident that antenna plays a vital role in IoT Technology. Traditional antennas can only operate in a particular frequency band and have a predetermined emission pattern and polarization (Mathur et al. 2021). An IoT device, on the other hand, needs great capacity, simultaneous use of many frequency bands, and high-speed data transfer. The gadgets utilize many wireless services; hence additional transmission capacity is actually required. Using carrier aggregation, a single user can access many channels. Consequently, carrier aggregation aids in boosting IoT capacity and throughput. Each frequency band must be independently tuned without influencing other functioning bands in order to do this (Subbaraj et al. 2019). As a result, reconfigurable antennas (RAs) are envisioned as a suitable system that can modify basic properties such as operating frequency, polarization, and E and H plane radiation patterns to meet the demands of various communication systems such as IoT sensors and mobile stations. Microstrip patch antennas are ideal candidates for IoT applications because they are small, lightweight, compact, and easy to incorporate antennas with low fabrication costs (Mahlaoui et al. 2017; Merlin Teresa and Umamaheswari 2020; Riaz et al. 2022). Various reconfigurable patch antennas for IoT, Wireless, and Cognitive radio applications have been described in the literature (Karthika and Kavitha 2021; Madhav and Anilkumar 2019; Vamsee Krishna et al. 2019; Boufrioua 2020; Tu and Sang 2021; Allam et al. 2019; AL-Muttairy and Farhan 2020; Balanis 2003; Singh et al. 2020; Ullah et al. 2021; Wang et al. 2020; Akinola et al. 2021; AL-Fadhali et al. 2021; Asadallah et al. 2017; Ojaroudi Parchin et al. 2020; Trinh et al. 2017; Haydhah et al. 2021; Santamaria et al. 2021; Palsokar and Lahudkar 2020; Rajagopalan et al. 2013; Shankar 2021; Lee and Choi 2017; Chen et al. 2019; Al-Yasir et al. 2018; Ingle et al. 2021; Rao and Govardhani 2021; Barakali 2019; Balcells et al. 2010; Schaffner et al. 2000; Kamran Shereen et al. 2019; Ahmad et al. 2021; Shereen et al. 2020).

Reconfigurable Antennas (RAs)

The primary idea of a RA is to adjust the typical parameters by changing the physical features of the antenna by joining or separating different sections of it. Reconfigurability in terms of frequency, polarization, and radiation pattern can be achieved in various ways (Karthika and Kavitha 2021).

Reconfigurable Antenna (RA)-Types

Based on the antenna parameters that are dynamically modified, often the operating frequency, radiation pattern, or polarization, RAs can be of several types. The classification of reconfigurable antennas is illustrated in Fig. 10.1. The primary types of RAs include frequency RA, polarization RA, pattern RA, and hybrid or compound RA. Combination of two or more reconfigurability in one antenna is known as hybrid or compound RA. Further this is sub-classified into frequency and pattern RA, frequency and polarization RA, pattern and polarization RA, and frequency, pattern and polarization RA as shown in Fig. 10.1.

Frequency Reconfigurable Antenna

Multiple antennae are used in a modern wireless communication technology to execute a variety of application-oriented activities. The result is the system gets increasingly complicated and bulky. To achieve portability in wireless devices, multiple antennas residing in the device are replaced with a one radiating element to

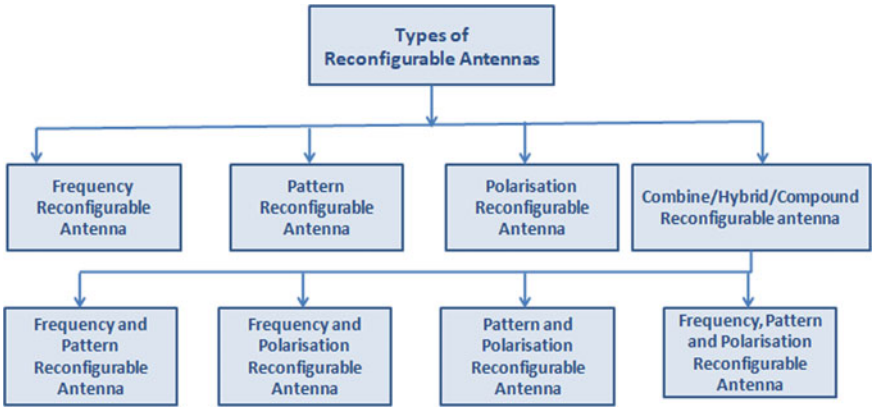

Fig. 10.1 Types of reconfigurable antennas based on change in parameters (Karthika and Kavitha 2021)

function at different frequencies, i.e., multi-band antennas were developed. Nevertheless, these antennas have a deterministic performance and unchangeable according to the user's needs. The concept of frequency reconfiguration is a great option in such situations. As a result, the radiating structure can change its operating frequency in response to demand. These antennas are crucial in technologies like 5G and IoT (Karthika and Kavitha 2021). (Mathur et al. 2021; Riaz et al. 2022; Madhav and Anilkumar 2019; Vamsee Krishna et al. 2019; Tu and Sang 2021; Allam et al. 2019; AL-Muttairy and Farhan 2020; Singh et al. 2020) presents various frequency-reconfigurable antennas for IoT devices (Subbaraj et al. 2019; Karthika and Kavitha 2021; Vamsee Krishna et al. 2019; Boufrioua 2020; Ullah et al. 2021; Rajagopalan et al. 2013) for Wireless communications and (Rajagopalan et al. 2013) for Cognitive Radio Applications. Table 10.1 illustrates the comparison between the suggested antenna and several frequency RAs mentioned in the literature.

Pattern Reconfigurable Antenna

A one only radiating element can substitute multiple single-purpose antennae by including reconfigurability in diverse parameters. Adaptive and non-adaptive radiation patterns are the two types of antenna radiation patterns. Compared to non-adaptive, adaptive radiation patterns gives greater network capacity (Lee and Choi 2017). Literature (Trinh et al. 2017; Haydhah et al. 2021; Santamaria et al. 2021; Palsokar and Lahudkar 2020) presented various pattern reconfigurable antennas for IoT Applications. In (Trinh et al. 2017), a cylindrical metal antenna with a maximum size of 0.58λ, 4 dBi Gain at 2.4 GHz frequency with 80% efficiency for IoT networking Applications is presented. The antenna is switched between three directional patterns and an omnidirectional pattern using PIN diodes as a switch (Haydhah et al. 2021). A novel antenna with four patterns of reconfigurability which include electric, magnetic omnidirectional, and two-directional patterns in two modes at 868 MHz is obtained by employing PIN diodes with 80×55 mm^2 sizes for IoT applications. An electronically pattern (EP) RA consisting of four-wire patches is reported in Santamaria et al. (2021). The patch is switched between four end-fire radiation states from 2.25 to 2.54 GHz and a SP4T switch is used to enable the radiation pattern steering. This method limits the use of electronic components in the reconfiguration process.

Polarization Reconfigurable Antenna

Polarization establishes the direction of the electric field of the transmitting or receiving RF transmission. Based on the type of orientation, it is categorized as Linear, Elliptical, or Circular Polarization. Vertical, Horizontal Polarizations are two types of linear polarization. Elliptical polarization is classified as Right-Hand (RH) and Left-Hand Elliptical Polarization (LHEP). Similarly, based on the direction of rotation (DoR) of RF signal, Circular Polarization is also classified as Right-Hand

Table 10.1 The comparison of constructed antenna with various frequency-reconfigurable antennae is reported in the literature

Ref	Antenna size (mm^2)	No. of bands	Operating bands (GHz)	Reconfiguration Techniques	Applications
Mathur et al. (2021)	59 × 61	2	2.398–2.955 and 2.234–2.944	Mechanical	IoT
Subbaraj et al. (2019)	25 × 10	4	0.9, 2.4, 3.5, and 5.5	Varactor diodes	Handheld Wireless devices
Riaz et al. (2022)	40 × 40	Continuous Tenability	1.4 to 2.9	Varactor diodes	IoT
Madhav and Anilkumar (2019)	40 × 30	4	2.2, 2.45, 4.26, and 7.34	PIN diodes	Vehicular IoT Communication Platforms
Vamsee Krishna et al. (2019)	8 × 27.5	3	1, 2.4, 10 and 18	PIN diodes	IoT and Wireless Applications
Boufrioua (2020)	55 × 55		4 to 5.5	PIN diodes	Wireless Communications
Tu and Sang (2021)	30 × 30	8	0.9; 1.8; 2.6; 5, 2.4; 3.3; 5.5; 8.2	PIN diode	IoT
Allam et al. (2019)	33 × 31	6	2.47, 7.18, 12.14, 8.4, 3.42, 14.55	PIN Diode	IoT
AL-Muttairy and Farhan (2020)	33.5 × 16	2	2.4 and 5	PIN Diode	IoT
Singh et al. (2020)	25 × 25	5	3.85, 4.14, 4.43, 4.91, and 6.01	PIN Diode	IoT
Ullah et al. (2021)	37 × 35	4	2.1, 2.45, 3.2, and 3.5	PIN Diode	Portable Wireless Applications
Akinola et al. 2021)	23 × 23.4	4	16, 16.5, 21.9, and 21.7	Diode	Covid-19 Tracking
Rajagopalan et al. (2013)	100 × 120	2	2.0–2.6 and 2.6–3.2	RF-MEMS	Cognitive Radio
Rajagopalan et al. (2013)	50 × 50	4	4.5, 3.5, 2.4, and 1.8	PIN Diode	RF Harvesting
Proposed	7 × 7	2	28 and 60	Structural change	IoT and 5G applications

and Left-Hand Circular Polarization (LHCP) as presented in Fig. 10.2. The RF signal can travel numerous paths to reach its target in a wireless environment, causing multi-path fading, path, and shadowing losses. As a result, information loss occurred to the variation in polarization of the transmitted signal. This may be prevented by adopting polarization-diversity antennae. Reconfiguring the feed or changing the radiating structure can both be used to achieve polarization variety (Karthika and Kavitha 2021). The literature reported in Lee and Choi (2017); Chen et al. (2019); Al-Yasir et al. (2018); Ingle et al. (2021); Rao and Govardhani (2021), Balcells et al. (2010) reports various polarizations-reconfigurable antennae and techniques for IoT applications.

A polarization reconfigurable antenna with felt fabric as substrate material for wearable IoT is presented. As shown in Fig. 10.3, PIN diodes are connected to the edge truncations of the radiating patch to achieve three possible reconfigurable polarizations, which includes linear polarization, Right-hand, and Left-hand circular polarization. The antenna resonates at a 2.4 GHz ISM band with an average gain of 5.96 dBi among all three polarizations (Lee and Choi 2017). Overall Structure of polarization reconfigurable antenna with switches is reported in Fig. 10.1 of Lee and Choi (2017). In Al-Yasir et al. (2018), authors have designed and fabricated a prototype of a microstrip antenna that can be reconfigured between right hand and left-hand circular polarization. The circular polarization reconfigurability is achieved by adjusting the DC biasing of PIN diodes. The antenna has a fractional bandwidth

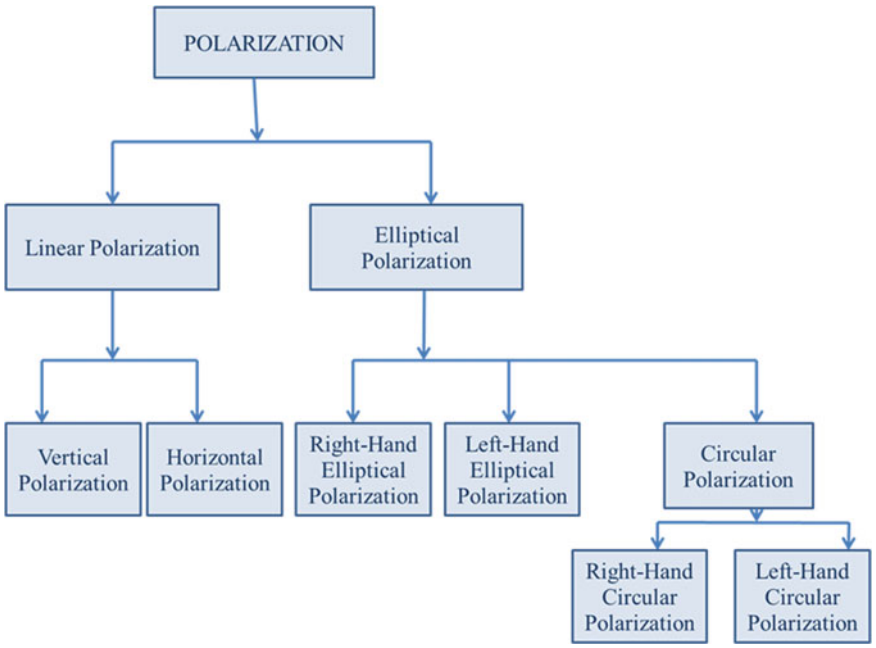

Fig. 10.2 Basic classification of polarization in antenna

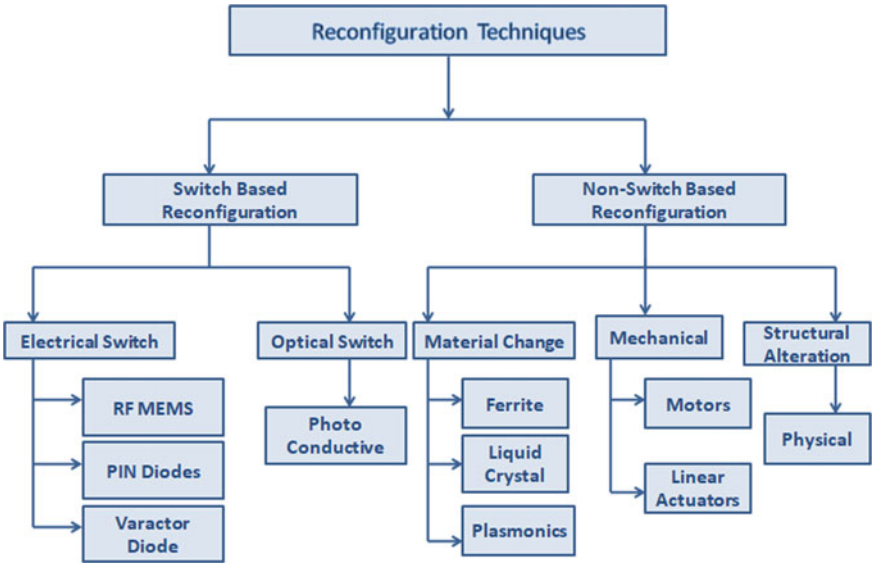

Fig. 10.3 Categorization of reconfiguration techniques (Karthika and Kavitha 2021)

of 9.11%, with a maximum realized gain of (3.1–4.8) dBic at 3.5 GHz. A Scopus data-based bibliometric study of a circularly polarized reconfigurable antenna is presented in Ingle et al. (2021), which helps researchers in this area quickly study various circularly polarized reconfigurable antennas published between 2002 and 2021. Authors in Rao and Govardhani (2021) have designed a rectangular microstrip antenna with a defective ground structure that can be reconfigured between linear and Right-hand circular polarization (RHCP) using a PIN diode for WLAN applications. In Balcells et al. (2010), a millimeter-wave antenna resonating at 60 GHz is designed with the ability to reconfigure between right-handed, circular polarization (CP), or linear polarization (LP) using RF-MEMS switches.

Hybrid/Combined/Compound Reconfigurable Antenna

Any antenna's properties, such as frequency of operation, radiation pattern, and polarization, can be reconfigured based on the use cases. Space vehicles, radar and military, and aviation applications demand a fast and secure link between the communication end-users (Schaffner et al. 2000). Its performance may be hampered by electromagnetic interference and pollution. The single reconfiguration would not be a practical option for these applications. As a result, it requires a cognitive antenna that can transition between different operating frequencies, polarization types, and radiation patterns (Karthika and Kavitha 2021). Palsokar and Lahudkar (2020); Barakali (2019) presents antennas with pattern and frequency reconfigurability. Figure 10.5 of Palsokar and Lahudkar (2020) represents the prototype of the fabricated antenna

which has the ability to switch between pattern and frequency reconfigurability. A few compound reconfigurable antennas are reported in Barakali (2019); Schaffner et al. (2000); Kamran Shereen et al. (2019).

Classification of Reconfiguration Techniques (Karthika and Kavitha 2021)

The technique used to reconfigure an antenna plays a vital role because it changes the current distribution of the radiating structure by connecting and disconnecting various elements of the structure. As demonstrated in Fig. 10.3, many switching mechanisms employ switches such as electrical, optical and also mechanical switches, external adjustment, and the use of reconfigurable materials, etc. (Mathur et al. 2021). Switching techniques for the reconfigurable antennas are reported in Ojaroudi Parchin et al. (2020).

Proposed Antenna Structure and Dimensions

The constructed antenna structure and its overall dimensions are presented in Fig. 10.4a–c. Figure 10.4a shows the patch layer, and Fig. 10.4b presents the bottom layer of the proposed slotted patch antenna for 28 GHz frequency, and Fig. 10.4c presents the bottom layer for 60 GHz frequency. The top layer of the antenna consists of radiating slotted patch antenna and an insert feed line with a quarter-wave transformer with the full ground. An antenna's ground is known to use a defective ground structure (DGS) to minimize antenna size and increase bandwidth (Mahlaoui et al. 2017). The bottom layer of the antenna is made DGS by etching a square slot of 0.2 mm width on a full ground plane. The outer layer of the slot is of 3.62×2.2 mm^2 size; the shift in frequency from 28 to 60 GHz is achieved by defective ground structure or the slot made in the bottom layer of the proposed antenna. The proposed antenna is realized on FR4 material substrate (thickness = 0.8 mm and $\varepsilon_r = 4.4$). The overall antenna is etched on a substrate material possessing size of $7 \times 7 \times 0.8$ mm^3, which can be employed to the Internet of Things (IoT) devices and portable wireless devices. Slot S_1 on the patch has 0.05×1.8 mm^2, and width is kept unchanged for all the slots, and the length of each adjacent slot is reduced by 0.2 mm. The gap between two adjacent slots is 0.2 mm is maintained. The detailed dimensions of the constructed antenna are noted in Table 10.2. The simulated antenna structure is shown in Fig. 10.5. The antenna is designed using HFSS simulation tool. The reconfigurability of an antenna is achieved using structural change in the ground.

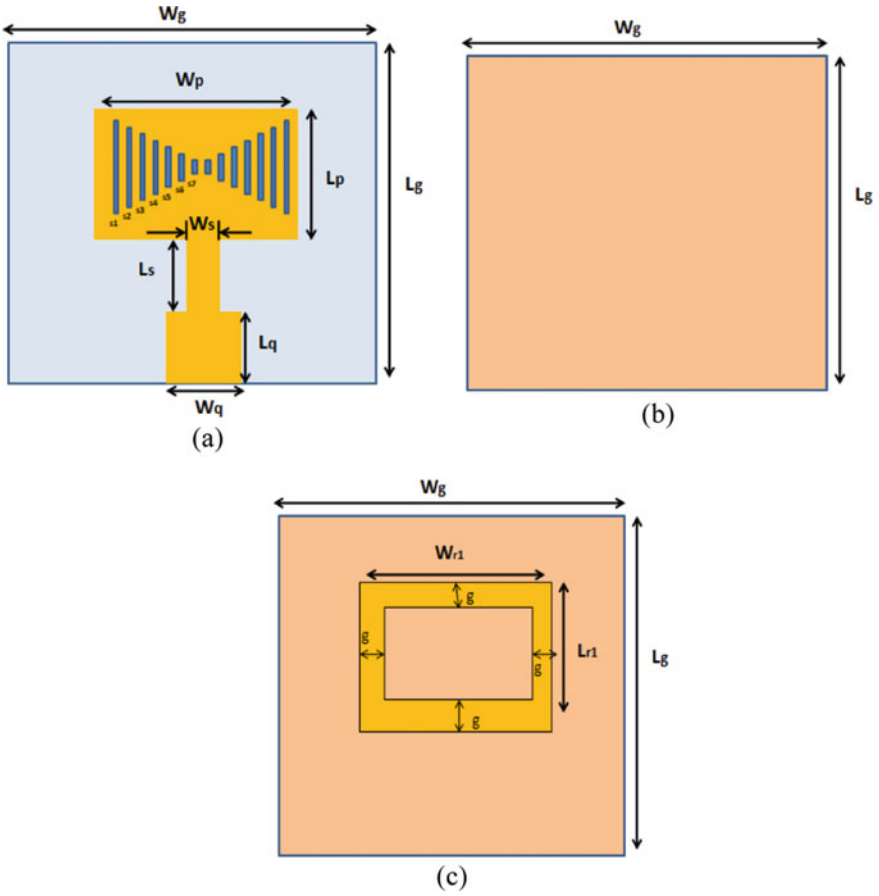

Fig. 10.4 **a** The top layer and **b** the bottom layer of the constructed antenna for 28 GHz. **c** the bottom layer of the constructed antenna for 60 GHz

Simulation Results and Discussions

The performance of the proposed slotted patch antenna is analyzed; HFSS version 15 was used in the simulations. Figures 10.6 and 10.10 illustrate the S_{11} characteristics of the constructed antenna at 28 and 60 GHz frequencies, respectively. The reflection coefficient of −24.99 dB at 28 GHz with a bandwidth of 2490 MHz is shown in Fig. 10.6. Similarly, −24.18 dB reflection coefficient and bandwidth of 6800 MHz is achieved at 60 GHz as reported in Fig. 10.10. The VSWR at all the resonating frequency ranges is less than two (<2) for both 28 and 60 GHz antenna modes. The realized gain of 6.54 dB is achieved at 28 GHz and 2.27 dB at 60 GHz, as shown in Figs. 10.7 and 10.11, respectively. Figures 10.8 and 10.12 illustrate realized 2D gain polar plots along with the XZ and YZ plane of the simulated

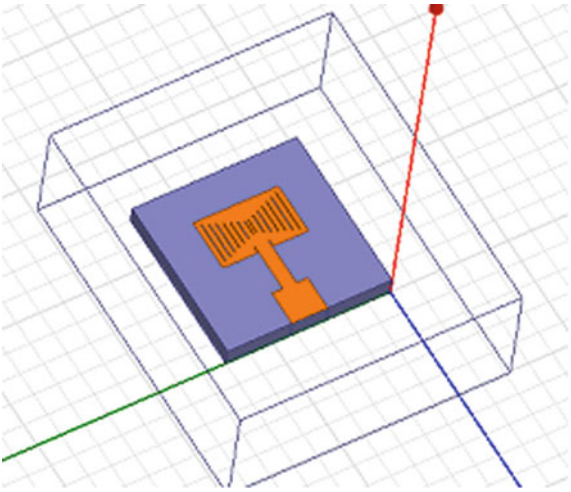

Fig. 10.5 Constructed antenna structure in simulation environment

Table 10.2 Dimensions of the proposed antenna structure

Dimensions of patch layer		Dimensions of ground layer	
Symbol	Dimension (mm)	Symbol	Dimension (mm)
W_g	7	W_g	7
L_g	7	L_g	7
W_p	3.62	W_{r1}	3.62
L_p	2.2	L_{r1}	2.2
W_s	0.58	W_{r2}	3.6
L_s	1.35	L_{r2}	2.18
L_q	1.47	G	0.02
w_q	1.53	–	–

antenna with full and defected ground, respectively. From Figs. 10.9 and 10.13, it is observed that the antenna with the full ground obtained a radiation efficiency of 81% at 28 GHz frequency, and the antenna with defected ground structure achieved a radiation efficiency of 83% at 60 GHz frequency.

Conclusion

This chapter presents a review of various reconfigurable antennas for IoT, and a reconfigurable microstrip slot antenna is proposed for emerging 5G and IoT applications. A compact antenna at 28/60 GHz with multiple slots on the rectangular patch and defected ground structure is designed and simulated. The simulated antenna exhibits good performance characteristics, such as a realized gain of 6.54 dB at 28 GHz and

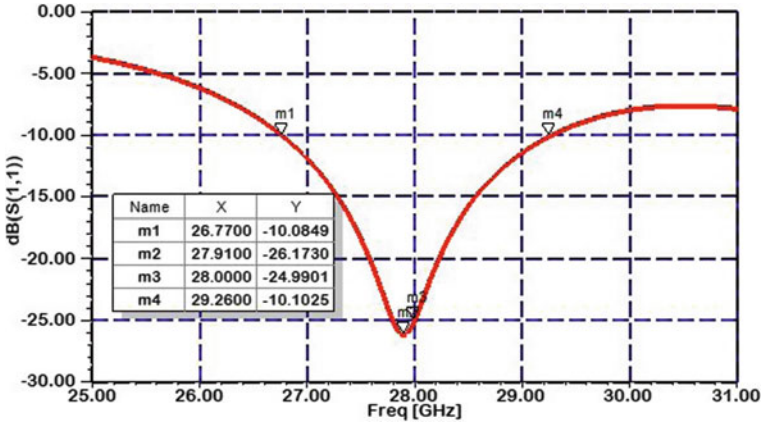

Fig. 10.6 S_{11} characteristics of a simulated antenna with the full ground

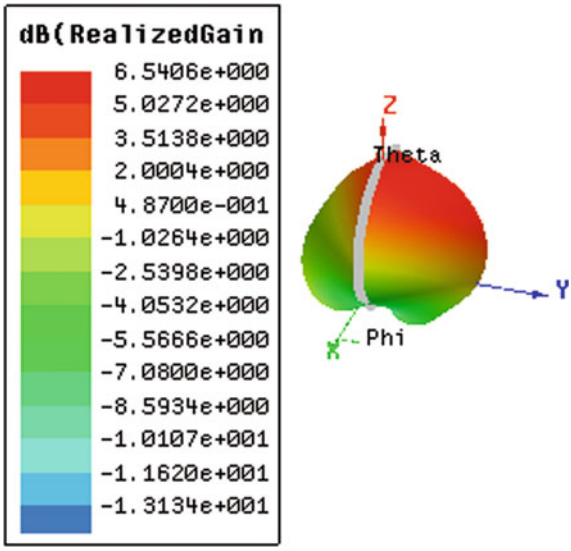

Fig. 10.7 3D realized gain plot of the simulated antenna with the full ground

2.27 dB at 60 GHz. A bandwidth of 8.8 and 11.25% at 28 GHz, 60 GHz, respectively, is achieved. The radiation efficiency of 81% at 28 GHz and 83% at 60 GHz are obtained. An antenna is constructed using an FR4 substrate with an overall size of 7 mm × 7 mm × 0.8 mm. An inset feed with a quarter-wave transformer is used for good impedance matching.

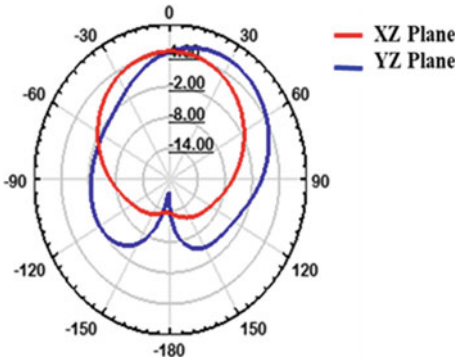

Fig. 10.8 Polar plot along with the XZ and YZ plane of a simulated antenna with full ground

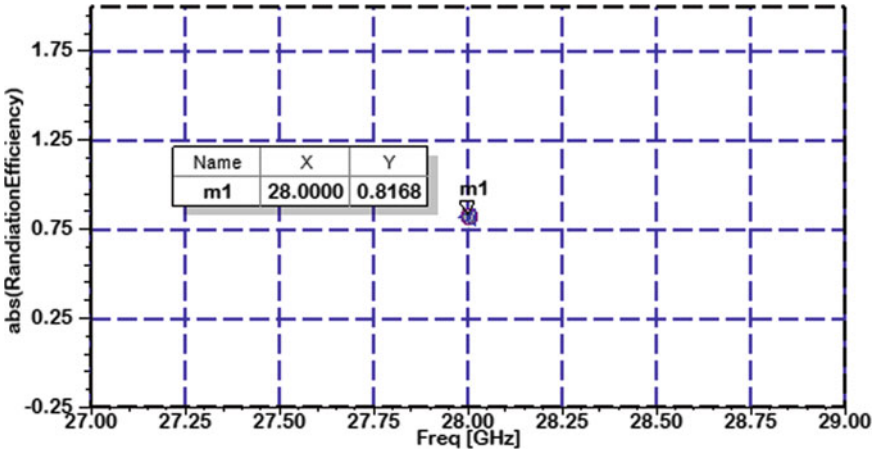

Fig. 10.9 Radiation efficiency versus Frequency plot of a simulated antenna with the full ground

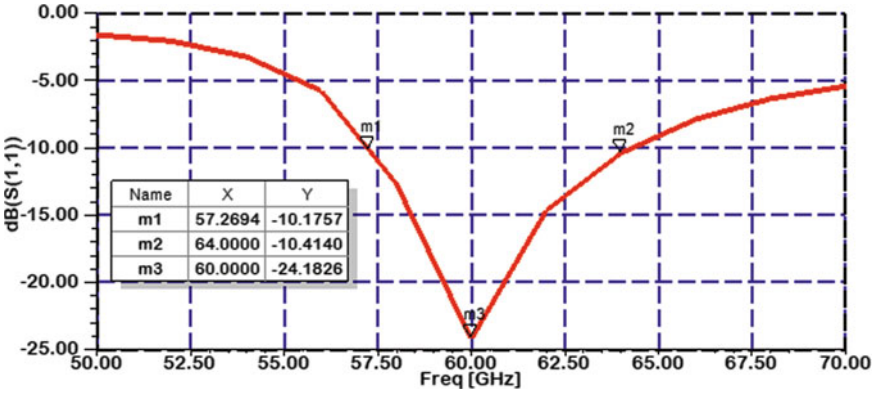

Fig. 10.10 S_{11} characteristics of a simulated antenna with defected ground structure (DGS)

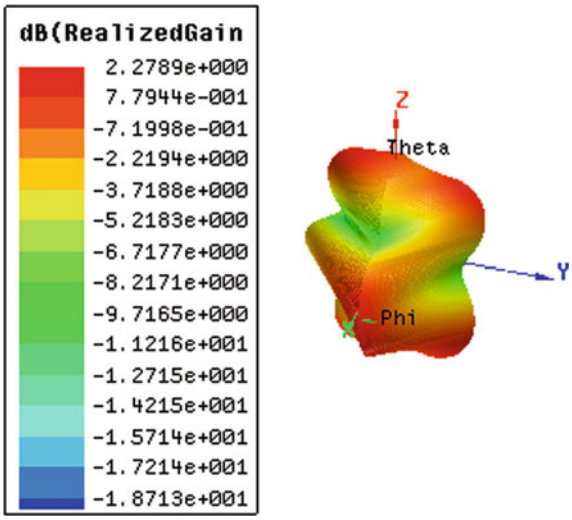

Fig. 10.11 3D realized gain plot of a simulated antenna with defected ground structure (DGS)

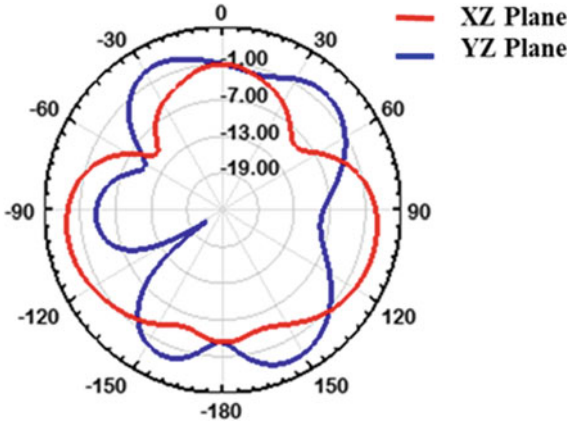

Fig. 10.12 Polar plot along with the XZ and YZ plane of a simulated antenna with defected ground structure (DGS)

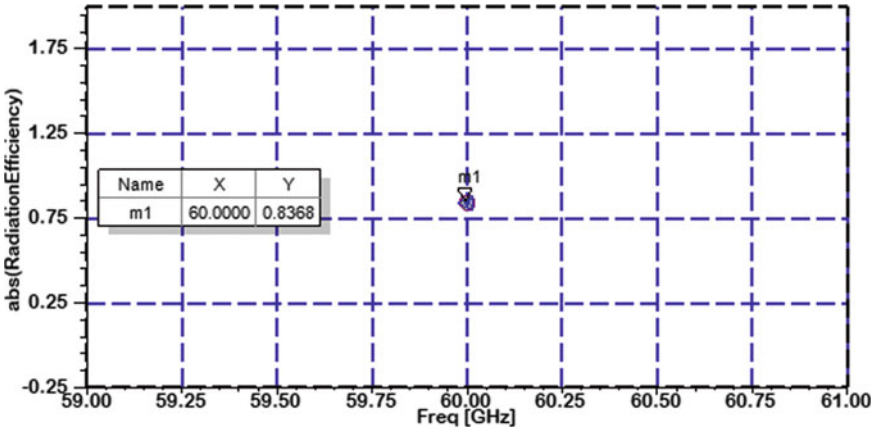

Fig. 10.13 Radiation efficiency versus frequency plot of a simulated antenna with defected ground structure (DGS)

References

Ahmad I, Dildar H, Khan WUR, Shah SAA, Ullah S, Ullah S, Umar SM, Albreem MA, Alsharif MH, Vasudevan K (2021) Design and experimental analysis of multiband compound reconfigurable 5G antenna for sub-6 GHz wireless applications. Wireless Commun Mob Comput

Akinola A, Singh G, Ndjiongue A (2021) Frequency-domain reconfigurable antenna for COVID-19 tracking. Sens Int 2:100094

AL-Fadhali N, Majid HA, Omar R, Abdul Sukor J, Rahim MK, Zainal Abidin Z, Al-Bukhaiti, M, Momin AM, Abo Mosali N (2021) Review on frequency reconfigurable antenna using substrate-integrated waveguide for cognitive radio application. J Electromagn Waves Appl 35(7):958–990

Allam VK, Madhav BT, Anilkumar T, Maloji S (2019) A novel reconfigurable bandpass filtering antenna for IoT communication applications. Progress Electromag Res C 96:13–26

AL-Muttairy AI, Farhan MJ (2020) Frequency reconfigurable monopole antenna with harmonic suppression for IoT applications. TELKOMNIKA (Telecommun Comput Electron Control 18(1):10–18

Al-Yasir YI, Abdullah AS, Ojaroudi Parchin N, Abd-Alhameed RA, Noras JM (2018) A new polarization-reconfigurable antenna for 5G applications. Electronics 7(11):293

Asadallah FA, Costantine J, Tawk Y, Lizzi L, Ferrero F, Christodoulou CG (2017) A digitally tuned reconfigurable patch antenna for IoT devices. In: 2017 IEEE international symposium on antennas and propagation & USNC/URSI national radio science meeting. IEEE, pp 917–918

Balanis CA (2003) Smart antennas for future reconfigurable wireless communication networks. In: IEEE topical conference on wireless communication technology, pp 181–182

Balcells J, Damgaci Y, Cetiner BA, Romeu J, Jofre L (2010) Polarization reconfigurable MEMS-CPW antenna for mm-wave applications. In: Proceedings of the fourth European conference on antennas and propagation. IEEE, pp 1–5

Barakali B (2019) Pattern and polarization reconfigurable antennas for gain enhancement. Ph.D. thesis, University of Sheffield

Boufrioua A (2020) Frequency reconfigurable antenna designs using PIN diode for wireless communication applications. Wireless Pers Commun 110(4):1879–1885

Chen Z, Wong H, Xiang J, Liu SZ (2019) Polarization-reconfigurable antennas for internet of things. In: 2019 international conference on microwave and millimeter wave technology (ICMMT). IEEE, pp 1–3

Haydhah SA, Ferrero F, Lizzi L, Sharawi MS, Zerguine A (2021) A multifunctional compact pattern reconfigurable antenna with four radiation patterns for sub-GHz IoT applications. IEEE Open J Antennas Propag 2:613–622

Ingle U, Chaurasia V, Basu M, Arjun C, Kumar S, Tupe-Waghmare P (2021) Circularly polarised reconfigurable antenna in 5G application: a bibliometric study using Scopus database. Library Philos Pract (e-journal) 5761

Kamran Shereen M, Khattak MI, Witjaksono G (2019) A brief review of frequency, radiation pattern, polarization, and compound reconfigurable antennas for 5G applications. J Comput Electron 18(3):1065–1102

Karthika K, Kavitha K (2021) Reconfigurable antennas for advanced wireless communications: a review. Wireless Pers Commun 120(4):2711–2771

Lee H, Choi J (2017) A polarization reconfigurable textile patch antenna for wearable IoT applications. In: 2017 international symposium on antennas and propagation (ISAP). IEEE, pp 1–2

Madhav BTP, Anilkumar T, Vaishnavi V, Chand TB, Naga Lakshmi PG, Hawanika YS (2019) Switchable fractal antenna for LTE and vehicular IoT communication platforms. Int J Sci Technol Res 8(11)

Mahlaoui Z, Antonino-Daviu E, Ferrando-Bataller M, Benchakroun H, Latif A (2017) Frequency reconfigurable patch antenna with defected ground structure using varactor diodes. In: 2017 11th European conference on antennas and propagation (EUCAP). IEEE, pp 2217–2220

Mathur P, Madanan G, Raman S (2021) Mechanically frequency reconfigurable antenna for WSN, WLAN, and LTE 2500 based internet of things applications. Int J RF Microwave Comput Aided Eng 31(2):e22318

Merlin Teresa P, Umamaheswari G (2020) Compact slotted microstrip antenna for 5G applications operating at 28 GHz. IETE J Res 1–8

Ojaroudi Parchin N, Jahanbakhsh Basherlou H, Al-Yasir YI, Abdulkhaleq M, Abd-Alhameed R (2020) Reconfigurable antennas: switching techniques—a survey. Electronics 9(2):336

Palsokar AA, Lahudkar SL (2020) Frequency and pattern reconfigurable rectangular patch antenna using single PIN diode. AEU Int J Electron Commun 125. https://doi.org/10.1016/j.aeue.2020.153370

Rajagopalan H, Kovitz JM, Rahmat-Samii Y (2013) MEMS reconfigurable optimized E-shaped patch antenna design for cognitive radio. IEEE Trans Antennas Propag 62(3):1056–1064

Rao DS, Govardhani I (2021) A switchable polarization slotted WLAN antenna with DGS for IOT and medical applications. In: IOP conference series: materials science and engineering, vol 1057, No. 1. IOP Publishing, p 012090

Riaz S, Khan M, Javed U, Zhao X (2022) A Miniaturized frequency reconfigurable patch antenna for IoT applications. Wireless Pers Commun 123(2):1871–1881

Santamaria L, Ferrero F, Staraj R, Lizzi L (2021) Electronically pattern reconfigurable antenna for IoT applications. IEEE Open J Antennas Propag 2:546–554

Schaffner JH, Loo RY, Sievenpiper DF, Dolezal FA, Tangonan GL, Colburn JS, Lynch JJ, Lee JJ, Livingston SW, Broas RJ, Wu M (2000) Reconfigurable aperture antennas using RF MEMS switches for multi-octave tunability and beam steering. In: IEEE antennas and propagation society international symposium. Transmitting waves of progress to the next millennium. 2000 Digest. Held in conjunction with: USNC/URSI national radio science meeting, vol 1. IEEE, pp 321–324

Shankar BJ (2021) An Iot controlled octahedron frequency reconfigurable antenna for Rf sensing applications. In: Proceedings of the international conference on IoT based control networks & intelligent systems

Shereen MK, Khattak MI, Al-Hasan MA (2020) A frequency and radiation pattern combo-reconfigurable novel antenna for 5G applications and beyond. Electronics 9(9):1372

Singh PP, Goswami PK, Sharma SK, Goswami G (2020) Frequency reconfigurable multiband antenna for IoT applications in WLAN, Wi-Max, and C-band. Progress Electromagnet Res C 102:149–162

Subbaraj S, Kanagasabai M, Alsath MGN, Palaniswamy SK, Kingsly S, Kulandhaisamy I, Shrivastav AK, Natarajan R, Meiyalagan S (2019) A compact frequency-reconfigurable antenna with independent tuning for hand-held wireless devices. IEEE Trans Antennas Propag 68(2):1151–1154

Trinh LH, Le TN, Staraj R, Ferrero F, Lizzi L (2017) A pattern-reconfigurable slot antenna for IoT network concentrators. Electronics 6(4):105

Tu DTT, Sang NV (2021) Frequency reconfigurable multiband MIMO antenna base on gradient arcs for IoT devices. Adv Electromagnet 10(2):85–93

Ullah S, Ullah S, Ahmad I, Khan WUR, Ahmad T et al (2021) Frequency reconfigurable antenna for portable wireless applications. Comput Mater Continua 68(3):3015–3027

Vamsee Krishna A, Madhav BTP, Avinash R, Koukab (2019) A novel H-shaped reconfigurable patch antenna for IoT and wireless applications. Int J Innov Technol Exploring Eng (IJITEE) 8(7)

Wang Z, Dong Y, Ning Y (2020) Frequency reconfigurable SRR-based compact antenna FOR IoT application. In: 2020 IEEE Asia-pacific microwave conference (APMC). IEEE, pp 148–150

Chapter 11
Microstrip Antenna for Internet of Things (IOT) Applications

Dharmendra V. Chauhan, Amit Patel, Alpesh Vala, Keyur Mahant, Sagar patel, and Hiren Mewada

Abstract The Internet of Things (IoT) is a technical tool for experts. It does this by using existing network infrastructures to turn physical resources into new things. The primary objective is to provide intelligent and effective services without user disruption. The Internet of Things paradigm aims to build a complex information system by fusing, among other technologies, big data, clouds, machine learning, artificial intelligence, effective data interchange through networking and sensor data collection. The diverse applications and uses of the Internet of Things (IoT) in various industries explain the trend toward IoT acceptability in the modern world. However, as with all IoT requirements, developing an efficient antenna on all relevant IoT frequency bands is necessary. A compact microstrip antenna based on monopole feed and the coplanar ground plane has been designed, optimized and fabricated, operated in dual band of IoT applications. The operating bands of the proposed antenna are 2.5 GHz and 5.2 GHz having a bandwidth of more than 500 MHz and providing the gain of 2.03 dB and 3.37 dB, respectively. Placement of the superstrate into the antenna makes the dual-band operation as well as improves the bandwidth. The proposed antenna is designed on FR4 epoxy, having a dielectric constant of 4.4

D. V. Chauhan (✉) · A. Patel · A. Vala · K. Mahant · S. patel
V T Patel Department of E&C Engineering, Chandubhai S Patel Institute of Technology, Charotar University of Science and Technology (CHARUSAT), Changa 388421, India
e-mail: dharmendrachauhan.ec@charusat.ac.in

A. Patel
e-mail: amitvpatel.ec@charusat.ac.in

A. Vala
e-mail: alpeshvala.ec@charusat.ac.in

K. Mahant
e-mail: keyurmahant.ec@charusat.ac.in

S. patel
e-mail: sagarpatel.ec@charusat.ac.in

H. Mewada
Prince Mohmmad Bin Fahad University, Al Khobar, Saudi Arabia
e-mail: hmewada@pmu.edu.sa

P. K. Malik and P. N. Shastry (eds.), *Internet of Things Enabled Antennas for Biomedical Devices and Systems*, Springer Tracts in Electrical and Electronics Engineering,
https://doi.org/10.1007/978-981-99-0212-5_11

and loss tangent (tan δ) 0.02. The overall size of the antenna is 30 mm x 30 mm × 1.6 mm, which is smaller than the previously published work.

Keywords Gain and Return loss · Internet of Things (IoT) · Microstrip Antenna · Radiation pattern · Superstrate

Application of Internet of Thing (IoT)

The primary goal of this section is to explore IoT applications discussed in current studies. The main application fields are healthcare, the environment, intelligent towns, trade, industry and infrastructure (Souri et al. 2017, 2018). The applications and utilization of IoT in the various fields lead and explain the trend towards IoT acceptability for the innovative world (Chettri and Bera 2019). Furthermore, learning the IoT requirements enhances IoT technology's understanding and development and, therefore, develops new systems for new cases (Tun et al. 2021; Kim and Kim 2018).

Environment Applications

Several evaluations of IoT's use in environmental applications have been conducted. To initiate, (Li et al. 2015) designed an internet surveillance system for hen houses that included a WSN and monitored environmental factors such as temperature, humidity, ammonia (NH3) and carbon dioxide. However, the majority of applications in the studies mentioned above, the authors, were tied to the creation of systems, with information transmission reliability not being considered. The authors of this work proposed a transport protocol that focuses on recovering from data loss in an effort to address the issue. In order to predict the data rate and improve the system's dependability, duplicated data was automatically filtered out, and missing data was filled in.

Additionally, the internet remote control system was developed so that administrators could view the data gathered via computers and mobile devices, enabling them to better manage the henhouse environment. Furthermore, future extensions of this research include strengthening the system's data-collecting precision and dependability and lowering tiny update and repairing costs. Energy use, on the other hand, was not assessed in this investigation.

Smart City Applications

Expand the Internet of Things (IoT) for creative city applications. (Montori et al. 2017) presented a SenSquare structural architecture that would provide a mobile sensing population to witness customer tests of existing smart city data flows. To assess the option for the proposed strategy, the present facility structure used a data mining categorization technique. However, the quality of the data and data privacy of the user was not measured. For a specific experimental prototype of numerical forensics, (Zia et al. 2017) developed a software design. In their study, they examine the methodology of forensics to review conventional regulations and production methods. In an Internet of Things numerical forensics solicitation, it assists with data collection, investigation, evaluation, and storage. The suggested methodology was evaluated using three IoT application scenarios: flexible devices, modern houses and shrewd cities. It introduced a paradigm applicable to assessing forensic data collection in an adaptable IoT setting. The presented approach does not account for security measures, although it appears prudent to make the process safer and more efficient.

Commercial Applications

In recent years, the prevalence of commercial Internet of Things demand has grown. (Alodib 2016) derived a framework method for automating the Quality of service-familiar facility construction and incorporating actual-time control into an experiment. The writer expressed grave concerns on the violation of Service Level Agreements. As a result, the Service Level Agreement was developed to link the Petri net to the Unified Modelling Language Quality of Service model via a user indicator. The discrete event system (DES), which demonstrates that the suggested technique may be utilized to develop a shared facility for the Petri network model, is an essential concept to consider. It developed a review for the cost-effective evaluation of implementation to meet QoS; the scalability in the research was not considered. In another research endeavour, (Han and Crespi 2017) presented the model for semantic maintenance provisioning for intelligent devices. The main aim was to create a Internet service that was compatible with the limits of smart devices, such as their limited resources (Read Only Memory, Random Access Memory and Central Processing Unit), sluggish communication channels and microcontrollers. Utilizing a number of conventional application programming interfaces, this was accomplished (API).

ContikiCooja tested it in a variety of scenarios using samples and web functions (simulator). The conclusions of this study have influenced the development of important service delivery features for IoT applications on the web, such as security, dependability and scalability.

Industrial Applications

The industrial sector is another key use of Internet of Things technology (Park 2019). The application of Internet of Things in this area has necessitated numerous investigations. (Li et al. 2014) created a 3-stage process for enhancing Quality of Service using the top-down judgment-making methodology in Markov. With the help of MATLAB, the authors made a model for the situation and tested the suggested method. During the assessment, various Quality of Service factors were taken into account, such as the latency, one-way delay, ease of access and transmission capacity. The recommended approach to resource planning was assessed to lower the overall latency of the network. Venticinque and Amato have studied a new strategy (Venticinque and Amato 2019) to answer and clarify the issue of Fog service deployment to Internet of Things Fog applications. It will be decided on the ideal component for processing power and IoT applications, like those in the intelligent energy sector. This study is significant because it makes use of numerous computational resources to better programme planning and analyse energy profiles. A CONCISE-based subject-based multidimensional framework for Internet of Things applications is proposed in another paper by Jin et al. (2017). It provides a standard that supervises and gathers data/Information using Time Synchronized Channel Hop-Ping (TSCH) planning. The outcomes include decreased end-to-end latency, enhanced communication dependability and decreased network traffic congestion.

Infrastructural Applications

At the same time, Programmable Object Interface/Internet of Things can be used for a variety of purposes. As a result, this section goes over the research that has been done on IoT infrastructure. For IoT/Fog and SDN, (Diro et al. 2018) developed a combined framework. Important factors like lowering packet delay, eliminating the chances of lost packets, avoiding space conflicts and achieving the maximum output are all aided by this. The importance of flow space allocation in producing both critical and dangerous flows is highlighted in this study. It illustrates how the Fog communication paradigm balances the programmability of SDN processes with conventional packet flows. This structure selects a level of flow space distribution variation based on the Quality of Service requirements. According to the findings, critical flow classes provided more proficient support. The main focus of the research is on improving QoS elements such data rate, delay and likelihood. However, we did not examine cases involving several virtualized devices. A technique for resource management of fog computing with energy efficiency was another option put up by Naranjo et al. (2018). To maintain interacting virtualized assets alive, the suggested structure utilizes middleware and has quick clearance. It has acceptable QoS characteristics, especially in terms of energy consumption, however there are no prior data or proof. A novel resource processing model for IoT intelligent applications was lastly proposed

by Chen et al. (2018). The researchers created a technique for resource-efficient computation offloading using a hybrid approach.

Healthcare Applications

From the perspective of the provider, (Kim and Kim 2018) is a manual for users of Internet of Things healthcare services. The research identifies some key characteristics that substantially impact users, allowing them to authenticate healthcare services. The procedure includes looking at elements like account risks and privacy in order to qualify and validate services.

This research serves as a roadmap for manufacturers looking to improve the dependability and trustworthiness of IoT healthcare services. In (Damis et al. 2018), three epidermal loop antennas were theoretically and experimentally studied for the purpose of detecting biological factors in Internet of Things healthcare applications. The purpose of this research is to support the accuracy of GSM and BLE communications by examining the bit BER and error-vector magnitude (EVM) characteristics in quadruple loop antennas. The results reveal that the reflection factor and radiation forms are trustworthy and steady. Additionally, the data transmission assessment demonstrates that the BER is capable of working in quadrature amplitude modulation and fits what is known about the antenna (QAM).

Elappila et al. 2018) conducted yet another research on healthcare applications, in which an improvement in interference, energy efficiency after blocking, and interface perception of energy efficiency were the main goals of a routing approach for Wireless Sensor Network. Due to excessive network traffic and delays connecting devices, many IoT devices share a single focal point. Because multiple Internet of Things devices use the similar emphasis, the network experiences high traffic and delays in connecting devices. The method that was made uses a function to find the next party node. This function is controlled by three factors: (1) the signal-to-interference-plus-noise ratio, (2) the route's ability to stay up and (3) the node's ability to be blocked. As shown, the data provided using the suggested way increased data rate while lowering energy use and packet loss. Additionally, (Jebadurai and Peter 2018) proposed a brand-new architecture for Internet of Things healthcare applications that allows the processing of retinal pictures obtained by a smartphone fundoscopy. A super-resolution approach based on the Kernel support vector regression procedure was suggested to improve the image quality. The collected findings suggest that the proposed approach outperforms several current super-resolution algorithms in terms of effectiveness. For the study (Malik et al. 2018), the authors investigated the performance of an IoT (NB-IoT) narrowband, which requires effective communication for simple captors and long-term batteries with low performance. The research aims mainly to examine and assess NB-IoT latency and performance in health services.

Additional study by Hamdan (2018) examined the human elements in the healthcare setting that affect information exchange. The project's goal was to collect information from healthcare professionals and disseminate it so that new applications for

the Internet of Things in healthcare might be developed. Additionally, LoRa and My Signals made use of the body temperature, oxygen saturation, electrocardiograms and pulse speed sensors.

Many antennas have been proposed for wireless and satellite applications (Jilani and Alomainy 2018; Patel et al. August 2017; Kachhia et al. 2015; Patel et al. 2016). However, we have proposed the design of a multilayer antenna for IoT applications here, which resonates at 2.5 GHz and 5.2 GHz frequencies. The suggested antenna is built on a FR4 material, which is cost-effective and easy to fabricate. Moreover, the gain and the radiation efficiency of the proposed antenna are suitable for the proposed applications (Smart Antennas 2022; Malik et al. 2021; Rahim and Malik 2020).

Design of Antenna

In Fig. 11.1, the suggested antenna is shown, it is a multilayer structure designed on FR4 substrate with a ε_r of 4.4 and tan δ of 0.02. The antenna's top view, bottom view and perspective view are represented in Fig. 11.1a, b, c, respectively. As shown in Fig. 11.1, it contains a monopole feed with a coplanar ground plane. The dimensions of the monopole have been optimized using CST Microwave Studio software. Initially, we have kept the entire ground plane and vary the width of the monopole from 2 to 6 mm. The same return loss is represented in Fig. 11.2, which shows that the optimum value of return loss at 3.2 mm width. Next, we have optimized the monopole's width, and a similar approach is applied for the length of the monopole. The length of the monopole feed is tuned from 15 to 29 mm. That is derived that the dual-band response is achieved at the length of 29 mm that is illustrated in Fig. 11.3. However, the return loss is shallow, so we need to think in another direction to improve the antenna's performance.

Next, we have fixed the width and the length of the monopole feed as 3.2 mm and 29 mm and changed the length of the ground plane (Jilani and Alomainy 2018). The width of the ground plane is kept fixed at 30 mm because the reduction causes too much degradation in the return loss. Hence, the ground plane length changes from

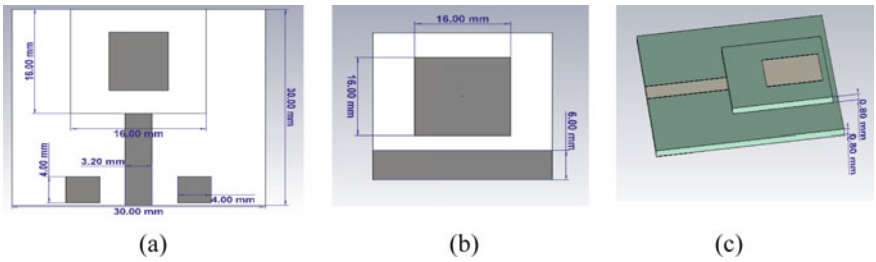

Fig. 11.1 (**a**) top view, (**b**) side view and (**c**) perspective view of the proposed antenna

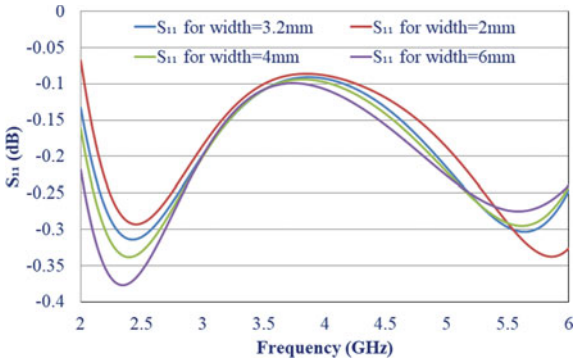

Fig. 11.2 Reflection coefficient performance with the width variation of monopole feed

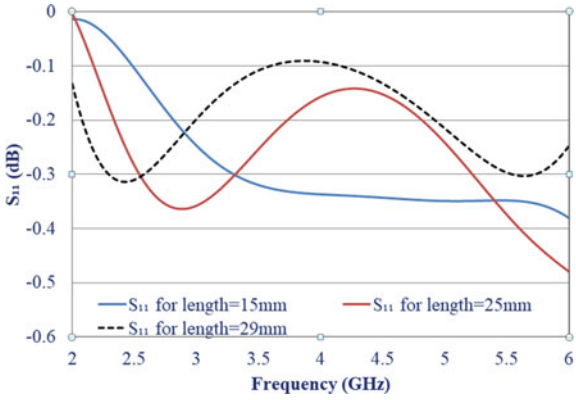

Fig. 11.3 Reflection coefficient performance with a variation of monopole feed length

30 to 3 mm and simulates the structure using CST software. The simulation result of the S_{11} is illustrated in Fig. 11.4. It shows that for the variation in length for 3 mm, 6 mm and 10 mm, the antenna is resonated at 2.45 GHz, 2.62 GHz and 3.05 GHz with the return loss of 16.5 dB, 47 dB and 25 dB, respectively. So we have now fixed the width and length of the ground plane as 30 mm and 6 mm. The 3D gain plot of the antenna at 2.62 GHz is shown in Fig. 11.5. It gives a gain of 2.31 dBi. However, the performance is not achieved as per the mentioned specifications.

Furthermore, to improve the performance, we have added a second substrate on the top of a patch with the dimensions is shown in Fig. 1a. The small square patch with different dimensions is created on this top of a substrate, and its simulated results are represented in Fig. 11.6. However, the return loss performance of the square patch is still improved by transforming it into the rectangle patch. It is now resonated at 2.5 GHz and 5.25 GHz. To measure the -10 dB impedance bandwidth, we have highlighted that region in the dotted box. It gives a bandwidth of 2.38 GHz to 2.64 GHz and 4.94 GHz to 5.65 GHz centre at 2.5 GHz and 5.2 GHz, and gain of 2.09 dBi and 3.48 dBi, respectively, which is represented in Fig. 11.8. Furthermore, to improve the performance of the proposed antenna, the square patch has been created in the

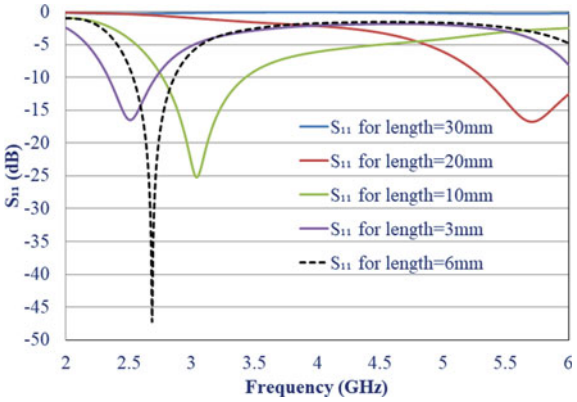

Fig. 11.4 Reflection coefficient performance with variation in ground plane length

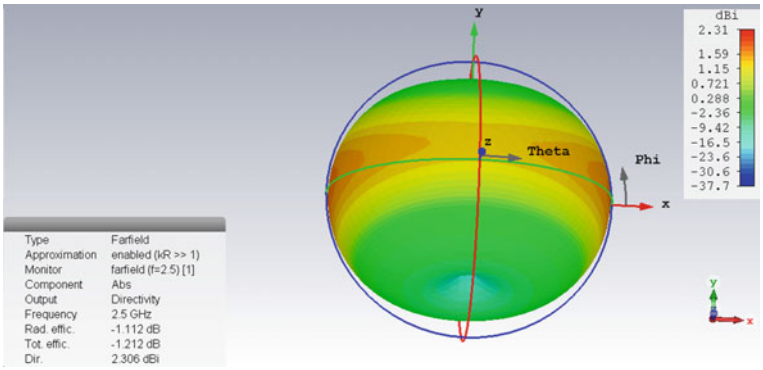

Fig. 11.5 3D gain plot of monopole feed with the partial ground plane at 2.5 GHz

ground plane. Figure 11.9 shows the return loss performance concerning changes in the square patch dimensions at the ground plane. The optimized dimension of the square patch is 8 mm × 8 mm, which gives the -10 dB bandwidth of 2.4 GHz to 2.62 GHz and 4.75 GHz to 5.7 GHz centre at 2.5 GHz and 5.4 GHz, respectively. The 3D gain plot of the proposed antenna at 2.5 GHz and 5.2 GHz is shown in Figs. 11.10, 11.7.

The surface current distribution of the proposed antenna at 2.5 GHz and 5.2 GHz is shown in Fig. 11a and Fig. 11b, respectively. It shows that the current is maximally coupled at those frequencies and also radiates. The voltage standing wave ratio (VSWR) of the proposed antenna is shown in Fig. 11.12. It gives the VSWR of 1.2 and 1.09 at 2.5 GHz and 5.2 GHz, respectively, matching our design specifications. The radiation efficiency plot for the proposed antenna is shown in Fig. 11.12. It represents the radiation efficiency of 92.4% and 94.5% at 2.5 GHz and 5.2 GHz, respectively. To prove the proposed design's superiority, we have compared the simulation results

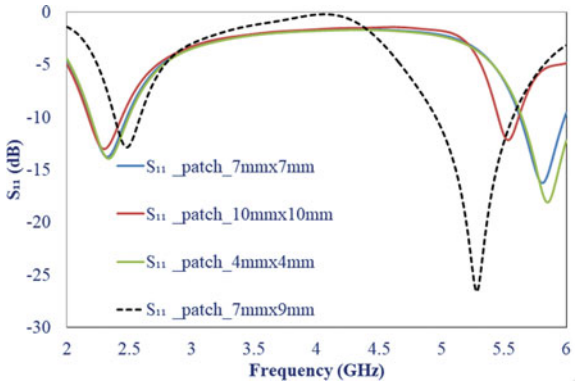

Fig. 11.6 Reflection coefficient variation with respect to variation in top patch dimensions

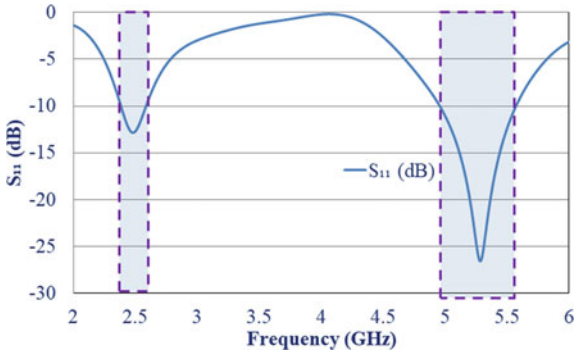

Fig. 11.7 –10 dB impedance bandwidth for the proposed antenna

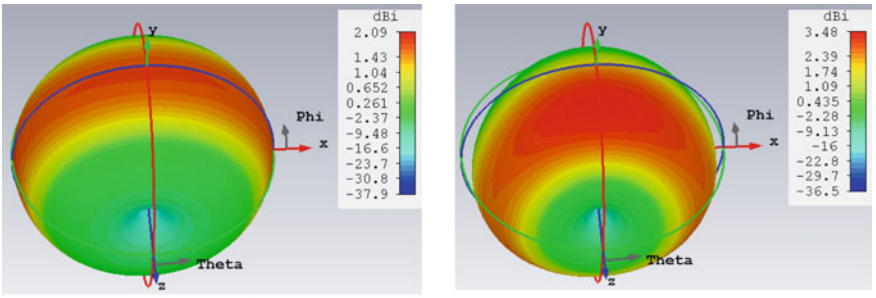

(a) (b)

Fig. 11.8 3D gain plot at (**a**) 2.5 GHz and (**b**) 5.2 GHz

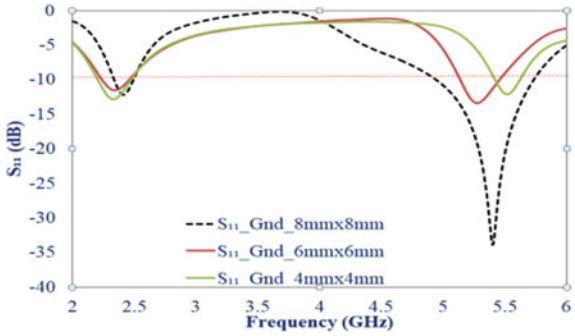

Fig. 11.9 Reflection coefficient performance while variation in ground plane of the patch

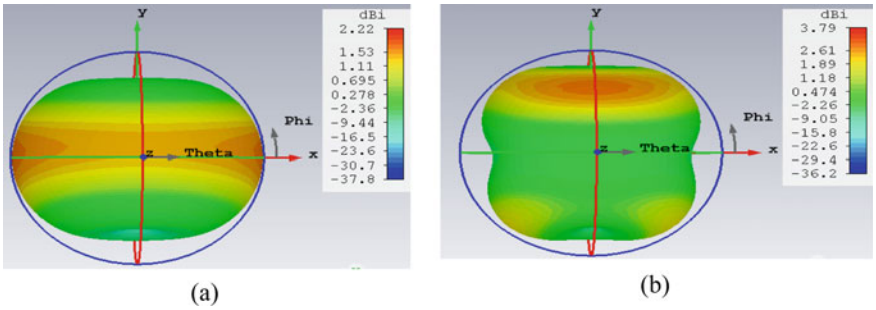

Fig. 11.10 3D gain plot of the proposed antenna at (**a**) 2.5 GHz and (**b**) 5.2 GHz

with the other already proposed designs, as illustrated in Table 11.1. The proposed antenna gives higher gain and better radiation efficiency compared to other designs (Fig. 11.13).

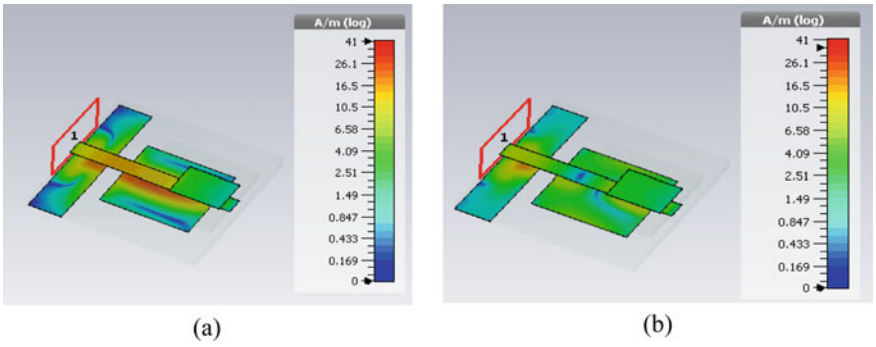

Fig. 11.11 Current distribution of the proposed antenna at (**a**) 2.5 GHz and (**b**) 5.2 GHz

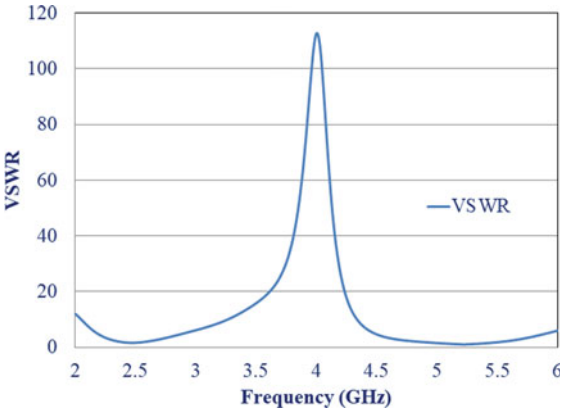

Fig. 11.12 VSWR of the proposed antenna

Table 11.1 Performance comparison of the proposed antenna vs. other models

Reference	Resonant frequency (GHz)	– 10 dB impedance Bandwidth (MHz)	Gain (dB)	Efficiency (%)	Physical dimensions (mm^3)
Refaat et al. 2021)	2.42, 5.22, 5.92	< 100	1.72, 7.86, 6.97	–	55.5 × 42.75 × 1.5
Kumar et al. 2018)	1.8, 5.2, 7	> 300	1.83,0.73, 3.6	97, 90, 77	30 × 20 × 1.52
Munir and Soba 2015)	1.5, 2.43, 2.86	> 200	> 1	–	78.6X8.4X1.6
Satheesh et al. 2017)	2.38, 1.53	> 200	0.78, 2.5	–	110 × 65 × 1.6
Elijah and Mokayef 2020)	5.775	> 100	2.54	–	24.7 × 20.8x1.6
This work	2.5, 5.2	> 500	2.21, 3.79	92.4, 94.5	30 × 30 × 1.6

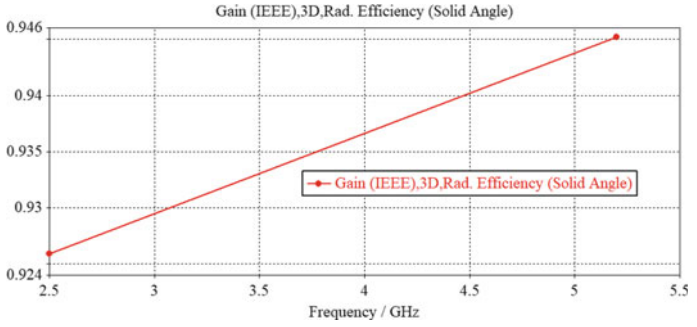

Fig. 11.13 Radiation efficiency of the proposed antenna

Conclusion

The proposed multilayer antenna is resonated at 2.5 GHz and 5.2 GHz for IoT applications. The proposed structure gives more than 100 MHz impedance bandwidth and better radiation efficiency at both the operating bands. The gain of the proposed antenna is 2.21 dBi and 3.79 dBi at 2.5 GHz and 5.2 GHz frequencies. The total volume of the antenna is $30 \times 30 \text{x} 1.6 \text{mm}^3$. The obtained results show the superiority, which can be used in the IoT applications.

References

Alodib M (2016) QoS - Aware approach to monitor violations of SLAs in the IoT. J Innov Digit Ecosyst 3:197–207. https://doi.org/10.1016/j.jides.2016.10.010

Chen X, Shi Q, Yang L, Xu J (2018) ThriftyEdge: Resource efficient edge computing for intelligent IoT applications. IEEE Network 32(1):61–65. https://doi.org/10.1109/MNET.2018.1700145

Chettri L, Bera R (2019) A comprehensive survey on Internet of Things (IoT) toward 5G wireless systems. IEEE Internet Things J 7:16–32. https://doi.org/10.1109/JIOT.2019.2948888

Damis HA, Khalid N, Mirzavand R, Chung HJ, Mousavi P (2018) Investigation of epidermal loop antennas for biotelemetry IoT applications. IEEE Access 6:15806–15815. https://doi.org/10.1109/ACCESS.2018.2814005

Diro AA, Reda HT, Chilamkurti N (2018) Differential flow space allocation scheme in SDN based fog computing for IoT applications. J Ambient Intell HumIzed Comput. pp 1–11, https://doi.org/10.1007/s12652-017-0677-z

Elappila M, Chinara S, Parhi DR (2018) Survivable path routing in WSN for IoTapplications. Pervasive Mob Comput 43:49–63. https://doi.org/10.1016/j.pmcj.2017.11.004

Elijah AA, Mokayef M (2020) Miniature microstrip antenna for IoT application. Materials Today: Proceedings 29(1):43–47. https://doi.org/10.1016/j.matpr.2020.05.678

Hamdan R (2018) Human factors for IoT services utilization for health information exchange. J Theor Appl Inf Technol 96(8):2095–2105, E-ISSN 1817–3195

Han SN, Crespi N (2017) Semantic service provisioning for smart objects: Integrating IoT applications into the web. Futur Gener Comput Syst 76:180–197. https://doi.org/10.1016/j.future.2016.12.037

Jebadurai J, Peter JD, (2018) Super-resolution of retinal images using multi-kernel SVR for IoT healthcare applications. Futur Gener Comput Syst 83:338–346. https://doi.org/10.1016/j.future.2018.01.058

Jilani SF, Alomainy A, (2018) Millimeter-wave T-shaped MIMO antenna with defected ground structures for 5G cellular networks. IET Microwaves Antennas Propag 12(5):672–677, https://doi.org/10.1049/iet-map.2017.0467

Jin Y, Raza U, Aijaz A, Sooriyabandara M, Gormus S (2017) Content centric cross-layer scheduling for industrial IoT applications using 6TiSCH. IEEE Access 6:234–244. https://doi.org/10.1109/ACCESS.2017.2762079

Kachhia J, Patel A, Vala A, Patel R, Mahant K (2015) Logarithmic slots antennas using substrate integrated waveguide. Int J Microw Sci Technol. https://doi.org/10.1155/2015/629797

Kim S, Kim S (2018) User preference for an IoT healthcare application for lifestyle disease management. Telecommun Policy 42(4):304–314. https://doi.org/10.1016/j.telpol.2017.03.006

Kumar P, Ghivela GC, Sengupta J (December 2018) Design and analysis of multiple bands spider web shaped circular patch antenna for IoT application. In: 2018 8th IEEE India International Conference on Power Electronics (IICPE) (pp 1–5) (13–15 December 2018), https://doi.org/10.1109/IICPE.2018.8709444

Li L, Li S, Zhao S (2014) QoS-aware scheduling of services-oriented internet of things. IEEE Trans Ind Inform 10(2):1497–1505. https://doi.org/10.1109/TII.2014.2306782

Li H, Wang H, Yin W, Li Y, Qian Y, Hu F (2015) Development of a remote monitoring system for henhouse environment based on IoT technology. Future Internet 7(3):329–341. https://doi.org/10.3390/fi7030329

Malik H, Alam MM, Le Moullec Y, Kuusik A (2018) NarrowBand-IoT performance analysis for healthcare applications. Procedia Comput Sci 130:1077–1083. https://doi.org/10.1016/j.procs.2018.04.156

Praveen Kumar Malik, Pradeep Kumar, Sachin Kumar, Dushyant Kumar Singh, (2021) Smart antennas: recent trends in design and applications, Bentham Science, Sharjah, United Arab Emirates, Aug 2021, ISSN: 2717–5421 (Print), ISSN: 2717–543X (Online), ISBN: 978–1–68108–860–0 (Print), https://doi.org/10.2174/9781681088594121020l

Montori F, Bedogni L, Bononi L (2017) A collaborative internet of things architecture for smart cities and environmental monitoring. IEEE Internet Things J 5(2):592–605. https://doi.org/10.1109/JIOT.2017.2720855

Munir A, Soba J (2015) Multiband printed antenna composed of an array of split ring resonator, 2015 European Radar Conference (EuRAD), Paris, France, pp 9–11 (Sept. 2015), https://doi.org/10.1109/EuMC.2015.7346036.

Naranjo PGV, Baccarelli E, Scarpiniti M (2018) Design and energy efficient resource management of virtualized networked Fog architectures for the real-time support of IoT applications. J Supercomput 74:2470–2507. https://doi.org/10.1007/s11227-018-2274-0

Park JH (2019) Advances in future Internet and the industrial Internet of Things. Symmetry 11(2):244. https://doi.org/10.3390/sym11020244

Patel A, Vala A, Goswami R, Mahant K (2016) Square loop slots loaded substrate integrated waveguide based horn antenna. Microw Opt Technol Lett 58(7):1577–1582. https://doi.org/10.1002/mop.29857

Patel A, Vala A, Goswami R, Mahant K (August 2017) SIW Based Wideband Horn Antenna. In IOP Conference Series: Materials Science and Engineering 225:012263

Abdul Rahim, Praveen Kumar Malik, (2020) Design methodologies and tools for 5G network development and application, Ch 10: Analysis and Design of planner wide band antenna for wireless communication applications: Fractal Antennas, Pages: 13 (196–208), ISBN13: 9781799846109, Dec 2020 IGI Global USA https://doi.org/10.4018/978-1-7998-4610-9.ch010

Refaat SM, Abdalaziz A, Hamad EK (2021) Tri-Band slot-loaded microstrip antenna for internet of things applications. Adv Electromagn 10(1):21–28. https://doi.org/10.7716/aem.v10i1.1514

Satheesh A, Chandrababu R, Rao IS (2017) A compact antenna for IoT application. In: 2017 International Conference on Innovations in Information, Embedded and Communication Systems (ICIIECS), Coimbatore India, 17–18 March 2017, https://doi.org/10.1109/ICIIECS.2017.8275921

Smart Antennas: Latest Trends in Design and Application (2022) "Springer" Malik P, Lu J, Madhav BTP, Kalkhambkar G, Amit S (Eds), ISBN 978–3–030–76636–8. https://doi.org/10.1007/978-3-030-76636-8

Souri A, Asghari P, Rezaei R (2017) Software as a service based CRM providers in the cloud computing: Challenges and technical issues. J Serv Sci Res 9:219–237. https://doi.org/10.1007/s12927-017-0011-5

Souri A, Rahmani AM, JafariNavimipour N (2018) Formal verification approaches in the web service composition: A comprehensive analysis of the current challenges for future research. Int J Commun Syst 31(2):e3808. https://doi.org/10.1002/dac.3808

Tun SYY, Madanian S, Mirza F (2021) Internet of things (IoT) applications for elderly care: a reflective review. Nat Libr Med 33(4):855–867. https://doi.org/10.1007/s40520-020-01545-9

Venticinque S, Amato A (2019) A methodology for deployment of IoT application in fog. J Ambient Intell Humaniz Comput 10:1955–1976. https://doi.org/10.1007/s12652-018-0785-4

Zia T, Liu P, Han W (2017) Application-specific digital forensics investigative model in internet of things (IOT). In Proceedings of the 12th International Conference on Availability, Reliability and Security, Reggio Calabria, Italy No. 55, pp 1–7, (29 August—1 September 2017), https://doi.org/10.1145/3098954.3104052

Chapter 12
Design of a Low Profile Dielectric Resonator Antenna Beyond 6 GHz for Next Generation Bio-medical Sensing Application

Sovan Mohanty, Maleeha Khan, and Baibaswata Mohapatra

Abstract Radiofrequency and microwave technologies are the front runners for wireless bio-sensing, imaging, hyperthermia, and other clinical applications. The Internet of Things with 5G communication technology is the root of the exponential expansion of modern digital high-speed technologies. IoT is disruptive and alters the way of fundamental communication between an implanted bio-sensor and its ever-changing dynamic bio-medical environment. Ultra-narrow band facilitates ultra-sensitive (−137 dBm) modulation scheme, whereas 5G and beyond 5G wireless networks concentrate on 100 Gbps high-speed connectivity with low latency. This article provides a design solution for a low-profile bio medical dielectric resonator antenna as a front-end telecommunication device in a deeply implanted biosensor for sensing and drug delivery applications. The radiation pattern is stable within dielectric discontinuities due to the complex nature of lossy biological tissues. However, the heterogeneity of the surrounding tissue determines its efficiency and accuracy. $|S11| < 10$ dB is between 6.78 and 7 GHz with a maximum dip of −41 dB at 6.9 GHz with an impedance bandwidth of 3.19%. The DR antenna produces a monopole-like radiation pattern due to the excitation of the hybrid mode. Further, meta-material inclusions make the field distribution more uniform than a conventional structure.

Keywords Dielectric resonator antenna · Ultra narrow band · Chu limit · Finite element method · Bio-sensor

S. Mohanty (✉)
SRMS College of Engineering and Technology, Bareilly, India
e-mail: mohanty.sovan@gmail.com

M. Khan
McGill University, Montreal, QC, Canada
e-mail: maleeha.khan@mail.mcgill.ca

B. Mohapatra
Chandigarh University, Chandigarh, India

P. K. Malik and P. N. Shastry (eds.), *Internet of Things Enabled Antennas for Biomedical Devices and Systems*, Springer Tracts in Electrical and Electronics Engineering,
https://doi.org/10.1007/978-981-99-0212-5_12

Introduction

The last decade shows the surge in the application of radio frequency and microwave signals for disease tracking and estimation to improve the quality of life. The RF and microwave signal in medical sensing can extend its applications in photodynamic therapy, microwave-assisted anastomosis, thermally molded stents for cardiology, urology, etc. (Kraus and Fleisch 2010). The medical body area network system provides low-power wireless network of a plurality of body-worn sensors, actuators as well as hub devices placed on and around the human body. An implantable dielectric resonator antenna provides a seamless, reliable, and efficient connectivity for biomedical communication and telemetry link between an implanted biomedical device and outside the peripheral processor (Skrivervik and Merli 2011; Singhwal et al. 2022). Through adaptive power control for frequency sharing, low-power active medical implants and associated peripherals to improve bandwidth (Islam et al. 2014; Bazaka and Jacob 2013). Further, performance improvement is through adequate spectrum access and spectrum-sharing mechanisms like listening before the talk, adaptive frequency agility, etc. The massive IoT will provide intelligent connectivity of physical devices and can be directed towards assisted living and health monitoring. It will muscle up the 5G communication link by bringing a paradigm shift in the healthcare industry. It will integrate sensing, computing, and information-processing techniques.

Why beyond the 6 GHz spectrum is so vital? According to the FCC fact sheet dated: 02 Apr 2020, there is the availability of 1200 MHz of unlicensed spectrum across 6 GHz from 5.925 to 7.125 GHz. This band is used for standard and low-power operations, especially for the near-field point-to-point communication link. Beyond 6 GHz unlicensed band creates an opportunity for inventors to provide the most advanced wireless services on various platforms including medical technologies. It can work in association with 5G wireless services. It can mitigate existing and anticipated congestion for new intensive applications. This band is creating new standards and protocols like IEEE 802.11ax and 5G NR–U standard. Therefore ISM band between 2.4 and 2.5 GHz is extended to 5.295–7.125 GHz to achieve high channel capacity, low latency, and enhanced mobile broadband in numerous applications.

Because of its low profile design and ease of integration with Microwave Integrated Circuit (MIC), the micro-strip antenna found widespread applications, especially in Wireless communication architecture. But it has inherent limitations like narrow bandwidth, low gain, high conductor loss, low-temperature handling capability, limited radiation surface, and the impact of the surface wave. These limitations can be addressed effectively by Dielectric Resonator Antenna. The dielectric used in the human body can be made biocompatible by using biocompatible materials such as Zirconia ($\varepsilon_r = 29$), PEEK ($\varepsilon_r = 3.2$), MDX: 4210 ($\varepsilon_r = 3.3$), etc. (Gabriel et al. 1996) This article proposes the design of a probe-fed futuristic dielectric resonator antenna at 6.9 GHz for biomedical operations. The main objective here is to find the electromagnetic field of the sensitive detector with high accuracy in a dynamic body

environment where permittivity changes rapidly with variation in charge distribution and flow of current. The concept of non-linearity, non-homogeneity, and non-isotropic are components of the design (Harrington 2001; Ramo et al. 2004; Johnson 1993; Pozar 1992). The designed DR antenna will act as a bio-electrically controlled device. The genuine computational technique to study DRA is the Finite element method. It contains unique qualities like geometrical adaptability and effective transient analysis in the time domain (Balanis 2013). This study uses a High-frequency structured simulator (HFSS) based on the Finite element method (FEM) and other integral equations-based computing technologies.

In this article, the first section describes the introduction, and the second section is dedicated to antenna design criteria. The third section proposes a design methodology. The fourth section focuses on result analysis and intrinsic problems associated with bio-antenna measurement in a dynamic biological environment.

Antenna Design

The major problem in bio-medical analysis is the design and development of microwave antennas for near-field communication with significant variations in coupling impedance. Considering the radial and tangential elements of the E-field, the most complicated field is the reactive near field and the radiative near field (Mohanty et al. 2020; Mohanty and Mohapatra 2020; Mongia and Ittipiboon 1997). The antenna and its transmission line may cause unintended thermal injury to the living tissues apart from the affected tissues inducing cellular toxicity. Therefore, while designing the antenna, it is essential to direct and control energy to the affected tissue volume. This design concentrates on the development of DRA with the associated coaxial line as the feeder. The radiation signature and electrical characteristics of the implanted antenna must be analyzed and evaluated both by numerical technique and suitable measurement setup. For the simulation, the air box surrounding the bio antenna will be completely different from other antenna technology. It is observed that temperature distribution due to the EM field is Gaussian in shape. Therefore tissue damage can be detected along the two sides of the antenna. DRA is tuned to 50 Ω to operate within 6.78–7.0 GHz. The electrical characteristics of the tissues and their dielectric phenomenon with the molecular processes are analyzed in the Fresnel zone. The parametric study as a lossy multi-layered sphere can be obtained through Green's function expansion.

The dielectric properties of the bio tissues result due to the energy deposition and strong interaction of electromagnetic radiation at the cellular and molecular level. Energy absorption can be determined from the specific absorption rate. Relative permittivity becomes very high i.e. 10^6 to 10^7 below 100 Hz. However relative permittivity increases along with increment in frequency due to α, β, and γ dispersion. The α and β dispersion occurs at the lower frequency of operation whereas γ dispersion occurs at the GHz range. It happens due to the polarization of water molecules (Kim and Rahmat-Samii 2004).

There will be an initiation of conduction and polarization current because of the free and bound charges. For biological tissues SAR can be estimated from the complex permittivity expressed by the Cole–Cole model (Gabriel et al. 1996):

$$\varepsilon = \varepsilon_\infty + \frac{\varepsilon_s - \varepsilon_\infty}{1 + (j\omega\tau)^{(1-\alpha)}} + \frac{\sigma}{j\omega\varepsilon_0} \tag{12.1}$$

where ε_∞= permittivity at high frequency, ε_s = static permittivity, τ = relaxation time, σ = conductivity, and α, β = broadening distribution of the transit time.

The complex permittivity can be modeled as:

$$\hat{\varepsilon}(\omega) = \varepsilon_\infty + \sum_{n=1}^{n=4} \frac{\Delta\varepsilon_n}{(j\omega\tau_n)^{(1-\alpha_n)}} + \frac{\sigma_i}{j\omega\varepsilon_0} \tag{12.2}$$

The power absorbed will be:

$$P_{abs} = \frac{1}{2}\int \sigma |E|^2 dV \tag{12.3}$$

The SAR is the ratio of incremental energy to that of incremental mass in W/ kg. The SAR can be computed as:

$$SAR = \frac{\sigma \left|E^2\right|}{\rho} \tag{12.4}$$

σ is the conductivity of the body tissues, ρ is the mass density, and E is the r.m.s electric field. According to IEEE C 95.1 guideline SAR of 1 g tissue <1.6 W/Kg and as per C 95 1-2005 SAR of 1 gm of tissue <2 W/kg.

Design Methodology

Modeling of DRA

DRA technology will prove to be viable alternative antenna technology. In dielectrics, the electric displacement current $\frac{\delta D}{\delta t}$ is a motion of the bound charge (Mongia and Bhartia 1994; Mc Allister and Long 1984; Mohanty and Mohapatra 2021a).

$$\varepsilon(\omega) = \varepsilon' - j\varepsilon'' = |\varepsilon| e^{-j\delta} \tag{12.5}$$

where ε', ε'', $\eqsim$ are real quantities. ε' is the a-c capacitivity, ε'' is the dielectric loss factor, and $\eqsim$ is the dielectric loss angle. The time average power dissipation and electric energy will be:

$$P_d = \iiint \omega\varepsilon''|E|^2 d\tau \tag{12.6}$$

$$W_e = \frac{1}{2}\iiint \varepsilon'|E|^2 d\tau \tag{12.7}$$

Here ε' contributes to stored energy and $\omega\varepsilon''$ contributes to power dissipation. In a good dielectric a–c capacitivity ε' is almost constant whereas dielectric loss factor ε'' is very small. The major loss in a dielectric is due to the imperfect dielectric material. DRA which is operating at fundamental lower-order modes usually radiates like a magnetic dipole.

Low Profile and Compact DRA

An electrically small antenna is one whose dimensions ≤ wavelength of the operating frequency. The effect of antenna miniaturization includes the following (Petosa 2007; Mohanty and Mohapatra 2021b):

- The increment in reactive impedance especially capacitive reactance
- The reduction in the radiation resistance
- The matching becomes difficult as bandwidth reduces considerably
- It is difficult to place and excite the source.

However higher gain can be achieved and controlled by Malik et al. (2021a, b):

- Increasing the electrical length and aperture area of the radiator.
- Exciting the radiator with the higher order mode.

DRA can be miniaturized by adopting various techniques such as:

- Inserting a PEC boundary to reduce the resonant frequency
- Through reactive loading
- Meandering
- Self-resonant structures
- Termination with a tuned reactive element
- Realization of an effective medium to match with free space and afford miniaturization
- Distributed loading to reduce phase velocity (Roges and Malik 2021; Rahim et al. 2021; Malik et al. 2020).

The Q factor of the electrically small antenna will be (Petosa 2007):

$$Q = \frac{1 + 3(kR)^2}{(kR)^3[1 + (kR)^2]^{e_r}} \tag{12.8}$$

where k = wave number of the surrounding, e_r = radiation efficiency, and kR is the normalized radius. The maximum gain of an electrically small antenna will be:

$$G = \begin{cases} e_r\left[(kR)^2 + 2kR\right] \text{ for } kR \geq 1 \\ 3e_r \text{ for } kR < 1 \end{cases} \tag{12.9}$$

The largest dimension of the electrically small DRA will be:

$$L = \frac{c}{f_0\sqrt{\varepsilon_r}} \tag{12.10}$$

Let the radiation efficiency is 100%, then the Q-factor and maximum gain will be:

$$Q = \frac{1 + 3\left(\pi/\sqrt{\varepsilon_r}\right)^2}{\left(\pi/\sqrt{\varepsilon_r}\right)^3\left[1 + \left(\pi/\sqrt{\varepsilon_r}\right)^2\right]} \tag{12.11}$$

$$G = \begin{cases} \left[\left(\pi/\sqrt{\varepsilon_r}\right)^2 + 2\left(\pi/\sqrt{\varepsilon_r}\right)\right] \text{for } \varepsilon_r \geq \pi^2 \\ 3 \text{ for } \varepsilon_r < \pi^2 \end{cases} \tag{12.12}$$

Here these equations will be valid for the infinite ground plane and when the DRAs are in the isolated state. However for a finite ground plane and coupled DRA there'll be the occurrence of ripple at the output characteristics curve.

Structure of the DRA

The designed antenna is based on the stacked configuration of a lower cylindrical and upper hemispherical structure. Figures 12.1 and 12.2 show the side and top views of the antenna. The DR antenna is placed over a copper plate of a thickness of 0.1 mm, a width of 13 mm, and a length of 13 mm. The top portion of the copper plate is assumed to be a perfectly electrical conductor (PEC). The probe-fed antenna is excited by passing the core of the conductor through the metallic plane into the dielectric resonator at the center to excite the isotropic TM mode. For biological applications, the magnetic mode is preferred to couple energy into an inhomogeneous environment created due to the presence of human tissue in the skin, muscle, fat, cortical bone, etc. The stacked DRA is having $\varepsilon_r = 36.2$ with a total height of 12.37 mm in which the height of the cylinder is 6.4 mm whereas the radius of the hemisphere is 5.975 mm. The length of the probe that is inserted into the DRA is 9.7 mm with a radius of 0.63 mm. For optimum coupling of the excited energy. The excitation is done by the core of an unbalanced transmission line fitted with an SMA connector. The core of the transmission line is surrounded by Teflon $\varepsilon_r = 36.2$ followed by the mesh of wire.

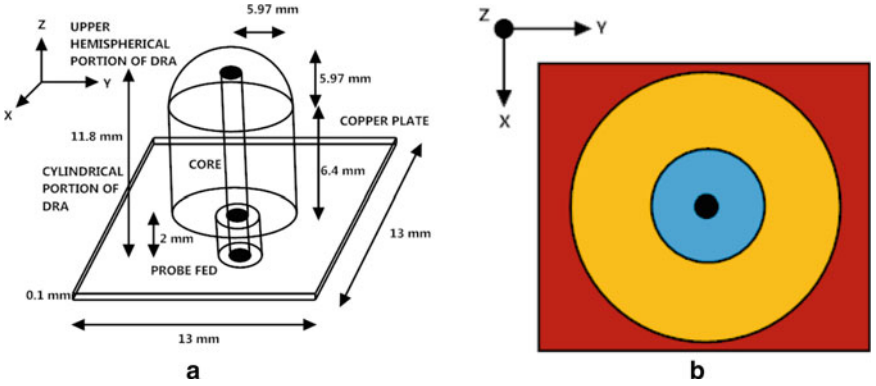

Fig. 12.1 **a** Side view of the DRA. **b** Top view of the DRA

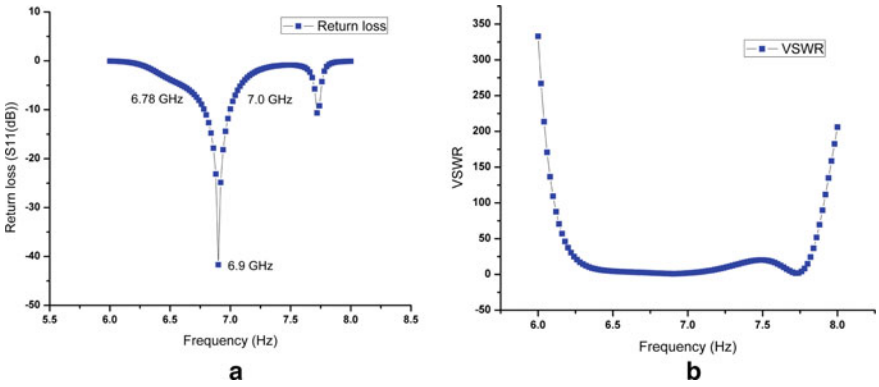

Fig. 12.2 **a** Return loss in dB versus frequency. **b** VSWR

Result Analysis

Accurate estimation of propagation constant, characteristics impedance, and wave impedance results the correct prediction of resonant resistance and resonant frequency. This antenna resonates between 6.78 and 7.0 GHz with a maximum dip of −41 dB at 6.9 GHz. It provides a 10 dB return loss impedance bandwidth of 3.19%. Figure 12.2a, b represent simulated return loss in dB versus frequency and VSWR respectively. Because of the complex environment the antenna is facing, bandwidth is not the criteria to indicate antenna quality. Quality depends upon the medium in which the antenna operates. Figure 12.3 shows the Re and Imj part of the input impedance Z(1,1). The antenna sees the real impedance of 50 Ohms at 6.9 GHz, whereas at other frequency reactive parameters dominate. The excitation method is probe feed considering the internal body environment and the necessity of a uniform radiation pattern around the antenna.

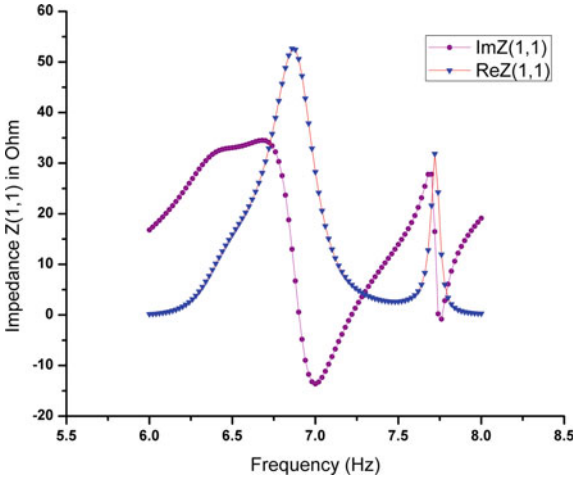

Fig. 12.3 Real and imaginary impedance Z(1,1)

Radiation Mechanism

Because of the circularly symmetric structure this antenna supports $TM_{01\delta}$ as the lowest order mode. The electric field inside the structure can be expressed as:

$$E_z = A|J_0(hr) + BY_0(hr)|\cos(\beta_z) \tag{12.13}$$

where h and β imply z-directed wave numbers inside the DR, J_0 and Y_0 are zero-order Bessel and Neuman function. The $TM_{01\delta}$ has unique external and internal fields associated with it to form unique radiation patterns. However the far field of the $TM_{01\delta}$ mode is similar to the electric dipole.

Figure 12.4a, b plotted E-plane and H-plane co and X polarization at 6.9 GHz under phi equals to 90° and 0° respectively. It is observed that there is a maximum difference of about 30 dB between co and cross-polarization at 90° and 270°. It indicates the effectiveness of this antenna at these angles when fitted with a transmitter or a receiver. As antenna seems to be bidirectional it is suitable for drug delivery systems. However, the effectiveness of this antenna is least at 0° and 180°. Figure 12.5a plots total gain versus theta in deg. It is found that a maximum gain of 1.8 dB occurs when the angle of elevation will be −75° and 125°. Figure 12.5b plots the total gain in dB versus frequency.

Table 12.1 shows various parameters of the proposed antenna. The field pattern due to electric, magnetic field, surface current density, and a combination of all is plotted in Fig. 12.6a–d. Figure 12.7a implies the electric and magnetic field distribution within and outside of the DRA. Figure 12.8 shows the structure of the proposed DRA as a medical device with associated connections.

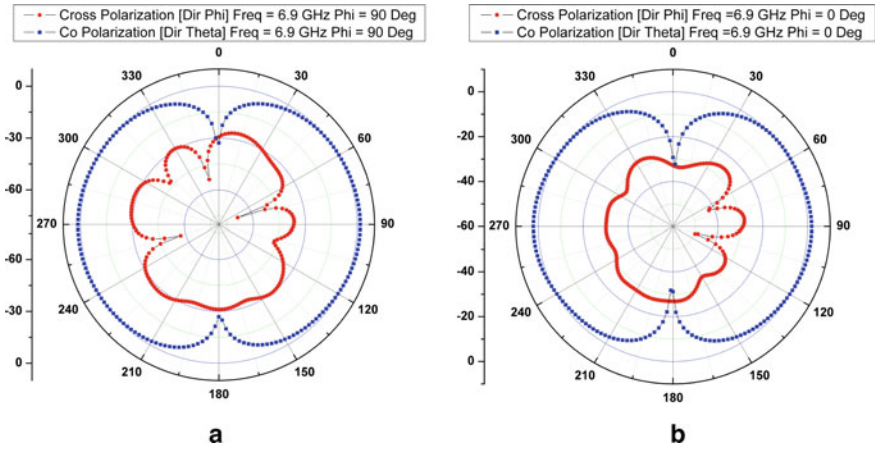

Fig. 12.4 **a** E plane co and cross polarization. **b** H plane co and cross polarization

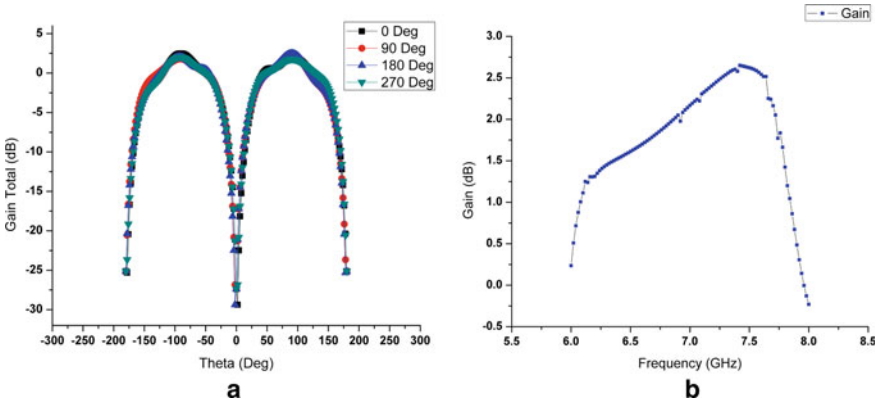

Fig. 12.5 **a** Plot of total gain versus theta (°). **b** Plot of gain versus freq (GHz)

Table 12.1 Antenna parameters

Operating frequency (GHz)	Resonating frequency (GHz)	10 dB impedance bandwidth (%)	Radiation intensity (W/Sr)	Peak directivity (dB)	Peak gain (dB)	Radiated power (W)	Radiation efficiency (%)	Front to back ratio (dB)
6.78–7.0	6.9	3.19	0.14	1.65	1.79	1.08	107.6	1.12

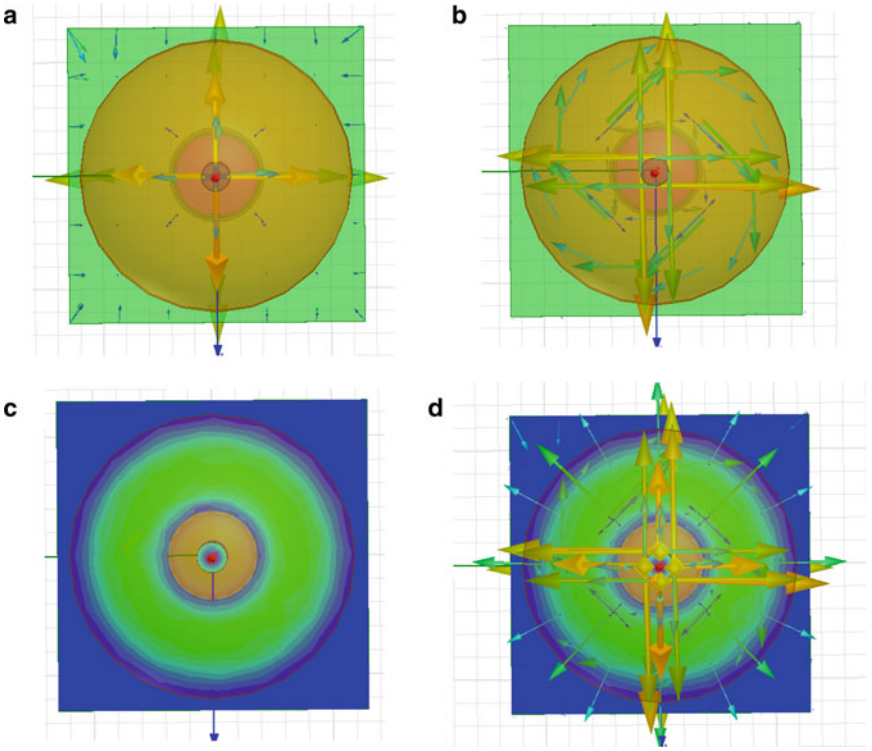

Fig. 12.6 **a** E-field vector. **b** H-field vector. **c** Surface current. **d** Combination of E, H, J Vector

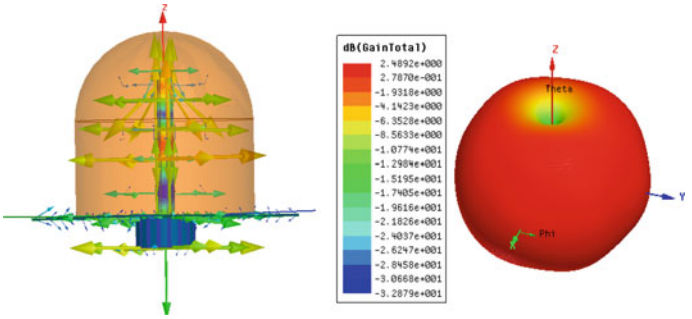

Fig. 12.7 Electric and magnetic field within and outside of the DRA

Bio-hazard: Uncontrolled and excessive emission may cause microwave syndrome and biohazard (Table 12.2). A potential hazard is a function of electromagnetic exposure and sensitiveness to various agents. The complex geometry and heterogeneous nature of human tissues provides a complex correlation between the outside exposed electric field and the inside electric field under thermal and

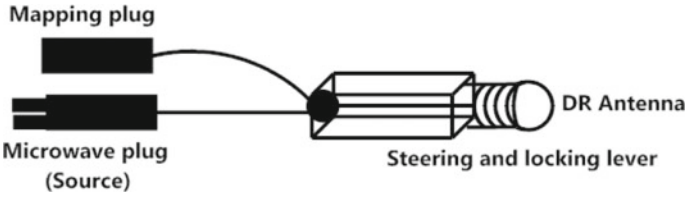

Fig. 12.8 Proposed DRA as a medical device with associated connection

Table 12.2 A comparative analysis

Refs.	Physical dimension (including substrate)	Feeding mechanisms	Advantages
Islam et al. (2014)	$19 \times 8 \times 3.2$ mm^3	Microstrip line	Provides biocompatibility and create buffer to prevent antenna detuning
Bazaka and Jacob (2013)	$54 \times 31 \times 11$ mm^3	Microstrip line	High reliability in supporting real time stimulation and data transmission
Singhwal et al. (2022)	$40 \times 40 \times 5.5$ mm^3	CPW feed	Compact and light with SAR analysis is within permissible limits
This article	$13 \times 13 \times 11.8$ mm^3	Probe feed	Miniaturized design with bidirectional radiation pattern suitable for drug delivery system

isothermal effects. Therefore the relationship between the electric and magnetic field associated with the dose effect at high frequency and low magnitude is not yet conclusive.

Conclusion

There is a huge surge in communication design and the demand for physiological information for disease estimation. This chapter proposes the design of a novel low profile, futuristic dielectric resonator antenna beyond the 6 GHz unlicensed spectrum for next-generation bio-medical sensing applications. Further, this antenna can become multifunctional by changing the matching network and a booster can be fitted to improve its sensing power.

References

Balanis CA (2013) Advanced engineering electromagnetics. Wiley India Private Limited, New Delhi

Bazaka K, Jacob MV (2013) Implantable devices: Issues and challenges. Electronics 2(1):1–34

Gabriel C, Gabriely S, Corthout E (1996) The dielectric properties of biological tissues: I. Literature survey. Phys Med Biol 41:2231–2249

Harrington RF (2001) Time harmonic electromagnetic fields. IEEE press series on electromagnetic wave theory

Islam MS, Esselle KP, Bull D, Pilowsky PM (2014) Converting a wireless biotelemetry system to an implantable system through antenna redesign. IEEE Trans Microw Theory Tech 62(9):1890–1897

Johnson RC (1993) Antenna engineering handbook. Mc-Graw-Hill

Kim J, Rahmat-Samii Y (2004) Low-profile antennas for implantable medical devices: optimized designs for antennasmuman interactions. IEEE Trans Antennas Propag 1331–1334

Kraus JD, Fleisch DA (2010) Electromagnetic with applications. Tata Mc-GrawHill, pp 119–166, Chap 03

Malik PK, Wadhwa DS, Khinda JS (2020) A survey of device to device and cooperative communication for the future cellular networks. Int J Wirel Inf Netw Springer 27:411–432. https://doi.org/10.1007/s10776-020-00482-8

Malik PK, Mohanty S, Mohapatra B (2021a) Multifunctional integrated hybrid rectangular dielectric resonator antenna for high-speed communication. In: Microstrip antenna design for wireless application, 1st edn, chapter 14. CRC Press, Taylor and Francis Group, pp 211–225. ISBN: 9780367554385

Malik PK, Mohanty S, Mohapatra B (2021b) Design of micro-strip fed aperture coupled broadside cylindrical dielectric resonator antenna array. In: Planar antenna: design, fabrication, testing, and application. Nova Science Publishers, NY, USA, p 11788. ISBN: 978-1-53619-898-0

Mc Allister MW, Long SA (1984) Rectangular hemispherical dielectric antenna. IEE Electron Lett 20:657–659

Mohanty S, Mohapatra B (2020) Leaky wave-guide based dielectric resonator antenna for millimeter-wave applications. Trans Electr Electron Mater 21(6), Online ISSN 2092-7592, Print ISSN 1229-7607. https://doi.org/10.1007/s42341-020-00240-w

Mohanty S, Mohapatra B (2021b) Dual band dielectric resonator antenna for high speed applications. J Math Comput Sci 11(4):4395–4410. ISSN: 1927-5307. https://doi.org/10.28919/jmcs/5870

Mohanty S, Khan A, Mohapatra B (2020) Stacked rectangular dielectric resonator antenna for biomedical electromagnetic application. National conference on biomedical engineering, NCBE-2020, NITTR, Chandigarh, pp 80–86. ISBN: 978-81-948668-9-3

Mohanty S, Mohapatra B (2021a) Design and analysis of embedded dual band rectangular dielectric resonator antenna. Int J Microw Opt Technol 16(6):536–554

Mongia RK, Bhartia P (1994) Dielectric resonator antennas—a review and general design relations for resonant frequency and bandwidth. Int J Microw Millim-Wave Comput-Aided Eng 4(3):230–247

Mongia RK, Ittipiboon A (1997) Theoretical and experimental investigations on rectangular dielectric resonator antennas. IEEE Trans Antennas Propag 45:9

Petosa A (2007) Dielectric resonator antenna handbook. Artech House, 685 Canton Street, Norwood, MA 02062

Pozar DM (1992) Microstrip patch antenna. IEEE Press, 203–259

Rahim A, Malik PK (2021) Analysis and design of fractal antenna for efficient communication network in vehicular model. Sustain Comput Inform Syst Elsevier 31:100586. ISSN 2210-5379. https://doi.org/10.1016/j.suscom.2021.100586

Ramo S, Whinnery JR, Duzer TV (2004) Fields and waves in communication electronics. Wiley

Roges R, Malik PK (2021) Planar and printed antennas for Internet of Things-enabled environment: opportunities and challenges. Int J Commun Syst 34(15):e4940. https://doi.org/10.1002/dac.4940ISSN:1099-1131

Singhwal SS, Matekovits L, Peter I, Kanaujia BK (2022) A study on application of dielectric resonator antenna in implantable medical devices. IEEE Access 10:11846–11857

Skrivervik AK, Merli F (2011) Design strategies for implantable antennas. Loughborough antennas & propagation conference, Loughborough, UK

Chapter 13
Implantable Dual Band Low-Profile Meandered Patch Antenna for Adhesive Skin Mimicking and Skin Contact Applications

K. C. Rajarajeshwari, K. R. Gokul Anand, E. L. Dhivya Priya, Dheeraj Kumar, and Joan Lu

Abstract An implantable low profile spiral-shaped meandered patch antenna is designed in this work exclusively for biomedical devices applications mainly for skin mimicking. The often-used frequency for biomedical applications for Medical Implant Communication Service (MICS) is 401–406 MHz and the Industrial, Scientific, and Medical (ISM) band of 2.4–2.48 GHz which is covered in this chapter. This antenna covers the frequency range of 405 MHz with a Reflection Coefficient of − 45 dB, and a gain of 8 dB. The next range is at 2.45 GHz with a Reflection Coefficient of −36 dB and 7 dB gain. The constructed antenna is just 0.32 mm thick, with dimensions of 35 mm and 28 mm. To achieve this gain many iterations were carried out and finally eight step meandered antenna suits the preferred frequency band. The meandered antenna is used in this work because it gives a high Reflection Coefficient, gain and low losses compared to normal conventional microstrip patch antenna. Also, they occupy less space compared to the normal antenna with minimised size. This antenna is mainly used for skin contact applications and skin-mimicking adhesive applications.

Keywords MICS · ISM · IMD · Meandered antenna

K. C. Rajarajeshwari (✉) · K. R. Gokul Anand
Department of ECE, Dr Mahalingam College of Engineering and Technology, Pollachi, Tamilnadu, India
e-mail: rajeswari.kc93@gmail.com

E. L. Dhivya Priya
Department of ECE, Sri Krishna College of Technology, Coimbatore, Tamilnadu, India

D. Kumar
Department of Physics and Electronics, Rajdhani College (University of Delhi), Delhi, India

J. Lu
Department of Computer Science, University of Huddersfield, West Yorkshire, HD1 3DH, Huddersfield, UK
e-mail: j.lu@hud.ac.uk

P. K. Malik and P. N. Shastry (eds.), *Internet of Things Enabled Antennas for Biomedical Devices and Systems*, Springer Tracts in Electrical and Electronics Engineering,
https://doi.org/10.1007/978-981-99-0212-5_13

Introduction

In recent years the need for Implantable Medical Devices (IMD's) has increased due to the increase in different diseases. The information or data can be sensed by an IMD sensor which is nothing but an antenna. The design of biomedical antenna has become a major role in medical industries. Implantable medical devices comprise embedded devices that can communicate wirelessly with an output device. Electromagnetic phenomena have been employed in clinical uses. Ever since the 1900s, applications have been transformed to the frequency of radio transmission Embedded gadgets are gaining popularity. They are being used in Pacemaker, Skin Patches for testing Blood pressure and Skin mimicking, Hypothermia treatment, Blastoma and so on. In this chapter we discuss briefly on Meandered antenna which is also called as serpentine antenna most widely used an antenna in medical industry for diagnosis and treatment purposes. Because of the human body's lossy tissues, the design of such sensors presents several obstacles. Certain characteristics of an implanted antenna features/characteristics like compact size and a broad working range bandwidth and adequate radiation efficiency and must address Patient security. Unlike standard antennas that function in open space, antennas utilised within the body must meet a number of requirements.

This implanted meandered antenna must fulfil the specifications. WBANs (wireless body area networks) were created in 1995 primarily for wearable computer device applications. Wearable computing devices can now be worn for extended periods of time and used to measure body signals such as electrocardiography (ECG), electroencephalography (EEG), electromyography (EMG), pulse oximeter, and body temperature data, thanks to the rapid development of wireless communication and low-power integrated circuits. These signals can be wirelessly transferred to a central process node (CPN), allowing medical personnel to examine the data and give clinical health care from afar. These potential applications have converted wireless sensor networks into a new generation of networks that have enhanced the quality of medical services and health care by allowing health care practitioners to continually and wirelessly monitor patients. A wireless medical gadget requires tiny high-performance antennas to execute these functions. The medical sector, healthcare personnel, and patients all benefit from antenna research and development. First, the antennas eliminate the need for actual cables that would otherwise flow through or rest on the body to assist in monitoring, diagnosis, and therapy and bind a patient to a medical bed. This improves patient mobility and comfort while also providing real-time data communication with healthcare professionals (doctors, nurses, and so on) around the clock, independent of the patients' location (hospital, home, office etc.).

Second, antennas make medical devices portable and wearable, as opposed to the massive importable medical equipment now in use in the business. This speeds up the development and distribution of potentially low-cost medical gadgets. There are mainly three types of antennae used in Biomedical industries which are classified in Fig. 13.1. External antennas mounted on monitoring/control equipment such as moving ambulances, distant doctor's clinics, and so on that set up strong connections

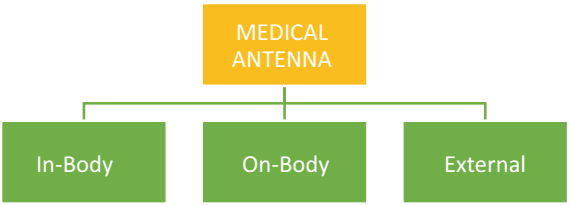

Fig. 13.1 Classification of medical antenna

with healthcare systems or protracted stationary remote access between emergency rooms, and in-body antennas placed inside the human body such as implantable, orally ingested, or parenteral antennas.

The chapter states the design of a U-shaped microstrip patch antenna with meandered slots. It operates at 2.45 GHz and is intended for biomedical applications. Simulation results show that two patch antenna designs are presented: one with and one without meandered slots. A study was comparatively made between the both. The antenna with meandered slots is found to have good functionality, appropriate bandwidth, minimal losses, and the ability to be used in biomedical applications. Furthermore, the suggested antenna is compact, with the ground accounting for about 14% of the entire size of the antenna (Sukhija* and Sarin 2017).

This antenna can be utilized in autonomous health monitoring systems because of its wide bandwidth capabilities. The compactness of this antenna, its progressive frequency response over loss response, and its radiation pattern all make it an excellent option for biological applications. The suggested antenna's future scope will be featuring compactness and a SAR calculation for the proposed design of the antenna (Nachiappan et al. 2020).

For biotelemetry applications, a patch design combining a Meandered and Sharp Edged Meandered shape is proposed in this paper. The antenna's structure has been created to suit the specifications. The antenna design's resonance frequency is between 2.4 and 2.5 GHz (Padmalatha et al. 2020). Medical antennas will be implanted in their bodies to help them and improve their standard of living. Implantable medical antennas based on radio frequency are utilized in a wide range of applications, including pacemakers, thermometers, electrical stimulators (FES), defibrillators, insulin level detection and blood flow. This paper shows a modest rectangular patch made up of a variety of Meandered shapes. The criteria used to choose the most efficient and suitable protocol in a variety of shapes and sizes. The data rate, low battery power needs, range, reliability, security, safety and data latency are the protocols stated in the paper. The device can be set up to work in two bands, allowing it to operate with one band while sleeping in the other (Yoshida et al. 2016).

The Paper Proposes designing of antenna using 3D EM simulation. The antenna checks out the metrics such as VSWR, input impedance and reflection coefficient using RF equipment. The experimental and modeling findings coincide well, indicating that it is a good option for biomedical applications. The suggested Micro strip patch antenna is shrunk by $\lambda 0/2$ for lower dimensions and a small footprint, the patch is created using the meandering line approach, and the simulated results are

provided by CST microwave studio for biomedical applications running at 2.4 GHz. The proposed antenna is designed successfully with metrics such as 74% of bandwidth efficiency and 38 dB return loss (Rahman et al. 2018). This research reveals that by optimizing the patch length and breadth, the Micro strip patch antenna design improves performance. The proposed antenna could be used for medical data collection processes from patients and rescue teams in on-body application systems (Durbhakula and Caruso 2021).

This paper describes an implanted antenna with a small meandering patch that operates in the Medical Implant Communications Service (MICS) band, which ranges from 402–405 MHz. The suggested antenna, which includes the super star layer, has a small volume of 0.16 cm^3 and is powered by a coaxial cable. A three-layered block phantom of the human chest has the antenna placed into the muscle tissue. The suggested antenna has excellent performance inside a three-layered tissue model and a very tiny size. The goal of this work is to create and show a small, implantable patch antenna that operates in the MICS band (402–405 MHz) and can be easily included in medical equipment (Wang et al. 2018). Additionally, a three-layered human chest model with muscle tissue and various lossy materials is used to test the performance of the suggested antenna. It is determined that the SAR analysis complies with the IEEE standard safety requirements. Different lossy materials were used to compare and analyse the antenna's performance. It works well for biomedical implantable purposes due to its tiny size and satisfactory performance (Reid et al. 2018).

A 4 × 4 antenna array with a high gain in a small space is proposed in this paper using a meandering-fed, 4-layer stacked patch antenna. The structure's meandering feed ensures a broad operating bandwidth. The high gain is a result of the four-layer layered patches. Comparing patch antennas with various layer configurations. Simulated versions of the antenna array and element designs are available. The suggested patch antenna array's 10-dB impedance matching bandwidth is 31 percent, spanning 1.2 GHz to 1.64 GHz. The realized gain changes between 1.25 GHz and 1.55 GHz, going from 18.7 dBi to 20.5 dBi (Naik and Manikanta 2018).

The study of a small rectangular patch antenna for satellite use has been done in this chapter. Upon that top of the substrate, the rectangular patch antenna is etched with a round slit and an additional meander line. The ground plane is slightly etched in the substrate's bottom. These two methods are taken into consideration for applications that require numerous bands in the X-band. The suggested antenna produces twin bands at operating frequencies of 11 GHz and 11.9 GHz with return losses of −26.89 dB and −26.04 dB, respectively. Two resonant bands where the radiation pattern was seen in the E and H planes are plotted in the outcome. Dual-band gain is likewise seen to be 7.01 dBi and 8.75 dBi, respectively (Yoshida et al. 2016). The proposed antenna is utilized for broadcasting and reception in satellite communication. The Importance of Wearable Technology in Today's World Wearable antennas and sensors are used to monitor home medical devices that assist patients suffering from asthma, diabetes, epilepsy, dialysis, cancer, and neonatal conditions. Sensors, processors, and antenna. Low-cost medical treatment may be achieved through online

evaluation of a large number of patients' continuous measured medical information (Lavanya et al. 2021).

Design of Meandered Shape Antenna

The design process of this work is briefly discussed in Fig. 13.2. To design any antenna fixing the frequency band of operation based on the specific application is mandatory. Once the frequency band is fixed, we have to design the antenna based on the length, width and slot size has to be decided (Podamekala et al. 2019). Optimization is followed after this to achieve the desired antenna parameters. Initially a four-step meandered antenna was designed covering the MICS and ISM band of frequency. This four-step meandered antenna initially provides a low Reflection Coefficient and after some optimization a Reflection Coefficient of −28 dB and gain of 4 dB was obtained at 405 MHz. Similarly at 2.45 GHZ a Reflection Coefficient of −28 dB and 3 dB gain was obtained. The Size of the four-step meandered antenna is 1080.4 mm^3 with Rogers RO3210 substrate(Reid et al. 2018). Then in order to increase the gain and Reflection Coefficient an eight-step meandered antenna was designed to have a Reflection Coefficient of −45 dB and gain of 8 dB at 405 MHz. Similarly at 2.45GHZ a Reflection Coefficient of −36 dB and 9 dB gain was obtained (Fig. 13.3).

The process involved in the IOT health monitoring system is shown in the figure. Initially the implantable antenna is distributed over human body through antenna fused capsules, laparoscope, pacemaker or any medical devices. Then the patient's

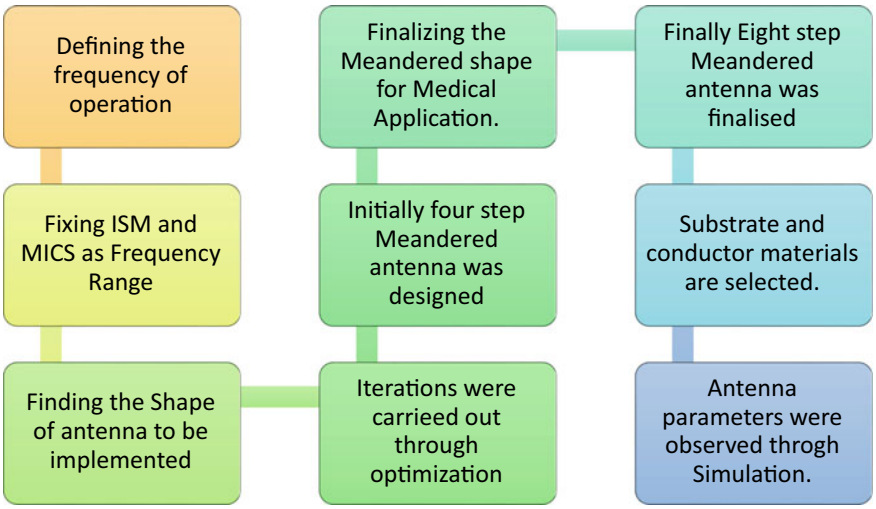

Fig. 13.2 Steps involved in design of meandered shaped antenna for MICS and ISM band for IMD applications

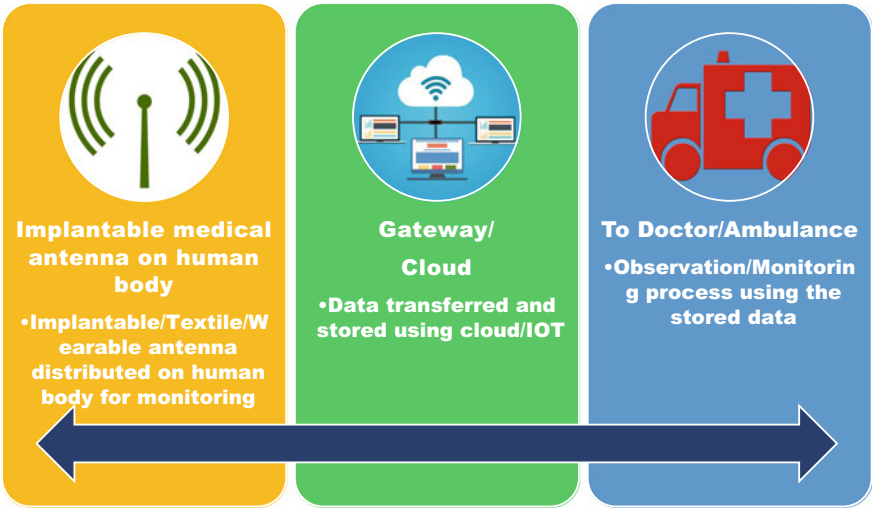

Fig. 13.3 Implantable antenna in IOT healthcare monitoring process

health is monitored using this IMA and stored in IOT cloud storage which can be further used for doctor reference about patients' health monitoring and treatment. The advantage of this process includes the data can be stored anywhere at any time and can be transferred to any gadgets through IOT cloud processing.

Antenna Design and Layout

To minimise the size of a straight monopole antenna, bend/twist/curve/stretch it to make a Meander line antenna (MLA). The antenna design was made based on the frequency usage or application and the microstrip patch antenna design. The impact of the antenna's meander segment is analogous to that of a foetus, and the meander line components are referred to as shorted-terminated transmission lines (Roy and Chakraborty 2017). The meander-line antenna can be dipole or ground planar in configuration. Bend the conductors back and forth to change the entire antenna shorter, as illustrated in Fig. 13.4. Although the size is lower, the Gain, Directivity, and Reflection coefficient are improved at the same time the radiation resistance, efficiency, and bandwidth are reduced.

An equivalent inductor can be depicted as a meander line section. Because magnetic fields cancel, the power lines of a meander line antenna do not transmit fields in the far-field pattern. Radiation fields will be emitted from the vertical sections of MLA. Various meander width values are simulated and analysed in order to determine the optimal antenna layout (Roy and Chakraborty 2017).

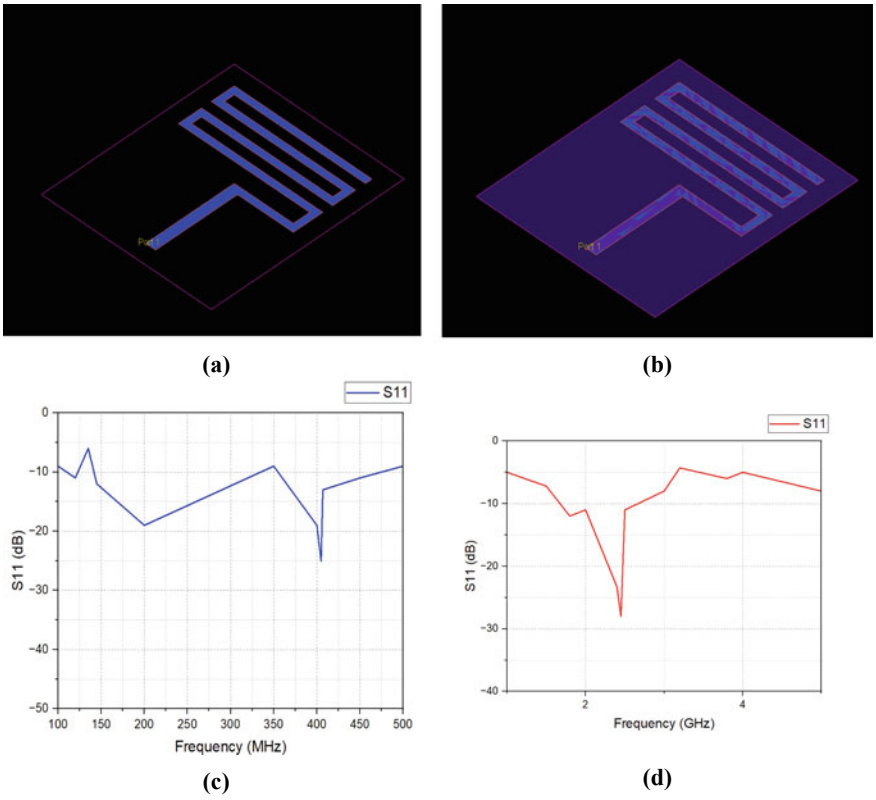

Fig. 13.4 **a** Simple four step meandered antenna design in 2-D view (**b**) Power distribution pattern of the proposed antenna (**c**) Antenna with DGS structure near feeding point (**d**) Antenna dimensions and layout (**e**) reflection coefficient S_{11} for ISM band (**f**) Reflection coefficient S_{11} for MICS band

Initially, a two-step S-shaped antenna was built that did not cover the needed frequency range; however, two additional steps were added to cover the required frequency band, as shown in Fig. 13.4. The dimensions of the antenna are given in Fig. 13.5. In addition, a defective ground structure was built to increase the reflection coefficient (S_{11} dB).

The antenna ground structure was made at lengths of 10.2 mm and 8.4 mm. At 405 MHz and 2.45 GHz, this results in a maximum reflection coefficient of −28 dB and a gain of 4 dB. This reflection coefficient and gain are inadequate for a high-performance antenna. As a result, we choose for an improved design with a higher step in the present antenna, which is an eight-step meandering antenna. This design provides and improved Reflection coefficient of −45 dB at 405 MHz and −36 dB at 2.45 GHz. The gain is also improved from 4 to 9 dB (Fig. 13.6).

The radiation pattern for XY, YZ and ZX plane was simulated and is shown in Fig. 13.7. The radiation pattern seems good for the proposed antenna at 2.4 GHz.Radiation is a term used to describe the emission or reception of a wave front

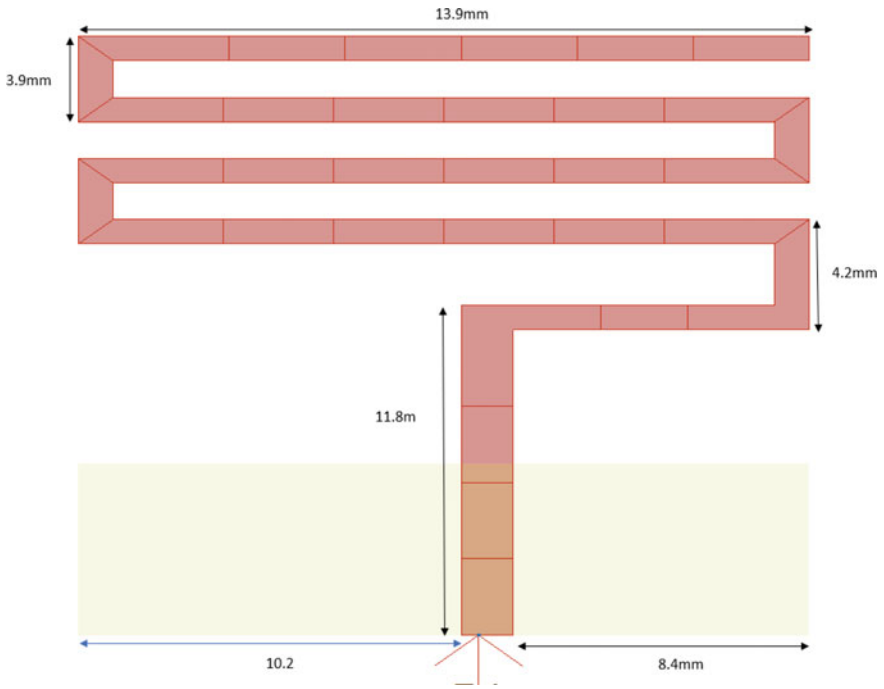

Fig. 13.5 Layout and dimensions of proposed meandered antenna

at an antenna, as well as its intensity (Ferdous et al. 2015a). The radiation pattern of an oscillator is represented by the sketch produced to depict its radiation in any picture. An antenna's function and quality factor may be easily assessed by looking at its radiation pattern. Many antenna designs and patch antennas have characteristics and radiation patterns that can be analysed but not easily visible. Fig. 13.7 displays the component parameters as well as the field patterns for a certain kind of antenna. The field pattern for a single element can be inspected by the user. The settings of these antennas or arrays can be changed manually or automatically using a swept parameter menu. There are common varieties of 1-D, 2-D, and 3-D arrays accessible, as well as a builder for any system of components (Ferdous et al. 2015b). The programme also includes synthesis and simulation tools for automatically selecting the optimum configuration for an array or element to fulfil a particular radiation characteristic (Roges and Malik 2021; Rahim et al. 2021; Malik et al. 2020).

Figure 13.8 depicts detailed research of the formation of various lobes in the ISM band's far-field lobes. We calculated the far-field distribution using an analytical model we developed. By comparing the observed and calculated far-field distributions, the mechanism producing the modulations may be identified conclusively. The model is then used to investigate the influence of various parameters on the far-field distribution. Finally, we demonstrate how to disable the modulations. Radiated power drops with the square of range in a directional antenna far-field area, and radiation

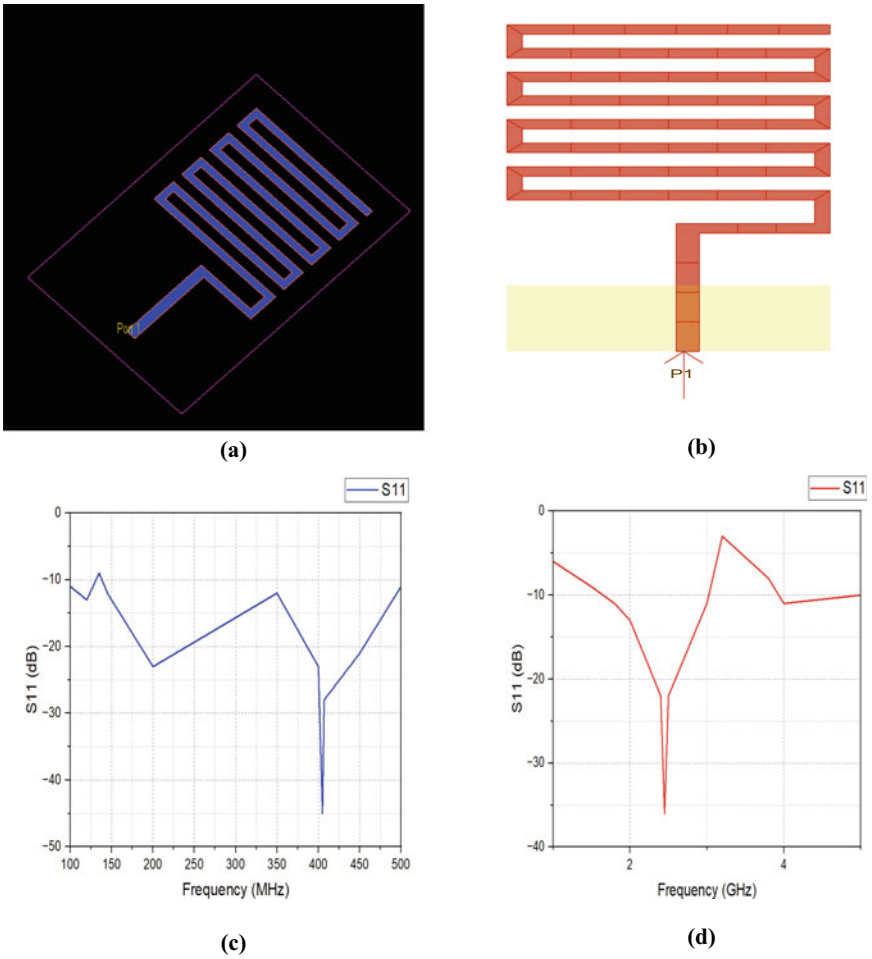

Fig. 13.6 **a** Eight step meandered antenna design in 2-D view (**b**) Eight step meandered antenna with DGS (**c**) Reflection coefficient S_{11} for ISM band (**d**) Reflection coefficient S_{11} for MICS band

absorption doesn't really feed back to the broadcaster. Conversely, in the near-field zone, radiation absorption does affect the transmitter's capacity. Magnetic induction, which can be seen in a transformer, is a very simple example of this sort of near-field electromagnetic interaction. In the far-field area, every half of the EM field is generated by a change in the other half, and the ratio of electric and magnetic field strengths is simply the medium's wave impedance.

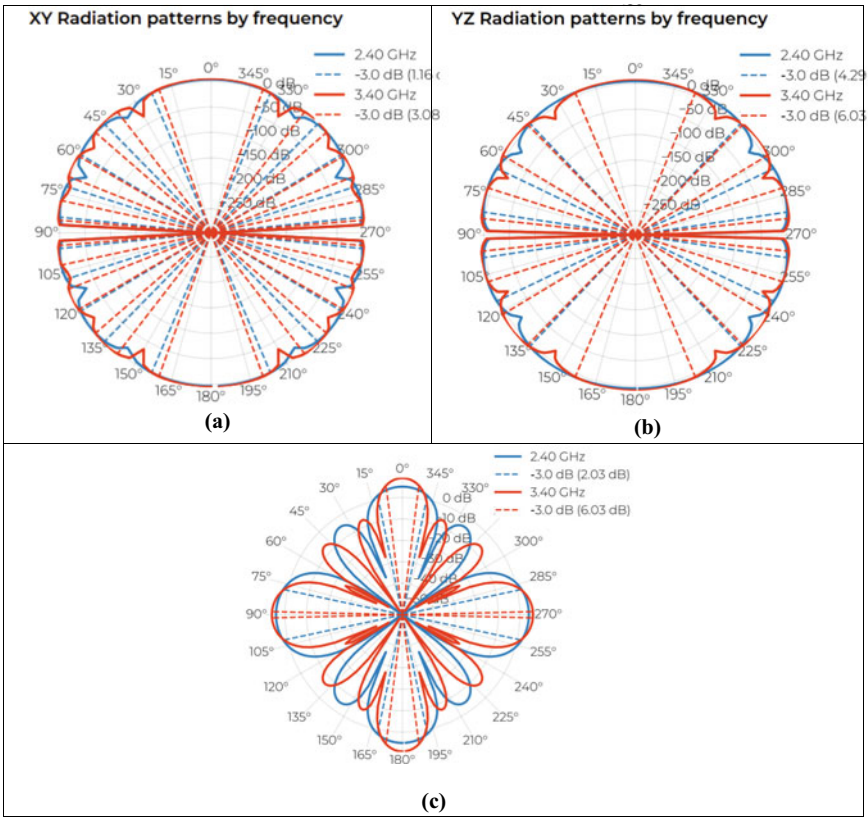

Fig. 13.7 **a** Radiation pattern in XY-plane (**b**) Radiation pattern in YZ-plane (**c**) Radiation pattern in ZX-plane

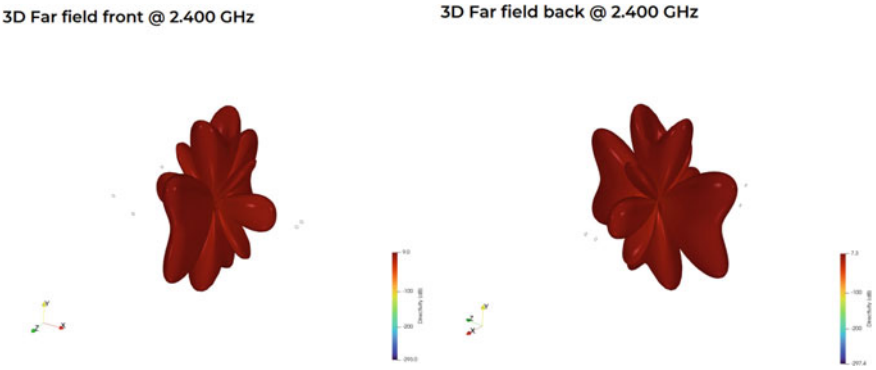

Fig. 13.8 Far field for front and back lobes

Result and Comparison

S11 is the most usually stated antenna parameter in practise. S11 denotes the amount of power reflected by the antenna and is hence known as the reflection coefficient (sometimes written as gamma: or return loss). If S11 = 0 dB, all power is reflected from the antenna and no radiation is produced. If S11 = −10 dB, then if 3 dB of power is given to the antenna, the reflected power is −7 dB. The remaining energy was "received by" or sent to the antenna. Radio and antenna performance are equally crucial in wireless communication. For the transmitter part to function properly, the matching between the radio's output port and the antenna must be as near to perfect as possible, which is achieved if VSWR is one. This received power is emitted or absorbed as antenna losses. Due to the fact that antennas are often built to be a low loss, the majority of the power given to the antenna should be radiated.

The results of ISM and MICS bands are compared in this section. The maximum return loss of −45 dB is obtained at 405 MHz for eight step meandered antenna and −28 dB for four step antenna the same is shown in Fig. 13.8. For both the frequency the eight-step meandered antenna gives better reflection coefficient and gain which is shown in Table 13.1. The S_{11} seems to be good at some MICS frequency like − 25 dB at 350 MHz, −28 dB at 405 MHz, −23 dB at 200 MHz and 400 MHz, − 28 dB at 407 MHz, −45 dB at 405 MHz. Similarly at ISM frequency band.

Antenna gain refers to an antenna's or an electromagnetic system's capacity to focus radiated power in a specific angle or, contrarily, efficiently absorption power coming from a specific direction. As it pertains to the effectiveness of the antenna system, gain is viewed as a fundamental parameter of an antenna. The gain of an antenna is strongly related to its directivity. The directivity, on the other hand,

Table 13.1 Comparison of reflection coefficient for four step and eight step

S. N0	Frequency (MHz)	Four step neandered antenna S_{11} (dB)	Eight step meandered antenna S_{11} (dB)	Frequency (Hz)	Four step meandered antenna S_{11} (dB)	Eight step meandered antenna S_{11} (dB)
	100	−6	−11	1	−5	−6
	120	−12	−13	1.5	−7.2	−9
	135	−19	−9	1.8	−12	−11
	145	−9	−12	2	−11	−13
	200	−19	−23	2.4	−23.3	−22
	350	−25	−12	2.45	−28	−36
	400	−13	−23	2.5	−11	−22
	405	−28	−45	3	−8	−11
	407	−9	−28	3.2	−4.3	−3
	450	−6	−21	3.8	−6	−8
	500	−12	−11	4	−5	−11

Table 13.2 Comparison of gain at 405 MHz and 2.45 GHz for the proposed antenna

Frequency	Gain of four step meandered antenna S11 (dB)	Gain of eight step meandered antenna S11 (dB)
405 MHz	3	8
2.45 GHz	4	7

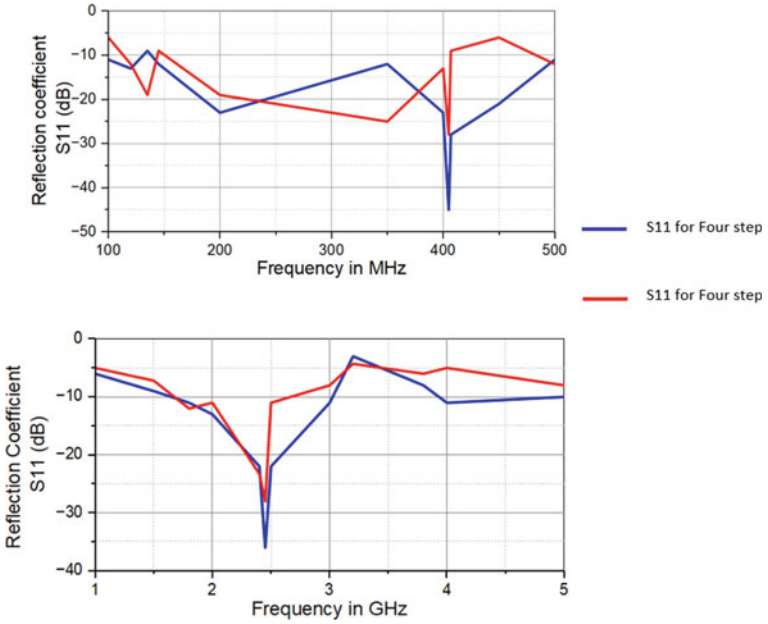

Fig. 13.9 Comparison of reflection coefficient shown in Table 13.1

is wholly reliant on the radiation pattern produced by the antenna. Nevertheless, when we wish to transmit equally throughout a whole room (or provide omni-directional exposure across our wifi signal), we don't need a lot of gain (or directivity). Remember that "gain" is merely borrowing radiated energy from one direction to amplify another. The maximum gain attained by the proposed antenna is 8 dB at 405 MHz and 7 dB at 2.45 GHz which is tabulated in Table 13.2 and compared in Figs. 13.9, 13.10.

Conclusion

In this work, an implanted low profile spiral shaped meandering patch antenna is constructed exclusively for Biomedical device applications, namely skin contact applications. The most often utilised frequency for biomedical applications for

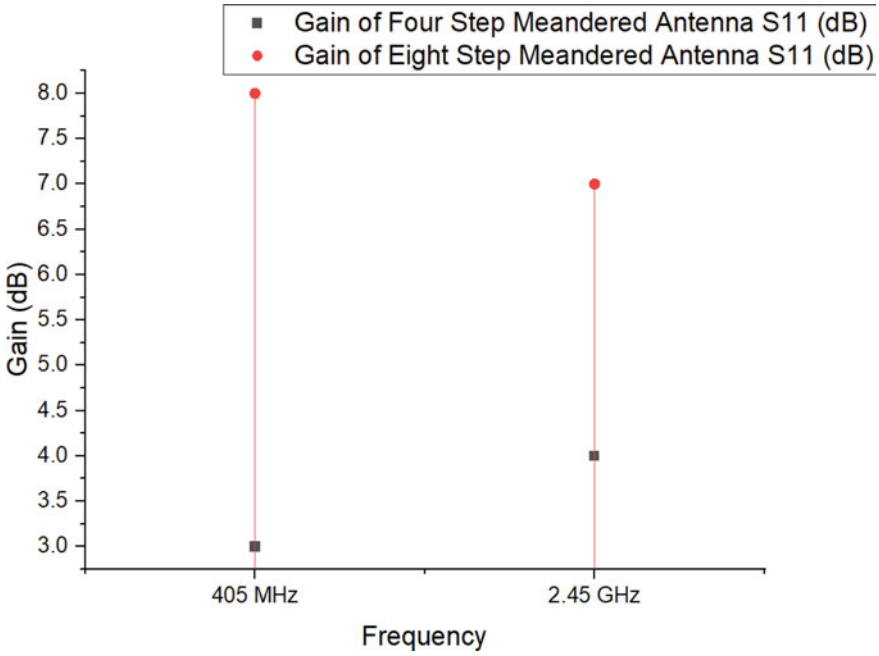

Fig. 13.10 Gain comparison of four step versus eight step meandered antenna at 405 MHz and 2.45 GHz

Medical Implant Communication Service (MICS) is 401–406 MHz, and this chapter covers the Industrial, Scientific, and Medical (ISM) band of 2.4–2.48 GHz. This antenna has a frequency range of 405 MHz, a reflectivity of −45 dB, and a gain of 8 dB. The following range is at 2.45 GHz, with a Reflection Coefficient of −36 dB and a gain of 7 dB. The antenna is only 0.32 mm thick and has dimensions of 35 mm 28 mm. Many iterations were performed to attain this gain, and eventually a twelve-slot meandering antenna fits the chosen frequency spectrum. Many iterations were performed to attain this gain, and the final Eight steps meandered antenna fits the intended frequency range. In this study, a meandered antenna is employed because it has a high Reflection Coefficient, gain, and low losses when compared to a standard microstrip patch antenna. They also take up less space than standard antennas of the same size.

References

Durbhakula KC, Caruso AN (2021) Characteristic mode analysis and optimization of meandering probe fed patch antenna for wide-bandwidth in UHF band. In: 2021 15th European conference on antennas and propagation (EuCAP), 2021, pp 1–5. https://doi.org/10.23919/EuCAP51087.2021.9411085

Ferdous N, Nainee NT, Hoque R (2015a) Design and performance of miniaturized meandered patch antenna for implantable biomedical applications. In: 2nd International conference on electrical engineering and information & communication technology (ICEEICT), 2015. Iahangirnagar University, Dhaka-I 342, Bangladesh, pp 21–23

Ferdous N, Nainee NT, Hoque R (2015b) Design and performance of miniaturized meandered patch antenna for implantable biomedical applications. In: International conference on electrical engineering and information communication technology (ICEEICT), 2015, pp 1–4. https://doi.org/10.1109/ICEEICT.2015.7307370

Lavanya P, Sujanth Narayan KG, Kumar DR, Murty VSCS, Baskaradas JA (2021) Design of CPW fed hexagonal patch antenna for LTE and Wi-MAX applications. In: 2021 IEEE Indian conference on antennas and propagation (InCAP), 2021, pp 462–465. https://doi.org/10.1109/InCAP52216.2021.9726455

Malik PK, Wadhwa DS, Khinda JS (2020) A survey of device to device and cooperative communication for the future cellular networks. Int J Wirel Inf Netw, Springer 27:411–432. https://doi.org/10.1007/s10776-020-00482-8

Naik KK, Manikanta MHV (2018) Design of circular slot on rectangular patch with meander line antenna for satellite communications. In: Second international conference on inventive communication and computational technologies (ICICCT), pp 1252–1255. https://doi.org/10.1109/ICICCT.2018.8473217

Nachiappan M, Jeyakumar V, Anand TP (2020) Design of compact implantable meandered and sharp edged meandered shaped antenna for biomedical application. Eur J Mol & Clin Med 7(11), ISSN 2515-8260

Padmalatha N, Deepa T, Susila M (2020) Design of miniaturized flexible planar antenna for biomedical application. Int J Recent Technol Eng (IJRTE) 9(2), ISSN: 2277-3878 (Online)

Podamekala M, Prathyusha ARL, Mamidi S, Verma P (2019) Design of a meandered line microstrip patch antenna with array implementation. In: International conference on wireless communications signal processing and networking (WiSPNET), 2019, pp 1–3. https://doi.org/10.1109/WiSPNET45539.2019.9032877

Roy S, Chakraborty U (2017) Dual band microstrip patch antenna with meandered ground plane. IEEE Appl Electromagn Conf (AEMC) 2017:1–2. https://doi.org/10.1109/AEMC.2017.8325720

Rahim A, Malik PK (2021) Analysis and design of fractal antenna for efficient communication network in vehicular model. Sustain Comput: Inform Syst, Elsevier 31:100586. ISSN 2210-5379. https://doi.org/10.1016/j.suscom.2021.100586

Roges R, Malik PK (2021) Planar and printed antennas for internet of things-enabled environment: opportunities and challenges. Int J Commun Syst 34(15):e4940. https://doi.org/10.1002/dac.4940ISSN:1099-1131

Rahman M, Ahmed F, Rahman AMA (2018) A compact MICS band operated implantable antenna for biomedical applications. In: 2018 4th international conference on electrical engineering and information & communication technology (iCEEiCT), 2018, pp 148–151. https://doi.org/10.1109/CEEICT.2018.8628087

Reid T, Sharma SK (2018) A 60 GHz 8×8 planar array antenna with corporate feed network using meandered probe fed patch in LTCC technology. In: 2018 11th global symposium on millimeter waves (GSMM), 2018, pp 1–4. https://doi.org/10.1109/GSMM.2018.8439240

Sukhija* S, Sarin RK (2017) A U-shaped meandered slot antenna for biomedical applications. Prog Electromagn Res M 62:65–77

Wang L, Wang J, Shi J (2018) Design of 4×4 meandering-fed stacked patch antenna array. Int Work Antenna Technol (iWAT) 2018:1–3. https://doi.org/10.1109/IWAT.2018.8379221

Yoshida S, Maruyama K, Matsushita D, Nishikawa K (2016) UHF-band meander line antenna and 60-GHz-band patch antenna with single feed structure for 5G terminal application. Int Symp Antennas Propag (ISAP) 2016:1044–1045

Chapter 14
THz Microstrip Patch Antenna for Wearable Applications

Mehaboob Mujawar and Md. Shakhawat Hossen

Abstract In this chapter, a THz-frequency microstrip patch antenna is constructed and analyzed, with the goal of using it in wearable applications. A novel form of THz wearable antenna is presented for wearable applications. Due to the shortage of spectrum accessible for wireless communication, this chapter was written with the intention of recognizing the needs and expectations of high data rates. As a result, the time has come to seriously consider the higher frequency portions of the electromagnetic spectrum for wireless communications. This chapter considers and analyses the usage of the terahertz frequency band in future compelling systems and devices.

Keywords THz antenna · Wearable · Microstrip · THz Applications · Wearable Applications · Denim · Return loss · Radiation parameters

Introduction to Terahertz (THz) Technology

THz is the frequency range from 300 to 3000 GHz, which is $1mmto100\mu m$ in wavelength, corresponding to the energy of about 1.2 to 12.4 meV and equivalent temperature of about 14 to 140 K. There are various applications for which the frequencies can be used depending on the electromagnetic spectrum. Starting from radio waves, which are used for broadcast radio and TV, going to higher frequencies which is the area of the cell phones then the THz region starts at the 300 GHz up to 3 THz. Going to higher frequencies in the infrared region then visible light region and ultraviolet region which is used in medicinal applications and x-ray imaging at higher frequencies and gamma rays, which are used for cancer therapy because it kills living cells.

M. Mujawar (✉)
Research Scholar, Glocal University, Saharanpur, Uttar Pradesh, India
e-mail: mehaboob311134@gmail.com

Md. S. Hossen
Rajshahi University of Engineering & Technology, Rajshahi 6204, Bangladesh

P. K. Malik and P. N. Shastry (eds.), *Internet of Things Enabled Antennas for Biomedical Devices and Systems*, Springer Tracts in Electrical and Electronics Engineering,
https://doi.org/10.1007/978-981-99-0212-5_14

Advantages of THz

THz has very strong interaction with all states of matter, i.e. liquid, solid and gases. The strong interaction results in interesting spectral effects. There are certain materials which are transparent in this frequency range such as plastics, ceramics and few dielectric crystals. There are naturally occurring spectral signatures, which have to do with molecular motion and these are mostly apparent when we have light weight gases under low pressure. It has got very high sensitivity for traditional signal detection because the techniques out of the microwave regime can be used. There are aperture advantages that we can compare directly with mm wavelength, we just scale the frequency up for the same antenna diameter and the pixel size or resolution can be scaled down linearly with aperture diameter and that gives real portability advantages. THz is non-ionizing radiation and compared to x-rays they don't cause harm to any genetic material or atomic structure when exposed to it. The optical tolerances are lower than near IR or optical regime. So the antennas don't have to be quite well surfaced even though they might be large. The huge bandwidth available from 300 to 3000 GHz, practically no signal bands in that range that have been assigned in that point of time. For wide dynamic signal range this frequency band is suitable.

THz Constraints

In this wavelength range, the material loss is very high irrespective of the material being plastic, crystalline material. The dielectric loss is very high compared to the optical regime. There is no such thing as the equivalent of optical fiber in the THz range because of the interaction of phone on the mode of dielectrics and because of high ohmic losses in metals. THz energy can be propagated in any material without suffering significant loss, whether it is a waveguide or quartz substrate having low loss. In the atmosphere water and oxygen absorb very heavily and cannot transmit to a very large distances interms of km at the low end of the THz band.

Interaction of THz Waves with Matter

One aspect which determines how THz waves behaves is their attraction with matter. THz waves have certain properties for example they can penetrate through materials which are not transparent for other parts of the electromagnetic spectrum packaging materials such as plastic, ceramic and so on (Failed 2021). Also the energy is very low that does not induce any chemical changes in the chemical structure. It can also be used to create imaging and transmit information.

Generation of THz Radiation

There are certain possibilities for the generation of THz radiation. One way is to do up conversion coming from the lower end of the spectrum and the other possibility is coming from the high end of the spectrum to do down conversion. Each of these waves has its own advantages and disadvantages. In the case of up conversion, electronic sources such as multiplier chains, RTD, transistors and diodes are used. The main advantages are as follows: It is compact, and it is at room temperature but disadvantages include limited bandwidth and limited efficiency. Coming from the upper part of this spectrum, that is for opto-electronics. Bit signal can be created using two lasers and bit signal can be mixed on the photodiode, and it is connected to antenna and then transmit THz radiation. It is tunable because lasers are tunable. It is at room temperature. Power and efficiency are limited.

Applications of THz Antennas

Traditional THz Applications: The investment of THz in the frequency regime has been significant and the reasons behind it mainly come from basically four areas (Plasma diagnostics, non-destructive evaluation, gas spectroscopy and quantum physics, ultra fast chemistry and nonlinear optoelectronics) in the historic development. The first is astrophysics, this is something that comes about because of the particular signatures that can be detected in this wavelength range that are unique, and have to do with molecular motion, especially in regions that are cold and low pressure, as you find outside the stars or in center of galaxies and out of space in general. The people doing plasma work in the early days were using THz for measuring electron zygotron resonance parameters and temperatures of heart gases in fusion reaction systems. There have been several non-destructive evaluation techniques that use THz for their very high sensitivity to order content. **Modern THz Applications**: One of the major applications of THz waves include non-destructive imaging, which can be used for security checks and material analysis. Another application is the analysis of molecules for diclofenac acid (Voltaren), which is a painkiller. The THz radiations can distinguish between two of its chemical forms. Chemical compound differences lie in the THz frequency region. The quick personnel security scanner used in airports and operates between 70 to 80 GHz and can create a 3D picture, which can easily detect suspicious objects. The security scanner consists of approximately 3000 transmitters and 3000 receiver antennas. Each transmit antenna radiates at a certain time successively and the 3000 receive antennas take the picture of the reflected waves at the same time. Which results in the collection of a lot of data and this data needs to be processed. The peak power is very low i.e. only 1mW. **Three main approaches to THz**: The first approach is the traditional radio frequency techniques, where we take microwave, transmission lines, waveguides, antennas, sources, and detector technology and we translate it up in frequency into the THz regime, in

order to capture these spectral contents that exists only in the wavelength band. A lot of this technology investment has really confirmed the astrophysics community basically in the 70 s as sources become available in this wavelength range and has undergone continuous development from then. The second approach is another technique that was developed in 1970s involves generating THz signals using Optical sources and using an interweaning crystals or photo-mixers to do optical rectification but narrow band sources like lasers are able to be applied to non linear crystals and down converting from optical into the THz regime became possible with narrow linewidth. The third technique is essential to use for the transform spectroscopy or to generate broadband THz energy through time domain technique using a fast femtosecond laser and the same kind of frequency conversion techniques that optics researchers used in 1980s to generate a very wide signal with microwatt levels of power throughout the THz range by making sure that the laser has pulse width of only few femtosecond, so that very broad THz signal response can be obtained from the fourier transform.

Millimeter Wave Effects on the Body

When THz imaging system comes into picture, in this technique human body is illuminated. When the human body is illuminated it will get heated apart from that, there will be also radiation effects on the body, which is a controversial statement. For many years it was thought that it was therapeutic approach for many diseases as well as for stimulating cells to behave in certain ways. For the frequency range of 60 GHz, which is approved for LAN systems and also used in Military applications for active denial. For the experiment in which rat tissue was exposed to millimeter waves, when the tissue was exposed to millimeter waves for 5 s, the neurons were less affected compared with the same tissue when exposed to 15 s.

Importance of Microstrip Patch Antenna

Antennas are the essential part of any wireless communication device because it is used to radiate and receive electromagnetic radiation preferably in the desired direction. Most of the time we want to radiate or receive from a desired direction. The efficiency of the antenna for the device is very important because without the efficient antenna the device will not be able to create a link with the receiving device or it will not be able to receive the information transmitted by the transmitter. The device bearing the antenna can be handheld, mobile or stationary. The efficiency of the antenna primarily determines the quality of the wireless communication and further the antenna characteristics determine the efficiency of the antenna. The main antenna characteristics which we need to focus on is return loss, gain, bandwidth in which the antenna is working, radiation pattern of the antenna and many other

parameters, which we need to examine during the design of the antenna. In general, the most preferred type of antenna is the small size planar antenna or microstrip patch antenna. The general structure of the microstrip patch antenna consists of two parallel conducting planes that are separated by dielectric substrate. The thickness of the conducting planes is very small, therefore we call it as microstrip (Mujawar October 2021). The bottom conducting plane is known as ground plane and the upper conducting plane is known as a radiating plane. The upper part is basically radiating and the lower part is basically spotting the radiation, therefore the ground plane has its own role. The thickness of the substrate and the dielectric constant of the substrate, these are the two major deciding factors of the characteristics of the antenna. The selection of the substrate is very crucial in the field of wearable antennas and flexible antennas. The upper conductor which is named as radiating patch that may have shape of rectangular then will call it as rectangular shaped microstrip patch antenna. Similarly we can have circular patch, square patch or ring type of radiating patch. If we are having fractal type of radiating patch, then will call it as fractal microstrip patch antenna. Depending on the shape of the radiating patch will name the antenna accordingly. The main advantages of microstrip patch antenna are (Mujawar 2021): Microstrip patch antenna are light weight and low volume, so these antennas are very light and the dimensions of the antenna are very compact and we can easily integrate these antennas to the devices. If the weight of the antenna is large, then the device will not be able to carry the antenna. We can easily design these antennas in planar configuration and we can also easily design these antennas which can be hosted on the conformal host surface. The wearable or flexible antennas can be easily designed using the microstrip patch antenna design principles, which can be conformal to the host surface. Many of the fabrication techniques of these antennas are low cost. We can fabricate these antennas with low cost fabrication process. We can integrate these antennas with microwave integrated circuits. In microwave integrated circuits, the antenna will become part of the circuit and some parts will behave as antenna and the other part will work as microwave integrated circuit for the desired function. The very popular application of antenna in the field of microwave integrated circuit is RF energy harvesting. In RF energy harvesting, antenna have been used to collect RF energy and get RF energy. Then we need to provide that energy to rectifier, so we can easily design that integrated rectifier along with antenna, which is very useful for RF energy harvesting applications. These antennas are also capable of multi-band frequency operations, that is we can design antennas which can work on two or more than two bands. So same antenna can be used for different bands.

Introduction to Wearable Antennas

These antennas find a number of applications in the smart devices and smart clothes. The upcoming technology would require that the antenna should be a part of clothing, therefore there is a need of flexible antenna. The interaction of the antenna with people and surrounding should be very easy, therefore there is a need for flexible antenna.

The major applications of the wearable antennas can be in the field of medical applications, for planning time or getting inputs from surrounding. The emerging of IOT applications, this is another reason for a special focus on flexible wearable antennas. For the IOT applications, many times we require that those components should be self powered or we should have energy storage components. So for self powered components, RF energy harvesting antennas are very useful for collecting ambient energy and giving that energy to the IOT device. In general we can say that the upcoming time is of flexible electronics systems. So flexible electronic systems will also require flexible antenna systems, especially interms of IOT. According to different surveys it is projected that billions of the devices will be connected to internet to form the IOT type of network, so these devices will be needing antennas. So these tens of billions of wireless sensing devices will be required in coming years, so all these devices will be required antennas. These antennas should have the properties of conformability or flexibility to mount on non-planar or curved surfaces. IOT is one special segment of application, which need flexible and durable antennas. Most of these antennas will be worned by the humans as part of wearable sensors. **Desirable Features of Wearable Antennas**: These antennas should be low cost, because IOT applications will require billions of wireless sensors or antennas. The cost of the antenna should be so low that it can be comparable to use and throw, disposable type. Flexibility should be large, so there should not be any deformation with the antenna conformal to the host surfaces. Light weight is another concern of the antenna, specially for human wearable devices. The size of the antenna also matters, because if the size of the antenna is large then it will not be easy to integrate that antenna with the wearable devices. Similarly these antenna should be low profile. Mechanically robust antennas are required since they are subjected sometimes to harsh environments, such as continuous change in temperature or other type of variations in physical environment (Hossen et al. 2021, 2020). The radiation characteristics should be desirable. If we have designed antenna for particular application, so even in the different harsh environments they should work desirably and we should be able to control the radiation characteristics of the antenna, so that we can design antenna accordingly for their use. **Applications of flexible wireless antenna**: These are mainly used for bio-medical monitoring / applications. They are also used in Wi-Fi and WLAN applications. They are also used in beam switching detection systems, RF energy harvesting, wearable glasses and UWB applications. **Major issues with wearable antennas**: (a) Non-invasive and invisible: Many of these antennas will be a part of smart clothes, these smart clothes will be interacting with the environment of the person, who is wearing that particular cloth. But at the same time the major challenge is our antenna should be non-invasive and it should be invisible to the user or to the person who is interacting with the user of that smart cloth. Making of invisible antennas is a major issue. (b) Durability of wearable clothes and devices: when antenna is made part of the cloth or wearable particular device, especially in case of clothes that are frequently washed or ironed frequently. The performance of the antenna is also affected. The antenna characteristics should not drift when it is subjected to the different operations interms of clothes. (c) Robustness to operating circumstances: This is another major issue, when the wearable or flexible antenna is a part of smart cloth or it is a part of wearable

device. Making antenna independent of the surrounding environment is also a major issue. (d) Drift in antenna RF characteristics due to bending and human body proximity: Since human body is hostile environment interms of antenna performance, so energy is absorbed by the human body, so we need SAR analysis during the design of antenna and our antenna should meet the desired standards which have been set up by different bodies interms of SAR deposition. Similarly how the body affects the performance of the antenna is also a major issue. (e) We cannot generalize the solution approach for flexible wearable antenna, so the design of flexible antenna or wearable antenna will be an application centric approach.

Recent Trends in THz and Wearable Antenna Technology

In this paper (Ghosh et al. 2020), terahertz structures have been designed in the terahertz window. Meander line-based split ring resonator in terahertz has been designed. The subsequent improvement in the structure can be achieved and multiband operation can be obtained operating at four to six distinct frequencies. The co-polarized level is higher compared to the cross polarized. The efficiency of the proposed antenna is around 50%. The return loss obtained by the proposed antenna is around 35 dB in the frequency range of 5 to 6 THz. This antenna finds applications in the field of medicine and point to point communication. In this paper (Zhang et al. 2017), optimization techniques in THz antenna is explained, basically consists of open loop resonator with multiple channels and dual surface. The feed line is wired to the same multiway open-loop resonator on both sides of the antenna substrate. In dual-band microstrip antennas, a T-shaped structure is commonly used. The study presents a unique dual-frequency THz microstrip antenna. In this paper (Paul and Islam 2017), Gain and bandwidth were increased as a result of optimizations. Antenna arrays, in addition to a single microstrip antenna, have greater directionality and gain. THz wireless communication is carried out from the transmitter to the receiver end with the help of THz antennas. Overall system's efficiency has a direct impact because of the effectiveness of the THz antennas. Which basically means that bandwidth will have a direct impact due to THz antenna performance. THz antennas have a good directivity. The unit size is significantly reduced due to the response of THz antenna in the higher band of frequencies. Materials and process methods restrict the packaging of THz antennas. Because of its small size in the high-frequency bands of THz waves, it has a high loss and lower fabrication accuracy. Another difficulty in terahertz antennas is obtaining effective radiation. As a result, THz antennas must meet higher standards with respect to design, operation and fabrication technology. At frequencies of 0.835, 0.635, and 0.1 THz, LCP is used as a substrate. Fabrication for a variety of medical applications, including THz tumour detection and Doppler radar or vitro technology for vital sign detection, may be done on a simple printed circuit board (PCB). However, because THz microstrip antennas have a low gain, researchers are concentrating their efforts on figuring out how to

boost the gain. The principle of suppression effect is employed to identify semiconductor features in this study (Failed 2017). TARC Value is also giving the bandwidth from 2 GHz to almost 8 GHz. MEG is almost 0.3. Surface current distributions in different frequency range has been observed, specifically for 2.4 GHz, 6 GHz and 6.425 GHz. For every frequency range the I shaped structure has reduced the coupling current in the second element. After placing the I shaped structure the bandwidth has been increased. Quality factor will be reduced and bandwidth will be increased. The overall gain will also be reduced. Therefore it can be concluded that after placing the I shaped structure gain of the antenna is reduced. So the major disadvantage of this design was with the increase in bandwidth, gain of the antenna reduces. In this paper (Mei et al. 2017), radar cross section of the antenna has been reduced with the help of frequency selective surfaces. The broadband absorber has been placed on the antenna along with periodic strip type of structure to get a notch band. Notch band is working in only vertical polarization. In horizontal polarization there will be only wide absorption band. The absorber structure acts like a ground plane for a dipole antenna. Radar cross section of the antenna has been observed when absorber structure acts like a ground plane for a dipole antenna. The frequency of operation of the antenna is chosen to be overlapping with the notch band of the absorber. Monostatic RCS for vertical polarization and horizontal polarization was observed. For horizontal polarization, the RCS of antenna with and without absorber is seen. The significant reduction in RCS was observed in both in band and out band for the horizontal polarization. For vertical polarization RCS is reduced only in the out band, RCS is not reduced in band. In this paper (Young et al. 1973), meander line polarizer has been discussed. meander line polarizer is a transmission type polarization converter. In meander line polarizer wave is incident diagonally over the polarizer, this incident field is broken into two components, one is E parallel and the other is E perpendicular. E parallel is incident in parallel with the surface of the meander line structure. E perpendicular is striking the meander line surfaces orthogonally. Meander line structures are periodically arranged and their surfaces are spaced at a distance of $\lambda/4$ with respect to each other. The basic approach is to make the array of structure which appeared to be predominantly inductive to one polarizer and predominantly capacitive to orthogonal polarization. In this paper (Syed et al. 2013), the desired axial ratio is achieved with the help of jerusalem cross shaped structure with inductive arms and capacitive coupling among unit cells. The arms are tuned to provide inductive and capacitive coupling between the unit cells, which helps in achieving the polarization conversion. The unit cell sizes are close to $\lambda/2$ at the operating frequency. The wave will be incident at 45 degree to the surface of polarizer and again by adjusting the dimensions of the arms meander line type of response can be obtained. The main disadvantage of this antenna structure is high insertion loss of about -3.1 dB. In this paper (Ayoub et al. 2020), reconfigurable polarization converter has been designed. The designed antenna has periodic array of hexagonal type of structure. This structure basically works in two modes. The incident wave is a linearly polarized wave and transmitted wave is a linearly polarized wave in one state of the converter and it will be circularly polarized wave in another state of the converter. The proposed converter is a reconfigurable polarization converter. The converter is

designed on a diclad 880 substrate. The antenna has hexagon type of structure with gap in the middle where PIN diodes are placed. The PIN diode can be operated in two modes. Hexagonal type of structure have been printed on both sides of the diclad substrate having thickness of 60 mil thick. In state 1, diode acts like a short circuit. In state 2, it is a hexagon structure with split in the central arm. In state 1 of the polarization converter, the magnitude of the transmission coefficient for the orthogonal component in the frequency band ranging from 13.6 to 17 GHz are both equal and close to 0 dB and phase difference among them varies between 13.3 to 19 GHz. Since the phase difference is not 90 degrees, it is not circularly polarized mode. For the state 2, magnitude of the orthogonally transmitted components are equivalent and they have phase difference varying from 85 to 100. it is providing circularly polarized wave. In this paper (Ridouane et al. 2017), innovative DGS structure has been used to design the antenna for WiMAX applications. The main aim of this paper is to design antenna which could shift the resonance frequency from 10 GHz to 3.5 GHz. The reduction in frequency can be achieved by using DGS structure. The use of DGS structure also makes the antenna compact. They have designed this antenna for WiMAX applications by shifting the frequency from 10 GHz to 3.5 GHz. In this paper (Arya and Kartikeyan Patnaik 2008), A simple dumbbell-shaped DGS structure has been used to design the antenna. The effect of dumbbell-shaped DGS structure on the antenna was observed. The efficiency of the antenna has been increased by using cavity backed model. The overall size of the antenna was reduced with the introduction of DGS. The antenna has been designed using IE3D software. The resonance frequency has been calculated by varying the structure dimensions. The change in the inductive and capacitive values of the LC circuit used depends on the size and area of the antenna structure. In this paper (Hamad and Gehad 2019), the antenna has been designed using periodic geometry. The use of a DGS structure in the antenna has provide compact antenna having low cost, antenna design involving less complexity and the antenna offering large bandwidth. FR4 substrate has been used to design the antenna. The overall structure of the antenna consists of X-shaped slots on the microstrip patch and it has four slots at the edges of the patch. The designed antenna has bandwidth ranging from 3.1 to 22.9 GHz. This antenna offered gain of 6.01 dB at a frequency of 8.8 GHz. In this paper (Gao et al. 2016), massive MIMO antenna has been designed which is having dual polarization. The designed antenna is having arrays with 132 ports. In the construction of this antenna power splitters have been used. These power splitters have vertically and horizontally connected ports. The ports connected to power splitters acts like feed provided to the antenna structure. The combination of four individual unit cells forms the subarrays in the design. The overall arrays used in the structure constitute for 18 subarrays. Many layers have been stacked one on top of the other to form stacked patch. This antenna design has 7 layers stacked one on top of the other. The metallic coupling strips are located between the two dielectric layers. Also the ground plane is also located between the two dielectric layers. The feeding ports are located at the bottom of the stacked layer. This antenna offers measured bandwidth of 159 MHz (3.55 to 3.80 GHz). The measured transmission coefficient of the antenna is -31 dB. The mutual coupling

between the power splitters is observed to be -44 dB. The simulated reflection coefficient of the antenna is -17 dB at 3.75 GHz and the measured reflection coefficient of the antenna is -23 dB at 3.75 GHz. In this paper (Sarkar et al. 2015), monopole antenna loaded with split ring resonator has been discussed. The monopole antenna has also been loaded with an inter-digital capacitor. The split ring resonator has also been loaded with an inter-digital capacitor because of which the antenna structure is offering four bands.but normally monopole offers single resonance. The overall performance of the antenna has been studied by considering four cases of operation. In the first case only the monopole antenna has been considered, which resulted in single resonance. The reflection coefficient for the first case was obtained to be –20 dB at 2.8 GHz. In the second case the monopole antenna was loaded with SRR, which resulted in two resonances. The reflection coefficient for second case was obtained to be –25 dB at 1.8 GHz and –20 dB at 2.8 GHz. In the third case inter digital capacitor has been introduced in the antenna structure, which resulted in two resonances. The reflection coefficient for third case was obtained to be –15 dB at 2.4 GHz and –20 dB at 2.8 GHz. In the fourth case inter-digital capacitor has been introduced along with split ring resonator in the antenna structure, which resulted in four resonances. The reflection coefficient for fourth case was obtained to be –17 dB at 1.8 GHz, –22 dB at 2.4 GHz, –21 dB at 2.7 GHz and –15 dB at 3.3 GHz. When the designed antenna was put on microstrip patch in the form of array of four antenna elements in the orthogonal pattern, the correlation parameters of the antenna reduced compared to the single antenna structure. In this paper (Sarkar et al. 2016), dipole antenna arrays loaded with CSRR have been designed. Two power dividers have been combined and placed on the antenna patch. The two dipoles are not feed with the same because of the additional delay lines introduced in the second power divider. Due to the additional delay line, the phase will be different at both the power divider locations. If the feed is given to port one, then proper radiation patterns are obtained. But if the feed is given to port two, then it can be clearly seen that the power has reduced along + 1 as well as in the x direction. From the radiation patterns at the different frequencies, it was concluded that the designed antenna offered good diversity patterns at 2.36 GHz. The introduction of Complementary split ring resonators in the antenna structure has resulted in making the proposed antenna compact, low profile and increasing the diversity of the antenna. In this paper (Sharma et al. 2015), quad band MIMO antenna has been designed. Two rings have been used to create two bands. The structure of the antenna is in the form of orthogonal style. In order to establish the quad band operation, slots have been created on the microstrip patch. These microstrip slots are loaded with split ring resonators. The proposed antenna finds very good application in WLAN, WiMAX and c-band operations. In this paper (Sharma et al. 2016), dipole antenna has been designed to achieve polarization and pattern diversity in the antenna elements. Two dipole antenna element structures have been created on the patch and in addition to this bottom side of the patch is behaving like reflector. The reflector is like some in fire radiation at the bottom of the patch antenna. The dipoles will radiate under + Y and -Y directions respectively. Circularly polarized patch has been placed at the center of the patch antenna. This patch will be radiating at the CP antenna in the + Z direction. It is also radiating in the

linearly polarized wave along the + Y and –Y direction. This three element system is very compact but it has the polarization and pattern diversity. The pattern is not only orthogonal polarization, it is also linearly polarized on one side and circularly polarized antenna on the other side. From the radiation patterns it can be clearly seen that the linearly polarized antenna is radiating in the –Y direction, + Y direction and also the Z direction it is radiating at Right Hand Circular Polarization. In this paper they have integrated pattern diversity and polarization. The simulated results of the reflection coefficient for the designed antennas are obtained to be -20 dB at 5.8 GHz. The measured results of the reflection coefficient for the designed antennas are obtained to be –35 dB at 5.8 GHz. In this paper (Dwivedy and Behera 2020), the antenna has been designed for frequency and CP re-configurability. The overall structure of the antenna consists of rectangular microstrip patch, feed network, varactor diodes. The antenna is fed with microstrip line feeds at port 1 and port 2. The ports are matched with quarter wave transformer. Four varactor diodes have been used to design the antenna. The selection of varactor diodes mainly depends on the capacitance and operating voltage. These varactor diodes are used for capacitance variation as well as frequency alteration. The primary aim of this antenna is to alter its resonant frequency or operating frequency. Therefore four varactor diodes are used to tune its frequency. In order to achieve circular polarization antenna has been fed using two ports. The two ports are fed with equal amplitude signal and 90 degree phase shift. The feeding network basically consists of phase shifting and switching circuit. The switching circuit handles the operation of + 90 or –90 degree phase shift. The proposed antenna offered a band width of –10 dB for the frequency range from 1.9 GHz to 2.5 GHz. The measured transmission coefficient of the antenna is varying from –5 dB to –6.2 dB. In this paper (Kumari et al. 2015), the sequential rotation technique has been used to achieve circular polarization within a wide bandwidth. The proposed antenna structure aims at four types of polarizations within a wide bandwidth. It is very difficult to achieve multiple polarizations with a single structure hence sequential rotation technique has been used to design the antenna. Rogers dielectric substrate has been used for the antenna design having a dielectric constant of 9.2. The radius and height of the DRA are 20 mm and 10 mm respectively. To achieve circular polarization all the four antennas are simultaneously excited from four sides by equal amplitude signals with 90 degree phase shift. The two antennas are excited at the same time with the phase difference of 180 degree to obtain vertical linear polarization. The other pair of antennas are excited with the phase difference of 180 degree to obtain horizontal linear polarization. Hence four types of polarizations are obtained within a wideband. In this paper (Bhattacharya et al. 2012), single band metasurface absorber has been designed. The metallic pattern have been printed on the unit cell of the structure. The substrate used to design this antenna is FR4. The absorption is achieved at a frequency close to 7.46 GHz. The scaling of the metallic structure has been carried out. The periodicity of the structure remains constant and only the dimensions of the structure have been scaled. Super cells have been formed which basically consists of sub-cell 1 and sub-cell 2. Sub cell 1 has been scaled by a factor of 1.2, which is deponent from the scaling factor of sub cell 2 that is 1.3. The designed structure is absorbing and resonating at two distinct frequencies. It has 48

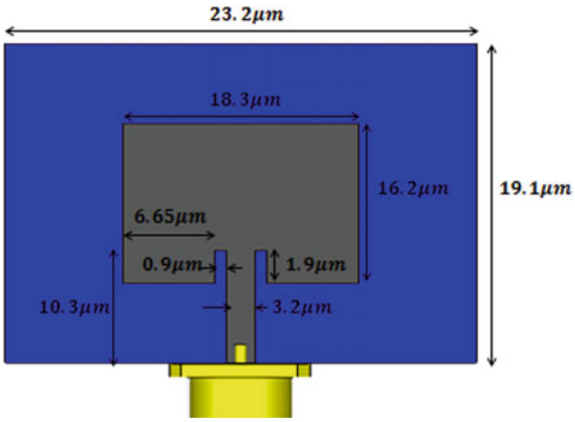

Fig. 14.1 The proposed THz microstrip wearable antenna

unit cells in the X direction and 48 unit cells in the Y direction. The dimensions of the fabricated structure is 230*230. It was observed from the electric field pattern that all the gaps are getting activated at 5.46 GHz. From the second frequency band that is at 9.54 GHz, the gaps are indicating absorption. At 7.40 GHz, the waves are adjacent on the metallic structures. Therefore all the capacitance in the structure gets excited at 7.40 GHz. Hence the structure contributes to triple band absorber.

Geometry of the Proposed THz Wearable Antenna

The suggested THz wearable antenna's top layer is comprised of copper with a thickness of $0.05\mu m$, and it is the antenna's radiating element. The substrate is made of denim, which has a thickness of $0.6\mu m$ and a dielectric constant of 1.6. CST software was used to design the antenna. The proposed antenna's ground plane measures $23.2 \times 19.1\mu m^2$ and the copper radiating patch measures $18.3 \times 16.2\mu m^2$ (Fig. 14.1).

THz Wearable Antenna Simulation Results

At the resonance frequency of 870.3 GHz, the return loss reaches a maximum of –28 dB. At a resonance frequency of 692.7 GHz, the return loss is as low as –26 dB. The tunability of the suggested antenna to resonate at multiple frequencies in the terahertz region, 692.7 GHz, 798.3 GHz, and 870.3 GHz, has been shown. CST was used to build and simulate a terahertz microstrip patch antenna. As a substrate, the suggested antenna uses Denim with a dielectric constant of 1.6 (Figs. 14.2, 14.3, 14.4).

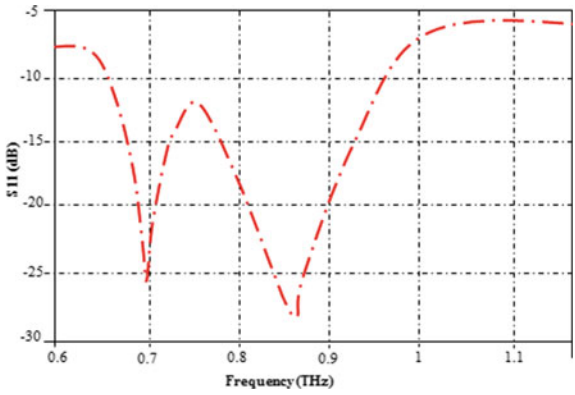

Fig. 14.2 Graph of S11 vs. Frequency

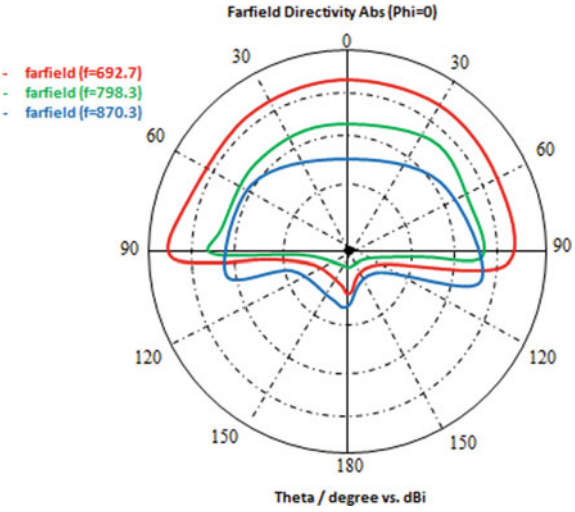

Fig. 14.3 Field radiation patterns in E-plane

SAR Analysis of the Proposed Antenna

The amount of power absorbed by human tissue per unit mass is known as the specific absorption rate. SAR values of all devices must be validated prior to fabrication and before the product is put on the market. The impact of human body interaction on wearable antennas must be investigated. According to the Federal Communications Commission, the SAR value for 1 g of tissue in the United States is 1.6 W/ kg, while the SAR value for 10 g of tissue in Europe is 2.0 W/ kg. CST microwave studio was used to determine the SAR values of the wearable device. The SAR values of the antenna obtained when placed on the forearm are 0.35, 0.61 and 0.72 at frequencies 692.7 GHz, 798.3 GHz, and 870.3 GHz respectively (Fig. 14.5).

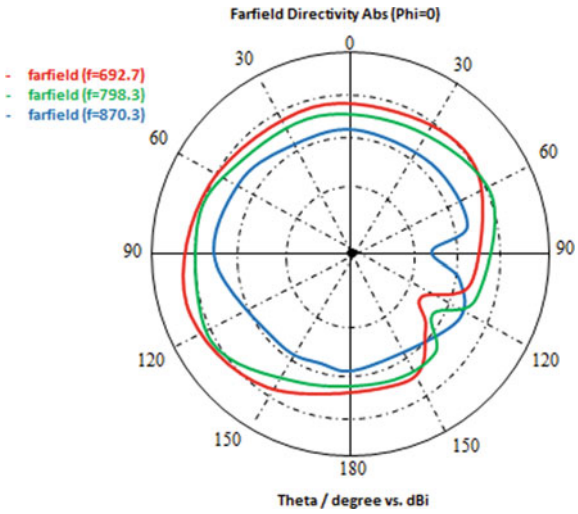

Fig. 14.4 Field radiation patterns in H-plane

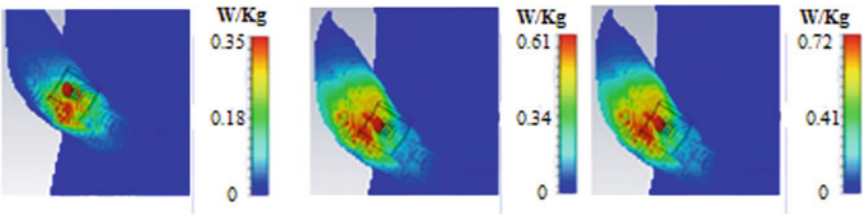

Fig. 14.5 SAR distribution on forearm

Conclusion

This chapter discusses a wearable antenna design that works well at terahertz frequencies. The tunability of the suggested antenna to resonate at multiple frequencies in the terahertz region, 692.7 GHz, 798.3 GHz, and 870.3 GHz, has been shown. CST was used to build and simulate a terahertz microstrip patch antenna. As a substrate, the suggested antenna uses denim with a dielectric constant of 1.6. The antenna reflection coefficient at resonant frequencies was also evaluated by analysis. The developed antenna's performance makes it ideal for wearable applications.

References

Arya Ashwini, Machavaram Kartikeyan, Patnaik A (2008) Efficiency enhancement of microstrip patch antenna with defected ground structure. 729–731. https://doi.org/10.1109/AMTA.2008.4763036

Ayoub Sofi Mohammad, Saurav Kushmanda, Koul, Shiban (2020). Reconfigurable polarization converter printed on single substrate layer frequency selective surface https://doi.org/10.1109/IMaRC45935.2019.9118663

Bhattacharya S, Baradiya H, Chaudhary Raghvendra, Srivastava, Kumar Vaibhav (2012) An electric field driven LC resonator structure as ultra thin metamaterial absorber

Dwivedy B, Behera S (2020) A square-shaped microstrip antenna with frequency and circular-polarization reconfigurability: an approach [Antenna Applications Corner]. IEEE Antennas Propag Mag 62:107–115. https://doi.org/10.1109/MAP.2020.2998813

Prince, et al. (2017) Rectangular terahertz microstrip patch antenna design for vitamin K2 detection applications. In: Preceding 2017 1st International Conference on Electronics, Materials Engineering and Nano-Technology (IEMENTech), pp 1–3

Mujawar M, Gunasekaran T, Rashid A, (2021) Design and analysis of X band pyramidal horn antenna using FEKO.In: 2021 International Conference on Advances in Electrical, Computing, Communication and Sustainable Technologies (ICAECT), pp 1–4, https://doi.org/10.1109/ICAECT49130.2021.9392523

Gao Y, Ma R, Wang Y, Zhang Q, Parini C (2016) Stacked Patch Antenna with Dual-Polarization and Low Mutual Coupling for Massive MIMO. IEEE Trans Antennas Propag 64:1–1. https://doi.org/10.1109/TAP.2016.2593869

Ghosh Soham, Das Sohom, Samantaray Diptiranjan, Bhattacharyya Somak (2020). Meander-line-based defected ground microstrip antenna slotted with split-ring resonator for terahertz range. Engineering Reports. 2. https://doi.org/10.1002/eng2.12088

Hamad Ehab, Nady Gehad, (2019) Bandwidth extension of Ultra-wideband microstrip antenna using metamaterial Double-side planar periodic geometry. Radioengineering. 28, 25–32. https://doi.org/10.13164/re.2019.0025

Hossen MS, Badrudduza ASM, Islam SMR, Hanif A, Kundu MK, Kwak K-S (2021) Opportunistic relay selection over generalized fading and inverse gamma composite fading mixed multicast channels: a secrecy tradeoff. IEEE Access 9:166184–166205. https://doi.org/10.1109/ACCESS.2021.3133727

Hossen MS, Badrudduza ASM, Hanif A, Kundu MK, Sarkar MZI (2020) Secrecy performance of multicasting over shadowed rician fading channel. In: 2020 IEEE Region 10 Symposium (TENSYMP), pp 1086–1089, https://doi.org/10.1109/TENSYMP50017.2020.9230729.

Kumari Runa, Behera SK, Sharma Sk (2015). Aperture coupled wideband dielectric resonator antenna array with polarization reconfiguration https://doi.org/10.1109/AEMC.2013.7045056

Mei Peng, Lin Xian, Yu Jia, Boukarkar Abdelheq, Zhang Peng, Yang Zi (2017). Development of a low radar cross section antenna with band-notched absorber. IEEE Trans Antennas Propag. pp 1–1. https://doi.org/10.1109/TAP.2017.2780903.

Mujawar M (2021) Antenna array design for massive MIMO system in 5G application. In: book: Future Trends in 5G and 6G, November 2021, https://doi.org/10.1201/9781003175155-18

Mujawar M (October 2021) Compact microstrip patch antenna design with three I-, Two L-, One E- and One F-Shaped patch for wireless applications. In Book: Microstrip Antenna Design for Wireless Applications. https://doi.org/10.1201/9781003093558-7

Paul LC, Islam MM (2017) Proposal of wide bandwidth and very miniaturized having dimension of μm range slotted patch THz microstrip antenna using PBG substrate and DGS. In: Preceding 2017 20th International Conference of Computer and Information Technology (ICCIT), pp 1–6

Ridouane Er-Rebyiy, ZBITOU, JAMAL, Tajmouati Abdelali, Latrach Mohamed, Ahmed Errkik, El Abdellaoui Larbi (2017). A new design of a miniature microstrip patch antenna using Defected Ground Structure DGS. 1–4. https://doi.org/10.1109/WITS.2017.7934598

Sarkar Debdeep, Singh Aditya, Saurav Kushmanda, Srivastava Kumar Vaibhav (2015) Four-element quad-band multiple-input–multiple-output antenna employing split-ring resonator and inter-digital capacitor. IET MicrowS Antennas & Propag. 9. https://doi.org/10.1049/iet-map.2015.0189

Sarkar Debdeep, Saurav Kushmanda, Srivastava Kumar Vaibhav (2016). Dual band CSRR-loaded printed dipole antenna arrays for pattern diversity MIMO applications. IET Microwaves Antennas & Propagation. 10. https://doi.org/10.1049/iet-map.2016.0004

Sharma Yashika, Sarkar Debdeep, Saurav Kushmanda, Srivastava Kumar Vaibhav (2015) Quad band annular slot and SRR based MIMO antenna system. 1–2. https://doi.org/10.1109/AEMC.2015.7509143

Sharma Yashika, Sarkar Debdeep, Saurav Kushmanda, Srivastava Kumar Vaibhav (2016). Three element MIMO antenna system with pattern and polarization diversity for WLAN Applications. IEEE Antennas and Wireless Propagation Letters. pp 1–1. https://doi.org/10.1109/LAWP.2016.2626394

Syed Irfan Sohail, Ranga Y, Esselle Karu, Hay SG (2013) A linear to circular polarization converter based on Jerusalem-Cross frequency selective surface. 2141–2143

Young L, Robinson L, Hacking C (1973) Meander-Line Polarizer. Antennas Propag, IEEE Trans on. 21:376–378. https://doi.org/10.1109/TAP.1973.1140503

Zhang G, Pu S, Xu X-Y, Tao C, Dun J-Y (2017) Optimized design of THz microstrip antenna based-on dual-surfaced multiple split-ring resonators. In: Preceding 2017 IEEE International Symposium on Antennas and Propagation and USNC/ URSI National Radio Science Meeting, pp 1755–1756

Chapter 15
ANN Modeling and Performance Comparison of X-Band Antenna

Shuchismita Pani, Malay Ranjan Tripathy, and Sumit Agarwal

Abstract Presently due to technological advancement in computational logic based on intelligent computing using neural networks, ANN has become one of the solution techniques which gives adaptability and self-learning capability to the antenna system. A technique of antenna parameter adaptation under different conditions has been carried out in this work. The present technology of machine learning and neural network computations give good support to various antenna parameters, design in an optimized manner. Demand for fast and highly accurate computations are often satisfied using the models of artificial neural network. The ANN training algorithms help in the simulation of the results to minimize the error with high-accuracy geometric dimensions. Various EM simulators are available for designing microstrip patch antenna, but they all need a number of iterations and time-consuming processes to get actual data and develop the real prototype. Artificial Neural Networks have the capability as a fast and flexible solution to EM modelling, simulation and optimization also has the ability to respond precisely to the inputs which are in the interval or having inequality constraints. This chapter presents the artificial neural network modeling of rectangular microstrip patch antenna in an X-band region and analysis of the ANN model by using nftool in MATLAB through three different kinds of training algorithms. The best validation and training performances are observed and noted with various epochs and varying the number of hidden neurons. The minimum error values and best regression plots are also observed. To verify this observation rectangular microstrip patch antennas are designed and studied. The results show the usefulness of the antenna in the X-band region.

S. Pani (✉) · M. R. Tripathy
Amity University, Uttar Pradesh Noida, India
e-mail: spani@amity.edu

M. R. Tripathy
e-mail: mrtripathy@amity.edu

S. Agarwal
Pennsylvania State University, State College, Pennsylvania Philadelphia 16802, US
e-mail: sua347@psu.edu

P. K. Malik and P. N. Shastry (eds.), *Internet of Things Enabled Antennas for Biomedical Devices and Systems*, Springer Tracts in Electrical and Electronics Engineering,
https://doi.org/10.1007/978-981-99-0212-5_15

Keywords Rectangular microstrip patch antenna · Resonant frequency · Dielectric constant · Artificial neural network · S11parameter · Gain

Introduction

The microstrip patch antenna design requires a set of complex requirements, which are calculated through some equations. The resonant frequency of MPA is a very important parameter related to its geometry which consists of the length, width of patch and dielectric constant of the substrate. Due to the compactness and excellent radiator, MPA has wide area usefulness in recent mobile antenna, aircraft, remote sensing and satellite communication. Various EM simulators are available for designing MPA, but they all need a number of iterations and time-consuming processes to get actual data and develop a real prototype. Though neural networks have the capability as a fast and flexible solution to EM modelling, simulation and optimization. Artificial neural network accurately respond to a new data set in a determined interval of interest, which is defined during the training phase. They are also able to provide results closer to the reality, once calculated data set is used (Güney et al. 2001; Haykin 2001; Silva 2006; Karaboga et al. 1999). MLP is a multi layer perception is very suitable for modelling high-dimensional and very non correlated problems.The multi layer perception mainly has three layers, which include one or more hidden layers.. The design of a rectangular patch antenna has been done using MLP (Ali Heidari 2011). A detailed study of multilayer perceptron neural networks has been conducted in Kala et al. (2013). Artificial Neural Network design of a microstrip antenna is clearly explained in Tamboli and Nikam (2013), Turker et al. (2004) and Thomas et al. (2014) displays the entire neural network toolbox concept. Levenberg–Marquardt (LM) algorithm, Bayesian Regularization(BR) training algorithm and Scaled Conjugate Gradient(SCG) training algorithm are generally used to train the multi layer perception for modelling. A stacked antenna with 2 radiating patches using neural network training algorithm has been proposed to find resonant frequencies (Jain et al. 2009). The network takes the various design parameters of the patch antenna as input and gives both upper resonant frequency and lower resonant frequency (Bisht and Malik 2022; Pandey et al. 2022; Vishnoi et al. 2023). In this chapter RMPA for the X-band region has designed with HFSS and S11 parameters and maximum gains are discussed. It also analyzed through ANN modelling and their performances are compared through different training algorithms, such as Levenberg–Marquardt training algorithm, Bayesian Regularization training algorithm and Scaled Conjugate Gradient training algorithm.

Methods of Analysis for Proposed Model

Artificial Neural Network is basically composed of several computational units known as neurons. They are mainly multiple processing units and connected through communication channels called links, associated with their respective weights. The weights used for storing the knowledge also represent the biological synapses of neurons, which are the existing connections between them. The model of an individual neuron consists of following components:

- Weights which are a set of synapses.
- A function that combines the weighted input signals.
- An activation function to limit the amplitude of the signal output of the neuron.

There are so many methods available for the design of microstrip patch antenna. To get proper result, it is very difficult to develop real prototypes for specific applications. So the ANN technique is the best option to get the design parameters.

From the physical parameters of microstrip antenna, the resonant frequency can be estimated to use a model. Other parameters like radiation pattern, bandwidth and directivity can also be calculated. Some methods commonly used are the transmission line, cavity and full wave. The transmission line method (TLM) is an approximate method which is considered to be the simplest method and it provides good insight of mechanism of radiation, however, is the least accurate (Turker et al. 2006).

In order to generate the network learning a training database has to create which must contain both the network input and the required output. In the proposed method of ANN design, one model has been analyzed as shown below in Fig. 15.1.

The analysis of proposed models has been developed by using the Levenberg–Marquardt training algorithm, Bayesian Regularization training algorithm and Scaled conjugate gradient training algorithm with MATLAB17. The data set is calculated from microstrip patch calculator. The generated data is used for training and testing of ANN for both the analysis model. In our case the database contains 25 examples.

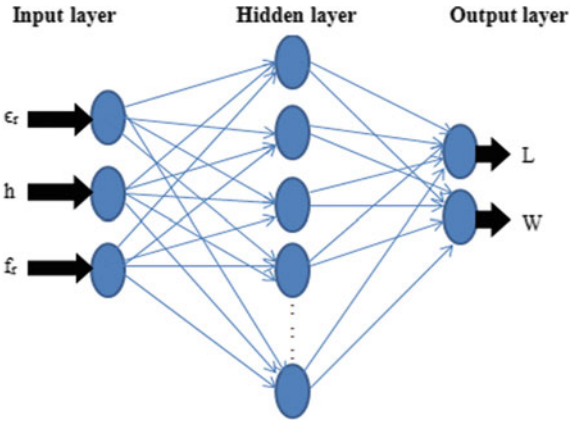

Fig. 15.1 The MLP3 ANN architecture at X-band frequencies

Table 15.1 Range validity of the proposed ANN model

Parameter of MSA	Minimum range	Maximum range
resonant frequency(fr)	8 GHz	12 GHz
Permitivity of dielectric substrate(ϵr)	2.2	4.4
Height of substrate(h)	0.5 mm	2.5 mm
Length of radiating patch(L)	4.615 mm	12.398 mm
Width of radiating patch(W)	7.557 mm	14.823 mm

Considering this ANN technique as an effective tool for nonlinear approximations has been used in this work to identify the relationship between the physical parameters of antenna system and its performances. In the analysis design as shown in Fig. 15.1, input data are resonant frequency(f_r), permitivity of dielectric substrate(ϵ_r) and height of substrate(h). The output data are length(L) and width(W) of a radiating patch antenna, whose ranges are given in Table 15.1.

Statistical Analysis of Proposed Method

In this proposed model, three statistical indices such as Levenberg–Marquardt, Scaled conjugate gradient and Bayesian Regularization training algorithms are used for the accuracy evaluation of the performances and results.

- Levenberg–Marquardt training algorithm: It is damped least square(DLS) used to solve the generic curve fitting problems with the local minimum finding which may not be the global minimum, shown in Eq. 15.1.

$$S(\alpha) = \sum_{j=1}^{n} \left[y_j - f\left(x_j, \alpha\right) \right]^2 \tag{15.1}$$

  where n is a given set of independent and dependent variable (x_j,y_j). The algorithm find the parameter α of the model curve f(x,α) so that sum of squares of deviations S(α) is minimized.
- Scaled conjugate gradient training algorithm: SCG algorithm is a feed-forward and supervised algorithm for Artificial Neural Network which shows that in connections there are no loops between the units, shown in Eq. 15.2.

$$S_k = [E(W_k + \sigma_k P_k) E(W_k)] / \sigma_k \tag{15.2}$$

- Bayesian Regularization training algorithm: BR algorithm reduces the need for lengthy cross-validation and it is more robust than the standard back-propagation methods, where to solve non-linear least squares problems, shown in Eq. 15.3.

$$X = \arg Max\, P(C_b)\pi np\left(\frac{y_i}{C_b}\right). \tag{15.3}$$

The neural fitting tool of MATLAB is mainly used to analyze the performances and results.

Antenna Designs

Within X-band 8–12 GHz four rectangular microstrip patch antennas are designed in HFSS with the Permitivity of dielectric substrate 2.2 for 8 GHz, 9 GHz, 10 GHz and 2.94 for 8.5 GHz as mentioned in Table 15.2.

The design of antenna which is operating in 8 GHz with inset fed is shown in Figure 15.2.

Results and Discussion

The proposed ANN model is trained with three different types of training algorithm, considering the number of hidden neurons 10,20,30,40 and 50. All are tested with two categories of number of data samples. In first category out of 25 samples, 17 samples are taken as training data, 4 samples are taken as validation data and 4 samples are considered to testing data. The performance with number of epoch, gradient, regression and zero error point values are noted and mentioned in Table 15.3. The average value of performances and average zero error point, for all 3 training algorithms are calculated.

All the readings for 3 training algorithms are taken from the respective plots, for the analysis. The best validation performance values are taken from the plot of mean square error vs number of epochs. With hidden neurons 10, for category I, the LM training algorithm gives the best validation performance as 0.12796 at epoch 5 as shown in Figs. 15.3 and 15.4 shows the gradient as 1.2112e-8. The error histogram diagram with 20 bins is shown in Fig. 15.5, for the three steps of training data, validation data and testing data in ANN modelling. The zero error has come at 0.006322 and illustrated with a yellow standing line in the graph with 35 instances in training set. The regression value comes best as 0.99764 for the same and shown in Fig. 15.6. With 40 hidden neurons in the same case, error comes to very minimum as −0.0171. Though its regression is 0.91083 less than the previous case but it is a good value. The average of performance with LM training algorithm is 1.9906. Similarly the average performance value for BR and SCR training algorithm are 1.21e-08 and 1.790274 respectively. Performance of LM training algorithm is better than BR and SCR training algorithm whereas error is minimum in BR training algorithm as compared to others.

Table 15.2 Parameters and results of designed RMPA

Sl. No	Resonant frequency (f_r) in GHz	Permitivity of dielectric substrate (ϵ_r)	Height of substrate (h) in mm	Length of radiating patch (L) in mm	Width of radiating patch (W) in mm	Simumated S11 parameter (dB)	Simulated Gain (dB)
1	8	2.2	1.5	12.39	14.82	−28.8	7.9
2	8.5	2.94	1.5	10.89	13.95	−10.8	7.6
3	9	2.2	1.5	10.21	13.18	−11	7.4
4	10	2.2	2.5	9.07	11.86	−18.7	6.8

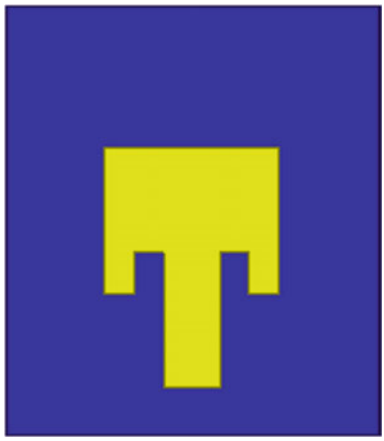

Fig. 15.2 RMPA with resonant frequency 8 GHz with $\epsilon_r = 2.2$

The number of epochs are very large in the Bayesian regularization training algorithm as compared to LM and SCR training algorithm. So regression is near about to 1 and error is also minimum in BR alg. Figure 15.7 shows the best training performance of category I with the Bayesian Regularization algorithm with 10 hidden neurons. When hidden neurons are 30, the zero error comes at −6.5e-5 shown in Fig. 15.8.

Similarly in the second category out of 25 data, 15 samples are considered for training data, 5 samples are for validation and 5 samples for testing. All of their performances with various epochs, gradient, regression and zero error point values are mentioned in Table 15.4. The number of epochs in BR is large as compared to SCR and LM algorithm. Regression values are near to 1 with less values of error. In this case average performance of SCR training algorithm is 9.654902 which is maximum as compared to other two training algorithm, but average zero error point value is minimum in the BR training algorithm as compared to LM and SCR training algorithms.

The S11 parameters of all four designed antennas are −28.8 dB, −10.8 dB, −11 dB and −18.7 dB for 8Ghz, 8.5 GHz, 9 GHz and 10Ghz respectively as mentioned in Table 15.2. The best value for S11 parameter comes for 8 GHz as shown in Fig. 15.9. Similarly the simulated maximum gain for designed antennas is 7.9 dB, 7.6 dB, 7.4 dB and 6.8 dB for 8Ghz, 8.5 GHz, 9 GHz and 10Ghz respectively. The best value for maximum gain is 7.9 dB for 8 GHz resonant frequency as shown in Fig. 15.10.

Conclusion

The physical parameters of rectangular microstrip patch antenna in X-band(8–12 GHz) region are considered as the dataset for ANN modelling in which input data are resonant frequency(fr), permitivity of dielectric substrate(ϵr) and height of substrate(h). The output data are length(L) and width(W) of radiating patch antenna.

Table 15.3 Performances of category I

Types of training algorithm	Category-I Training data-17 samples Validation data-4 samples Testing data-4 samples							
	No of hidden neurons	Performance	Average value (performance)	Epoch	Gradient	Regression	Zero error point	Average zero error point value
Levenberg–Marquardt training algorithm	10	0.12796	1.9906	5	1.2112e-8	0.99764	0.006322	5.69e-02
	20	1.385		1	2.5656e-9	0.94376	0.05366	
	30	0.19933		5	6.2925e-14	0.97704	0.09859	
	40	2.5447		3	6.2202e-14	0.91083	−0.0171	
	50	5.6962		1	3.771e-14	0.8827	0.1431	
Bayesian regularization training algorithm	10	3.7479e-8	1.21e-08	1000	7.3379e-6	0.99998	−0.0016	−1.40e-04
	20	6.0294e-15		1000	5.3659e-7	0.9998	0.001944	
	30	1.681e-9		1000	2.5646e-5	0.9999	−6.5e-5	
	40	2.1293e-8		1000	5.3207e-6	1	−0.00016	
	50	4.6477e-16		999	1.393e-7	1	−0.00082	
Scaled conjugate gradient training algorithm	10	0.74862	1.790274	29	0.20637	0.98731	−0.03004	0.049938
	20	0.94045		84	0.050934	0.97117	0.07735	
	30	1.9621		9	1.0016	0.9416	0.08008	
	40	3.4674		28	0.51157	0.86724	−0.1221	
	50	1.8328		232	4.4888e-5	0.81483	0.2444	

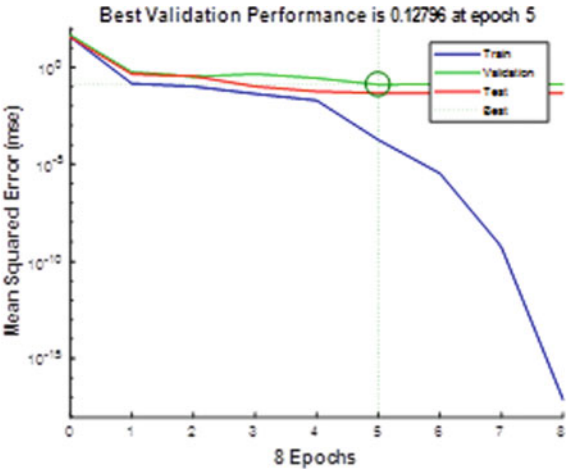

Fig. 15.3 Performance of data set in category I with LM algorithm with 10 HN

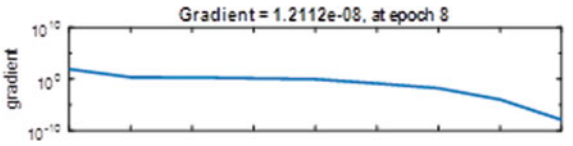

Fig. 15.4 Gradient in category I with LM algo with 10 HN

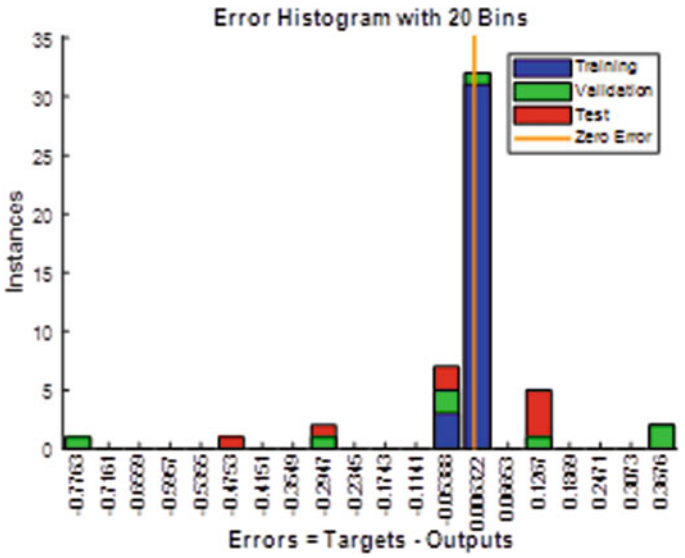

Fig. 15.5 Error histogram diagram showing zero error in category I with LM algo with 10 hidden neurons

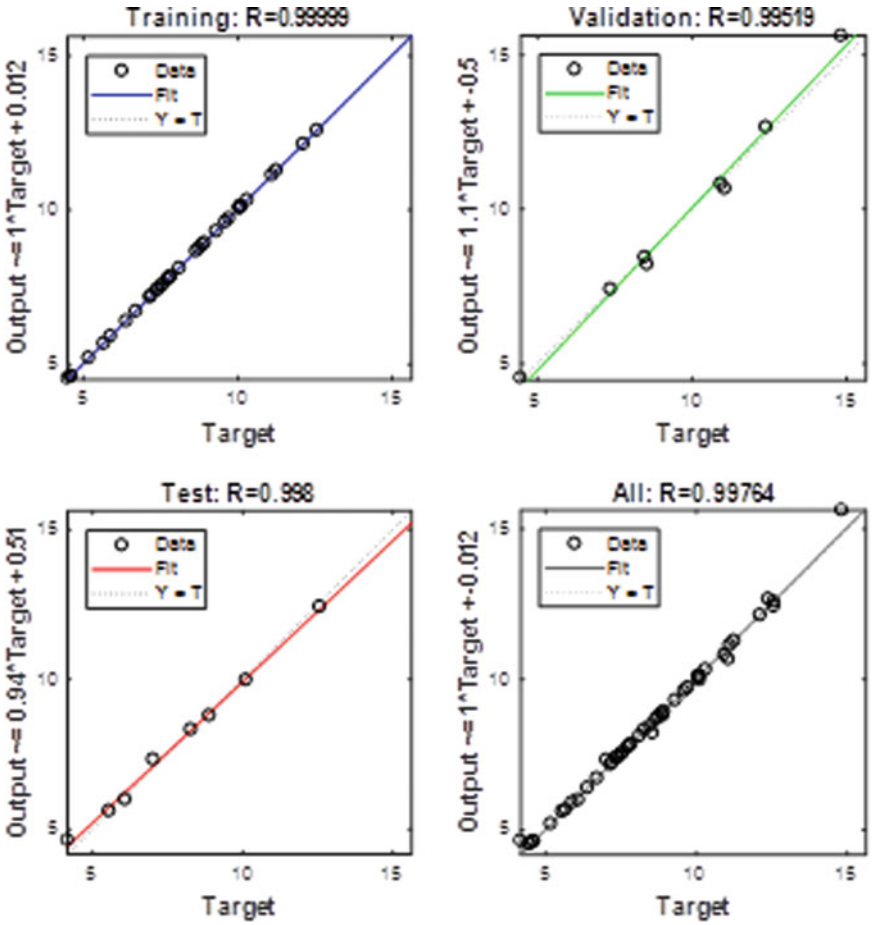

Fig. 15.6 Regression curve diagram in category I with LM algo with 10 hidden neurons

The model is analyzed with three different kinds of training algorithm such as Levenberg–Marquardt training algorithm, Bayesian Regularization training algorithm, and Scaled conjugate gradient training algorithm with MATLAB17. The analysis has been carried out by considering different numbers of data sets for training, validation and testing in two catagories. In each case a number of hidden neurons are varying for each of the three algorithms. For all cases performances with number of epochs, gradients, regression and error values are observed. The average value of performance and zero error point for all three training algorithms are calculated. RMPA is designed for different resonant frequencies within X band and simulated S11 parameters and maximum gains are observed.

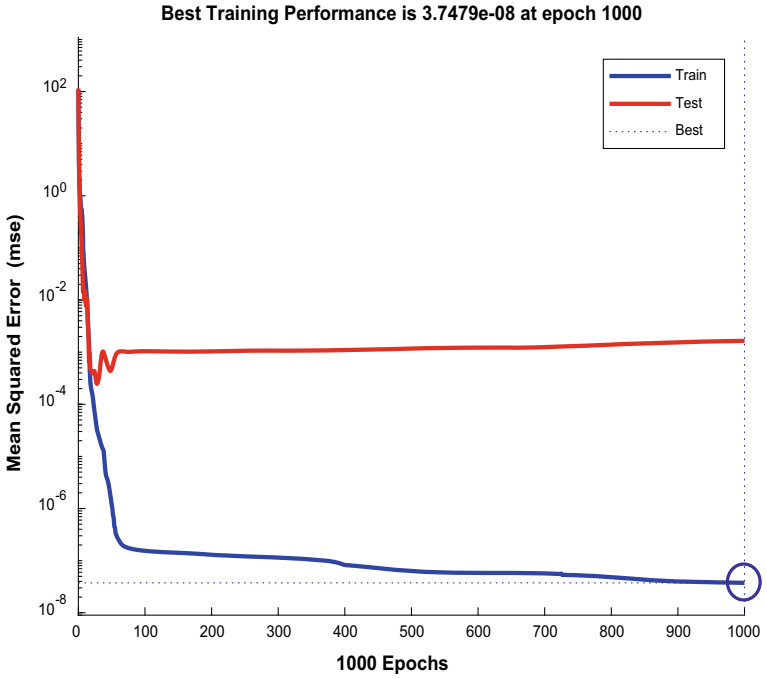

Fig. 15.7 Category I with BR algo with 10 hidden neurons

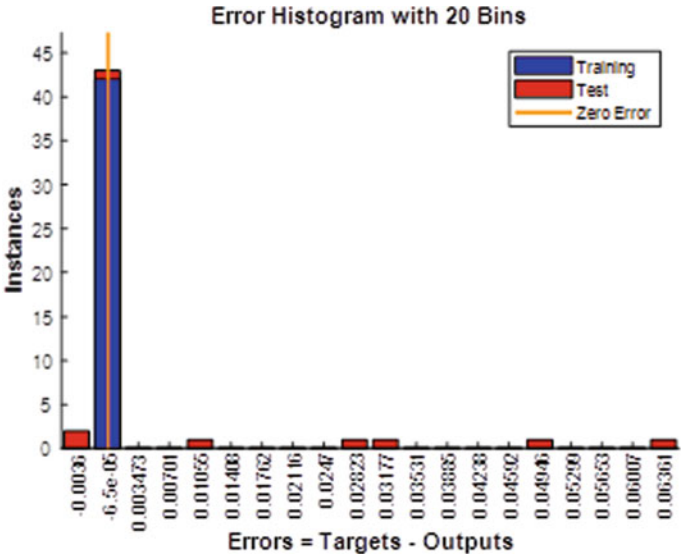

Fig. 15.8 Error histogram diagram in category I with BR algo with 30 hidden neurons

Table 15.4 Performances of category II

Types of training algorithm	Category-II Training data-15 samples Validation data-5 samples Testing data-5 samples							
	No of hidden neurons	performance	Average value (performance)	epoch	Gradient	Regression	Zero error point	Average zero error point value
Levenberg–Marquardt training algorithm	10	0.022	7.44	5	1.0471e-8	0.96206	0.01783	0.004138
	20	0.42491		3	8.8139e-14	0.9657	−0.04671	
	30	6.629		3	1.8385e-14	0.87859	−0.1849	
	40	6.9283		1	9.8957e-8	0.825	0.1782	
	50	23.1982		3	1.1145e-12	0.68386	0.05627	
Bayesian regularization training algorithm	10	2.4108e-9	8.53e-09	1000	2.6829e-6	0.99999	−0.00101	−9.5e-05
	20	7.0893e-10		1000	3.1521e-6	0.99998	0.002246	
	30	8.8733e-16		997	2.4692e-7	1	−0.00022	
	40	3.9526e-8		582	7.5711e-7	0.99998	−0.00179	
	50	5.5739e-16		705	7.6848e-6	0.99999	0.000298	
Scaled conjugate gradient training algorithm	10	0.79941	9.654902	8	0.4859	0.93222	0.06998	−6.13e-02
	20	9.5508		10	0.83774	0.74415	0.09682	
	30	2.4737		50	0.11884	0.93414	−0.0814	
	40	19.8755		10	1.678	0.78146	0.1796	
	50	15.5751		4	3.1467	0.30144	−0.5713	

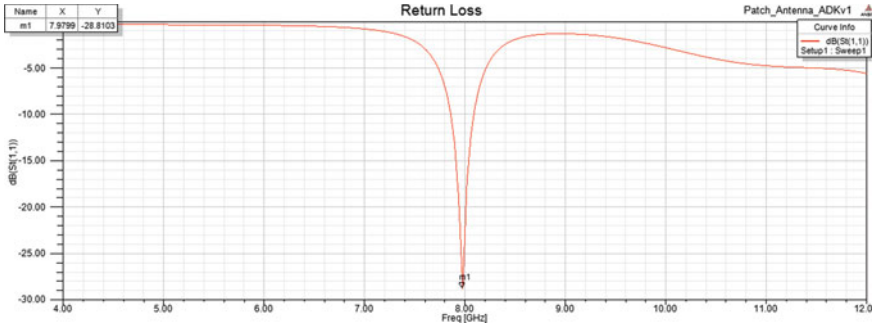

Fig. 15.9 S11parameter of RMPA at 8 GHz resonant frequency

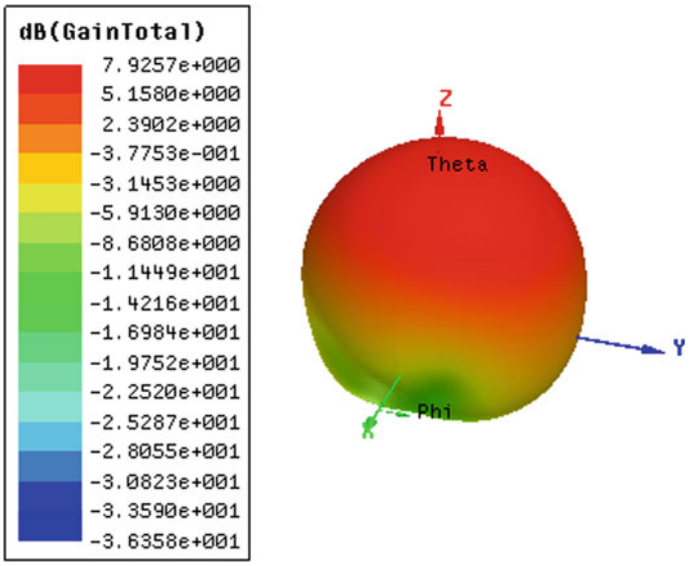

Fig. 15.10 Maximum gain of RMPA at 8 GHz resonant frequency

References

Ali Heidari A, Dadgarnia A (2011) Design and optimization of a circularly polarized microstrip antenna for GPS applications using ANFIS and GA, communication research laboratory. Yazd University, IEEE

Bisht N, Malik PK (2022) Adoption of microstrip antenna to multiple input multiple output microstrip antenna for wireless applications: a review. In: Singh PK, Singh Y, Chhabra JK, Illés Z, Verma C (eds) Recent innovations in computing. lecture notes in electrical engineering, vol 855. Springer, Singapore. https://doi.org/10.1007/978-981-16-8892-8_15

Güney K, Sagiroglu S, Erler M (2001) Generalized neural method to determine resonant frequencies of various microstrip antennas. Int J RF Microwave Comput Aided Eng 12(1):131–139

Haykin S, Neurais R (2001) Princípios e prática, Bookman, 2nd Ed

Jain SK, Sinha SN, Patnaik A (2009) Analysis of coaxial fed dual patch multilayer X/Ku band antenna using artificial neural networks. In: World congress on nature & biologically inspired computing (NaBIC), pp 1111–1114

Kala P, Saxena R, Kumar M, Kumar A, Pant R (2013) Design Of rectangular patch antenna using MLP artificial neural network. J Glob Res Comput Sci 3(5)

Karaboga D, Guney K, Sagiroglu S, Erler M (1999) Neural computation of resonant frequency of electrically thin and thick rectangular microstrip antennas. IEEE Proc Microw Antennas Propag 126(2), 155–159

Pandey U, Gupta NP, Malik P (2022) Review on miniaturized flexible wearable antenna for body area network. In: Singh PK, Singh Y, Chhabra JK, Illés Z, Verma C (eds) Recent innovations in computing. lecture notes in electrical engineering, vol 855. Springer, Singapore. https://doi.org/10.1007/978-981-16-8892-8_4

da Silva PL (2006) Modelagem de Superfícies Seletivas de Freqüência Antenas de Microstrip Utilizando Redes Neurais Artificiais. MSc thesis, Federal University of Rio Grande do Norte, Natal

Tamboli ZJ, Nikam PB (2013) Study of multilayer perceptron neural network for antenna characteristics analysis. Int J Adv Res Comput Sci Softw Eng 3(8)

Thomas JS, Thomas JS, Mary Neebha T, Nesasudha M (2014) Improvement of microstrip patch antenna parameters for wireless communication. IEEE Xplore Digit Libr

Turker N, Gunes F, Yildirim T (2004) Artificial neural design of microstrip antennas. Yildiz Technical University, Istanbul, Turkey

Turker N, Gunes F, Yildirim T (2006) Artificial neural design of microstrip antennas. Turkey J Elect Eng 14(3):445–453

Vishnoi V, Singh P, Budhiraja I, Malik PK (2023). Multiband dual-layer microstrip patch antenna for 5G wireless applications. In: Singh PK, Wierzchoń ST, Tanwar S, Rodrigues JJPC, Ganzha M (eds) Proceedings of third international conference on computing, communications, and cybersecurity. Lecture notes in networks and systems, vol 421. Springer, Singapore. https://doi.org/10.1007/978-981-19-1142-2_7

Chapter 16
Design and Analysis of Wideband Polarization Independent Absorber for L and S Band

Nitinkumar J. Bathani, Jagdishkumar M. Rathod, and Utkal Mehta

Abstract This chapter proposes a wideband polarization-independent microwave absorber for L and S frequency band applications. The structure comprises four resistors and 10*10 unit cells printed on an FR4 substrate with an ample airgap of 1 cm. The simulated structure consists of an ultra-wide bandwidth of 2.24 GHz with a fractional bandwidth of 95.8% occupied at above 90% absorptivity. The novelty of this structure is that it consists of wide bandwidth in TE and TM modes in long wave and short wave communication, which can be utilized in the LTE band and TV communication on satellite. The proposed structure is miniaturized to λ/12 in size and λ/16 in thickness. The results of a fabricated structure are also compared to the results of a simulation.

Keywords Absorber in L and S band · Wideband and polarization-independent absorber

N. J. Bathani (✉)
Department of Electronics and Communication Engg, Government Engineering College, Modasa, Gujarat, India
e-mail: nitinkumar@gecmodasa.org

J. M. Rathod
Electronics Department, B.V.M. Engineering College, Vallabh Vidhyanagar, Anand, Gujarat, India
e-mail: jmrathod@bvmengineering.ac.in

U. Mehta
Electrical and Electronics Engineering, The University of the South Pacific, Laucala Campus, Suva, Fiji Islands
e-mail: utkal.mehta@usp.ac.fj

P. K. Malik and P. N. Shastry (eds.), *Internet of Things Enabled Antennas for Biomedical Devices and Systems*, Springer Tracts in Electrical and Electronics Engineering,
https://doi.org/10.1007/978-981-99-0212-5_16

Introduction

Widespread research on metamaterial structures has been carried out due to their artificial properties, consisting of negative ϵ and μ, which causes advancement of the signal phase and an increment of evanescent waves towards the source. Victor Veselego was the first to represent the metamaterial property in 1968 (Veselago 1968). A great deal of research has been presented in the field of designing metamaterial absorbers. An absorber consists of a metal part with a single or multilayer dielectric material. Ultrathin, wideband, polarization independent, and oblique angle independent features are among the most recent metamaterial absorber developments (Tak and Choi 2016; Zhang et al. 2019). It is now well understood that frequency-selective absorbers can absorb electromagnetic waves within a specific frequency range. So it is highly applicable to aircraft, RF harvesting, radar, camouflage, solar cells, RFID tags, satellite communication, antennas, filters, cell phones, Wi-Fi devices, etc (Dincer et al. 2014; Liu et al. 2020; Amer et al. 2020; Bashiri et al. 2017).

An Eq. (16.1) can be used to calculate the absorptivity of a frequency-selective absorber (Munk 2000).

$$A(\omega) = (1 - T(\omega) - R(\omega)) * 100\% \tag{16.1}$$

In which $T(\omega)$ and $R(\omega)$ can be represented as transmissive and reflective coefficients respectively, which can be given as Eqs. (16.2) and (16.3)

$$T(\omega) = (S_{11})^2 \tag{16.2}$$

$$R(\omega) = (S_{21})^2 \tag{16.3}$$

Because most absorbers have a copper-backed ground plane, there is no transmission. The reflection coefficient can be used to calculate the absorptivity of a structure with a ground plane. Minimization of the reflection coefficient can increase the absorption rate. The suitable value of the reflection coefficient is less than − 10 dB for any structure which can work as a frequency-selective absorber, providing the absorptivity is greater than 90%.

It is a narrow band absorber with a single resonant frequency if the inductive impedance of the dielectric substrate with the ground plane may be equal and opposite to the capacitive impedance of the frequency selective surface. Suppose substrate thickness is increased than the quarter wavelength of operating frequency. In that case, the capacitive impedance of dielectric substrate with the ground plane can be equal and opposite to the inductive impedance of frequency selective surface (FSS). It causes a second resonance in which the input impedance of the dielectric substrate is infinite, consisting of pure real impedance with zero imaginary impedance of the FSS structure. This is the fundamental property of the wideband absorber (Costa et al. 2016). The Impedance of a frequency-selective absorber (FSA) can be determined by Eq. (16.4)

$$Z(\omega) = \eta\left(\frac{1 + R(\omega)}{1 - R(\omega)}\right) \tag{16.4}$$

It shows that minimizing the reflection coefficient at the resonance frequency causes the input impedance of FSA to be equal to η. So, the input impedance of the FSA structure compensated with the intrinsic impedance of free space causes the highest absorptivity at the particular frequency (Malik et al. 2022; Malik et al. 2021; Rahim and Malik 2020).

Intrinsic impedance can also be determined by Eq. (16.5)

$$\eta = \sqrt{\frac{\mu_0 \mu_r}{\varepsilon_0 \varepsilon_r}} \tag{16.5}$$

Depending on the permittivity and permeability of the structure, a wave is an incident, transmitted, or absorbed (Tirkey and Gupta 2019). The absorption rate of the structure can also be determined by Eq. (16.6)

$$A(\omega) = \frac{1}{2}\sigma E^2 + \frac{1}{2}\omega\varepsilon_0\varepsilon_r E^2 + \frac{1}{2}\omega\mu_0\mu_r H^2 \tag{16.6}$$

Equation (16.6) represents that the dielectric material with minimum conductivity absorptivity of the proposed structure can be increased by the stronger electric field and anti-parallel magnetic field at the resonant frequency.

Design Parameters

To occupy a more significant electrical metallic length inside the 2 cm unit cell structure is simulated. A complete structure can occupy 10*10 unit cells. The structure is engraved in a 0.5 mm FR_4 substrate comprising a dielectric constant of 4.4 with a loss tangent (tanδ) of 0.02. The structure also inhabits a 1 cm air gap for the betterment of bandwidth (Lan et al. 2018). The Optimized parameter in HFSS, as shown in Fig. 16.1, is as follows.

$L = 20$ mm, $a = 3.5$ mm, $b = 5.1$ mm, $c = 0.3$ mm, $d = 0.3$ mm, $x = 1.9$ mm, $h = 1$ cm and $h_1 = 0.05$ cm. For the higher absorption rate, four resistors of 220 Ω have been chosen. The unit cell size is 2 cm, which is miniaturized to λ/12 at the highest operating wavelength. The thickness of the proposed structure is 1.5 cm, miniaturized to λ/16 at the highest operating wavelength.

The solving method for the simulation is the finite element method calculated by HFSS software. This design simulates the unit cell with master and slave boundary and the absorber's parallel configuration to perform its periodicity. It is excited by the floquet port in the perpendicular propagating direction.

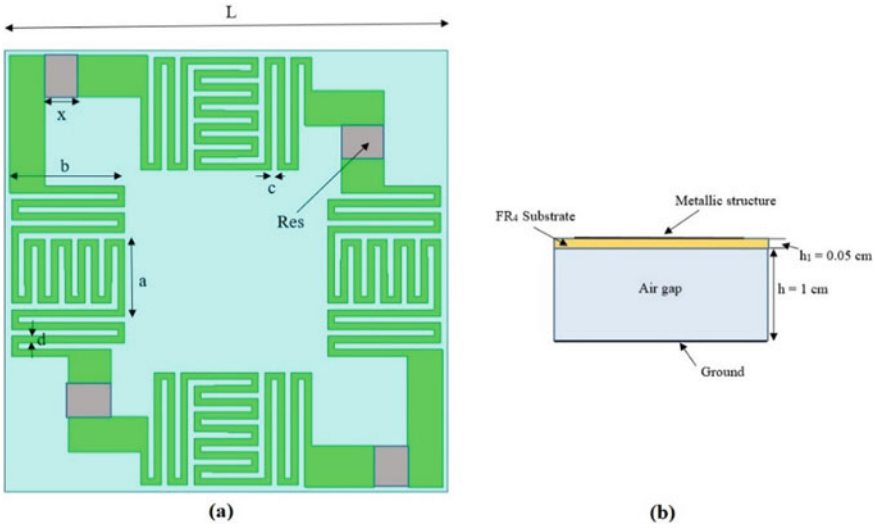

Fig. 16.1 (**a**) Front view. (**b**) Side view of LSMA structure

Simulated Result Discussion

The simulated result of absorptivity, which can be evaluated from the return loss derived from Eq. (16.1), is shown in Fig. 16.2 under TE and TM configuration. It offers a slight deviation of bandwidth concerning both configurations. The proposed structure works from 1.22 to 3.46 GHz with fractional bandwidth of 96% in TE configuration and 1.03 GHz to 3.34 GHz with fractional bandwidth of 105% in TM configuration. The input impedance can be evaluated and represented in Fig. 16.3. The real and imaginary parts of the input impedance can be compatible with free space impedance and zero value respectively at the operating bandwidth.

Absorption Mechanism of the Proposed Structure.

Wideband absorber working on L and S-band, more considerable electrical length with interspacing is simulated to provide the LC resonator. The Resistor can also be implanted in the LC Resonator structure for the absorption mechanism in terms of heat. So, the RLC circuit is a vital parameter for providing the higher absorptivity of a proposed structure. The long metallic structure is comprised of four-cornered resistors in the unit cell. The Large electrical length of the proposed structure is 6.81 cm. It can operate the highest wavelength of 27.24 cm (current length = $\lambda_h/4$), exciting the frequency of 1.1 GHz, which can compare with simulated 1.22 GHz in TE configuration. Multiple variations in the metallic structure are the main reason for the

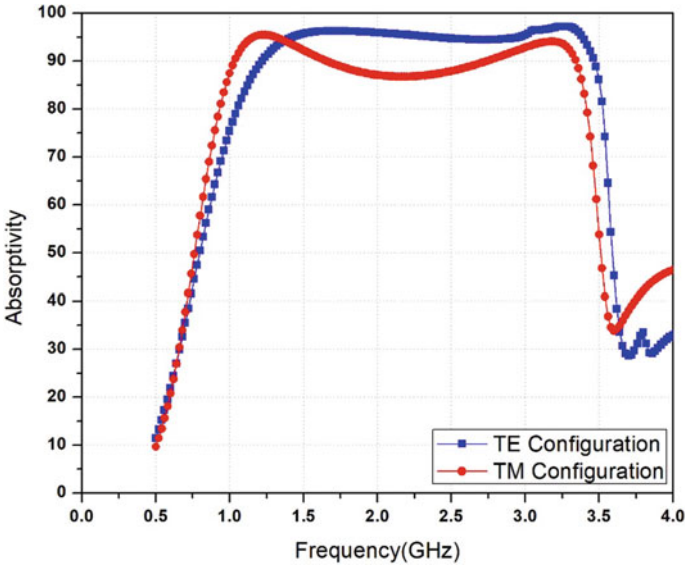

Fig. 16.2 Simulated absorptivity versus frequency under TE and TM configuration

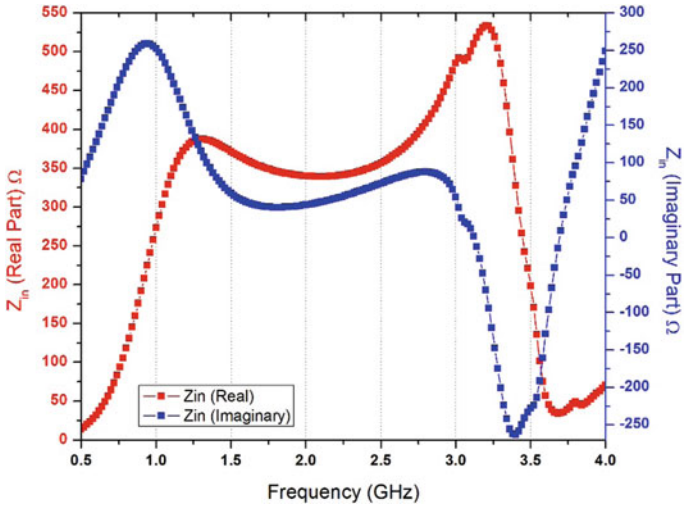

Fig. 16.3 Input impedance (Z_{in}) of the proposed structure

broader bandwidth in L and S-band. The lowest wavelength of the proposed structure can be determined from the unit cell structure, which is 2 cm which can be excited at the lowest wavelength of 8 cm (current length = $\lambda_l/4$), working at a frequency of 3.75 GHz, which can compare to simulated 3.46 GHz in TE configuration. The

interspacing between the metallic strip constructions determines the capacitance of the proposed structure.

Parameter Variation of the Proposed Structure

We can analyze the proposed structure after simulating this variation to observe the effect of physical and electrical parameters on absorption property. Airgap is a mandatory physical parameter of increasing the bandwidth represented in Fig. 16.4a, which shows that an increment in the height of airgap increases the absorptivity over a broad bandwidth. Increasing bandwidth increases the thickness of the overall structure with a low effective dielectric constant, causing more substantial wave confinement, resulting in matching the network and increasing bandwidth. So 1 cm of optimum air gap has been chosen for this proposed structure. The absorptivity of the proposed structure for multiple resistor values is shown in Fig. 16.4b. It shows that the absorptivity of the proposed structure is directly proportional to resistance having a value less than 220 Ω. However, for a resistance value of more than 220 Ω, the bandwidth of the proposed structure is reduced. Zero resistance loses absorptivity. So, the distributed and lumped RLC circuit parameter is an effective tool for deciding the absorptivity of the absorber. The resistor is used to determine the absorption rate, while the LC configuration decides the operating bandwidth of the proposed structure. An Optimized 220 Ω resistor is chosen for this structure.

The proposed structure is simulated in the θ and Φ plane for the optimum TE and TM configuration variation to determine the oblique incident angle independence. Magnetic and electric field components parallel to the incident surface in the TE and TM configuration, respectively. Figures 16.5a and b depict that the proposed structure is oblique angle independent up to 30° in TE and TM configuration.

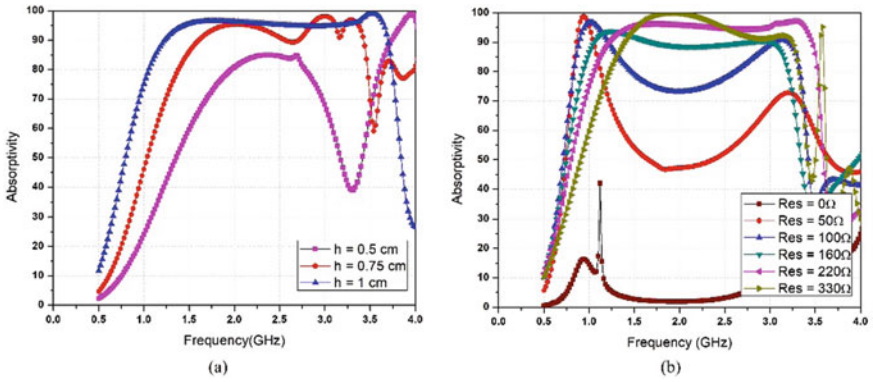

Fig. 16.4 Absorptivity response for (**a**) air gap variation (**b**) Resistor variation

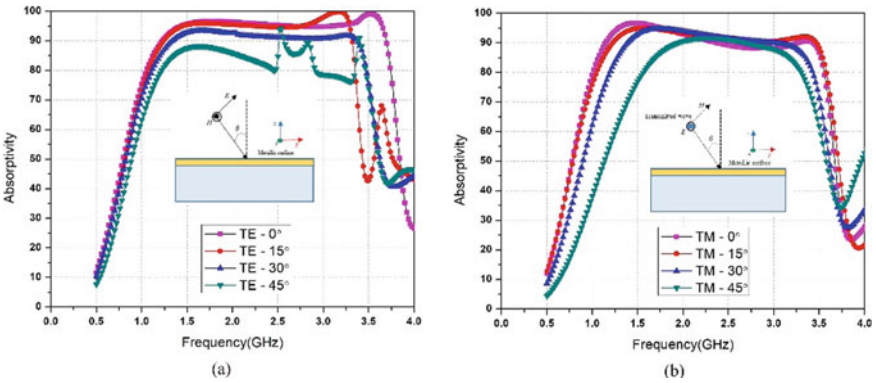

Fig. 16.5 Absorptivity for oblique angle incidence in (**a**) TE configuration (**b**) TM configuration

Fabricated Design with Experimental Verification

The proposed structure is fabricated on a 0.5 mm FR_4 substrate. The ground plane with copper is attached with the 1 cm airgap to enhance bandwidth, as shown in Fig. 16.6. 10*10 unit cells are fabricated on the dielectric substrate, so the proposed structure's total size is 20 cm*20 cm. The Transceiver ridged horn antenna was connected with the Anritsu vector network analyzer MS46322B-020 working from 1 MHz to 20 GHz. The proposed structure is positioned in an anechoic chamber at the far-field of the horn antenna, as shown in Fig. 16.7. First, the return loss with the copper plane can be measured, offering the maximum reflection coefficient. The spacer is used to space out.

the absorber on this copper plane to determine the reflection coefficient while reducing the S11 in the operating frequency. Subtracting these values from the previous value accessed from the copper plane will give the measured absorptivity of the proposed structure. Figure 16.8 depicts the measured results of the fabricated structure, representing that the operating frequency with absorptivity greater than

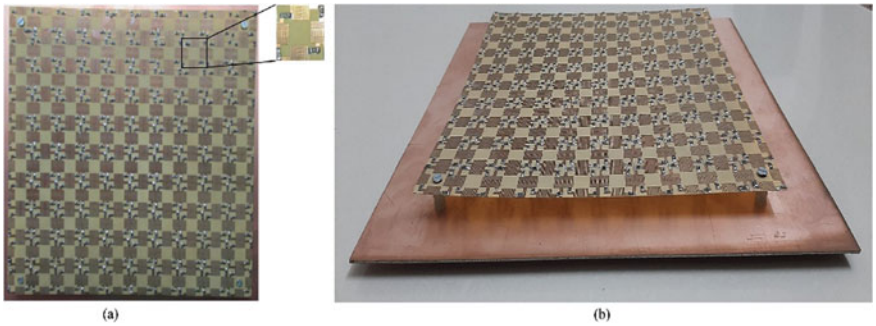

Fig. 16.6 Fabricated proposed structure (**a**) front view. (**b**) Side view

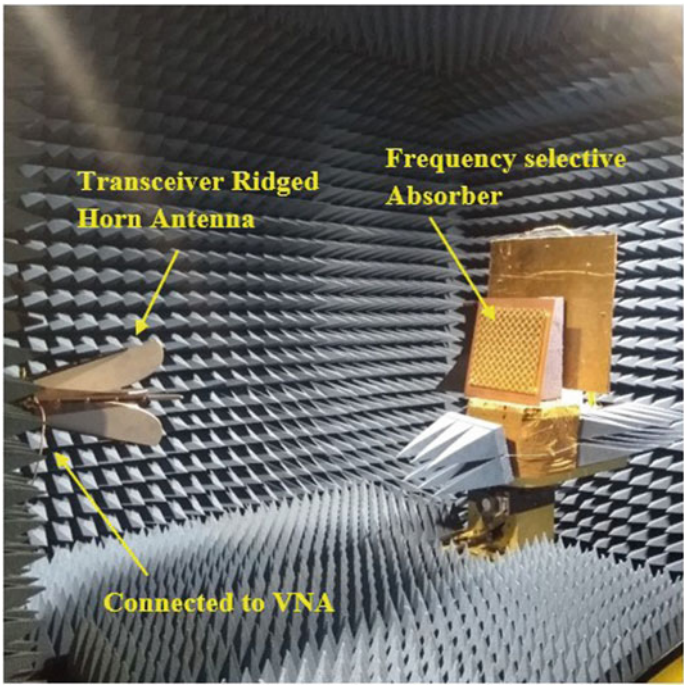

Fig. 16.7 Measurement Setup in the anechoic chamber

90% (Return loss is less than −10 dB) is 1.2–3.22 GHz, which is evaluated as 90% bandwidth of the proposed structure. Lossy dielectric with a tolerance of lumped resistor in the fabrication causes the measurement error from the simulated error.

Conclusion

The Novel wideband absorber is designed for L and S bands. The Proposed structure is experimentally working in the bandwidth of 90% with absorptivity greater than 90%. The value of S_{11} is less than −10 dB in this operating band. Because of its physical symmetry, the proposed structure has a minimum deviation of bandwidth working in TE ($\Phi = 0$ plane) and TM ($\Phi = 90$ plane) configuration. It also provides the miniaturization of $\lambda/12$ and $\lambda/16$ in length and thickness, respectively. So this type of structure is applicable for Radar and RF harvesting for low-power sensor networks.

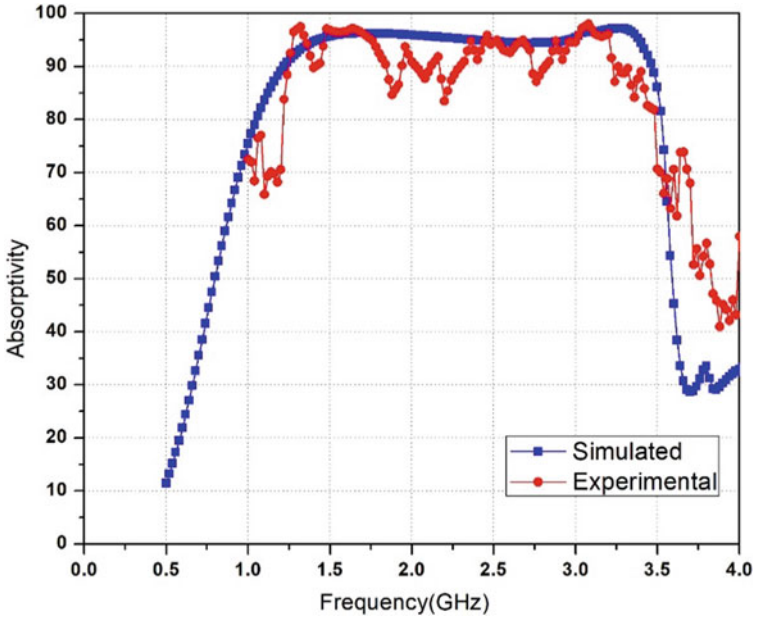

Fig. 16.8 Measurement result compared with the simulated result

References

Amer AAG, Sapuan SZ, Nasimuddin N, Alphones A, Zinal NB (2020) A comprehensive review of metasurface structures suitable for RF energy harvesting. IEEE Access 8:76433–76452

Bashiri M, Ghobadi C, Nourinia J, Majidzadeh M (2017) WiMAX, WLAN, and X band filtering mechanism: simple-structured triple-band frequency selective surface. IEEE Antennas Wireless Propag Lett 16:3245–3248

Costa F, Monorchio A, Manara G (2016) Theory, design and perspectives of electromagnetic wave absorbers. IEEE Electromagnet Compat Mag 5(2):67–74

Dincer F, Akgol O, Karaaslan M, Unal E, Sabah C (2014) Polarization angle independent perfect metamaterial absorbers for solar cell applications in the microwave, infrared, and visible regime. Progress Electromagnet Res 144:93–101

Lan J, Cao X, Gao J, Cong L, Wang S, Yang H (2018) Design of miniaturized wideband microwave absorber loaded with lumped resistance. Radioengineering 27(3):746–752

Liu Y, Jia Y, Zhang W, Li F (2020) Wideband RCS reduction of a slot array antenna using a hybrid metasurface. IEEE Trans Antennas Propag 68(5):3644–3652

Malik PK, Kumar P, Kumar S, Singh DK (2021) Smart antennas: recent trends in design and applications. Bentham Science, Sharjah, United Arab Emirates. ISSN: 2717–5421 (Print), ISSN: 2717–543X (Online), ISBN: 978–1–68108–860–0 (Print). https://doi.org/10.2174/978168108859412102 01

Malik P, Lu J, Madhav BTP, Kalkhambkar G, Amit S (eds) (2022) Smart antennas: latest trends in design and application. Springer. ISBN 978-3-030-76636-8. Dhttps://doi.org/10.1007/978-3-030-76636-8

Munk BA (2000) Frequency selective sufaces: theory and design. JohnWiley and Sons Inc

Rahim A, Malik PK (2020) Design methodologies and tools for 5G network development and application, Ch 10: analysis and design of planner wide band antenna for wireless communication applications: fractal antennas, vol 13. IGI Global USA, pp 196–208. https://doi.org/10.4018/978-1-7998-4610-9.ch010

Tak J, Choi J (2016) A wearable metamaterial microwave absorber. IEEE Antennas Wirel Propag Lett 16:784–787

Tirkey MM, Gupta N (2019) Electromagnetic absorber design challenges. IEEE Electromagnet Compat Mag 8(1):59–65

Veselago VG (1968) The electrodynamics of substances with simultaneously negative values of ε and μ. Sov. Phys. Uspekhi 509

Zhang GW, Gao J, Cao XY, Li SJ, Yang HH (2019) Wideband miniaturized met amaterial absorber covering L-frequency range. Radioengineering 27(1):154–160

Chapter 17
An Efficient Non-invasive Blood Glucose Measurement Using Microwave Antennas

R. Ramesh, E. Udayakumar, R. Sanjeev Kumar, and Ahmed J. Obaid

Abstract Medical technology is advancing very fast, as technology advances there is improvement in both diagnostic techniques and equipment design. Non-invasive diagnosis of biological data through microwave techniques has become the recent study pursued by researchers to help the medical industry, of which non-invasive glucose measurement has developed into a distinct class of diagnosis. In this work effort is made to use the microstrip antenna for non-invasive measurement of blood glucose in human at 2.4 GHz. The resonance frequency of the antenna undergoes a shift of 8 dB for the change in the glycaemia level in human tissue. This report is a part of work for the development of real-time painless glucometer.

Keywords Blood glucose · Diabetes mellitus · Microwave antenna · Non-invasive measurement

Introduction

Human body's capacity to utilize the energy found in food is significantly influenced by the disability in pancreas called Diabetes Mellitus. There are three major kinds of diabetes: Type 1 diabetes, Type 2 diabetes, and Gestational diabetes. The characterization is based on the causing agent of diabetes but the problem is same in all

R. Ramesh (✉)
Department of ECE, PSG College of Technology, Coimbatore, India
e-mail: vmramesh1993@gmail.com

E. Udayakumar
Department of ECE, KIT-Kalaignarkarunanadhi Institute of Technology, Coimbatore, India

R. S. Kumar
Department of Physics, Coimbatore Institute of Technology, Coimbatore, India

A. J. Obaid
Department of Computer Science, Faculty of Computer Science and Mathematics, University of Kufa, Najaf, Iraq
e-mail: ahmedj.aljanaby@uokufa.edu.iq

P. K. Malik and P. N. Shastry (eds.), *Internet of Things Enabled Antennas for Biomedical Devices and Systems*, Springer Tracts in Electrical and Electronics Engineering,
https://doi.org/10.1007/978-981-99-0212-5_17

three. In a normal adult, after consumption of food, the human body breaks down the sugars and starches in the food into a special sugar called glucose allows in the blood stream. Glucose is the fuel required by every cell in the body, but cells need the assistance of a hormone called "insulin" (secreted by pancreas) to take in the glucose and use it for energy. Hence, nonappearance or inadequate creation of insulin, or the incapable nature of the body to appropriately utilize insulin causes diabetes. Because of diabetes the glucose stays in the blood stream itself and on further intake of food the blood-glucose level increases. Significant levels of blood glucose damage the small veins in kidneys, heart, eyes, or the sensory system.

That is the reason diabetes—particularly whenever left untreated—can in the long run cause coronary illness, stroke, kidney disease, blindness and nerve damage in the feet. The control of normal blood glucose levels in diabetic patients includes persistent observing going either from week after week on several times each day itself. The current solid innovation is the finger-prick glucose meter or glucometer. The patient punctures his skin with a lancet and afterward presses his finger to gather a huge drop of blood on a test strip. The strip is then embedded into the glucometer for estimation as shown in Fig. 17.1.

In spite of the fact that the current glucometers are powerful in estimating blood glucose, it is an excruciating long-haul strategy. Consequently, huge exploration is completed towards "non-obtrusive" techniques for estimating glucose. The striking ones are optical investigation, temperature examination, and electromagnetic investigation of tissue. Non-intrusive glucose estimation kills the pricking experience (So et al. 2012), danger of contamination, and harm to finger tissue. The non-intrusive idea was imagined numerous many years back be that as it may, the greater part of the non-obtrusive advancements are still in their beginning phases of improvement. Numerous non-intrusive advances have been portrayed in the writing, and there is an expanding number of late exploration results. Figure 17.2 shows the classification of Non- Invasive Glucose Measurement Methods (So et al. 2012). This article is divided

Fig. 17.1 Invasive glucometer showing blood collected in the test strip after painful prick

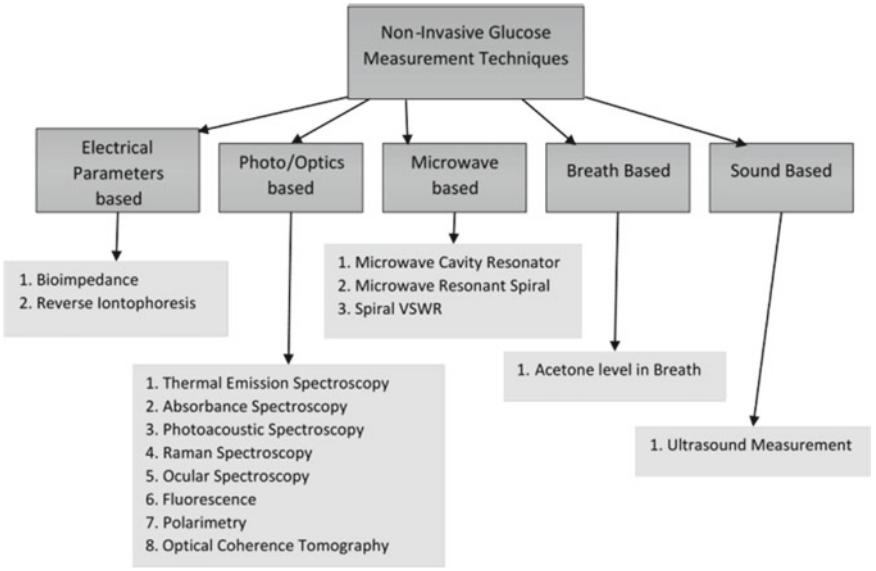

Fig. 17.2 Classification of non-invasive glucose measurement techniques

into three sections viz section "Dielectric Properties of Blood", section "Experiment Setup", and section "Result Analysis".

Dielectric Properties of Blood

Gabriel et al. (1996b) conducted a series of experiments to analyse the dielectric assets of human tissues based on the interaction of tissues with electromagnetic radiation. The research findings were beneficial in creating anatomically similar human EM-Models for experimental simulations known as the Cole–Cole model (Sidley and Venkataraman 2013). Blood is the fluid tissue in human body which is an intricate suspension of cells, proteins, hormones, glucose, and different particles in water. Its permittivity is recurrence subordinate, as affected by every one of its constituents. Further analysis reveal that permittivity is affected by the amount of glucose.

Hayashi et al. (2003) observed the permittivity of red blood cells affected by the concentration changes in blood glucose. The result was utilized for the development of a non-invasive glucometer.

Park et al. (2003) assembled a needle-type cell to fit over the tail of a hamster (rodent like rat) and the connection among glucose and dielectric consistent of blood was illustrated. This was the proof of in-vivo correlation between blood permittivity and glucose level.

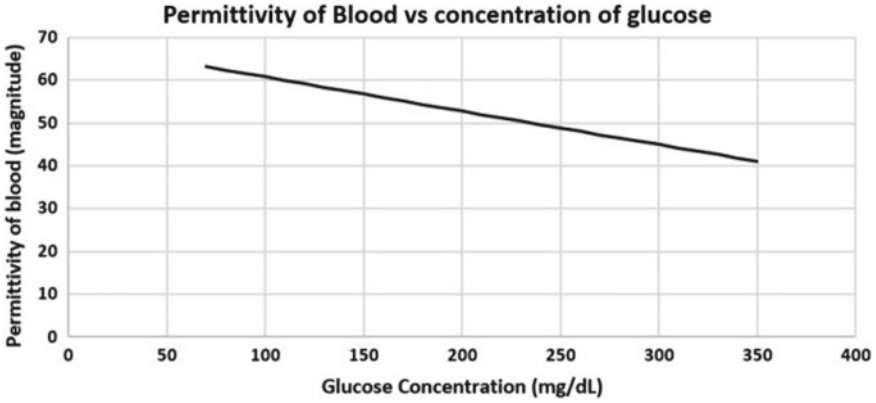

Fig. 17.3 Modified Cole–Cole plot showing the inverse relation of permittivity and blood glucose

Recent findings by Freer and Venkataraman (2011) presented a Modified Cole–Cole model which represents the parametric model of blood glucose and permittivity change. The modified cole–cole model is used for studying the variation in the permittivity of blood as a purpose of glucose attention g and angular frequency at 2.45 GHz frequency, where 'g', is the glucose concentration in mg/dL. From the above studies it is therefore found that the permittivity of human blood decreases with the increase in glucose concentration. An inverse proportional relation is well established. Hence a microwave antenna could be used to determine the glucose fluctuations based on the antenna's response to permittivity change in its near-field (Wang and Peng 2019) (Fig. 17.3).

The prime factor to decide for the design of antenna is the frequency (Kaur et al. 2019) of operation. From the literature studies on the dielectric properties of biological tissues it is found that below 100 MHz the rise in permittivity is exponential and would cause complete reflection of the microwave energy and it is not a good option. In accordance with the works done by Gabriel and Gabriel (Gabriel et al. 1996c) the penetration depth for blood is achieved in between 300 MHz and 4 GHz. At the ISM band centre frequency of 2.45 GHz the penetration achieved is 2 cm (Jafari et al. 2016). Thus, it can be used to leverage the license free spectrum usage as well as the required minimum penetration depth to pick up the changes in blood permittivity.

In order to respond for the changes, blood must be within the reactive near-field zone of the antenna which is within 9 mm.

Reactive Near field at 2.45 GHz.

$$\mathrm{R} \;=\; 0.62\,\mathrm{sqrt}\left(\mathrm{D}^3/\lambda\right) \;=\; 0.0092\,\mathrm{m}\ \text{or}\ 9.2\,\mathrm{mm}.$$

Experiment

A rectangular patch antenna with resonant frequency 2.45 GHz in free space was designed. The antenna was placed 1 mm above the wrist of the subject and measurements were observed for the shift in the resonant frequency. Two sets of readings were made on the subject viz. pre-prandial and postprandial test (Andrés-Sánchez 2018). For pre-prandial test, the human subjects were made to remain in fasting for 8 h and the blood glucose was estimated utilizing ONETOUCH glucometer and the thunderous recurrence of the radio wire was estimated using a network analyser. Similarly for the postprandial test the measurements were taken half-an-hour after the consumption of food by the subjects.

Results and Discussion

The resonant frequency of the antenna in free space is shown in Fig. 17.4. The antenna radiates at 2.4 GHz as desired (Fig. 17.5).

When pressed gently above the human subject's arm the following results were obtained. The resonant frequency of the antenna shifts rightward with 8 dB change when the blood glycaemia increases and shifts leftward on decrease (Fig. 17.6).

The graphs in Figs. 17.7 and 17.8 depict the variation of the resonant frequency of the antenna in accordance with the blood glucose measured using a traditional invasive glucometer. The shifts are appreciable for a large magnitude of variation

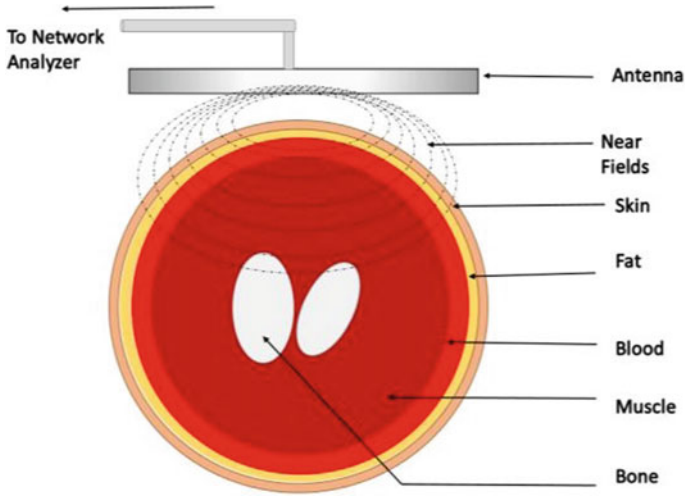

Fig. 17.4 Cross section of human hand

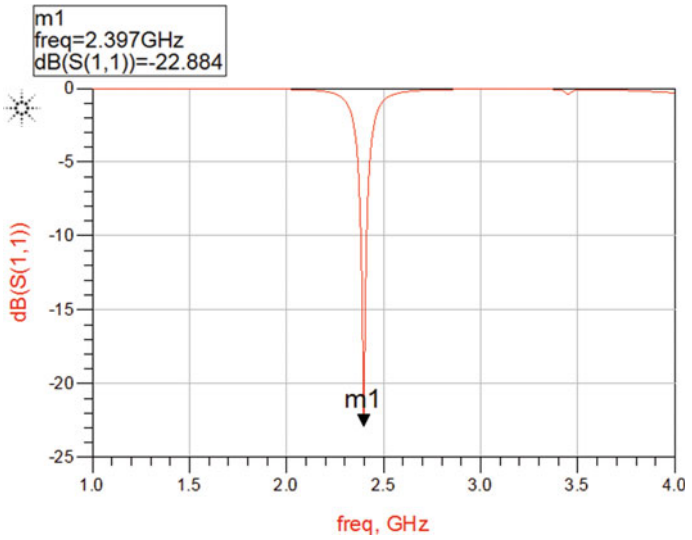

Fig. 17.5 Free-space resonance frequency of the antenna

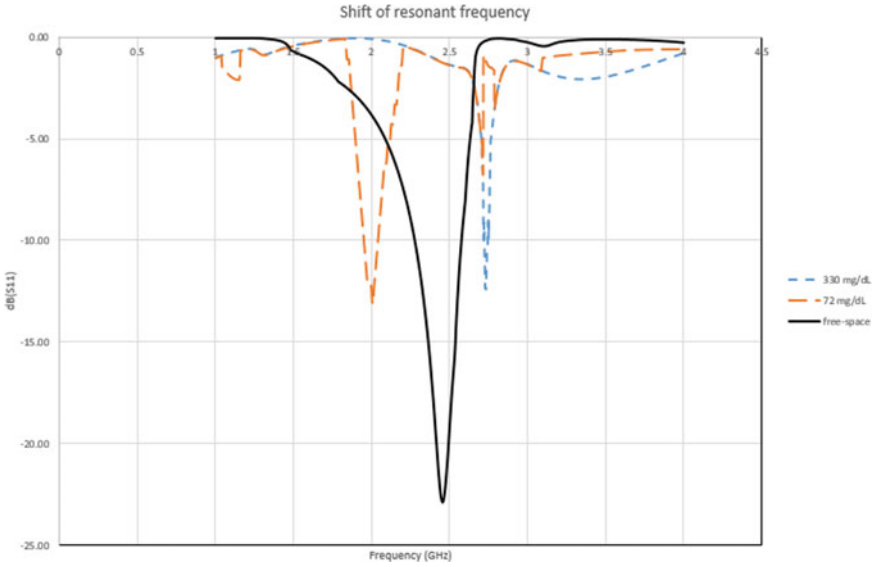

Fig. 17.6 Observed shift in the resonant frequency of the antenna while

in glucose concentration. The measurement systems have to be calibrated for more human volunteers for accuracy of prediction.

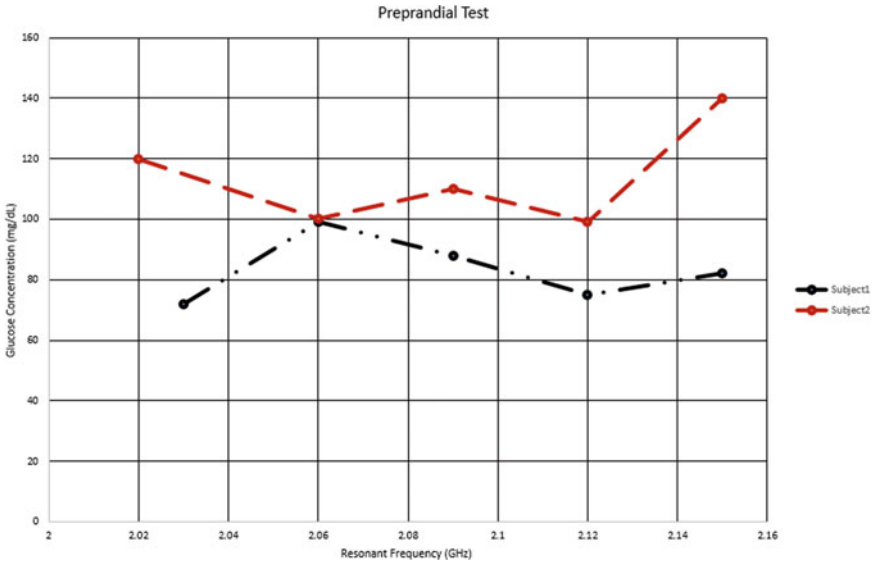

Fig. 17.7 Preprandial test results of the human subjects

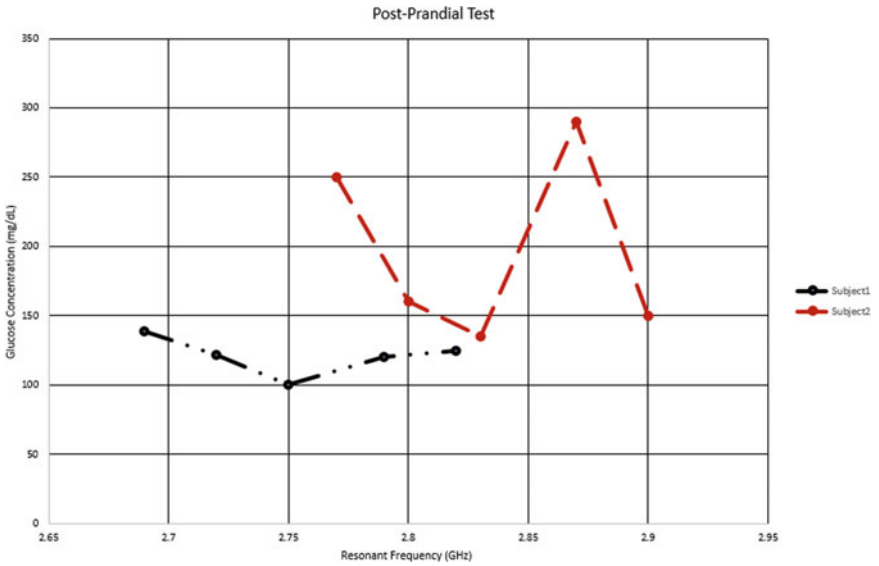

Fig. 17.8 Postprandial test results of the human subjects

Conclusion

Based on the in-vitro experiments on human subjects the antenna proves to be a good microwave sensor to track the changes in blood glucose. A new calibration and estimation methodology has to be developed for the calculation of glucose concentration based on the degree of shift in the resonant frequency.

Future Work

To develop a complete RF system for non-invasive glucose estimation based on the shift in resonant frequency as the fundamental principle.

References

Adhyapak A, Sidley M, Venkataraman J (2014) Analytical model for real time, non-invasive estimation of blood glucose level. In: 2014 36th annual international conference of the IEEE Engineering in Medicine and Biology Society

Andrés-Sánchez J (2018) Pricing European options with triangular fuzzy parameters: assessing alternative triangular approximations in the Spanish stock option market. Int J Fuzzy Syst 20:1624–1643

Freer B, Venkataraman J (2011) Feasibility of non-invasive blood glucose monitoring: in-vitro measurements and phantom models. In: IEEE antennas and propagation society international symposium, Spokane, July, pp 603–606

Gabriel C, Gabriel S, Corthout E (1996a) The dielectric properties of biological tissues: I. Literature survey. Phys Med Biol 41(11):2231

Gabriel S, Lau RW, Gabriel C (1996b) The dielectric properties of biological tissues: II. Measurements in the frequency range 10 Hz to 20 GHz. Phys Med Biol 41(11):2251

Gabriel S, Lau RW, Gabriel C (1996c) The dielectric properties of biological tissues: III. Parametric models for the dielectric spectrum of tissues. Phys Med Biol 41(11):2271

Hady KKA, Salam RAA, Hadad GM, Hameed EAA (2020) Simultaneous HPLC determination of vildagliptin, ampicillin, sulbactam and metronidazole in pharmaceutical dosage forms and human urine. J Iran Chem Soc

Hanna J, Costantine J, Kanj R, Eid A, Tawk Y, Ramadan AH (2018) Electromagnetic based devices for non-invasive glucose monitoring. In: 2018 IEEE conference on antenna measurements & applications (CAMA)

Hayashi Y, Livshits L, Caduff A, Feldman Y (2003) Dielectric spectroscopy study of specific glucose influence on human erythrocyte membranes. J Phys D Appl Phys 36(4):369–374

Jafari H, Bateni S, Daneshvar P et al (2016) Fuzzy mathematical modeling approach for the nurse scheduling problem: a case study. Int J Fuzzy Syst 18:320–332

Jean BR (2008) A microwave frequency sensor for non-invasive blood-glucose measurement. In: 2008 IEEE sensors applications symposium

Kaur A, Kumar A, Appadoo SS (2019) A note on "approaches to interval intuitionistic trapezoidal fuzzy multiple attribute decision making with incomplete weight information." Int J Fuzzy Syst 21:1010–1011

Marattukalam F, Sawant D (2017) Efficient microstrip ring resonator antennas for glucose measurement. In: 2017 international conference on wireless communications, signal processing and networking (WiSPNET), Chennai, pp 1106–1110

Nakamura M, Tajima T, Seyama M, Waki K (2018) A noninvasive blood glucose measurement by microwave dielectric spectroscopy: drift correction technique. In: 2018 IEEE international microwave biomedical conference (IMBioC), Philadelphia, PA, pp 85–87

Park JH, Kim CS, Choi BC, Ham KY (2003) The correlation of the complex dielectric constant and blood glucose at low frequency. Biosens Bioelectron 19(4):321–324

Sidley M, Venkataraman J (2013) Calibration for real-time noninvasive blood glucose monitoring. Masters' thesis, Rochester Institute of Technology

So C-F, Choi K-S, Wong TKS, Chung JWW (2012) Recent advances in noninvasive glucose monitoring. Med Dev Evid Res 45–47

Venkataraman J, Freer B (2011) Feasibility of non-invasive blood glucose monitoring: In-vitro measurements and phantom models. In: 2011 IEEE international symposium on antennas and propagation (APSURSI)

Wang G, Peng J (2019) Fuzzy optimal solution of fuzzy number linear programming problems. Int J Fuzzy Syst 21:865–881

Yilmaz T et al (2019) Radio-frequency and microwave techniques for non-invasive measurement of blood glucose levels. Diagnostics (Basel) 9(1):6

Chapter 18
Role of Antennas in Biomedical Applications for ISM/MICS/MED-RAD Bands Using Wireless Technology

Parminder Kaur, Manish Sharma, and Shivani Malhotra

Abstract In recent years, where microwave sensors have been deployed for communication, navigation, agriculture, remote sensing, etc. they are also being extensively used for biomedical applications. As people are getting more aware of health issues so there is a huge demand to develop healthcare devices for the early detection as well as treatment of disease. Nowadays microwave antenna sensors are used for continuous monitoring of glucose levels of the human body, blood pressure, and body temperature monitoring, in pacemakers to manage irregular heartbeats, in defibrillators, and some other physiological parameters. This chapter provides an overview of the requirements, designs, techniques, human body effects, and testing of antennas for biomedical applications in ISM, MICS, and MED-RAD bands. Moreover, the domains and standards used for body-centric networks in the present scenario have also been discussed.

Keywords Body centric networks · Implantable antennas · Biomedical · ISM · MICS

Introduction

Advancement in wireless technologies has led to the miniaturization of devices used in a plethora of daily life applications including entertainment, sports, defense, disaster management, and healthcare services (Farooq and Rather 2022). Biomedical applications hold their existence and importance as they serve to improve and save one's life. Many devices have been used to monitor patient health continuously, which has been made possible with the deployment of body-centric networks (BCNs). These networks have their areas restricted to personal area networks (PANs) and body area networks (BANs) and are used for monitoring physiological parameters like blood pressure, electrocardiogram (ECG), heartbeat rate, and oxygen level

P. Kaur · M. Sharma (✉) · S. Malhotra
Chitkara University Institute of Engineering and Technology, Chitkara University, Rajpura, Punjab, India
e-mail: manishengineer1978@gmail.com

P. K. Malik and P. N. Shastry (eds.), *Internet of Things Enabled Antennas for Biomedical Devices and Systems*, Springer Tracts in Electrical and Electronics Engineering,
https://doi.org/10.1007/978-981-99-0212-5_18

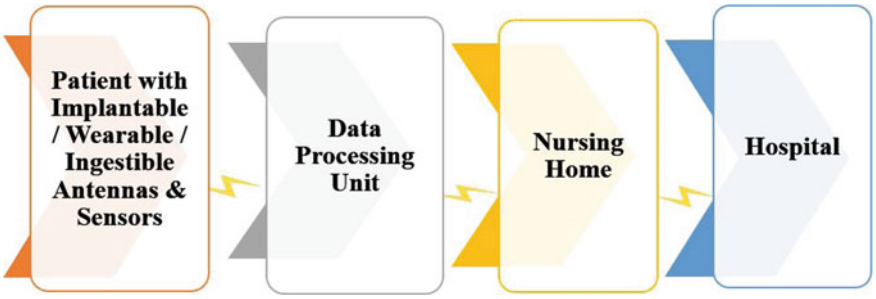

Fig. 18.1 Wireless communication through body centric networks

of patients continuously from inside the human body to the receiver placed outside the body. Figure 18.1 represents the process of wireless communication through body-centric networks. Data is collected from the patient either through wearable, implantable or ingestible devices placed on or in the body of the patient. It is then sent via wireless links using a specified frequency band (ISM/MED-RAD/MICS) to the data processing unit, from where it is further communicated to nursing homes for analysis and lastly to the hospitals where the doctors further investigate and interpret the reports for the treatment of the identified disease (Malik et al. 2020).

1.1 **Domains of Body-Centric Network's**: Figure 18.2a represents the three domains which are explained as follows.

(a) **On-Body**: When the communication channel as well as antennas are placed within the body, the network domain is named as on-body centric networks. It implements wearable devices as shown in Fig. 18.2b.
(b) **Off-Body**: When the communication channel is outside the human body and one antenna is placed on the body, the domain is termed as off-body centric networks.
(c) **In-Body**: When the communication channel is inside the body and the communication is carried through implanted transceivers and external devices. It is in-body, and it implements implantable medical devices (IMD) [3].

IEEE 802.15.6 Standard for WBANs

With the increase in the implementation of WBANs in medical and non-medical areas, there was a need to set an international standard for wireless communication for both medical and consumer-electronics applications. Institute of Electrical and Electronics Engineers (IEEE) has set IEEE 802.15.6 as a standard for short range, low power devices to be mounted or implanted in the human body. This standard

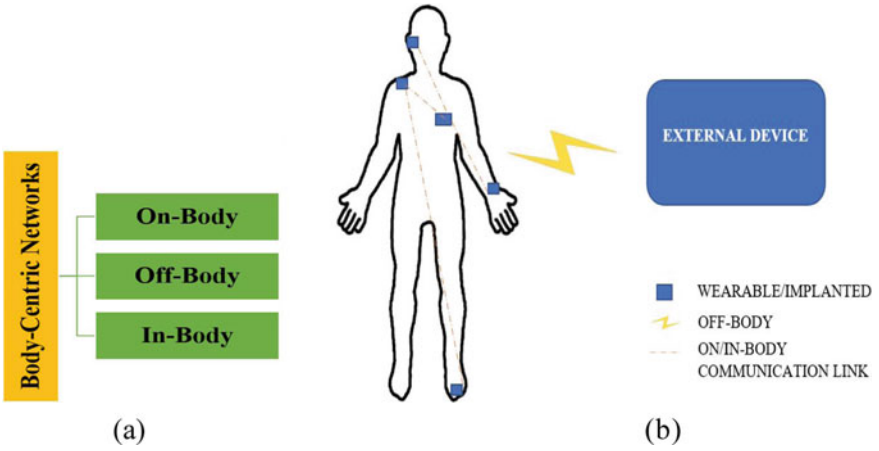

Fig. 18.2 **a** Domains of Body Centric Networks **b** On/In and Off-Body Communication

provides the specifications for communication in the surroundings of the human body. It specifies the use of ISM band along with other bands specified by medical authorities. Quality of service (QoS) and minimum SAR value along with the data rate of 10Mbps are the important features of this standard as shown in Fig. 18.3. It supports the new Medium Access Control (MAC) layer which controls the access of the channel and supports three physical (PHY) layers. Physical layer is responsible for modulation and error correction and is divided in to three parts named as Narrow-band (NB) layer(MICS/WMTS/ISM), Human-Body Communication (HBC) layer (5–50 MHz) and Ultra-Wideband (UWB) layer (3.1–10.6 GHz) (Ullah et al. 2013).

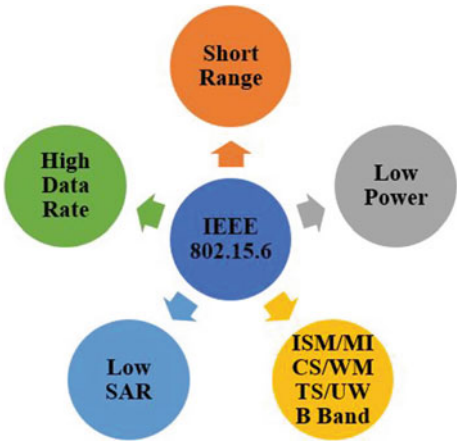

Fig. 18.3 Features of IEEE 802.15.6

Frequency Bands for Biomedical Applications

Body-centric devices consist of sensors, source of power supply, electronic circuit and an antenna. Among all the components antenna plays an important part as it acts as a transceiver for the body as well as for the external device. FCC has specified certain frequency bands for biomedical applications. All the wearable and implanted devices used for health-care services are operated in these bands as shown in Fig. 18.4. Implanted medical devices uses Medical Device Radio Band (MED-RAD) having different bands of (401–406, 413–419, 426–432, 438–444, 451–457 MHz) for diagnostic and therapeutic purposes, Medical Implantable Communication Service (MICS)(402–405 MHz),Industrial, Scientific and Medical (ISM) (2.45 GHz) frequency bands and wearables also use ISM, MICS Ultra-Wideband (3.1–10.6) (Malik et al. 2020; Ramanpreet et al. 2021; Zaki et al. 2021) and sub 6 GHz, unlicensed 61 GHz ISM as well (Puskely et al. 2014).

Requirements of Implantable Antennas

Implantable medical Devices (IMD) are used for wireless communication between the human body and externally mounted receiver. These devices are used for continuous monitoring of physiological parameters of the body and eliminate the need of frequent visiting to doctor. The device is embedded with antenna, sensors, batteries, camera and required electronic circuit. Antenna acts as transceiver as it is the only component which transmits the information collected in the form of images and videos to the external receiver and also receives the signals as wake up signals. The

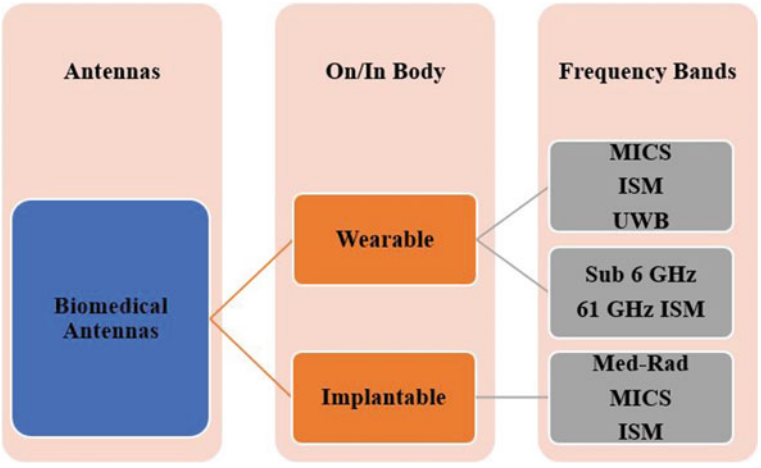

Fig. 18.4 Frequency spectrum for Bio-medical applications

information received by the receiver is transmitted to the hospital via wireless links where the doctor interprets the data and generates the reports as shown in Fig. 18.5 (Malik et al. 2020). These devices have found their applications in various healthcare services like capsule endoscopies, cardiac pacemakers, blood glucose monitoring systems, retinal implants, functional electrical stimulators (FES) and cardioverter-defibrillators etc. The design of the antenna depends upon the band of frequency used and is categorized as low frequency band antenna, MICS band antenna, ISM band, WMTS band and UWB band antenna (Zaki et al. 2021). As antennas need to be designed for biomedical applications, there are certain limitations, requirements and challenges which have been considered and are listed in Fig. 18.6.

(a) **Antenna Miniaturization**: Various techniques has been adopted and investigated for the compactness of implantable antennas such as the use of dielectric with high permittivity which shortens the wavelength and hence shifts the resonant frequency to the lower side. RogersRO3210/RO3010/6002 are usually used for implantable antennas. Secondly, by using Planar inverted F antenna with resonant length of quarter wavelength, and thirdly by Inductive and Capacitive Loading for impedance matching at the desired frequency band. Moreover by lengthening the current path of the radiator, the resonant frequency gets shifted to lower side, thereby reducing the size of antenna. Another method is to use a higher operating frequency which owing to its shorter wavelength helps in reduction of the antenna size. Last but not the least altering the ground plane

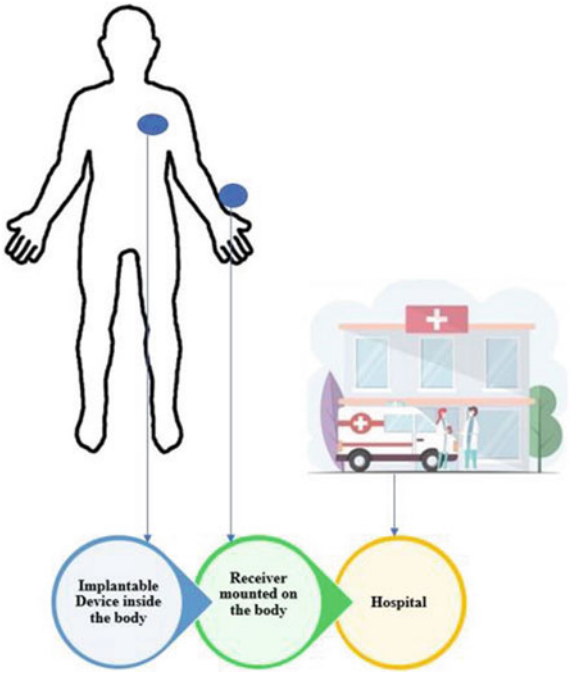

Fig. 18.5 Implantable antenna

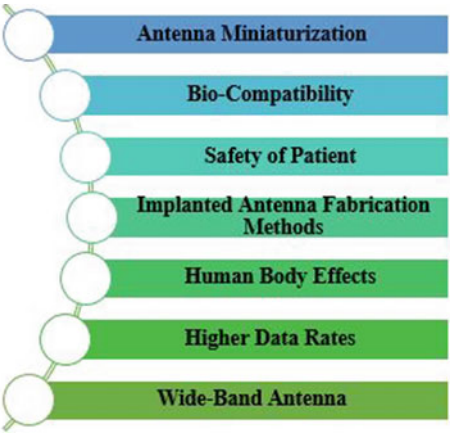

Fig. 18.6 Requirements of implantable antenna

(Malik et al. 2020; Liu et al. 2016) changes the impedance and hence the size of an antenna as summarized in Fig. 18.7.

(b) **Bio-Compatibility**: As stated in International Dictionary of Medicine and Biology, Bio-compatibility refers to the ability of the implant to exist in harmony with the tissues without causing any adverse effects. As the tissues of the human body are conductive in nature, they might get short circuited after coming in contact with the antenna. So biocompatible materials like Ceramic Alumina, Teflon, MACOR should be used for the fabrication of implantable antennas. Moreover, the antenna must be encapsulated with bio-compatible

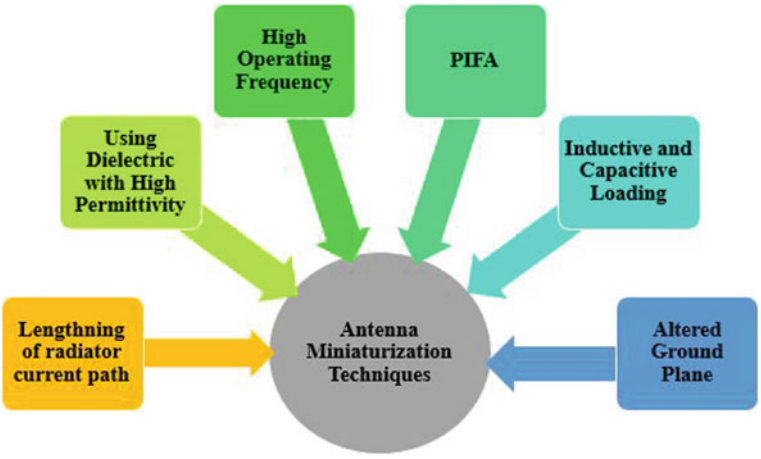

Fig. 18.7 Implantable antenna miniaturization techniques

superstrates having high permittivity and low loss tangent like Zirconia, Grade-base elastomer, Silastic-MDX 4210 and PEEK (Malik et al. 2020; Liu et al. 2016)

(c) **Safety of Patient**: Several precautions have to be taken while implanting antenna inside the body for the safety of the patient. Specific Absorption Rate (SAR), Effective Isotropic Radiated Power (EIRP) and Focalized Temperature limit are the parameters which must be up to the acceptable values to ensure patient's safety. Two standards have been set for SAR acceptable values. First is IEEE C95.1–1999 standard which defines that the SAR should be less than 1.6 W/kg averaged over 1 g cubic volume of the tissue and the other standard named IEEE C95.1–2005 specifies SAR to be less than 2 W/kg averaged over 10 g cubic volume of the tissue. Moreover, FCC has specified 1 g averaging whereas the International Commission on Non-Ionizing Radiation Protection (ICNIRP) considers 10 g averaging. 2 W/kg over 10 g cubic tissue would be equal to 4–6 W/kg averaged over 1 g cubic tissue. Specific absorption is calculated as:

$SA = SAR \times T_p$ …. where, T_p denotes the pulse duration and

$SAR = \frac{\sigma |E|^2}{2\rho}$ where, ρ (Kg/m^3) is the mass density, σ (S/m) is the conductivity and |E| is the electric field. The second parameter, EIRP of an implantable antenna in the Med-Radio band should be –16 and –20 dBm for the ISM band and third is the temperature around the implanted device which must not exceed 1–2°.

(d) **Implanted Antenna Fabrication Methods**: Fabrication method must be chosen wisely as antenna has to be placed inside the human body. Several methods have been proposed in literature such as antennas on fabric embroidery, polymer composites encapsulation, microfluidic antennas, photolithography and 3D printed antennas. Fabricating antenna with the combination of the conductive fabric along with PDMS allows easy implementation along with more robust flexible antenna structure.

(e) **Human Body Effects**: The human body consists of millions of cells which are organized to form several tissues to perform specific functions in the human body. These tissues experience changes in their electrical properties when exposed to changes in the operating frequencies of the implanted device. The more the conductivity and permittivity of the tissues; the more is the attenuation which is described by the equation given below:

$\boldsymbol{L_\alpha} = 20\log_{10}(e^{-\alpha L})$ where $\boldsymbol{\alpha}$ is the attenuation constant

$\boldsymbol{L}$ is the distance travelled by the signal in the human body.

Moreover, the human body losses also affect the radiated power, radiation efficiency, radiation pattern and bandwidth of the antenna (Malik et al. 2020).

(f) **High Data Rates**: Multiple-Input-Multiple-Output (MIMO) is employed now a days to enhance the data rate by reducing multipath distortion. Moreover, MIMO has high spectral efficiency than single–input–single–output which makes it more versatile for implanted antennas (Alazemi and Iqbal 2021).

(g) **Wide-Band Antenna**: As different tissues have different dielectrics, so signal travelling from the implanted device to the external receiver undergoes multipath propagation. So wideband antenna must be implemented for implants (Alazemi and Iqbal 2021).

Body Centric Implantable Antennas

Encapsulated two element (2 × 2) MIMO antenna is proposed in Alazemi and Iqbal (2021) with meandered geometry and slotted ground plane to achieve isolation of 28 dB and envelope correlation coefficient (ECC) of <0.1. It has been fabricated using Roger RO3010 substrate and is being encapsulated with thin alumina capsule cell for deep implantation. Antenna works in the ISM band with safe 10 g SAR of 402.8 W/Kg at an input power of 1 W and is shown in Fig. 18.8a along with its s-parameters in Fig. 18.8b.

Authors have investigated Coplanar-Waveguide (CPW) fed multiband antenna on Rogers Duroid 5880 substrate as shown in Fig. 18.9a in Yeap et al. (2021). It incorporates both in-body and off-body communication by providing 10 dB bandwidth of 420 MHz in the ISM band (2.07–2.49 GHz), 90 MHz for the WBAN band (3.16–3.25 GHz) and 460 MHz in the WLAN band (4.76–5.22 GHz). It can be easily adhered to any part of the human body as illustrated in Fig. 18.9b.

Planar implantable device incorporating two radiating elements for bio-telemetric applications has been reported in Singh et al. (2021) for the ISM band as depicted in Fig. 18.10 along with its s-parameters. It achieves high isolation of more than 37 dB with the implementation of neutralization line (NL) and defected ground structure technique (DGS). The bandwidth has also improved by 8.5%. 4 × 4 MIMO for head implants has been reported in Iqbal et al. (2021) to be operated in the ISM band. Meandered resonators in semicircular shape have been used for radiating elements. An isolation of more than 32.6 has been achieved with the implementation of centrally drilled via. SAR has also been reported with the value of 860 W/Kg which is within the human safety. Authors have reported an implantable antenna in Karacolak et al. (2008) for continuous monitoring of glucose in the human body for ISM as well as

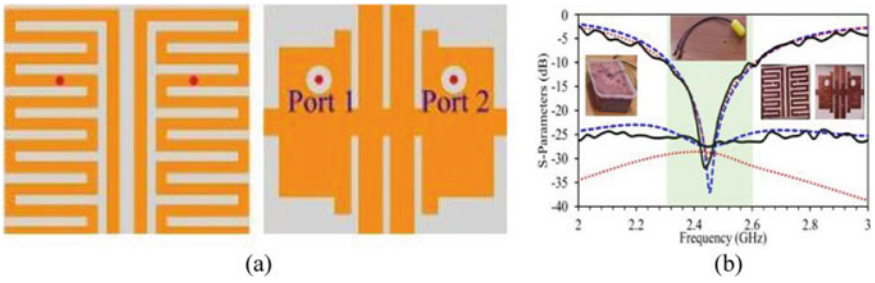

Fig. 18.8 **a** MIMO for deep penetration **b** S11 graph

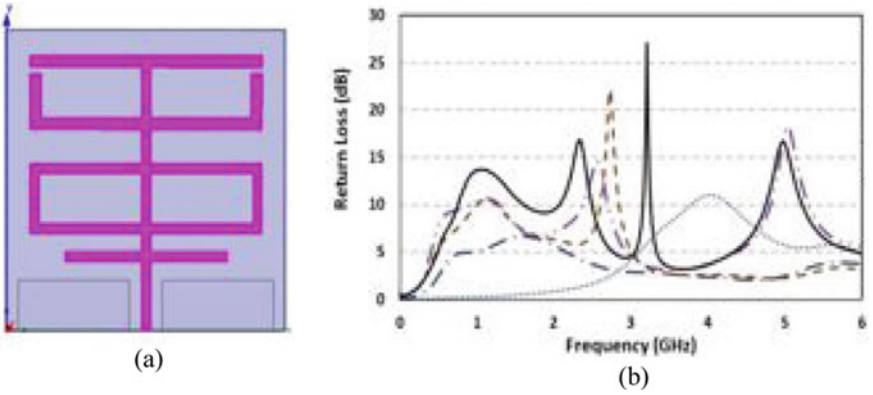

Fig. 18.9 **a** Structure of antenna **b** S11 graph

MICS bands. Gels resembling to the human skin structure have also been investigated in this paper. In Usluer et al. (2020) RO3010 substrate is used to design a dual band complementary split ring (CSR) based antenna that is designed to operate in MICS and ISM bands for bio-telemetry applications. Bandwidth of 23.5% is reported at 460 MHz and 12% at 2.3 GHz. A compact multiband antenna with spiral shape as shown in Fig. 18.11a with s-parameters in Fig. 18.11b has been reported in Kaim et al. (2020) for MICS, ISM and mid-field bands. Wireless pacemakers are also been investigated along with the wireless communication link budget specifying range at 7 and 100 Kbps.

In Faisal et al. (2019) a miniaturized antenna has been proposed for intracranial pressure monitoring of the human body. The antenna is required to operate at 915 MHz and 2.45 GHz and is used in scalp implantations. Authors have proposed

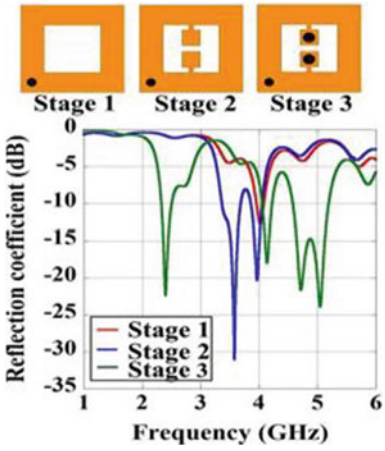

Fig. 18.10 Dual antenna system structure with S11 plot

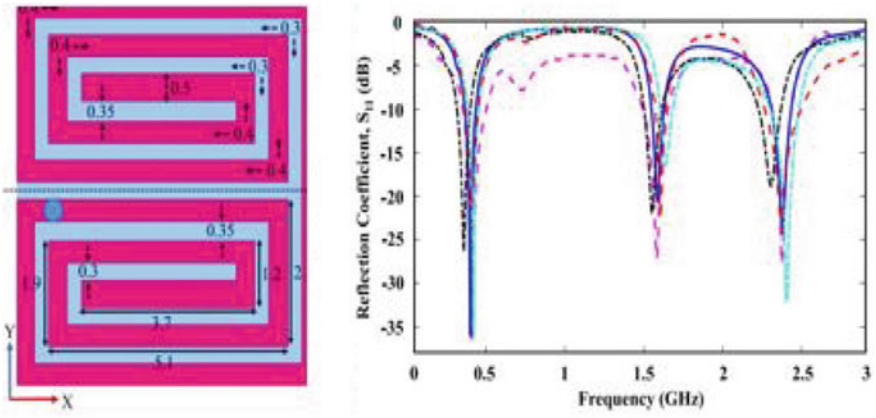

Fig. 18.11 **a** Structure of scalp implantable antenna **b** S11 graph with tri-band applications

a meandered shaped triple band Zada and Yoo (2018) antenna for multiple bio-telemetry applications in ISM/902-92 8MHz and 2400-2483.5 MHz/1824-1980 MHz. It consists of two devices to be implanted inside the body. One device is the capsule type for deep implantations and the other is the flat type for skin implantations as shown in Fig. 18.12a, b. In Zhang et al. (2018) a circularly polarized implantable antenna operating at 915 MHz is proposed. Slot technique has been used for achieving compactness and shorting pin is used for lowering the resonant frequency and to achieve the circular polarization.

Present State-of-the-Art—Implantable Antennas

Table 18.1 shows the comparison of the implantable antennas. It shows that the implanted antennas are very much smaller as the size is in millimeters and the Rogers RO3010 is the widely used substrate for implanted bio-medical applications in all prescribed frequency bands (Malik et al. 2021, 2022; Rahim and Malik 2020).

Conclusions

Antenna holds a great importance in saving one's life as it is the main component used for bio-telemetry applications. Its compact size makes it possible to be implanted or mounted on a person's body whose physiological parameters have to be monitored, but the design should meet the requirements of implantable devices. Various techniques have been identified for miniaturization of antenna such as meander shaped

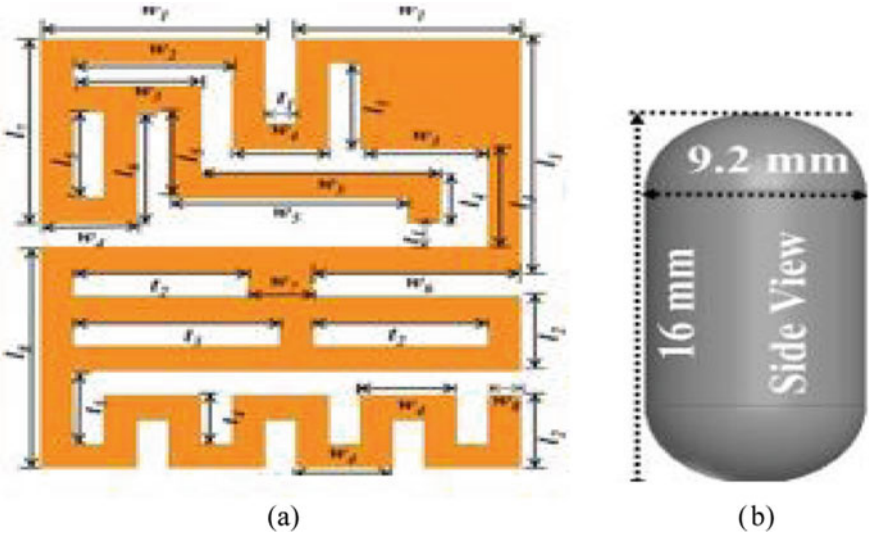

Fig. 18.12 **a** Skin implant antenna structure **b** Deep tissue implant

structures, PIFA, extending radiator current path, using higher operating frequencies, use of capacitive and inductive loading, by using high permittivity substrate etc. Moreover, the SAR, EIRP and temperature must be within the standard values for the sake of human safety and these antennas should ensure the use of biocompatible materials.

Table 18.1 Comparison of implantable antennas

Refs.	Size (mm^3)	Substrate	Frequency Band	SAR (W/Kg)	Input Power
Alazemi and Iqbal (2021)	3.98	Rogers RO3010	ISM	402.8	3.97 mW
Yeap et al. (2021)	453.312	Rogers 5880	ISM/WBAN-UWB/WLAN	NC	NC
Singh et al. (2021)	280.035	Rogers 6010	ISM	66.55	1 W
Iqbal et al. (2021)	23.6	Rogers RO3010	ISM	860	1 W
Usluer et al. (2020)	248.92	Rogers RO3010	ISM/MICS	482 at 2.44 GHz / 338 at 402 MHz	1 W
Kaim et al. (2020)	17.15	Rogers 6010	ISM/MICS/MID-FIELD	92.7 at 402 MHz / 85.3 at 1600 MHz and 81.7 at 2450 MHz	1 W
Faisal et al. (2019)	9.8	Rogers 6010	ISM 915 MHz	89.70 at 0.915 GHz/82.71 at 2.45 GHz	22.45 and 24.18 mW
Zada and Yoo (2018)	21	Rogers 6010 & ceramic alumina	ISM/MICS/MID-FIELD	40.4/38.2/40.3	1 W
Zhang et al. (2018)	88.0905	Rogers RO3010	ISM 915 MHz	778	1 W

**NC* Not Calculated

References

Alazemi AJ, Iqbal A (2021) A high data rate implantable mimo antenna for deep implanted biomedical devices. IEEE Trans Antennas Propag 70(2):998–1007

Faisal F, Zada M, Ejaz A, Amin Y, Ullah S, Yoo H (2019) A miniaturized dual-band implantable antenna system for medical applications. IEEE Trans Antennas Propag 68(2):1161–1165

Farooq U, Rather G (2022) A miniaturised Ka/V dual band millimeter wave antenna for 5G body centric network applications. Alex Eng J 61(10):8089–8096

Hall PS, Hao Y (2012) Antennas and propagation for body-centric wireless communications. Artech House

Iqbal A, Al-Hasan M, Mabrouk IB, Nedil M (2021) Scalp-implantable MIMO antenna for high-data-rate head implants. IEEE Antennas Wirel Propag Lett 20(12):2529–2533

Kaim V, Kanaujia BK, Kumar S, Choi HC, Kim KW, Rambabu K (2020) Ultra-miniature circularly polarized CPW-fed implantable antenna design and its validation for biotelemetry applications. Sci Rep 10(1):1–16

Karacolak T, Hood AZ, Topsakal E (2008) Design of a dual-band implantable antenna and development of skin mimicking gels for continuous glucose monitoring. IEEE Trans Microw Theory Tech 56(4):1001–1008

Liu C, Guo Y-X, Xiao S (2016) A review of implantable antennas for wireless biomedical devices. Forum Electromag Res Methods Appl Technol (FERMAT) 14(3):1–11

Malik NA, Sant P, Ajmal T, Ur-Rehman M (2020) Implantable antennas for bio-medical applications. IEEE J Electromag RF Microwaves Med Biol 5(1):84–96

Malik PK, Kumar P, Kumar S, Singh DK (2021) Smart antennas: recent trends in design and applications. Bentham Sci. Sharjah, United Arab Emirates. ISSN: 2717-5421 (Print), ISSN: 2717-543X (Online), ISBN: 978-1-68108-860-0 (Print). https://doi.org/10.2174/9781681088594121020l

Malik P, Lu J, Madhav BTP, Kalkhambkar G, Amit S (eds) (2022) Smart antennas: latest trends in design and application. Springer. ISBN 978-3-030-76636-8. https://doi.org/10.1007/978-3-030-76636-8

Puskely J, Pokorny M, Lacik J, Raida Z (2014) Wearable disc-like antenna for body-centric communications at 61 GHz. IEEE Antennas Wirel Propag Lett 14:1490–1493

Rahim A, Malik PK (2020) Design methodologies and tools for 5G network development and application. In: Analysis and design of planner wide band antenna for wireless communication applications: fractal antennas. https://doi.org/10.4018/978-1-7998-4610-9.ch010, 13(196–208), ISBN13: 9781799846109, Dec 2020 IGI Global USA

Ramanpreet N, Rattan M, Gill SS (2021) Compact and low profile planar antenna with novel metastructure for wearable MBAN devices. Wirel Pers Commun 118(4):3335–3347

Singh MS, Ghosh J, Ghosh S, Sarkhel A (2021) Miniaturized dual-antenna system for implantable biotelemetry application. IEEE Antennas Wirel Propag Lett 20(8):1394–1398

Ullah S, Mohaisen M, Alnuem MA (2013) A review of IEEE 802.15. 6 MAC, PHY, and security specifications. Int J Distrib Sens Netw 9(4):950704

Usluer M, Cetindere B, Basaran SC (2020) Compact implantable antenna design for MICS and ISM band biotelemetry applications. Microw Opt Technol Lett 62(4):1581–1587

Yeap KH, Tan EMF, Hiraguri T, Lai KC, Hirasawa K (2021) A multi-band planar antenna for biomedical applications. Frequenz 75(5–6):221–228

Zada M, Yoo H (2018) A miniaturized triple-band implantable antenna system for bio-telemetry applications. IEEE Trans Antennas Propag 66(12):7378–7382

Zaki AZ, Abouelnaga TG, Hamad EK, Elsadek HA (2021) Design of dual-band implanted patch antenna system for bio-medical applications. J Electr Eng 72(4):240–248

Zhang Y, Liu C, Liu X, Zhang K, Yang X (2018) A wideband circularly polarized implantable antenna for 915 MHz ISM-band biotelemetry devices. IEEE Antennas Wirel Propag Lett 17(8):1473–1477

Chapter 19
Study of SAR in Tumor for Biomedical Applications Based on Microstrip Patch Antenna

Sweety Jain, Vivek Singh Kushwah, Sanjay Chouhan, and Mohamed El Bakkali

Abstract In this chapter we have discussed the Microstrip patch antenna (MPA) that is designed to detect the tumor in the human brain. It is aimed so because the location of the tumor can be easily targeted by rotating the antenna array around the head. To achieve this aim, an FR4 substrate is used whose main characteristics include low cost, durability, low maintenance cost and easy to fabricate. The antenna is initially simulated on the computer simulation technology (CST) microwave studio software and is designed for size 40 mm × 40 mm while it works at a frequency of 2.4 GHz for the ISM (Industrial Scientific and Medical Band Frequency) Band. For accurate detection of the tumor and to check the efficiency of the antenna to study the different parameters, reflection coefficient, current density and SAR (Specific Absorption Rate) with 10 g and 1 g are determined for healthy and unhealthy brain. On the final analysis, it is found that the antenna is effective in operate at a designed frequency and can detect the tumor.

Keywords Tumor · Human brain · Current density · MPA · Reflection coefficient · SAR (10 g and 1 g)

S. Jain (✉)
Samrat Ashok Technological Institute, Vidisha, Madhya Pradesh, India
e-mail: 1502sweety@gmail.com

V. S. Kushwah
Amity University, Gwalior, Madhya Pradesh, India
e-mail: vskushwah@gwa.amity.edu

S. Chouhan
Jawaharlal Institute of Technology, Borawan-Khargone, India
e-mail: sanjaychouhanjit@yahoo.co.in

M. El Bakkali
Faculty of Sciences of Rabat, Mohammed Five University of Rabat, Agdal, Rabat, Morocco
e-mail: mohamed.elbakkali1617@gmail.com

P. K. Malik and P. N. Shastry (eds.), *Internet of Things Enabled Antennas for Biomedical Devices and Systems*, Springer Tracts in Electrical and Electronics Engineering,
https://doi.org/10.1007/978-981-99-0212-5_19

Introduction

It is well known that electromagnetic waves such as radio frequency are generally used in communication, mobile phones network and wireless communication. Due to the presence of these waves near to human surroundings it causes adverse effects on their body (Ozdemir and Kargi 2011; National Research Council 1993).

Brain tumor is the growth of abnormal cells in the human brain. Various types of brain tumors exist such as noncancerous (benign) and cancerous (malignant). However the growth rate of any tumor may vary. Nervous system factor that affects the nervous system via the tumor depends upon the location of the tumor in the brain. Its early detection is beneficial to save one's life.

On focusing this, various countries took steps to reduce the effects of radiations that guidelines are known as specific absorption rate (SAR). SAR is the exposure of radiation to the human body (Cleveland and Athey 1989). It is expressed as W/kg. SAR can be calculated for the amount of exposure to the whole body or some part of the body. According to this study, basic exposure for various parts of the body is 1.6 W/kg. Also, for other parts it varies around 4 W/kg (Lin 2006, 2003; Hossmann and Hermann 2003). Generally, SAR is calculated quantitatively and the temperature distribution (Voigt et al. 2012; Montaser et al. 2012; Su et al. 2005) was determined by finite difference time domain analysis (FDTD) (Morega et al. 2010) and finite element mesh (FEM) (Ishimiya and Takada 2007). However, the permitted value of SAR in India is 1.6 W/kg (Ishak and Seman 2017).

With adoption of technologies such as 4G and 5G, microstrip antenna, not only boom in the medical field but also in the agricultural field for detecting the moisture content in grains, detection of salt sugar (Jain 2020a, b; Jain et al. 2021, 2020a, b, 2019, 2018a, b; Jain and Mishra 2021; Kushwah and Jain 2021) etc. Hence, the human body's risk to exposure towards radiations has frequently increased. Though various steps taken by International Commission on Non- Ionizing Radiation Protection (ICNIRP) and Institute of Electrical and Electronics Engineers (IEEE), which show that the safety of mankind is very important, these institutions also doing continuous research studies to get more better results which will help to reduce the exposure towards radiation (Arul Jenshiya et al. 2019).

$$\text{SAR} = \frac{\sigma E^2}{2\rho}$$

where,

σ—conductivity of tissue (S/m)
E—Electric field strength of tissue (V/m)
ρ—Mass density (Kg/m^3).

Study of Dielectric Properties of Human Tissues

Microwave imaging technology is supposed to be based on the dielectric properties of the tumour and other human tissues. According to various studies it is known that the tumour and other tissues transmit different microwaves. Therefore, this concept is utilized in this study for detecting cancer cells. For that, an antenna array is conducted to send pulses of the microwave on human tissues, which suffer from cancer. The result is that by the phenomenon of backscatter in the signal this is reflected and later picked up by an array (Abu Bakar et al. 2012). By this process, it is easy to induct whether the tissue is suffering from cancer or not. UW040 is used to maintain the fidelity of the waveform (Fear et al. 2003). A planner structure printed circuit board is used to design the antenna (Lu and Tsai 2013) and also for high resolution and accurate images. The compact antenna requires to transmit on broad range of frequencies. The dielectric properties of numerous tissues are considered by permittivity, which is the mean of the complex-valued dielectric (Islam et al. 2018).

$$\varepsilon(\varepsilon = \varepsilon_r + i\sigma/\omega\varepsilon_0) \tag{19.1}$$

where,

ε_r = dielectric constant
σ = conductivity of the tissue against frequency
ε_0 = dielectric permittivity of vacuum
ω = angular frequency.

Another important parameter which has relation with SAR is the power loss density. It is defined to get knowledge of electromagnetic field distribution inside tissue structure. The field distribution on human tissues can be determined when the antenna reaches the human tissues. Hence, there are two methods to determine the SAR i.e., (a) Point SAR and (b) averaging SAR. The former is defined as the value for which averaging is not required and determines SAR for all grid cells. The latter is defined as a cube with a predefined mass and power loss density is geometrically interpreted on this cube (Aly and Piket May 2014; Gustrau and Bahr 2002).

In Table 19.1, SAR defined ICNIRP guidelines for SAR frequency above 10 GHz and FCC for above 6 GHz are given. Also according to FCC guidelines, application of power density rises when the exposure is above 6 GHz. It is required to be noted down. Here, power density is defined only power travelling towards the tissue and does not define power absorption and field distribution in tissues. Hence, power density has limited application in the near field (Wu et al. 2015).

Table 19.1 SAR exposure limit guideline (Fear et al. 2003)

Standard	SAR limit [W/kg]	Averaging mass for SAR
ICNIRP	2.0 (f < 10 GHz)	10 g of tissues
FCC/ANSI	1.6 (f < 6 GHz)	1 g of tissues

Table 19.2 Parameters of antenna

Parameters	Size (mm)
Length of the ground	40
Width of the ground	40
Length of substrate	40
Width of the substrate	40
Length of the patch	40
Width of the patch	40
Brain (centre) radius	30
Brain (top) radius	20
Brain (bottom) radius	20
Tumor (centre) radius	5
Tumor (top) radius	4
Tumor (bottom) radius	2

Biological tissues consist of layers of skin, fat muscle and bone. The structure of the tissue skin contains non-homogeneous dielectric properties. The skin layers have thickness varying from 50 to 1000 micron and thickness of fat and muscles vary from 300 to 20,000 micron (Miklavcic and Pavselj 2006).

The study of dielectric properties of the tissues is important because they control the reflection, propagation and attenuation of electromagnetic fields in the body. Also, permittivity is inversely proportional to frequency with rise in permittivity bringing down the frequency, while conductivity is directly proportional to frequency (Wang and Wang 2013; Tiwari and Malik 2020, Gupta et al. 2020; Roges et al. 2022).

Study of Antenna Performance

Antenna Design

General properties of the antenna are shown in Table 19.2. However, the antenna is designed on CST software.

Performance of Antenna

Analysis of the antenna is done on CST software in two ways including the performance of the antenna with the healthy brain and unhealthy brain. Based on this, the reflection coefficient, current density and SAR for 10 g and 1 g are determined.

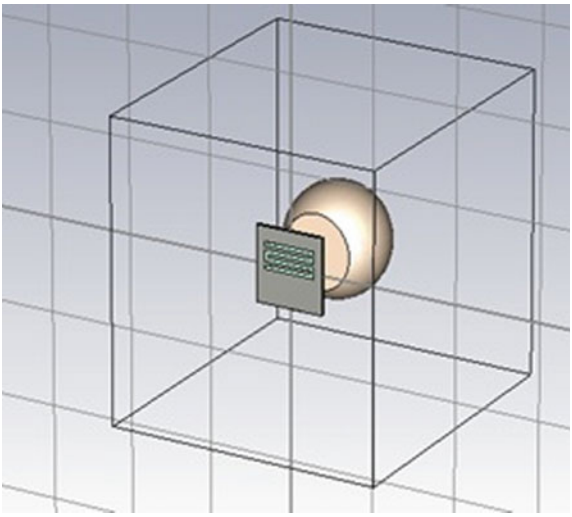

Fig. 19.1 Microstrip patch antenna with human head (healthy brain)

Table 19.3 Healthy brain

Parameters	Value on 2.4 GHz
Reflection coefficient	−25.68 dB
Current density	4.78A/m^2
SAR (10 g)	0.0232 W/kg
SAR (1 g)	0.00465 W/kg

Calculation of these parameters indicates the effectiveness of the designed antenna, which will be discussed in the later section.

(i) *Antenna in contact with Healthy brain*

Figure 19.1 shows when the antenna comes in contact with the healthy brain. After simulation, performance of the antenna found as shown in Table 19.3.

(ii) *Antenna in contact with Unhealthy brain*

Figure 19.2 shows when the antenna comes in contact with the unhealthy brain. After simulation, performance of the antenna found as shown in Table 19.4.

Comparison and Effectiveness of Antenna

When the performance of the antenna with healthy and unhealthy brain is compared then it is found that the antenna is effective in fulfilling the aim for which it is designed.

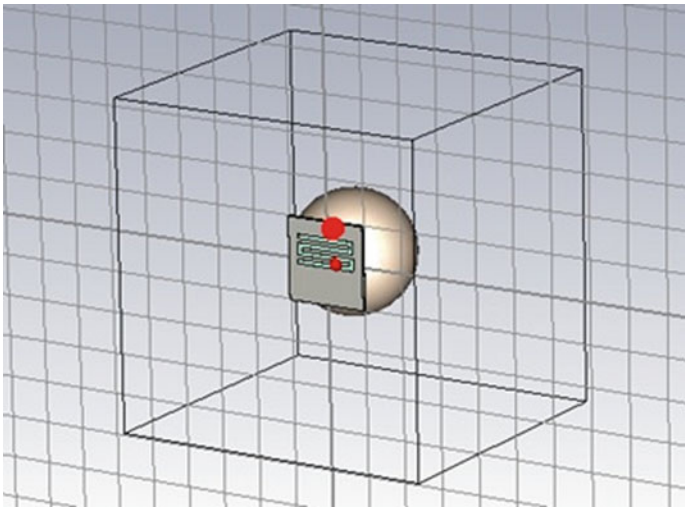

Fig. 19.2 Microstrip patch antenna with human head (unhealthy brain)

Table 19.4 Unhealthy brain

Parameters	Value on 2.4 GHz
Reflection coefficient	−2.75 dB
Current density	98 A/m^2
SAR (10 g)	0.069 W/kg
SAR (1 g)	0.0373 W/kg

(i) Reflection Coefficient: Reflection coefficient in healthy brain is found to be lower than unhealthy brain as shown in Fig. 19.3. The study shows that whenever the reflection coefficient is lower for healthy brain compared with unhealthy brain then it signifies that the antenna is accurate for this parameter.
(ii) Current density: It is also found to be lower in healthy brain as compared to unhealthy brain as shown in Fig. 19.4a, b. It signifies that the antenna is effective in performance.
(iii) SAR: It is found that in the healthy brain, SAR decreased while it increased in the unhealthy brain. Hence the antenna satisfies this condition also, as shown in Fig. 19.5a, b.

Figure 19.6b by analysis of these parameters, it can be concluded that the designed antenna is fully effective in the detection of tumor.

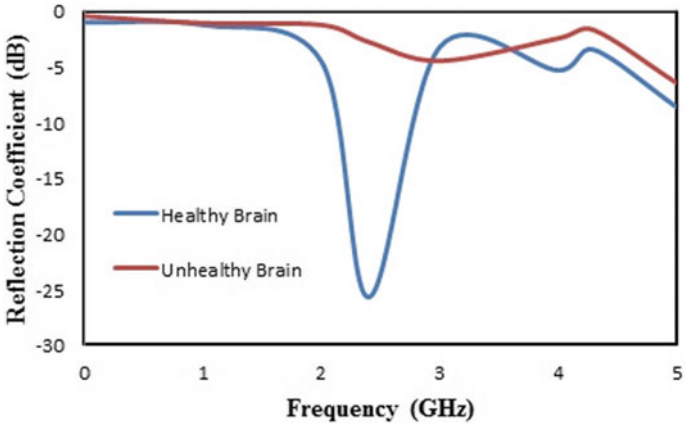

Fig. 19.3 Effect of reflection coefficient on healthy and unhealthy brain

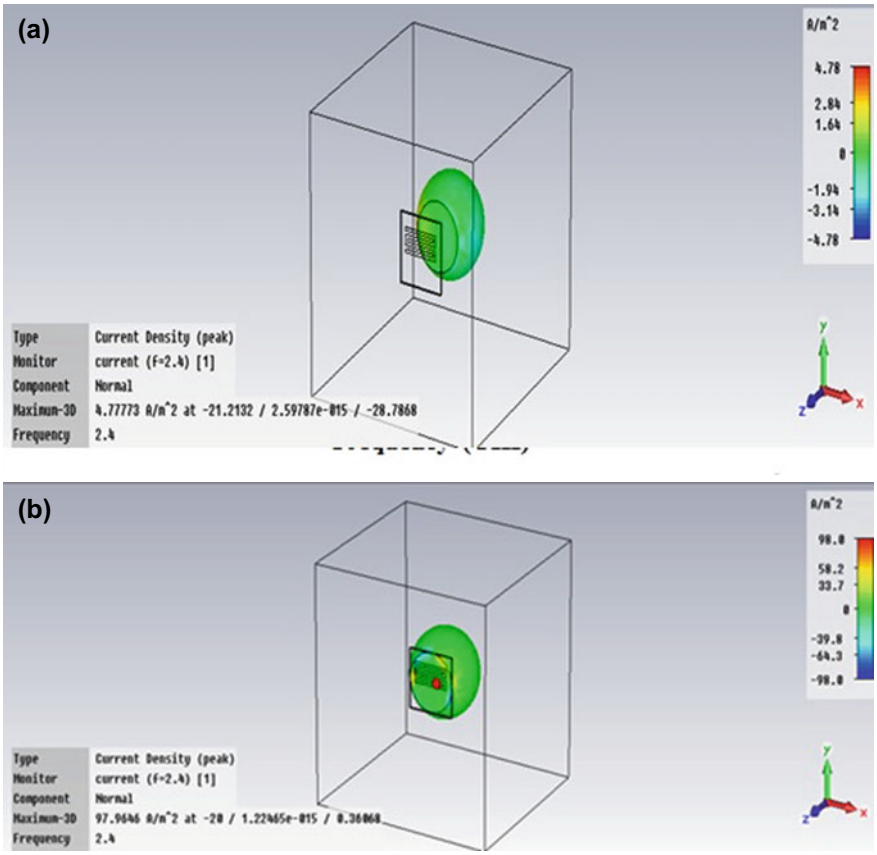

Fig. 19.4 Effect of current density on **a** healthy and **b** unhealthy brain

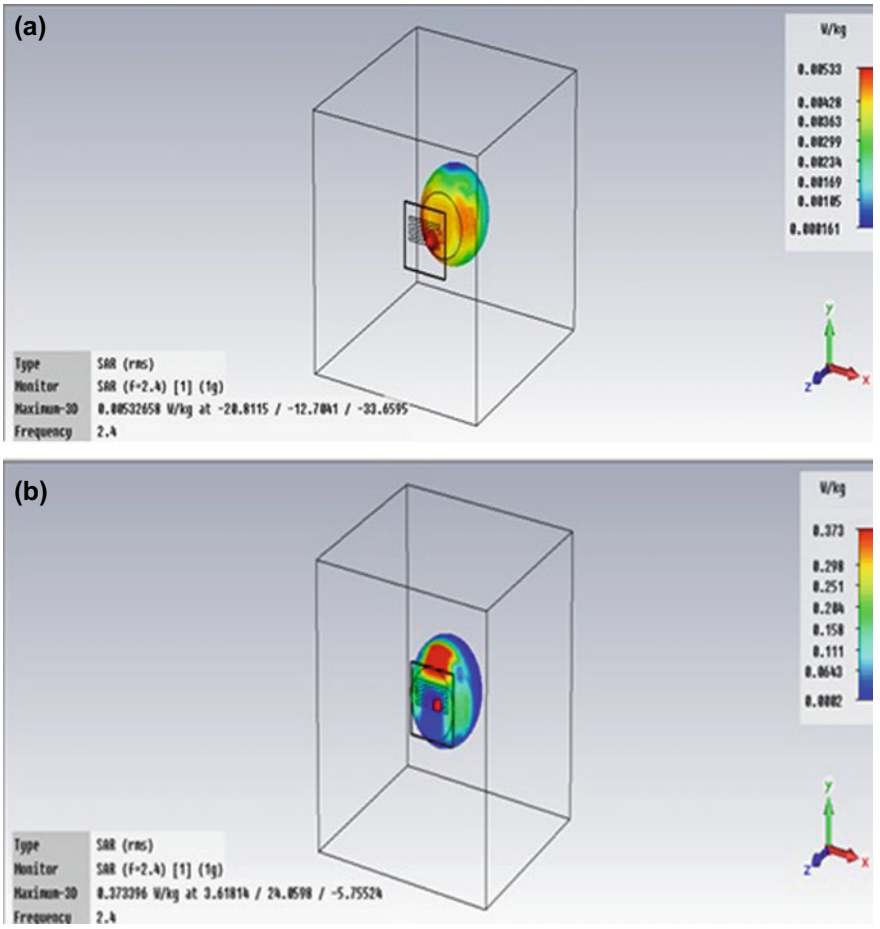

Fig. 19.5 Effect of SAR (1 g) on **a** healthy and **b** unhealthy brain

Conclusion

Adoption of this antenna will help in the early detection of tumor. So, inference can be made that the antenna is satisfying all criteria necessary for its performance. Also, it is low cost, easy to maintain and easy to fabricate on low cost FR4 substrate. Hence, it is recommended to adopt this MPA due to its high accuracy and better results.

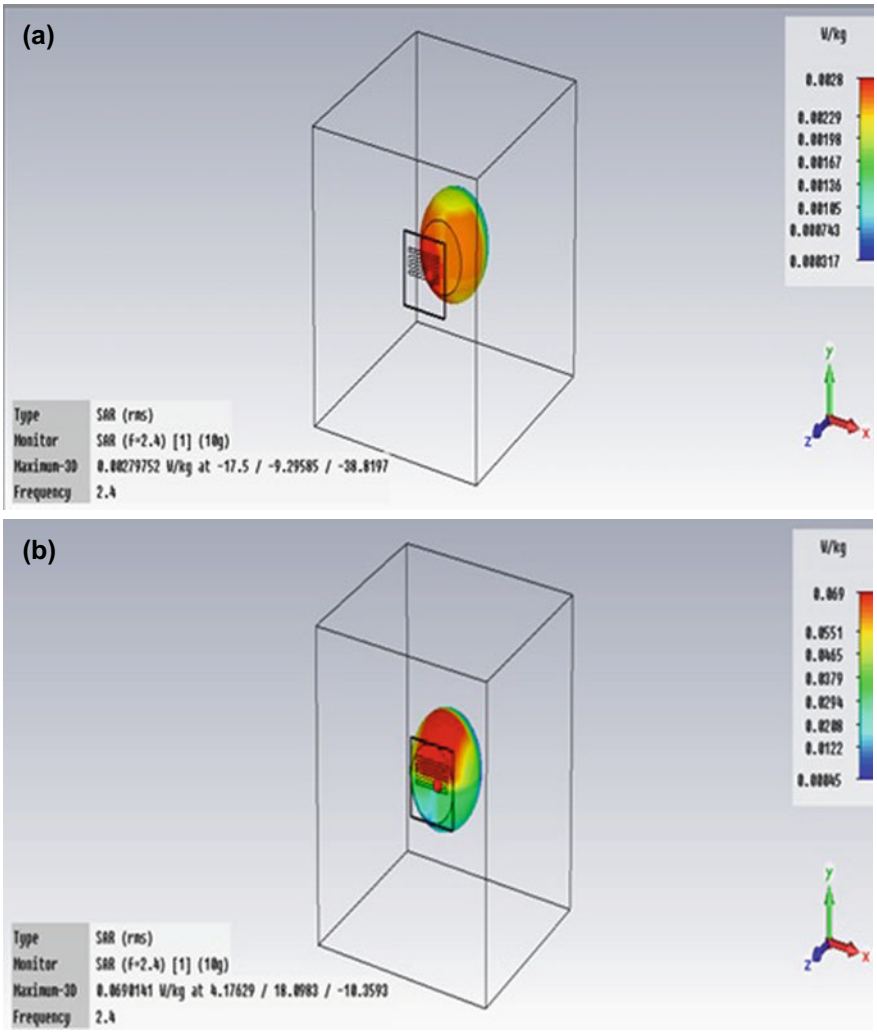

Fig. 19.6 Effect of SAR (10 g) on **a** healthy and **b** unhealthy brain

References

Abu Bakar A, Ireland D, Abbosh AM, Wang Y (2012) Experimental assessment of microwave diagnostic tool for ultra-wideband breast cancer detection. Progr Electromagn Res M 23:109–121

Aly AA, Piket May M (2014) FDTD computation for SAR induced in human head due to exposure to EMF from mobile phone. Int J Adv Comput 5

Arul Jenshiya PR, Madhan Kumar K, Riyaz Fathima H (2019) Evaluation of specific absorption rate of electromagnetic radiation on human brain: microstrip patch antenna. ICTACT J Commun Technol 10(issue 1):1923–1928. https://doi.org/10.21917/ijct.2019.0282

Cleveland RF Jr, Athey TW (1989) Specific absorption rate (SAR) in models of the human head exposed to handheld UHF portable radios. Bioelectromagn J Bioelectromagn Soc Soc Phys Regul Biol Med Eur Bioelectromagn Assoc 10(2):173–186

Fear EC, Meaney PM, Stuchly M (2003) Microwaves for breast cancer detection? IEEE Potentials 22:12–18

Gupta NP, Malik PK, Ram BS (2020) A Review on Methods and Systems for Early Breast Cancer Detection. In: 2020 international conference on computation, automation and knowledge management (ICCAKM), 2020, pp 42–46 (ISBN: 978-1-7281-0666-3). https://doi.org/10.1109/ICCAKM46823.2020.9051554; https://ieeexplore.ieee.org/document/9051554

Gustrau F, Bahr A (2002) W-band investigation of material parameters, SAR distribution, and thermal response in human tissue. IEEE Trans Microw Theory Tech 50:2393–2400

Hossmann KA, Hermann DM (2003) Effects of electromagnetic radiation of mobile phones on the central nervous system. Bioelectromagn J Bioelectromagn Soc Soc Phys Regul Biol Med Eur Bioelectromagn Assoc 24(1):49–62

Ishak NIA, Seman N, Kamarudin MR, Samsuri NA (2017) Specific absorption rate investigation on multiple antennas. In: Proceedings of international symposium on antennas and propagations, pp 1–2

Ishimiya K, Takada JI (2007) Multi-band folded dipole antenna for mobile phone. In: International workshop on antenna technology: small and smart antennas metamaterials and applications, pp 275–278

Islam MS, Kibria S, Islam MT (2018) Experimental breast phantoms for estimation of breast tumor using microwave imaging systems. IEEE Access 6:78587–78597. https://doi.org/10.1109/ACCESS.2018.2885087

Jain S, Mishra PK, Thakare VV, Mishra J (2018a) Microstrip moisture sensor based on microstrip patch antenna. Progr Electromagn Res M 76:175–185. ISSN number: 1937-8726. https://doi.org/10.2528/PIERM18092602

Jain S, Mishra PK, Thakare VV, Mishra J (2018b) Analysis and Optimal design of moisture sensor for rice grain moisture measurement. American Institute of Physics, pp 1–3, 060005. https://doi.org/10.1063/1.5028775

Jain S, Mishra PK, Thakare VV, Mishra J (2019) Design of microstrip moisture sensor for determination of moisture content in rice with improved mean relative error. Microw Opt Technol Lett 61(issue 7):1764–1768, ISSN number: 1098-2760. https://doi.org/10.1002/mop.31763

Jain S, Mishra PK, Thakare VV, Mishra J (2020a) Design and analysis of moisture content of hevea latex rubber using microstrip patch antenna with DGS. Mater Today Proc Elsevier 29(Part 2):581–586. https://doi.org/10.1016/j.matpr.2020.07.312

Jain S, Mishra PK, Mishra J, Thakare VV (2020b) Design and analysis of H-Shape patch sensor for rice quality detection. Mater Today Proc Elsevier 22(Part 2):556–560. https://doi.org/10.1016/j.matpr.2020.07.317

Jain S, Mishra PK, Thakare VV (2021a) Design and analysis of dual-frequency microwave moisture sensor based on rectangular microstrip antenna. Mater Today Proc Elsevier 47(part 18):6441–6448. https://doi.org/10.1016/j.matpr.2021.08.179

Jain S, Mishra PK, Thakare VV (2021b) The analysis and design of circular microstrip moisture sensor for rice grain. Mater Today Proc Elsevier 47(part 18):6449–6456. https://doi.org/10.1016/j.matpr.2021.08.180

Jain S (2022a) Determination of moisture content from microstrip moisture sensor with minimum mean relative error. Smart Antennas 345–357. https://doi.org/10.1007/978-3-030-76636-8_26

Jain S (2022b) Early detection of salt and sugar by microstrip moisture sensor based on direct transmission method. Wirel Pers Commun 122(Issue 1):593–601. ISSN: 0929-6212. https://doi.org/10.1007/s11277-021-08914-1

Kushwah VS, Jain S (2021) Enhancement of reflection coefficient for circular ring microstrip sensor. Mater Today Proc Elsevier, ISSN: 2214-7853. https://doi.org/10.1016/j.matpr.2021.05.106

Lin JC (2003) Reassessing exposure safety requirements for cell phones [telecommunications health and safety]. IEEE Antennas Propag Mag 55(1):218–220

Lin JC (2006) A new IEEE standard for safety levels with respect to human exposure to radio-frequency radiation. IEEE Antennas Propag Mag 48(1):157–159

Lu J-H, Tsai F-C (2013) Planar internal LTE/WWAN monopole antenna for tablet computer application. IEEE Trans Antennas Propag 61:4358–4363

Miklavcic D, Pavselj N (2006) Electric properties of tissues. Wiley Encyclopedia of Biomedical Engineering

Montaser AM, Mahmoud KR, Elmikati HA (2012) An interaction study between PIFAs handset antenna and a human head in personal. Progr Electromagn Res B 37

Morega M, Marinescu A, Morega AM (2010) Mobile phone sar analysis through experimental and numerical simulation. In: 12th international conference on optimization of electrical and electronic equipment, pp 95–102

National Research Council (1993) Effects of electromagnetic fields on organs and tissues. In: Assessment of the possible health effects of ground wave emergency network. National Academies Press (US)

Ozdemir F, Kargi A (2011) Electromagnetic waves and human health. In: Electromagnetic waves. IntechOpen

Roges R, Malik PK, Sharma S (2022) A compact wideband antenna with DGS for IoT applications using LoRa technology. In: 2022 10th international conference on emerging trends in engineering and technology—signal and information processing (ICETET-SIP-22), pp 1–4. https://doi.org/10.1109/ICETET-SIP-2254415.2022.9791725

Su T, Mittra R, Yu W, Wiart J (2005) Calculation of SAR using FDTD sub-domain approach. In: IEEE/ACES international conference on wireless communications and applied computational electromagnetics, pp 590–593

Tiwari P, Malik PK (2020) Design of UWB antenna for the 5G mobile communication applications: a review. In: 2020 international conference on computation, automation and knowledge management (ICCAKM), 2020, pp 24–30 (ISBN: 978-1-7281-0666-3). https://doi.org/10.1109/ICCAKM46823.2020.9051556; https://ieeexplore.ieee.org/document/9051556

Voigt T, Homann H, Katscher U, Doessel O (2012) Patient individual local SAR determination: in vivo measurements and numerical validation. Magn Reason Med 68(4):1117–1126

Wang J, Wang Q (2013) Body area communications: channel modeling, communication systems, and EMC, 1st edn. Wiley, Singapore PTE Ltd. ISBN: 978-1-118-18848-4

Wu T, Rappaport TS, Collins CM (2015) The human body and millimeter wave wireless communication systems: Interactions and implications. In: IEEE international conference on communications, London, UK

Chapter 20
Wearable Proximity Coupled Antenna for IoT Applications

E. L. Dhivya Priya, A. Sharmila, K. C. Rajarajeshwari, K. R. Gokul Anand, and Arshi Naim

Abstract Wearable antennas help people in many day-to-day activities inclusive of health monitoring, calorie burning, monitoring of oxygen level and the same measured data can also be shared to hospitals and attenders. Early, wearable antennas are found helpful for the elderly people and later a wide use of wearable antennas has been found in many fields. Wearable antennas found interest in medical, defence security and public entertainment fields. The antennas integrated with sporting cloths and being in shut proximity to the body are additionally appropriate for private wireless devices needed for maintaining quality of service, no matter the body movements. These wearable antennas can be body-worn antennas or wrist wearable ones and sometimes can be integrated with the dress materials. There are two types of wearable antennas, either on the layer of the skin or placed inside the body for the analysis of internal body parts. Some are made as capsules which are available for the patients to consume, for different analysis of body parts.

A wearable antenna is supposed to be part of the garb used for communique purposes, which incorporates monitoring and navigation, cellular computing and public safety. Specific necessities for wearable antennas are a planar shape and bendy production substances. Several residences of the substances have an effect on the traits of the antenna. For instance, the bandwidth and the performance of a planar microstrip antenna are particularly decided with the aid of using the permittivity and the thickness of the substrate. The use of textiles in wearable antennas calls for the

E. L. D. Priya (✉)
Department of ECE, Erode Sengunthar Engineering College, Erode, India
e-mail: dhivyapriyaloganathan@gmail.com

A. Sharmila
Department of ECE, Bannari Amman Institute of Technology, Sathyamangalam, India

K. C. Rajarajeshwari · K. R. G. Anand
Department of ECE, Dr. Mahalingam College of Engineering and Technology, Coimbatore, India
e-mail: Rajarajeshwari@drmcet.ac.in

A. Naim
Department of Information Systems, AlSamer, University Campus, King Khalid University, King Khalid University, Aseer, Abha, Kingdom of Saudi Arabia
e-mail: arshi@kku.edu.sa

P. K. Malik and P. N. Shastry (eds.), *Internet of Things Enabled Antennas for Biomedical Devices and Systems*, Springer Tracts in Electrical and Electronics Engineering,
https://doi.org/10.1007/978-981-99-0212-5_20

characterization in their residences. The proposed antenna is a rectangular microstrip MIMO antenna with a patch, with proximity coupled feed line. Two Nano strip feed lines are designed above substrate 1, which is placed above the perfect conducting ground plane. The Graphene based patch is placed above substrate 2. The feedlines are separated from the radiating material by substrate 2. Two excitation ports are assigned to the feed lines. The input for the excitation of the antenna is a Gaussian pulse.

Keywords Wearable antenna · IoT applications · Body parts · Proximity coupled · Microstrip patch · Antenna

Introduction

In recent years, the demand for wearable electronics are rapidly increasing. Wireless device miniaturization, wireless devices with rapid speed, ultra-compact and battery technologies are the key developments of wearable electronics. For making these wearable electronics communicate, antenna is integrated. The integrated antenna with wearable electronics are mentioned as wearable antenna. These antennas helps to sense, fetch and exchange data wirelessly from one node to another node in the network. The specific applications of wearable antennas are found in the bio medical RF systems. Categorization of wearable antennas includes on-body, off-body and in- body communication. Types of wearable sensors includes ECG sensor, Insulin sensor, Temperature sensor, Motion sensor, Blood pressure sensor, Heart rate sensor oximetry sensor and IoT Gateway. The impact of the human body on the antennas can be addressed using a variety of approaches, depending on the application. The positioning and direction of the antenna is one of the important factors. The effect of the human body on antennas is greatly reduced by the antenna's optimal position, orientation, and distance from the body. Automatic tunable circuits and programmable antennas can also be used in high performance systems. Antenna designers also implement EBG ground plane and High Impedance Surfaces to address the impact of body on wearable antennas.

The wearable antenna finds applications in military, navigation, entertainment and also in health monitoring systems. These types of antennas cause impact on the body based on its type. When it is placed integrated with other gadgets like watch, then the impact is low. Suppose if it is made to consume inside the body for the internal parts monitoring, then it may cause internal part damage. But in case of elderly people, where no one is at home to take care of them, then these wearable monitoring devices, help a lot. Continuous monitoring of health conditions, immediate reporting to the hospital and the care taker, is possible through these wearable devices. The conditions of the patients are to be considered while using these wearable devices.

People of age group above 75, suffering from severe health abnormalities are to be monitored closely and are to be reported to the hospital immediately if the severe condition reached. Comparative to such health problems, the impact of these wearable

devices are found to be very minimal. So these wearable devices are recommended in these conditions. Also the data collected are to be transmitted at a faster rate for offering immediate first aid. Thus in these conditions antennas working faster than the existence is required. The antenna operating in the range of Terahertz is proposed in this chapter. For making the antenna reach its Terahertz operating frequency range, graphene is used as patch. The proposed antenna has a rectangular patch with dual proximity feed. The antenna deigned is made to work in the THz frequency band with the properties of Graphene. It is a two port Multi input Multi output antenna with two substrates (Varshney et al. 2019). Two Nano strip feed lines are designed above substrate 1, which is placed above the perfect conducting ground plane. The Graphene based patch is placed above substrate 2. The feed lines are separated from the radiating material by substrate 2. Two excitation ports are assigned to the feed lines. The input for the excitation of the antenna is a Gaussian pulse.

These wearable sensor integrated devices can be controlled with the smart phone. The data collected are stored and sent to the users mentioned. The users can be either patients, care takers, doctors, nurse, hospital and ambulance. The data collected will be compared with the saturation point prefixed. As per the comparison made, if the measured data reaches beyond the prefixed saturation point, then it will be immediately reported to all users as mentioned above. The antenna designed as a part of this system will help in transmitting the data at Terabits/seconds. These fast data transmission helps in saving lots of human life. The measurements of the proposed antenna are mentioned in the next sub heading. Graphene is a single layer (monolayer) of carbon atoms, tightly bound in a hexagonal honeycomb lattice. This material helps in radiating the data at terabits/second. Thus the proposed antenna is designed with the Graphene material. As mentioned, the increased data rate can affect the human system at times, but comparative to the illness, this increase in data rate will help in saving human lives. Graphene based proximity dual feed antenna is proposed so as to safe guard life at risk.

Literature Survey

For THz applications, two port MIMO proximity coupled graphene patch antennas are implemented and tested for results in Varshney et al. (2019). The parameters such as diversity performance, ECC, Diversity gain and Mean effective gain are calculated. The transmission of Terabits per second is possible through this designed antenna (Varshney et al. 2019).

A harmonic terahertz (THz) having two distinct frequency stripes circularly polarized (CP) dielectric resonator (DR) antenna (DRA) is algorithmically examined, accomplished (Vishwanath and Sahana 2022). At first, an aperture coupled dual-band rectangular DRA was outlined which works accompanied by radical manner in the underneath stripe and third order fashion in the topmost stripe and proffers the linearly polarized reply. The angular edges of the rectangular DR are diminished

for procuring the perpendicular degraded elements of the employed fashion, as an outcome CP retort is attained (Vishwanath and Sahana 2022).

The pattern and enlargement of an emerging, operating in more than one directional swopped beam antenna functions at 2.45 GHz assisting wireless sensor network applications is entitled in paper (Sowmyadevi et al. 2019). The beam of the antenna is swopped, with regard to the peak gain 0 0, as an angle of ±80 0 in the pair of azimuth and elevation planes. The pair of ports were energized with a 90 0 phase variation guide to a discoid polarization in the beam directed with regard to the peak gain (Sowmyadevi et al. 2019). In addition, it is valued as the resonance frequency of an antenna continues to stay inside the 2:1 VSWR bandwidth regardless of the en route towards the switched beam.

The work proposed in Német et al. (2021) grants a textile-dependent antenna for the right now installed fifth-generation (5G) wireless bands (Német et al. 2021). The proposed antenna comprises a coplanar-waveguide (CPW)-fed patch over diminished edges and a twin L-shaped tail end as a portion of base geometry. The antenna has a bandwidth of 3.3–3.8 GHz, a peak gain of 3.17 dBi at 3.7 GHz, a proficiency of 64%. The antenna was outlined on denim fabric as it proffers preferred adaptability, effortlessness as a section of an attire, conservationist, compostable aspects of graphene owing to the property of non-metal, and modest on account of fabrication cost (Német et al. 2021).

The work done in Varshney et al. (2018) replicates an adjustable graphene-based antenna for terahertz applications. The target antenna can operate as a tunable dual–band besides tunable multi–input–multi–output (MIMO) antenna. The proposed work employs a pair of patches rather than the single patch. The technique permits the manufacturers to employ the variation in graphene chemical potential in the target antenna (Varshney et al. 2018). The calibration of two ports can be attained by employing diverse chemical possibilities. In case of two of the ports having similar chemical prospects the pattern can be operated as a dual–band reconfigurable antenna (Varshney et al. 2018).

The proposed system shares the pattern, reproduction and manufacturing of a pair of graphene antennas (Sharad and Upadhayay 2022). CPW fed rectangular patch antennas including U-shaped slot and inverted U-shaped slot are designated as design1 and design 2 sequentially (Sharad and Upadhayay 2022). The resonance frequency of the two antennas is 2.4 GHz (sub 6 GHz range). The antennas are projected to operate inside the extent available for Wi-Fi. Polyamide kapton tape of depth 100 μm and dielectric constant of 3.5 is employed as an underlayer. Graphene is engaged to form the governing patch, sustain, and bedrock of the antenna layout. Both the antenna patterns are collated and focus on a diverse antenna framework. The finest one is inspected and experimented in the entire proposed work.

The exploit of graphene for fabricating fault tolerant, diminutive, and efficacious terahertz (THz) antennas, analogous nurshing networks, and endeavour to recognize progression investigation fashion, medial and extended disputes and possibilities (Correas-Serrano and Sebastian Gomez-Diaz 2017). Initially clarify the upto to minute in resonant, leaky-wave and reflec tarray antennas, delivering a capacious evaluation of its execution, restrictions, and supreme provocations still to be labelled.

proceeded by inspecting various assimilation nurshing networks, embracing ingredients like circuit breakers, filters, and phase shifters, investigating the concussion of graphene's essential dimensional dissipation if it has in its execution (Correas-Serrano and Sebastian Gomez-Diaz 2017). The anticipation distinctly elaborates in what way graphene can conduct fascinating performance to its devices, inclusive of partial real-time redefine abilities and magnet-less non-reciprocal responses. Few stimulating applications of THz antennas are handed over and elaborated, inclusive of transceivers, biosensors, initial investigational observations of detectors and modulators. It is terminated by summarizing creativity for the assuring time ahead of graphene-based THz antennas (Correas-Serrano and Sebastian Gomez-Diaz 2017).

Fixing rigorous wearable gadgets to an individual's skin is a provocation to make it habitual. In view of this, the bearers would be unprotected with accommodating isolation, in particular in case if the gadget is implemented for keep see on neurological or medical circumstances (Golparvar et al. 2021). The enlargement of resilient, long term wearable, diffusivity nanomaterials with elevated fealty can promote perpetual and communally disconnected ambulatory electroencephalography (EEG) considering the perceiving materials are the garment fibres of each other (i.e., 3 rd generation intelligent clothing), and not a a strict gadget (Golparvar et al. 2021).

Wearable gadgets play a pivotal role in countless applications in healthcare covering from anatomical diseases, inclusive of cardiovascular diseases, hypertension and muscle disorders to neurocognitive disorders, such as Parkinson's disease, Alzheimer's disease and diverse psychological diseases (Iqbal et al. 2021). Various categories of wearables were employed for health care applications, for instance, skin-dependent wearables comprise tattoo-dependent wearables, textile cloth-dependent wearables, and biofluidic-dependent wearables. Later, wearables can be employed for promoting upgradation as a drug dispatch process; besides, intensify its efficacy with regard to customized health protection (Iqbal et al. 2021).

The restrictions of silicon competency are already outreached, accordingly, the detection of graphene with its distinctive nano-scale possessions is paving the way to possible replacement for the upcoming generation of rapid and lesser electronics in the twenty-first century (Taghiouskoui 2009). Considering the outcomes of the ensuring attributes of graphene, the investigation in this domain is captivating huge awards and promoters with a gradual flow in the numerous publications. The fashion in graphene examination is delivered in Taghiouskoui (2009). The vital provocations in this domain are figured out, and few attainable anticipations in the domain are elaborated in Taghiouskoui (2009).

Depending on the attributes of graphene nano-patch antennas, the work proposed a reconfigurable multiple-input multiple-output (MIMO) antenna system for Terahertz (THz) communications (Zheng et al. 2014). Initially, the mannerism of the graphene was examined and a beam restructuring antenna was patterned. The beamwidth and the transmission and receiving of gestures are dominated regarding the categories of individual graphene patches in an antenna. This is proceeded by enquiring the path loss and reflection models of the THz channel. As an outcome, put together the graphene-based antenna and the THz channel model, proffers an emerging MIMO

Table 20.1 The dimensions of the proposed antenna

Parameter	Dimension
Length of the substrate	65
Width of the substrate	45
Height of substrate 1	2.2
Height of substrate 2	2.2
Length of the feed	25
Width of the feed	1.7
Length of the patch	38
Width of the patch	16
Thickness of the patch	2

antenna pattern (Zheng et al. 2014; Bisht and Malik 2022; Pandey et al. 2022; Vishnoi et al. 2023).

Proposed Antenna Design

The proposed antenna is a graphene based proximity coupled two port MIMO antenna. The dimensions of the proposed antenna are given in the Table 20.1.

The Proposed antenna has been initially tested for results with Single port and now it is with Dual port.

Results and Discussion

The Two port Graphene based MIMO antenna is simulated using CST microwave studio and verified for its output. The antenna was designed for the frequency of 1.72 THz frequency following the procedure in Varshney et al. (2019). The Fig. 20.1 represents the simulated design of the proposed antenna in CST microwave studio.

A. ***Designed MIMO based Graphene antenna***

The antenna deigned is made to work in the THz frequency band with the properties of Graphene. It is a two port Multi input Multi output antenna with two substrates (Varshney et al. 2019). Two Nano strip feed lines are designed above substrate 1, which is placed above the perfect conducting ground plane. The Graphene based patch is placed above substrate 2. The feed lines are separated from the radiating material by substrate 2. Two excitation ports are assigned to the feed lines. The input for the excitation of the antenna is a Gaussian pulse.

B. ***Radiation pattern***

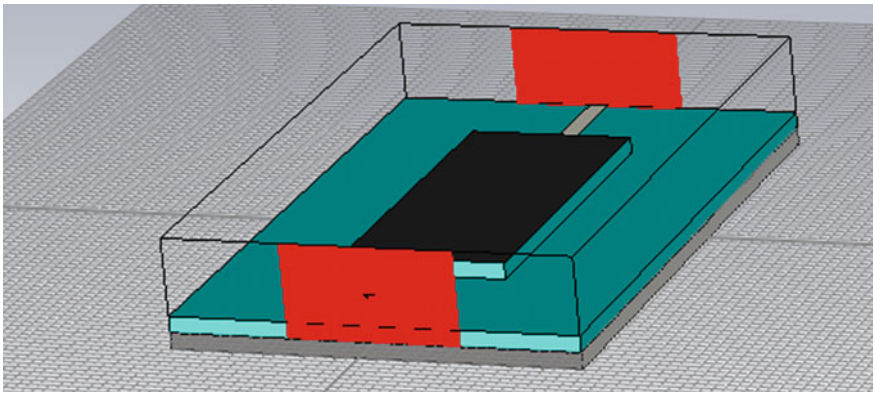

Fig. 20.1 Graphene based Two port MIMO antenna

The radiation pattern is the variation of power radiated along the defined direction of the antenna. Figure 20.2 shows the radiation pattern of the antenna designed (Taghiouskoui 2009).

C. ***S parameter***

Scattering parameter defines the input–output relationship between the ports. The designed two ports have four S (S_{11}, S_{12}, S_{21}, S_{22}) parameter values. Figures 20.3 and 20.4 represent the S parameter of the proposed graphene antenna.

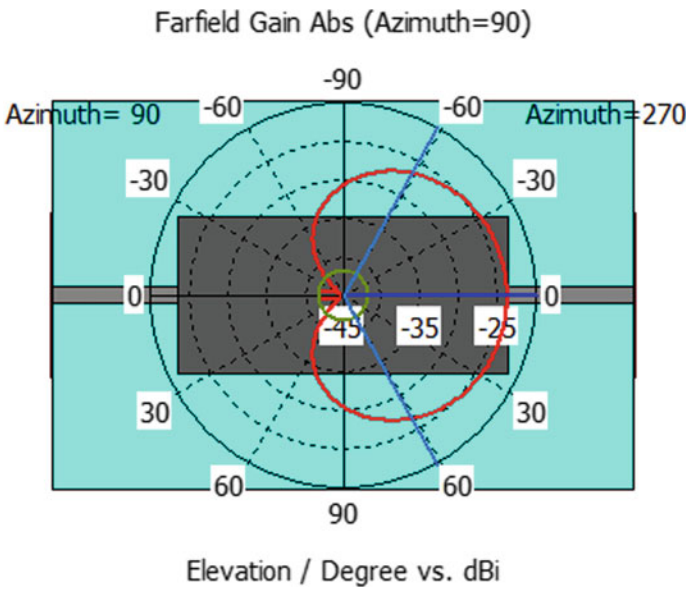

Fig. 20.2 Radiation pattern at 1.72 THz frequency

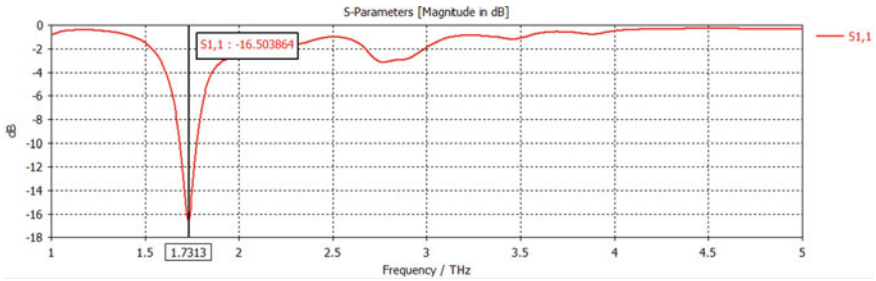

Fig. 20.3 S parameter response of the designed antenna

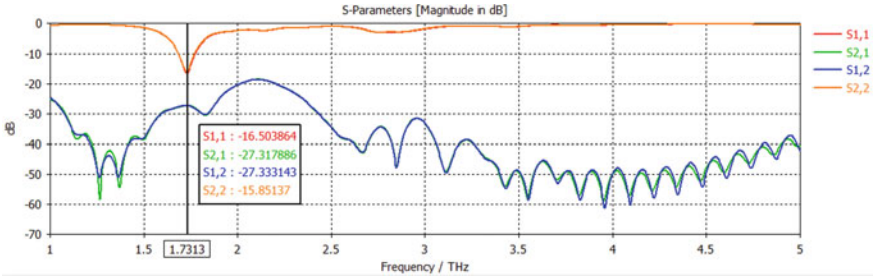

Fig. 20.4 S parameters (S_{11},S_{12},S_{21},S_{22})

The S parameter of the antenna is used to verify the correctness of excitation dip for the designed frequency.

D. ***Voltage Standing Wave Ratio***

The VSWR is the voltage standing wave ratio, defines the effectiveness of power transmitted from the power source for the designed frequency (Taghiouskoui 2009). Figure 20.5 represents VSWR of the proposed antenna.

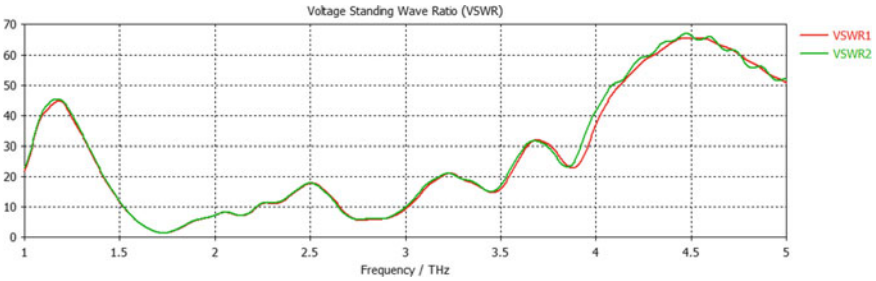

Fig. 20.5 VSWR of the designed antenna

Conclusion

Proximity coupled graphene patch antenna is designed and tested for results. The designed antenna can be used as Bio-medical wearable devices for testing various parameters of the body parts. The measurements such as pressure, sugar level and heart monitoring can be done. The range of Terabits per second transmission was found to be the fastest among all and thus the critical data ranges measured can be shared to the hospitals immediately. Elderly people, above 75 years of age can use these wearable devices for fastest and early detection of risky stages of human body parts.

References

Bisht N, Malik PK (2022) Adoption of microstrip antenna to multiple input multiple output microstrip antenna for wireless applications: a review. In: Singh PK, Singh Y, Chhabra JK, Illés Z, Verma C (eds) Recent innovations in computing. Lecture notes in electrical engineering, vol 855. Springer, Singapore. https://doi.org/10.1007/978-981-16-8892-8_15

Correas-Serrano D, Sebastian Gomez-Diaz J (2017) Graphene based antennas for Terahertz systems—a review. In: Forum for electromagnetic research methods and application technologies (FERMAT), pp 1–26, Correas-Serrano-ART, vol 20

Dai H, Ng K-W, Li M, Wu M.-Y (2013) An overview of using directional antennas in wireless networks. Int J Commun Syst 26(4):413–448

Varshney G, Gotra S, Pandey VS, Yaduvanshi RS (2019) Proximity-coupled two port multi-input-multi-output graphene antenna with pattern diversity for THz applications. Nano Commun Netw 21:1–11. https://doi.org/10.1016/j.nancom.2019.05.003

Golparvar A, Ozturk O, Yapici MK (2021) Gel-free wearable electroencephalography (EEG) with soft graphene textiles. IEEE Sens 2021:1–4. https://doi.org/10.1109/SENSORS47087.2021.9639711

Iqbal SM, Mahgoub I, Du E et al (2021) Advances in healthcare wearable devices. npj Flex Electron 5(1):1–14

Német A, Alkaraki S, Abassi QH, Jilani SF (2021) A biodegradable textile-based graphene antenna for 5g wearable applications. In: 2021 IEEE international symposium on antennas and propagation and USNC-URSI radio science meeting (APS/URSI), pp 1583–1584. https://doi.org/10.1109/APS/URSI47566.2021.9704120

Pandey U, Gupta NP, Malik P (2022) Review on miniaturized flexible wearable antenna for body area network. In: Singh PK, Singh Y, Chhabra JK, Illés Z, Verma C (eds) Recent innovations in computing. Lecture notes in electrical engineering, vol 855. Springer, Singapore. https://doi.org/10.1007/978-981-16-8892-8_4

Pawar AY, Sonawane DD, Erande KB, Derle DV (2013) Terehertz technologies and its applications. Sciverse Sci Direct, Drug Invention Day, Rev Art 157–163. https://doi.org/10.1016/j.dit.2013.03.009

Sharad S, Upadhayay MD (2022) Graphene antenna on polyamide for 2.4 GHz WLAN applications. In: 2022 IEEE Delhi section conference (DELCON), pp 1–5. https://doi.org/10.1109/DELCON54057.2022.9752959

Sowmyadevi A, Mathur P, Chandran AR, Timmons N, Morrison J, Raman S (2019) 2.45 GHz pattern reconfigurable antenna for wireless sensor network applications. URSI AP-RASC 2019, New Delhi, India, 09–15 March 2019

Taghiouskoui M (2009) Trends in graphene research. Mater Today 12(10)

Tarter G, Mottola L, Picco GP (2013) Directional antennas for convergecast in wireless sensor networks: are they a good idea? In: IEEE 13th international conference on mobile ad hoc and sensor systems, pp 172–182. https://doi.org/10.1109/MASS

Varshney G, Verma A, Pandey VS, Yaduvanshi RS, Bala R (2018) A proximity coupled wideband graphene antenna with the generation of higher order TM modes for THz applications. Opt Mater 85:456–463. https://doi.org/10.1016/j.optmat.2018.09.015

Vishnoi V, Singh P, Budhiraja I, Malik PK (2023) Multiband dual-layer microstrip patch antenna for 5G wireless applications. In: Singh PK, Wierzchoń ST, Tanwar S, Rodrigues JJPC, Ganzha M (eds) Proceedings of third international conference on computing, communications, and cybersecurity. Lecture notes in networks and systems, vol 421. Springer, Singapore. https://doi.org/10.1007/978-981-19-1142-2_7

Sahana BC, Varshaney G (2022) Tunable terahertz dual-band circularly polarized dielectric resonator antenna. Optik 253:168578. ISSN 0030–4026. https://doi.org/10.1016/j.ijleo.2022.168578

Xu Z, Dong X, Senior Member, IEEE, Bornemann J (2014) Design of a reconfigurable MIMO system for THz communications based on graphene antennas. IEEE Trans Terahertz Sci Technol 4(5):609–617

Chapter 21
Developing an Effective Antenna for IoT Applications in 5G

Mukesh Chand, Garima Mathur, and K. S. Nisaar

Abstract In last few years the wireless technology has been changing rapidly in India. The 5G wireless technology has emerged as a major player in the wideband antenna. Wireless research is a tough and fascinating field. This article outlines the high level of the Internet of Things in the context of 5G wireless broadband antennas. In the future of wireless technology, IoT in the 5G system will be a key changer. It will act as a catalyst for innovative antenna architecture and smart services. In 5G IoT systems, we present a complete overview of the issues and vision of several communication industries. One of the important challenges in the development of smart antenna services in industrial Internet-of-Things (IIoT), which includes automation, smart cellular devices. 5G has a lot of promise to promote IIoT as an advanced wireless antenna transmission technique in the future of IoT. This chapter presents a complete assessment of 5G supported smart devices in the IoT field. This chapter creates a significant overview of current IoT research in terms of antenna architecture, technology, and its applications. The prime objective of this chapter is built a thorough list of the advance techniques in IIoT as well as in the subject of IoT and their relevant trends. It will be beneficial in the future studies.

Keywords Industrial Internet-of-Things (IIoT) · Internet of Things (IoT) · 5G antenna

M. Chand (✉)
Poornima College of Engineering, Jaipur, India
e-mail: mukeshchand19@poornima.org

G. Mathur
Poornima College of Engineering, Jaipur, India
e-mail: drg.mathur@poornima.org

K. S. Nisaar
Salman Bin Abdul Aziz University, Al-Kharj, Kingdom of Saudi Arabia

P. K. Malik and P. N. Shastry (eds.), *Internet of Things Enabled Antennas for Biomedical Devices and Systems*, Springer Tracts in Electrical and Electronics Engineering,
https://doi.org/10.1007/978-981-99-0212-5_21

Introduction

Nowadays wireless communication techniques are highly in demand in terms of high-speed data rates internet connectivity. The IoT device market is booming concurrently with the rapid development of wireless communications. IoT devices will have wide applications in the future as wireless technology and the Internet of Things advance. Regarding the communication interface of wearable technology, the device is connected to the mobile phone via Bluetooth and linked to the mobile application (Liao et al. 2021). The advancement of the Internet of Things creates numerous scientific and engineering challenges. This is the main goal of innovative research work to develop efficient, economical, scalable and reliable antenna systems in the field of Internet of Things (IoT). The antenna design of UWB and RFID tags in the Internet of thing arena, the transmission technology of MIMO antenna systems, massive MIMO systems, and the position tolerance design method and the influence of the randomness of the antenna array element position are particularly emphasized in the contribution of this special issue (Chattha et al. 2018). Internet of Things applications play an important role in the field of wireless communication and computer networking. The devices used in Internet of things are cost effective, easy to use and energy efficient to operate at different frequencies (Liao et al. 2021; Chattha et al. 2018; Shameena et al. 2012).

Antenna Design

In "A compact CPW fed slot antenna for ultra-wide band applications" V. A. Shameena et al., the author proposes a compact UWB slot antenna with a wide (B.W.) bandwidth, a consistent radiation pattern, and a constant gain. The size of the compact antenna is 26 mm × 26 mm, printed on the substrate. The VSWR bandwidth range for UWB slot antenna is 3.1 –11.1 GHz and is used to cover broadband frequencies between 3.38, 4.8, and 9.5 GHz (Shameena et al. 2012). Comparing the simulation results with the actual measurement results, there is generally a good combination. The proposed antenna has wide application in UWB and IoT applications (Fig. 21.1).

In "A Compact Chip-less RFID Tag for IoT Applications" Usman A. Haider et al. the author presents a compact RFID antenna with cost effective, encoding bit capability, compact in size and easy fabrication. The code density of 6.122 bits/cm^2 and antenna size of 1.4 × 1.4 cm^2 were made on FR4 Substrate with planar construct. The operating bandwidth is 4–14 GHz and is suitable for a wide range of IoT applications (Haider et al. 2020) (Fig. 21.2).

In "Electronically Pattern Reconfigurable Antenna for IoT Applications" Luca Antamaria et al. the author, purposed an electronical reconfigurable Antenna for the application in IoT. The antenna has four wire patches with 4 end fire radiation which is less than 5 ms. The reconfigurable antenna achieves a bandwidth of 2.25–2.54 GHz of frequency of 290 MHz. The reconfigurable antenna is compact, cost

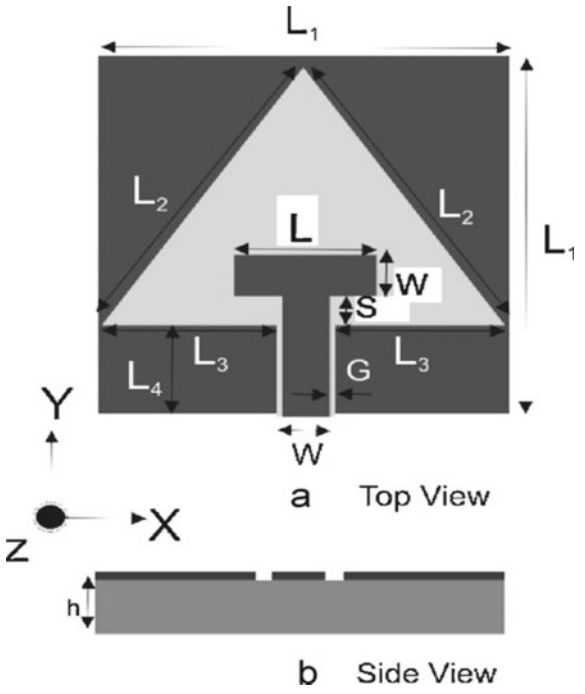

Fig. 21.1 Proposed geometry view antenna

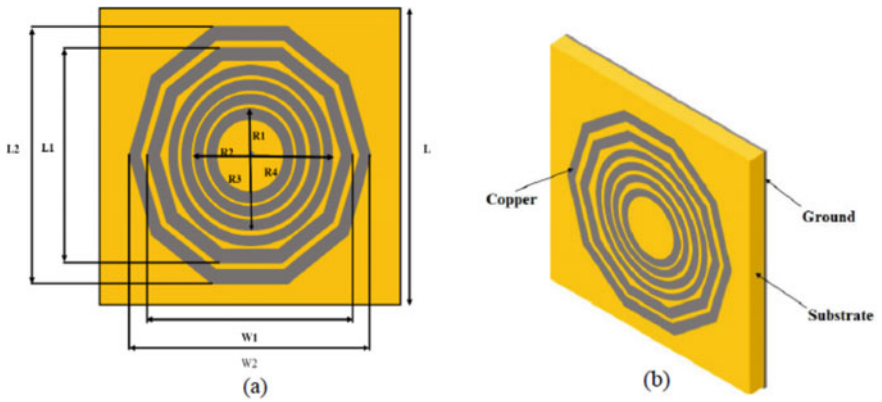

Fig. 21.2 Proposed structural model of antenna: **a** front **b** perspective view

effective with printed on substrate FR4 (Liao et al. 2021). The proposed antenna has maximum performance, is inexpensive, is of compact size, and has low power (Fig. 21.3).

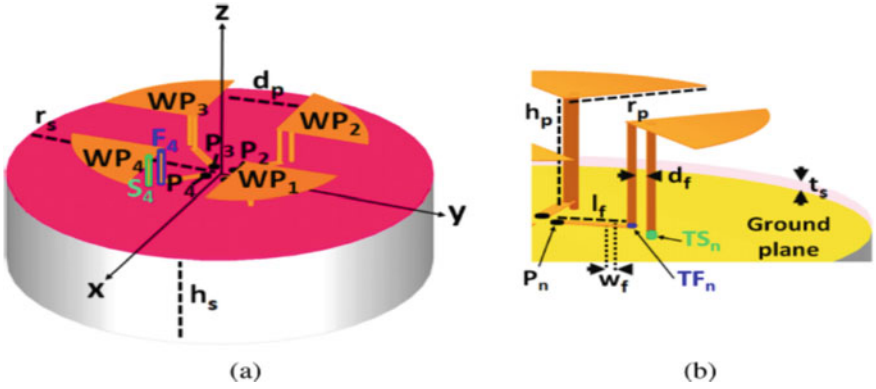

Fig. 21.3 Antenna model: **a** 3-D isometric view and **b** wirepatch elements (zoom view)

In "Multiple Integrated Antennas for Wearable Fifth-Generation Communication and Internet of Things Applications" Chia-teliao et al. the authors, present a multiple integrated antenna for the IoT application. The dedicated antennas covered frequency of 2.4–5 GHz. The integrated antenna has three modes, namely the slot mode, the monopole mode, and the loop coupled monopole mode (Santamaria et al. 2021) (Fig. 21.4).

In "A Novel Dual Ultrawideband CPW-Fed Printed Antenna for Internet of Things (IoT) Applications" Qasim Awais et al., the authors, purposed a dual-band co-planar waveguide antenna with rectangular implementation on a FR4 substrate and a size of 25–35 mm. The frequency of the CPW-Fed printed antenna is 1.1–2.7 GHz and 3.15–3.65 GHz, so it covers the 2.4 GHz Wi-Fi/ Bluetooth frequency and most of the 3G/4G frequency bands, as well as the expected 5G frequency band in the future, namely 3.4–3.6 GHz (Awais et al. 2018; Roges and Malik 2021; Rahim et al. 2021; Malik et al. 2020). The presented antenna has wide application in wireless communication 5G Technology and IoT (Fig. 21.5; Table 21.1).

Conclusion

This article performs a thorough survey of various 5G antennas by comparing and analysing their performance enhancement technologies. During aIoT antenna review, it was found that the dual band different coplanar wave guide antenna is used based on their frequency. The small chipless RFID antennas are ideal for use with 5G devices that support IoT.

It is possible to make a simple and compact UWB (Ultra wide Band) slot antenna. The antenna's main selling point is its wide impedance bandwidth, stable radiation pattern, and constant gain. The antenna's fidelity indicates that the antenna has been introduced. The baseband signal has a low level of distortion.

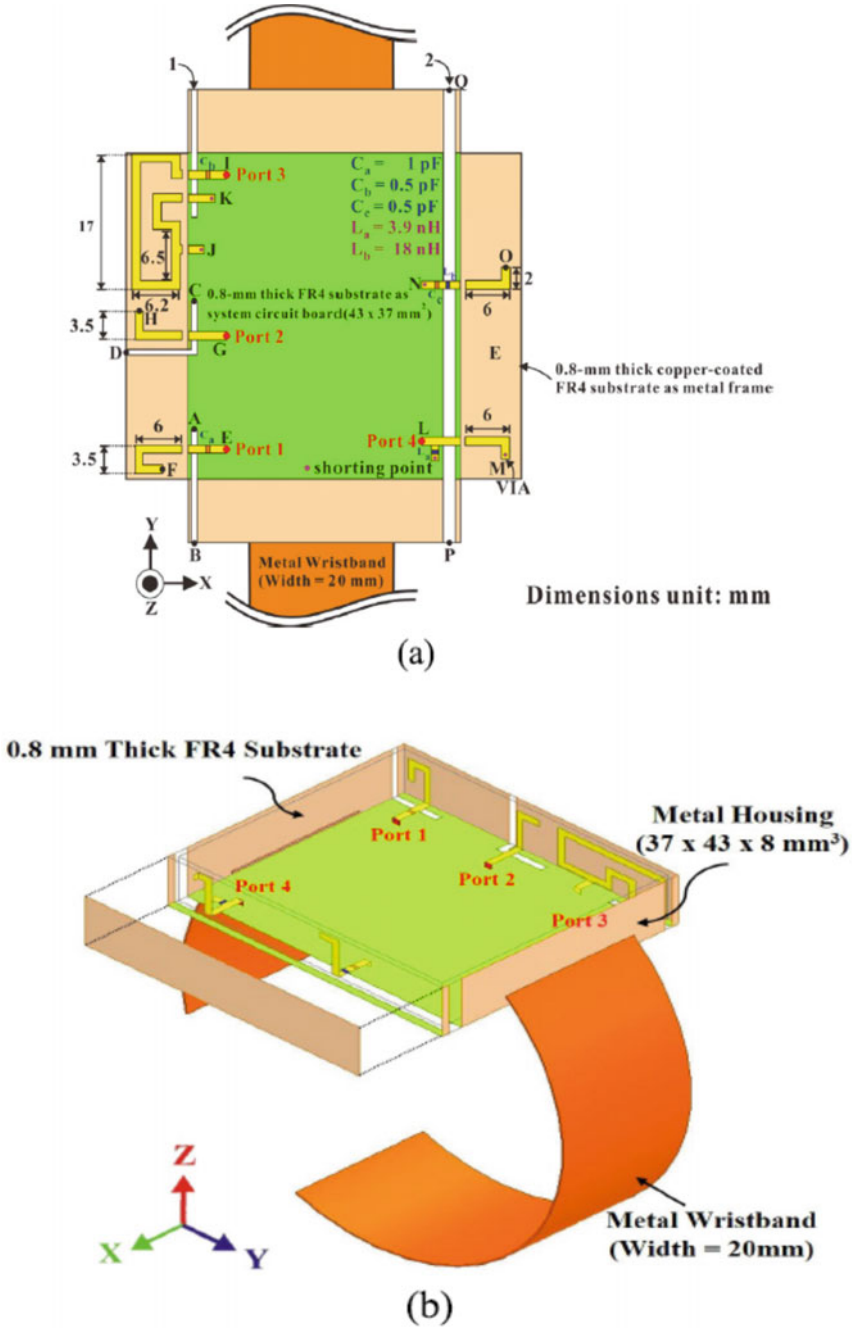

Fig. 21.4 **a** and **b** Top and side views of the suggested antenna's geometry

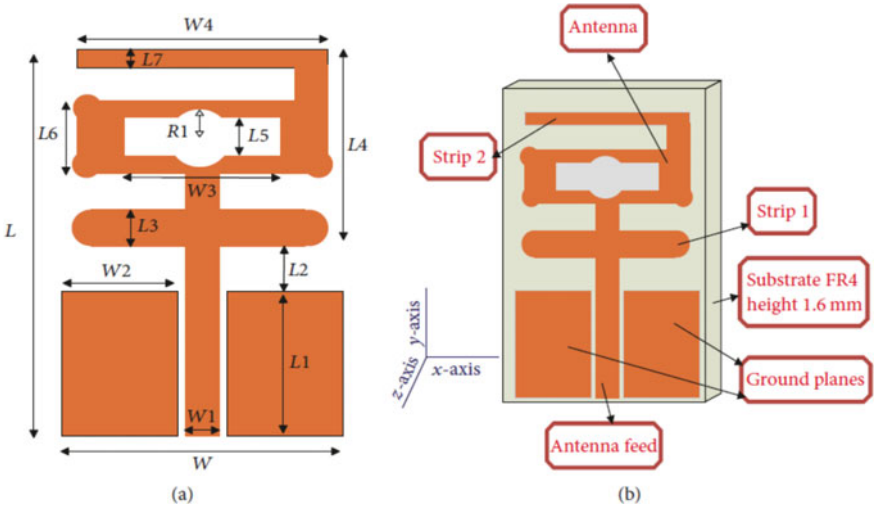

Fig. 21.5 Geometry view of the antenna structure: **a** geometrical structure and **b** major antenna components

Table 21.1 Comparison between different antennas

References	Total area (mm^2)	Bandwidth	Peak gain (dBi)
Shameena et al. (2012)	676	3.1–11.1 GHz	5.5
Haider et al. (2020)	1.96	4–14 GHz	–
Santamaria et al. (2021)	–	2.25–2.54 GHz	3.9
Liao et al. (2021)	676	3.4, 4.8 and 9.6 and 10.6 GHz	5.5
Awais et al. (2018)	875	1.1–2.7 GHz and 3.15–3.65 GHz	8.9

A novel pattern reconfigurable antenna structure is made up with only two FR4 PCBs, through holes, and one metal component. The antenna is simple to build and has a low production cost. The proposed antenna is an ideal one due to its simple reconstruction mechanism, limited volume, and low-cost implementation. CPW antennas on the top and bottom strips effectively control the 2.4 and 3.4 GHz resonance bands, respectively.

References

Awais Q, Chattha HT, Jamil M, Jin Y, Tahir FA, Rehman MU (2018) A novel dual ultrawideband CPW-fed printed antenna for Internet of Things (IoT) applications. Wirel Commun Mob Comput

Chattha HT, Abbasi QH, Ur-Rehman M, Alomainy A, Tahir FA (2018) Antenna systems for internet of things

Haider UA, Noman M, Ullah H, Tahir FA (2020) A compact chip-less RFID tag for IoT applications. In: 2020 IEEE International symposium on antennas and propagation and North American radio science meeting. IEEE, pp 1449–1450

Liao CT, Yang ZK, Chen HM (2021) Multiple integrated antennas for wearable fifth-generation communication and internet of things applications. IEEE Access 9:120328–120346

Malik PK, Wadhwa DS, Khinda JS (2020) A survey of device to device and cooperative communication for the future cellular networks. Int J Wirel Inf Netw (Springer) 27:411–432. https://doi.org/10.1007/s10776-020-00482-8

Rahim A, Malik PK (2021) Analysis and design of fractal antenna for efficient communication network in vehicular model. Sustain Comput Inform Syst (Elsevier) 31:100586. https://doi.org/10.1016/j.suscom.2021.100586. ISSN 2210-5379

Roges R, Malik PK (2021) Planar and printed antennas for Internet of Things-enabled environment: opportunities and challenges. Int J Commun Syst 34(15):e4940. https://doi.org/10.1002/dac.4940ISSN:1099-1131

Santamaria L, Ferrero F, Staraj R, Lizzi L (2021) Electronically pattern reconfigurable antenna for IoT applications. IEEE Open J Antennas Propag 2:546–554

Shameena VA, Mridula S, Pradeep A, Jacob S, Lindo AO, Mohanan P (2012) A compact CPW fed slot antenna for ultra wide band applications. AEU-Int J Electron Commun 66(3):189–194